NOVA SCHOOL OF SCIENCE & TECHNOLOGY

DEPARTMENT OF CHEMISTRY

BIOLOGICAL UPCYCLING OF MIXED PET WASTE INTO HIGH VALUE PRODUCTS

ANA TERESA MATALOTO REBOCHO

Master in Biotechnology

DOCTORATE IN CHEMICAL AND BIOLOGICAL ENGINEERING

NOVA University Lisbon

April, 2025

DEPARTMENT OF CHEMISTRY

BIOLOGICAL UPCYCLING OF MIXED PET WASTE INTO HIGH VALUE PRODUCTS

ANA TERESA MATALOTO REBOCHO

Master in Biotechnology

Adviser: Cristiana Andreia Vieira Torres
Assistant Researcher, NOVA School of Science and Technology, NOVA University Lisbon

Co-advisers: Maria Filomena Andrade de Freitas
Assistant Professor, NOVA School of Science and Technology, NOVA University Lisbon

Examination Committee:

Chair: Rui Manuel Freitas Oliveira,
Full Professor, NOVA School of Science and Technology,
NOVA University Lisbon

Rapporteurs: José António Couto Teixeira,
Full Professor, School of Engineering, University of Minho

Paula Maria Lima Castro,
Full Professor, Faculty of Biotechnology, Catholic University of Porto

Adviser: Cristiana Andreia Vieira Torres,
Assistant Researcher, NOVA School of Science and Technology, NOVA University Lisbon

Members: Maria Teresa Ferreira Cesário Smolders,
Researcher, Institute for Bioengineering and Biosciences,
Instituto Superior Técnico

Rui Manuel Freitas Oliveira,
Full Professor, NOVA School of Science and Technology,
NOVA University Lisbon

Mónica Isabel Gonçalves Carvalheira,
Assistant Researcher, NOVA School of Science and Technology, NOVA University Lisbon

DOCTORATE IN CHEMICAL AND BIOLOGICAL ENGINEERING

NOVA University Lisbon
April, 2025

Biological upcycling of mixed PET waste into high value products

Dedicada à minha avó Teresa

ACKNOWLEDGMENTS

Esta tese marca o final de uma das mais desafiantes jornadas da minha vida. Foi um percurso longo e bastante exigente, que colocou diariamente à prova as minhas capacidades de resiliência, trabalho e perseverança. Ao fim de quase cinco anos, torna-se difícil colocar em palavras os agradecimentos a todos os que acompanharam, de perto ou de longe, e contribuíram, tanto a nível científico como pessoal para a concretização deste objetivo. Tive a oportunidade de conhecer e de crescer com pessoas que não só tornaram os momentos bons em memórias inesquecíveis, mas também ajudaram a transformar os desafios em valiosas lições de vida. A todas elas, muito obrigado por tudo!

Em primeiro lugar, gostaria de expressar o meu agradecimento às minhas orientadoras, Doutora Cristiana Torres e Professora Doutora Filomena Freitas, por toda a orientação, ensinamento e partilha de conhecimento científico e espírito critico ao longo do desenvolvimento deste projeto. Agradeço também por terem acreditado nas minhas capacidades e no meu potencial, integrando-me no projeto de investigação BioICEP, no qual este trabalho de doutoramento foi desenvolvido. Gostaria de deixar um agradecimento, em particular, à Prof. Filomena, pelo acompanhamento exemplar e por todas as oportunidades que me proporcionou ao longo dos últimos oito anos.

Quero ainda expressar o meu sincero agradecimento à Professora Doutora Maria Ascensão Reis, por me ter deixado fazer parte do grupo BIOENG e por disponibilizar todos os recursos e condições de trabalho que tornaram este percurso possível.

Agradeço também aos parceiros do projeto BioICEP, nomeadamente à AVECOM e ao TUS, por terem gentilmente fornecido os microrganismos isolados e o resíduo de PET despolimerizado que foram utilizados durante o desenvolvimento desta tese, bem como à Microlife Solutions pela análise 16S rDNA.

Agradeço o apoio financeiro da Fundação para a Ciência e Tecnologia pelo financiamento da bolsa de doutoramento 2020.06470.BD e às instituições que me acolheram para o desenvolvimento deste doutoramento, a Unidade de Ciências Biomoleculares Aplicadas (UCIBIO).

É para mim impossível, terminar esta etapa, sem um enorme agradecimento a todas as pessoas do grupo BIOENG, que todos os dias estiveram ao meu lado e que contribuíram para um bom ambiente de trabalho e de partilha de conhecimento. Foram muitas e longas horas, tanto no Lab 407 como no 610, e com quem acabei por criar boas recordações e uma ligação de amizade.

À Patrícia Reis, pela amizade, infinitas horas de boa conversa, partilha de conhecimento, e pelo exemplo do que é ser-se cientista e rainha do step. Ao João Pereira, pela amizade, contagiante alegria, e por mostrar que é possível ir sempre mais longe quando impulsionamos os outros e estamos disponíveis para partilhar o melhor de nós com aqueles que nos rodeiam. À Cátia Gil, agradeço pela amizade, e partilha de momentos de alegria, mas acima de tudo pela paciência e a prontidão em relembrar-me, nos momentos mais difíceis e de maior frustração, que eu era capaz de fazer isto, és grande miúda! À Diana Araújo, obrigada pelos conselhos, desabafos e gargalhadas, mas acima de tudo por ser um grande exemplo de dedicação e perseverança. À Rita Bernardino, por ser uma das pessoas mais ponderadas, focadas e trabalhadoras que tive a oportunidade de conhecer, mas acima de tudo a quem agradeço imenso pela grande amizade que temos. À Patrícia Freitas, pelo grande companheirismo e amizade que continua até hoje, bem como o exemplo de valores, dedicação e entreajuda que sempre mostrou em prol da equipa. Ao Francisco Santos, o maior opinador profissional que conheço, obrigada pela partilha de conhecimento e pela pronta disponibilidade e discernimento em ajudar nos momentos de bloqueio. À Marta Catalão, comparsa das mistas, obrigada pela gigantesca ajuda nas noites sem fim dos ensaios de produção do team sapal. À Beatriz Almeida, pela ajuda na maratona que foi a fase final com os testes mecânicos e ensaios de permeabilidade. À Asiyah Esmail e à Maria Batista, por terem partilhado comigo os stresses e mil e uma tarefas de projeto sempre com boa disposição. Ao Thomas Rodrigues e ao Bruno Serafim, pelo apoio no laboratório, pelo bom ambiente de trabalho e momentos de descontração animados.

Não poderia deixar de agradecer à Elsa Mestre e à Elisabete Freitas pelo suporte e pelo exemplo de dedicação ao vosso trabalho, o que elevou o meu. Obrigada pela preocupação e por terem sempre uma palavra de apoio! À Eliana Guarda, pelas suas palavras de motivação, preocupação para comigo e de amizade, especialmente nos momentos de neura. À Juliana Almeida, pelo companheirismo e por ter partilhado comigo a insanidade do final do doutoramento, especialmente durante a escrita. À Marta Rodrigues, pela sua calma, preocupação pelo próximo e por me relembrar sempre que há vida para além do trabalho. À Claúdia Duarte, pelo apoio nos períodos de provação que tive no final do doutoramento, por estar sempre disposta a ouvir cada um dos dilemas do doutoramento e da vida, e pelos bons momentos de diversão. Ao João Carvalho e ao Miguel Palhas pelos momentos de boa disposição e pela entreajuda no laboratório nos últimos anos.

Ao Rafael, que viveu a meu lado todos os momentos deste doutoramento, o meu maior agradecimento pelo teu apoio infindável, que nunca deixaste dar em tudo. Por seres o meu melhor amigo. Por

acreditares em mim, mesmo quando eu não acreditava. E, acima de tudo, por fazeres de mim uma pessoa melhor.

Teria sido impossível ter chegado aqui sem o apoio incondicional dos meus pais. Não há palavras suficientes para agradecer os sacrifícios que fizeram para que eu tivesse a oportunidade de seguir os meus sonhos e chegar até aqui. Agradeço, do fundo do meu coração, pela vossa presença, pelos valores e pela educação que me transmitiram, e por acreditarem em mim todos os dias. Este doutoramento também é vosso!

Não poderia deixar de agradecer, à minha avó Teresa, que apesar de já não estar junto a mim, continua a ser um dos meus maiores exemplos, presente em mim todos os dias. Agradeço por teres acreditado sempre em mim e me teres ensinado que não importa de onde viemos, nem as limitações que a vida nos impõe, mas que, com dedicação, honestidade e humildade, conseguimos superar os nossos maiores desafios.

Finalmente, quero também deixar uma palavra de agradecimento aos meus amigos e à restante família, que sempre me ofereceram uma palavra de apoio e suporte e que ajudaram a tornar todos os momentos mais leves ao longo desta jornada.

O meu maior obrigado a todos!

"Working hard is important. But there is something that matters even more: believing in yourself."

-*Harry Potter and the Order of the Phoenix,* J.K.Rowling

ABSTRACT

Polyethylene terephthalate (PET) is a recalcitrant non-biodegradable petrochemical-based plastic contributing to environmental pollution. Therefore, it is urgent to develop strategies to mitigate PET disposal impacts and develop sustainable alternatives, such as biobased biodegradable biopolymers. This thesis address those challenges by developing upcycling strategies for the biotechnological conversion of post-consumer PET (pcPET) waste, which was chemically depolymerized via reactive extrusion, composed primarily of terephthalic acid (TPA). Single bacterial cultures and a microbial consortium (MMC) were investigated for their ability to use TPA as sole feedstock to produce polyhydroxyalkanoates (PHAs), biodegradable bioplastics with properties comparable to conventional plastics.

Two strains, isolated from plastic-contaminated environments, were tested for PHA production using TPA as feedstock. Response Surface Methodology was used to determine the optimal concentrations of TPA and ammonium for maximal cellular growth and PHA content. *Rhodococcus* sp. Ave7 was selected given its efficiency in converting TPA into biomass and PHA. This strain also accumulated triacylglycerols (TAGs), which were considered of interest for further exploitation. In a bioreactor, *Rhodococcus* sp. Ave7 efficiently converted TPA into PHA and TAG, representing 15.01 ± 0.68 and 15.40 ± 0.29% of the biomass dry weight, respectively. The culture produced the copolyester poly(3-hydroxybutyrate-co-3-hydroxyvakerate) (PHBV), with a 3HV content of 90wt.%, and TAGs comprising octadecenoic acid ($C_{18:1}$) (43.3-50.8wt.%), hexadecanoic acid ($C_{16:0}$) (32.1-38.9wt.%) and octadecanoic acid ($C_{18:0}$) (8.5-8.7wt.%).

An MMC selected from marshland sediments was enriched in PHA-storing organisms using cyclic TPA feeding (feast-and-famine, F/f, approach) in a 2 L bioreactor with 4-day cycles. A stable culture was established within one sludge retention time (40 days), an F/f ratio of 0.1, dominated by *Gammaproteobacteria*, including *Halomonadaceae* and *Zoogloeaceae*. Under permanent feast conditions (in a 1 L bioreactor) with growth-limiting conditions imposed by nitrogen exhaustion, the culture achieved a PHA content in the biomass of 65.14 ± 5.37wt%. The produced biopolymer was poly(3-hydroxybutyrate) (PHB) with an average molecular weight of 352 kDa, with melting and maximum degradation

temperatures of 174 °C and 253 °C, respectively. PHB films presented tensile strength of 18.8 ± 1.9 MPa and Young's Modulus of 422.5 ± 142.3 MPa, coupled with good gas and moisture barrier properties.

Overall, this thesis demonstrated the feasibility of biologically upcycling pcPET waste into PHA using TPA from PET depolymerization as feedstock for microbial cultivation. Different PHAs were obtained: PHB using an MMC, PHBV by *Rhodococcus* sp. Ave7 that also produced TAGs, further adding value to the bioprocess.

Keywords: Polyhydroxyalkanoates (PHA), Plastic waste, Polyethylene terephthalate (PET) waste, Pure cultures, Mixed microbial cultures (MMC), Terephthalic acid, PHA Films

RESUMO

O polietileno tereftalato (PET) é um plástico petroquímico recalcitrante e não biodegradável que contribui significativamente para a poluição ambiental. Portanto, é urgente desenvolver estratégias para mitigar os impactos do descarte de PET e desenvolver alternativas sustentáveis, como biopolímeros biodegradáveis de base biológica. Esta tese aborda esses desafios, desenvolvendo estratégias de upcycling para a conversão biotecnológica de resíduos de PET pós-consumo (pcPET), que foram quimicamente despolimerizados por meio de extrusão reativa, compostos principalmente por ácido tereftálico (TPA). Culturas bacterianas isoladas e um consórcio microbiano (MMC) foram investigados pela sua capacidade de utilizar o TPA como único substrato para produzir polihidroxialcanoatos (PHAs), bioplásticos biodegradáveis com propriedades comparáveis aos plásticos convencionais.

Duas estirpes, isoladas de ambientes contaminados por plásticos, foram testadas para a produção de PHA utilizando TPA como substrato. O Método de Superfície de Resposta (RSM) foi usado para determinar as concentrações ideais de TPA e amónia para maximizar o crescimento celular máximo e o conteúdo em PHA. *Rhodococcus* sp. Ave7 foi selecionada devido à sua eficácia na conversão de TPA em biomassa e PHA. Esta estirpe também acumulou triacilglicéridos (TAGs), os quais foram considerados de interesse para exploração futura. Em bioreactor, *Rhodococcus* sp. Ave7 converteu eficientemente TPA em PHA e TAG, representando 15.01 ± 0.68% e 15.40 ± 0.29% do peso seco da biomassa, respetivamente. A cultura produziu o copóliester poli(3-hidroxibutirato-co-3-hidroxivalerato) (PHBV), contendo 90wt% de 3HV, e TAGs compostos por ácido octadecenóico ($C_{18:1}$) (43.3-50.8wt.%), ácido hexadecanóico ($C_{16:0}$) (32.1-38.9wt.%) e ácido octadecanóico ($C_{18:0}$) (8.5-8.7wt.%).

Selecionou-se uma cultura microbiana mista (MMC) a partir de sedimentos de sapal, a qual foi enriquecida em organismos acumuladores de PHA através de um regime de fome e fartura (F/f), utilizando uma alimentação cíclica de TPA num bioreactor de 2 L, com ciclos de 4 dias. Foi estabelecida uma cultura estável dentro de um tempo de retenção de lamas (40 dias), com um rácio F/f de 0.1, dominada por *Gammaproteobacteria*, incluindo *Halomonadaceae* and *Zoogloeaceae*. Em condições de fartura permanente (num bioreactor de 1L) com condições limitantes de crescimento impostas pela exaustão de

azoto, a cultura atingiu conteúdos de PHA na biomassa de 65.14 ± 5.37wt%. O biopolímero produzido foi um poli(3-hidroxibutirato) (PHB) com um peso molecular médio de 352 kDa, uma temperatura de fusão e de degradação máxima de 174 °C e 253 °C, respetivamente. Os filmes de PHB apresentaram resistência à tração de 18.8 ± 1.9 MPa e um módulo de Young de 422.5 ± 142.3 MPa, juntamente com boas propriedades de barreira a gases e à humidade.

No geral, esta tese demonstrou a viabilidade do upcycling biológico de resíduos de pcPET em PHA, utilizando TPA proveniente da despolimerização do PET como substrato para cultivo microbiano. Foram obtidos diferentes PHAs: PHB utilizando uma MMC e PHBV por *Rhodococcus* sp. Ave7, que também produziu TAGs, acrescentando ainda mais valor ao bioprocesso.

P**alavas chave:** Polihidroxialcanoatos (PHAs), Resíduos Plásticos, Resíduo Polietileno tereftalato (PET), Culturas puras, Culturas microbianas mistas (MMC), Ácido Tereftálico, Filmes de PHA

LIST OF CONTENTS

LIST OF FIGURES

LIST OF TABLES

ABBREVIATIONS

3HB	3-hydroxybutyrate
3HHx	3-hydroxyhexanoate
3HV	3-hydroxyvalerate
3HO	3-hydroxyoctanoate
3HD	3-hydroxydecanoate
3HDd	3-hydroxydodecanoate
3HTd	3-hydroxytetradecanoate
ADF	Aerobic dynamic feeding
ANOVA	Analysis of Variance
ATR	Attenuated total reflectance
BHET	Bis(hydroxyethyl) terephthalate
BTEXs	Benzene, toluene, ethylbenzene, p-xylene
CCRD	Central Composite Rotatable Design
CDW	Cell dry weight
CSTR	Continuous stirred tank reactors
DMT	Dimethyl terephthalate
DO	Dissolved oxygen
DSC	Differential scanning calorimetric
EG	Ethylene glycol
FAME	Fatty acid methyl esters
FID	Flame ionization detector

FTIR	Fourier Transform Infra-Red
GC	Gas chromatography
HAAs	Hydroxyalkanoyloxy-alkanoates
HPDE	High-density polyethylene
HPLC	High performance liquid chromatography
HRT	Hydraulic retention time
ICP-AES	Inductively Coupled Plasma – Atomic Emission Spectroscopy
LDPE	Low-density polyethylene
lcl-PHA	Long Chain Length - Poly(HydxroxyAlkanoate)
LLDPE	Linear-low density polyethylene
mcl-PHA	Medium Chain Length - Poly(HydxroxyAlkanoate)
MMC	Mixed microbial culture
MSM	Mineral salt media
Mw	Average molecular weight
PA	Polyamide
PBS	Poly(butylene succinate)
pcPET	Post-consumer PET
PCL	Polycaprolactone
PCA	Protochatecuate
PDI	Polydispersity index
PE	Polyethylene
PET	Polyethylene terephthalate
PHAs	Polyhydroxyalkanoates
PHB	Poly(3-hydroxybutyrate)
PHBHHx	Poly(3-hydroxybutyrate-co-3-hydroxyhexanoate)
PHBO	Poly(3-hydroxybutyrate-co-3-hydroxyoctanoate)
PHBP	Poly(3-hydroxybutyrate-co-3-hydroxypropionate)
PHBV	Poly(3-hydroxybutyrate-co-3-hydroxyvalerate)
PLA	Polylactic acid

PP	Polypropylene
PS	Polystyrene
PVC	Polyvinyl chloride
PUR	Polyurethane
REX	Reactive extrusion
REX-PET	Reactive extrusion - polyethylene terephthalate
REX-TPA	Reactive extrusion - terephthalic acid
RSM	Response Surface Methodology
SBR	Sequencing batch reactor
scl-PHA	Short Chain Length - Poly(HydxroxyAlkanoate)
SE-HPLC	Size exclusion-High performance liquid chromatography
SEM	Scanning electron microscopy
SLPM	Standard Liters per Minute
SRT	Sludge retention time
TAG	Triacylglycerols
$\mathbf{T_m}$	Melting temperature
$\mathbf{T_{max}}$	Maximum Degradation Temperature
$\mathbf{T_{5\%}}$	Degradation temperature at 5% weight loss
TGA	Thermogravimetry analysis
TSS	Total suspended solids
TPA	Terephthalic acid
VSS	Volatile suspended solids
WVP	Water vapour permeability
WWTP	Wastewater treatment plant
$\mathbf{X_c}$	Crystallinity index

VARIABLES

ΔHm	Melting enthalpy (J/g)
ε	Elongation at break (%)
E	Young's modulus (MPa)
F/f	Feast and famine ratio
μ_{max}	Maximum specific cell growth rate (h^{-1})
P	Permeability (barrer)
r_{PHA}	Polyhydroxyalkanoate volumetric productivity (g/(L.day))
r_{TAGs}	Triacylglycerols volumetric productivity (g/(L.day))
σ	Tensile strength at break (MPa)
w/w	Weight-per-weight
X	Active biomass (g/L)
$Y_{PHA/TPA}$	PHA yield on TPA basis (g_{PHA}/g_{TPA})
$Y_{TAG/TPA}$	TAG yield on TPA basis (g_{TAG}/g_{TPA})
$Y_{X/TPA}$	growth yield on TPA basis (g_X/g_{TPA})

I.

BACKGROUND AND MOTIVATION

I.1. Background

I.1.1. Plastics: sources, manufacturing and their global impact

Plastics are high molecular weight polymers derived from organic monomers (Jansen, 2016; Van der Vegt, 2002) that are chemically linked through covalent bonds in polymerization reactions, such as addition and condensation, to form long chains of repeating structural units (Cantor & Watts, 2011; Jansen, 2016). These chains constitute the backbone of the polymer structure, resulting in materials with a wide range of properties and applications (Jansen, 2016).

The two primary sources for plastics' manufacturing are either fossil-based or renewable (Kumar et al., 2023). The majority of raw feedstocks used for plastics production come from fossil sources, such as crude oil, natural gas, and coal. However, there is an increasing, though still limited, share from renewable sources, such as sugarcane or biomass (https://www.european-bioplastics.org/, accessed on 10 January 2025; Walker & Rothman, 2020). Depending on their origin, plastics can be grouped as natural, derived from microorganisms and plants, or synthetic, meaning man-made by chemical synthesis (Kumar et al., 2023).

The plastic industry experienced a significant growth during the second half of the19th century, largely driven by the use of fossil-fuels as raw material. This development was a major contributing factor to the rapid expansion of the plastic industry (Tilsted et al., 2023), leading to plastic products becoming an inevitable presence in every aspect of our lives (Kibria et al., 2023). This progress boosted the continuous economic growth of the modern consumer society, resulting in a global plastic production of 2 million tons by 1950 (Geyer, 2020) and, since then, the production increased at an annual rate of 10%, reaching approximately 413.8 million tons in 2023 (https://www.statista.com/, accessed on 28 February 2025), as illustrated in Figure I.1. At the current production rate, it is estimated that plastic production will double during the next 20 years (Lebreton & Andrady, 2019). Despite the slight decrease during 2020 due to the worldwide pandemic (Chang, 2023), production is forecast to hit over 800 million tons by 2050 (Koppala et al., 2024).

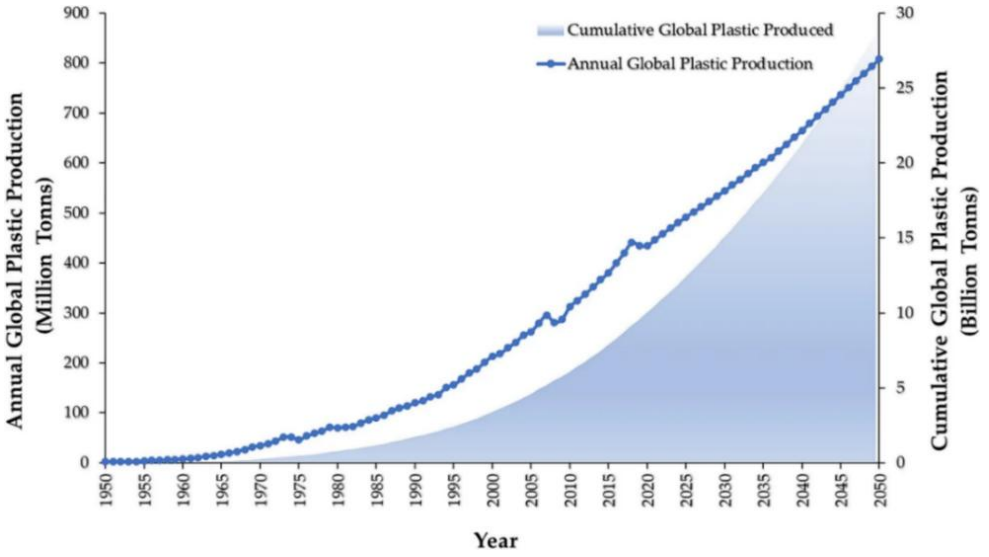

Figure I. 1 - Annual and cumulative global production of plastic (Adapted from Koppala et al., 2024)

Currently, approximately 4% of the world's oil production is used to produce most of the fine and bulk polymers necessary for plastics' manufacturing (Pilapitiya & Ratnayake, 2024). The production process begins with the refining of crude oil through fractional distillation or by removing impurities when natural gas is used as source, yielding key hydrocarbons components such as naphtha and ethane (Marczak, 2022). These became major feedstocks to produce hydrocarbons, for example ethylene, propylene, styrene benzene, toluene and xylenes (Zhou et al., 2021), through chemical steps such as refining, steam cracking and reforming (Ren et al., 2008; Singh et al., 2022). These monomers subsequently undergo polymerization reactions, catalysed by specific agents, to form plastics (Atiwesh et al., 2021).

The most relevant thermoplastics in the market, accounting for 92% of plastics, include polyethylene (PE), polyvinyl chloride (PVC), polypropylene (PP), polyethylene terephthalate (PET), high, low, and linear-low density polyethylene (HDPE, LDPE, and LLDPE), polystyrene (PS) and polyamide (PA) (Chamas et al., 2020; Kibria et al., 2023; Kumar et al., 2023). Upon heating, these materials soften and can be shaped through extrusion, moulding or pressing, and hardened upon cooling at ambient temperature (Kumar et al., 2023). On the other hand, polyurethanes (PUR), epoxies, diallyl phthalates and acrylates are among the examples for thermosetting plastics (Pascault & Williams, 2013). These undergoes an irreversible solidification process when heated or cured, maintaining their rigid structure (Kumar et al., 2023).

Petrochemical-based plastics hold outstanding properties such as toughness, durability, tensile strength, low weight, and plasticity, making them indispensable across all industrial sectors and providing considerable benefits to society (Andrady & Neal, 2009; Geyer, 2020; Shen et al., 2020). Their versatility and distinct features enables their use in a broad spectrum of applications across multiple industries, namely packaging (44%), in building and construction (18%),

automotive design (8%), electronics (7%), household (7%) , agriculture (4%), and others (12%), such as paints, coatings, adhesives and energy production and a countless of other applications including medical sector (Geyer, 2020; Gibb, 2019; Kunwar et al., 2016; https://plasticseurope.org/, accessed on 10 January 2025).

Unfortunately, the essential role plastics play in society, combined with a shift in consumer behaviour toward single-use items led to a worldwide increase in plastic production, which resulted in widespread plastic pollution that impacts ecosystems (Chen et al., 2021). Given the inherent durability of plastics, their elimination from the environment is challenging, with some taking hundreds of years to break down, thus accumulating in waste streams and posing potential risks to human health (Koller & Braunegg, 2018; Walker & Fequet, 2023). The degradation process depends on material properties and environmental factors, such as water, temperature, light, air and abrasion or through the action of microorganisms able to breakdown plastics (Acharjee et al., 2023; Danso et al., 2019).

Recent estimates indicate that 70% of the plastics produced globally became waste, representing 240 million tons (Mt) of plastic waste generated annually (Soong et al., 2022). In the overall faith of plastic (Figure I. 2), only 9% of post-consumer plastics are recycled, while 12% are incinerated and the overwhelming majority (79%) end up in landfills or improperly discarded in the environment, where they slowly degrade and persist for centuries (Geyer et al., 2017; Koller & Braunegg, 2018). Plastics in landfills are problematic not only because they continue to increase due to low recycling rates, do not degrade easily, but also, they occupy large amounts of space and contribute to serious leachate issues, releasing harmful chemicals into the environment and serve as major reservoirs of microplastics from plastic waste degradation (Acharjee et al., 2023; Chamas et al., 2020; Wojnowska-Baryła et al., 2022). Although incineration reduces the waste volume, it requires a substantial amount of energy and releases hazardous organic compounds (e.g. heavy metals, persistent organic compounds and emission of greenhouse gases), which raise environmental and public health concerns (Huang et al., 2022; Wojnowska-Baryła et al., 2022).

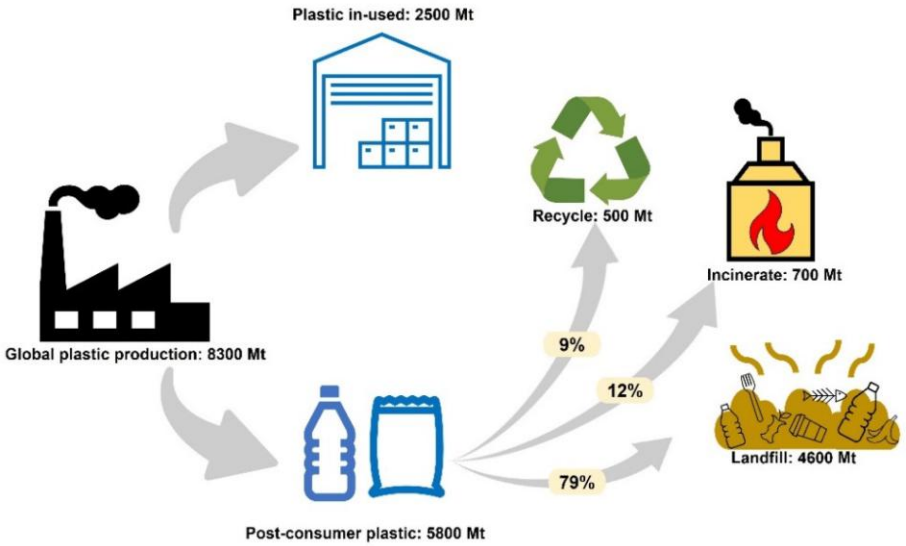

Figure I. 2 - The faith of worldwide plastic (Adpated from Lomwongsopon & Varrone, 2022b).

Increasing recycling rates is seen as the most promising approach to reduce plastic waste in landfills and minimize reliance on petrochemical plastics (Huang et al., 2022). Strategies to manage plastic waste vary considerable across countries, depending on local policies aimed at mitigating plastic pollution. (Kumar et al., 2021). For example, Europe has seen a strong shift toward recycling and energy recovery, with a substantial decrease in landfilling (https://plasticseurope.org/, accessed on 12 September 2024). However, future projections suggest that by 2050, 9,000 Mt of plastic waste will have been recycled, 12,000 Mt incinerated, and 12,000 Mt discarded in landfills or the environment (Geyer et al., 2017). In this context, aiming to address the growing plastic pollution crisis, innovative approaches are needed to manage and permanently eliminate plastic waste, which is one of the main environmental challenges of the 21st century (Geyer et al., 2017; Satti et al., 2024).

I.1.2. Polyethylene Terephthalate

- **PET Synthesis**

PET is one of the most widely used synthetic thermoplastics. First developed in the 1940s (Scheirs & Long, 2005), PET is synthesized by the condensation of two key subunits: terephthalic acid (TPA) and ethylene glycol (EG) linked through ester bonds (Figure I. 3). Alternatively, it can also be produced via the transesterification of dimethyl terephthalate (DMT) and EG terephthalate to yield bis(hydroxyethyl) terephthalate (BHET), followed by polymerisation of BHET into PET (Chamas et al., 2020; Webb et al., 2013).

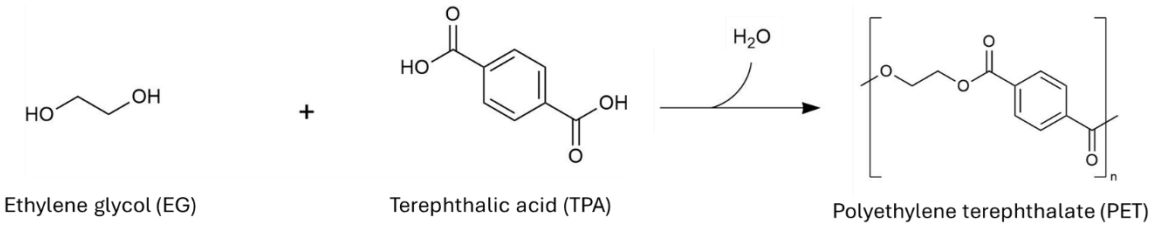

Figure I.3 - Chemical structure of polyethylene terephthalate (PET) and constituent monomers terephthalic acid (TPA) and ethylene glycol (EG) (Adapted from Carr et al., 2020).

Currently, the industrial routes to manufacture TPA consist in the direct chemical oxidation of p-xylene (obtained from the fractional distillation of naphtha) with air in the presence of transition-metal catalyst (Lapa & Martins, 2023), while ethylene is oxidized in the presence of oxygen or air on a silver catalyst, into ethylene oxide, followed by hydration reaction into EG (Cheng et al., 2022).

- **PET market**

PET presents low density, high mechanical strength, toughness, low gas permeability (Andrady & Neal, 2009; Webb et al., 2013), which combined with its simple synthesis, low-priced production, thermostability, and durability, renders it one of the most consumed plastics. Its manufacture accounts for 6.2% of global plastics' production (Thomsen et al., 2023). PET is extensively used in the packaging industry, particularly for soft drink bottles, food jars, and plastics films (Andrady & Neal, 2009; Koshti et al., 2018; Samak et al., 2020), and in the textile industry for producing fibers for clothing (Maurya et al., 2020). The majority of these materials, especially those used in packaging, are designed for single-use purposes. For example, the life cycle for a PET bottle is notably short, often culminating as plastic waste after its use (Ncube et al., 2021).

Between 2010 and 2023, worldwide demand increased from 17 million to 30 million metric tons, with an increasing tendency for the next years (https://www.statista.com/, accessed on 10 December 2024). The packaging material sector predominantly drives the global PET demand, with a significant segment used for single-use items, such as water and carbonated drink bottles (Nisticò, 2020).

- **PET waste management**

PET is highly resistant to physical, chemical and biological degradation (Carr et al., 2020). However, this resilience, combined with its increasing demand, consumption and disposal, has significantly contributed to the accumulation of PET waste in the environment (Raj et al., 2023). Reports indicate that PET accounts for approximately 8% of global solid waste by weight and around 12% by volume (Suhaimi et al., 2022).

A substantial portion of PET waste escapes waste management systems, polluting oceans and ecosystems due to its slow degradation rates. For instance, a single PET bottle can take approximately 450 years to be decomposed (Joo et al., 2018), leading to prolonged environmental presence and accumulation over decades (Sang et al., 2020). Furthermore, exposure to natural weathering conditions causes PET to fragment into smaller particles, generating PET microplastics (Sang et al., 2020). These pose serious environmental and health risks, such as groundwater and drinking water contamination due to migration of antimony from PET coloured bottles into mineral water (Dhaka et al., 2022). Moreover, PET particles and additives (e.g, heavy metals, brominated flame retardants and other types of plasticizers) (Pavlovskyi & Vorobyova, 2025) are reported as endocrine disruptors, further raising concerns about their potential impact on human health (Dhaka et al., 2022; Sang et al., 2020).

To address these issues, several pathways are available for PET waste management, including (1) reuse and four main recycling methods: (2) primary, (3) secondary (mechanical recycling), (4) tertiary (chemical) and (5) quaternary (energy recover) recycling (Barredo et al., 2023):

(1) Reusing PET materials, namely containers or bottles, is a direct and effective first step to reduce the demand for disposable packaging. Reusing these materials 25 to 35 times reduces PET waste and the consumption of disposable PET products by over 70%, thereby significantly lowering the carbon footprint (Soong et al., 2022). However, safety considerations must be addressed, primarily involving the need to thoroughly clean them before use, particularly for food and beverage storage (Soong et al., 2022).

(2) Primary recycling, also known as closed-loop process, involves the reconversion of clean and single-type PET waste through mechanical re-extrusion (Singh et al., 2017). This process is mainly for post-use PET packaging, that has been collected, sorted and reprocessed to produce materials with similar properties and end-use as the original products, for example for PET bottle-to-bottle recycling (Faust et al., 2023; Pinter et al., 2021). It is a simple and cost-effective method mostly used by manufacturers, although being limited to uncontaminated waste and is constrained by the number of reuse cycles (approximately six cycles), often limited due to cumulative thermal polymer degradation that the material can endure (Damayanti & Wu, 2021; Grigore, 2017; Singh et al., 2017).

(3) Secondary, or mechanical, recycling is a well-established and widely used method for processing post-consumer PET waste. This process involves collecting, cleaning and separating the waste from contaminants, followed by mechanical shredding through processes such as extrusion, inject and blow moulding materials (Faust et al., 2023; Singh et al., 2017). The shredded PET is further reduced into smaller particles, such as flakes, enabling larger volumes of PET waste to be recycled in a shorter time. These are then melted and extruded into pellets, which are used in the production of secondary plastic

(Francis, 2016; Joseph et al., 2024). A critical step in this process is washing, which is required to remove contaminants such as dirt, labels, and other plastics. However, this consumes extensive volumes of fresh water and generates large amounts of wastewater, raising environmental concerns (Jabłońska, 2018; Jabłonska et al., 2019).

(4) Tertiary, or chemical, recycling refers to the depolymerization of PET to recover its chemical constituents, such as monomers, dimers, oligomers' mixtures, or resins, which can later be of use for repolymerization into PET, used as refinery feedstocks or fuels, or converted into other value-added materials (Martínez-Narro et al., 2024; Sinha et al., 2010; Thachnatharen et al., 2021). Chemical recycling can occur via pyrolysis, hydrolysis, methanolysis, glycolysis or aminolysis (Damayanti & Wu, 2021). These methods are carried out using temperature, a combination of heat and solvent, and often with the aid of catalysts (Martínez-Narro et al., 2024). The end products vary depending on the chemical processing applied and the reactants used (Webb et al., 2013). While these methods are more effective for processing heterogeneous and contaminated PET waste streams, they are expensive, and energy demand may produce hazardous compounds and waste solvents (Cao et al., 2022; Soni et al., 2021).

(5) Quaternary recovery consists in energy recovery during plastic combustion (incineration) to obtain heat, steam and electricity, exploiting the high calorific value of plastics. However, this process is typically associated with the generation of toxic residues and fumes (Meneses et al., 2022).

Most PET waste is mixed with high volumes of other heterogenous waste streams, such as municipal solid waste containing paper, metals and organic materials. Such mixtures pose additional challenges for the effective recovery of PET (Al-Maaded et al., 2012; Al-Salem et al., 2009). Additionally, many PET-based products are combined with various materials, such as multilayered products or composites with rubber, aluminium and other additives, such as fillers, plasticizers and colourants (Aguado et al., 2014; Eriksen et al., 2018). While these additives are intended to enhance the products' properties, such as barrier to gas, moisture, or light, they make the recycling process much more difficult or impractical (Biermann et al., 2021; Ding & Zhu, 2023). Those materials' heterogeneity hinders mechanical recycling, since their presence deteriorate the quality and properties of recycled PET in each recycling cycle (Francis, 2016).

Chemical recycling offers a promising strategy for handling mixed PET waste streams with high contamination levels, multilayered structures, and limited recyclability, which hindered the effectiveness of mechanical recycling (Martínez-Narro et al., 2024). However, contaminants also pose challenges, particularly in thermochemical recycling, where pyrolysis oils are often contaminated with heteroatoms such as oxygen from organic residues, additives and metals (Kusenberg et al., 2022). Their presence leads to complications such as high viscosities, equipment corrosion

and catalyst deactivation (Martínez-Narro et al., 2024). To mitigate these issues, additional pre-treatments like washing or in-situ additives, are often applied to reduce contaminant levels, thought this increases the overall complexity and cost of the process (Kusenberg et al., 2022).

Currently, only 25% of PET is recycled in Europe, primarily into lower-grade applications (e.g. trays, films), leaving a substantial amount of PET waste unmanaged (Kim et al., 2022; Thomsen et al., 2023). Despite legislative efforts to improve PET recycling, existing limitations continue to hinder efficiency of current strategies. This highlights the urgent need for innovative solutions to enhance the management of post-consumer PET and drive greater circularity in plastic waste management (Lomwongsopon & Varrone, 2022a; Ronkay, 2023).

- **Biological strategies for PET waste management**

Despite the advancements in plastic waste management, additional approaches for PET recycling and valorisation are necessary to enhance and/or complement the existing ones. In this context, biological strategies, such as biodegradation, are gaining more attention as sustainable and eco-friendly alternatives for reducing plastic waste. Certain microorganisms have shown potential for waste plastic degradation, including PET (Lv et al., 2024; Salam et al., 2021). Biodegradation occurs when plastic materials are exposed to abiotic factors (e.g., solar light, abrasion, oxygen, moisture and temperature) and microorganisms capable of colonizing their surface and secrete extracellular enzymes that break down their macromolecular structure into smaller molecules, which are then converted into carbon dioxide, water and methane by mineralization, via aerobic and anaerobic conditions (Salam et al., 2021; Soong et al., 2022). Although this method requires less energy and operates under mild conditions, PET's recalcitrant nature poses challenges for biological degradation and valorisation (Soong et al., 2022; Thachnatharen et al., 2021). One promising alternative is the combination of PET waste chemical depolymerization with microbial conversion of its breakdown products. This integrated process contributes to mitigate the negative impacts of PET waste while enabling the production of new valuable products such as single-cell protein, β-ketoadipic acid and PHA (Lomwongsopon & Varrone, 2022b; Schaerer, Wu, et al., 2023; Werner et al., 2021).

I.1.3. Bioplastics: the eco-friendly alternative

Bioplastics, which are increasingly gaining attention as sustainable alternatives to traditional fossil-based plastics, comprise a diverse group of materials that can be biobased, biodegradable, or both (Figure I. 4) (https://www.european-bioplastics.org/, accessed on 8 October 2024). They can be derived from various renewable resources, such as corn, starch, sugarcane or cellulose, making them biobased. Examples include bio-based PE, PP, or PET, which exhibit properties

comparable to their synthetic ones (Fredi & Dorigato, 2022). On the other hand, biopolymers such as polycaprolactone (PCL) and polybutylene adipate-co-terephthalate (PBAT), though derived from crude oil, are considered bioplastics due to their biodegradability (Goel et al., 2021).

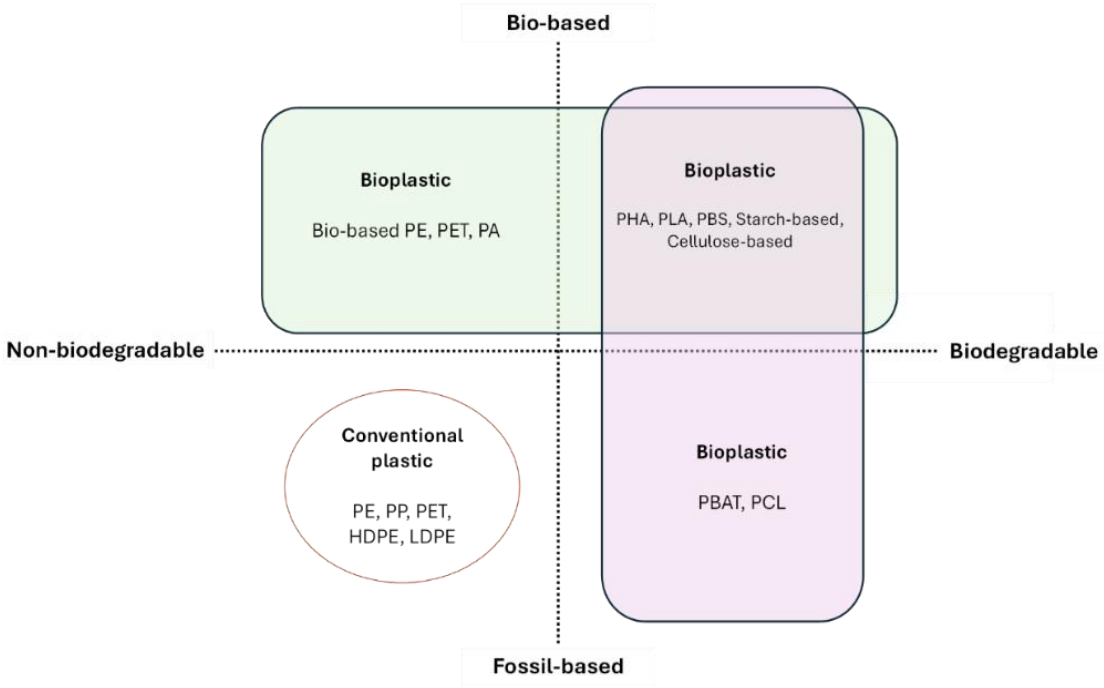

Figure I. 4 - Classification of plastic material and their degradability (adapted from Fredi & Dorigato, 2022).

Biobased and biodegradable plastics present chemical structures that can be decomposed by microorganisms. This category includes bioplastics such as polylactic acid (PLA), poly(butylene succinate) (PBS), PBAT and polyhydroxyalkanoates (PHAs) (Abang et al., 2023). These bioplastics offer a promising and sustainable alternative to fossil-fuel plastics. PHAs, in particular, stand out for their versatility and biodegradability under various environmental conditions, making them a promising solution to combat plastic pollution (Suzuki et al., 2021).

Currently, bioplastics represent less than 1% of the total annual plastic production with the packaging field leading this niche market. However, global bioplastics production capacity is projected to grow 62% by 2028, an estimated 2.43 million tons compared to 2.18 million tons in 2023 (https://www.european-bioplastics.org/, accessed on 20 January 2025; https://plasticseurope.org/, accessed on 30 January 2025).

The high production cost remains one of the main barriers to the broader adoption of PHAs, primarily due to expensive substrates, which account for 30–50% of total costs (Bhola et al., 2021). Additionally, inefficient and environmentally concerning downstream processes further hinder the competitiveness of industrial PHA bioprocesses compared to cheaper fossil-fuel plastics like PP and PE (Bhola et al., 2021; Jaffur et al., 2021). Currently, the market price for PHAs

ranges from 2-5 €/kg, which could be up to six times higher than synthetic plastics (0.8-1.5 €/kg) (Acharjee et al., 2023). However, the PHA market is expected to grow at an annual rate of 12.2% until 2028, supported by the availability of renewable feedstocks and the implementation of favourable green policies (https://www.marketsandmarkets.com/, accessed on 12 January 2025).

- **PHAs: structure, properties and applications**

PHAs are naturally synthesized by several Gram-negative and Gram-positive bacteria, as well as a wide range of archaea and cyanobacteria, as energy and carbon storage material (de Souza et al., 2020; Mezzolla et al., 2018; Muhammadi et al., 2015), being accumulated in the form of granules in the cell cytoplasm, to levels as high as 90% of the cells´ dry weight (Obruca et al., 2017).

The general chemical structure of PHAs (Figure I. 5) consists of linear polyesters composed of R-hydroxyalkanoid acid monomers (Wei & Fang, 2022). PHAs are typically classified based on the number of constituent carbon atoms in their monomer units. Short-chain-length PHAs (scl-PHA) contain monomer units with 3–5 carbon atoms, with the most common monomers in this category being 3-hydroxybutyrate (3HB) and 3-hydroxyvalerate (3HV). Medium-chain-length PHAs (mcl-PHA) include monomer units of 6–14 carbon atoms, such as 3-hydroxyhexanoate (3-HHx) and 3-hydroxyoctanoate (3HO). Lastly, long-chain-length PHA (lcl-PHA), which feature monomer units with more than 14 carbon atoms, an example being the case of 3-hydroxytetradecanoate (3HTd) (Muhammadi et al., 2015; Samrot et al., 2021; Tan et al., 2014).

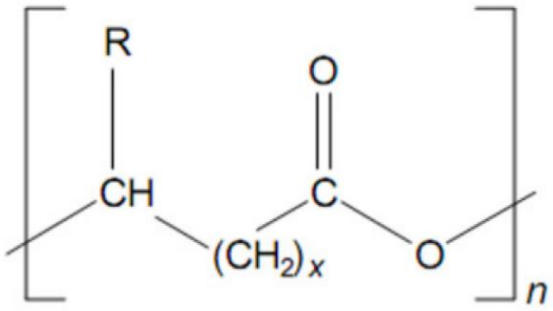

Figure I. 5- General chemical structure of PHA molecules, where x is the number of carbon atoms in the linear structure of the polymer, R is the side chain and n indicate the number of repetitive monomer units that vary between 100-30000 (Adapted from Miu et al., 2022)

PHAs are insoluble in water and biocompatible to living organisms, which contribute to their stability in various applications (Verlinden et al., 2007). They have a high degree of polymerization and possess distinct characteristics, such as optical activity, piezoelectric properties, and an isotactic structure due to the stereospecific enzymes involved in their biosynthesis (Reddy et al., 2003). These characteristics impart unique and functional properties, including the ability to form

films with good barrier performance against oxygen and low water vapour permeability, as well as a good resistance to UV light. However, they have poor resistance towards acids and bases (Bugnicourt et al., 2014). In addition, PHAs are biodegradable in various environmental conditions and exhibit thermoplastic properties similar to petrochemical plastics (LDPE and PP) making them highly attractive for diverse market applications (Bugnicourt et al., 2014; Diankristanti et al., 2024; Keskin et al., 2017; Zhang et al., 2024).

Depending on their monomeric units, PHAs' physical and chemical properties are highly diverse. This variety impacts melting and glass transition temperature, degree of crystallinity, and mechanical behaviour, which can range from hard and crystalline to elastic and flexible materials (Anjum et al., 2016; Keshavarz & Roy, 2010). In general, scl-PHAs are characterized by high melting (~179 ºC) and decomposition temperatures (between 200 and 300 ºC), high crystallinity (60 - 80%), and relative brittleness and stiffness, with poly(3-hydroxybutyrate) (PHB) being the main example (Mai et al., 2024). The incorporation of other monomers has been studied to improve PHB features resulting in a more flexible and less crystalline polymer with tunned mechanical properties. Among the copolymers formed are poly(3-hydroxybutyrate-co-3-hydroxyvalerate) (PHBV), poly(3-hydroxybutyrate-co-4-hydroxybutyrate) (P3HB4HB), poly(3-hydroxybutyrate-co-3-hydroxypropionate) (PHBP), poly(3-hydroxybutyrate-co-3-hydroxyoctanoate) (PHBO), poly(3-hydroxybutyrate-co-3-hydroxyhexanoate) (PHBHHx) (Mai et al., 2024). On the other hand, mcl-PHAs are distinguished with lower crystallinity (below 40%), as well as lower melting (between 40 and 60 ºC) and glass transition (between -50 and -25 ºC) temperatures, with elastomeric behaviour, and present low tensile strength (lower than 10 mPa) and high elongation to break (~300%) (Khanna & Srivastava, 2005; Reddy et al., 2022; Silva et al., 2021).

PHAs are versatile biopolymers with applications spanning multiple industries (Figure I. 6). In packaging, they are used for flexible and rigid materials, single-use containers, and durable products (https://www.european-bioplastics.org/, accessed on 20 January 2025; Philip et al., 2007). They have also been explored in agriculture for mulch films and coatings, and as encapsulating agents for seeds and fertilizers to enable slow release (Pandey et al., 2022; Yogesh et al., 2012). Their biocompatibility and tailored properties make them suitable for biomedical applications, including drug delivery systems, tissue engineering, implants and wound dressings (Diniz et al., 2023; Kalia et al., 2023). Additionally, PHAs are promising materials in other areas, namely plasticizers, fibbers, adhesives, and biofuels (Pandey et al., 2022; Reddy et al., 2022).

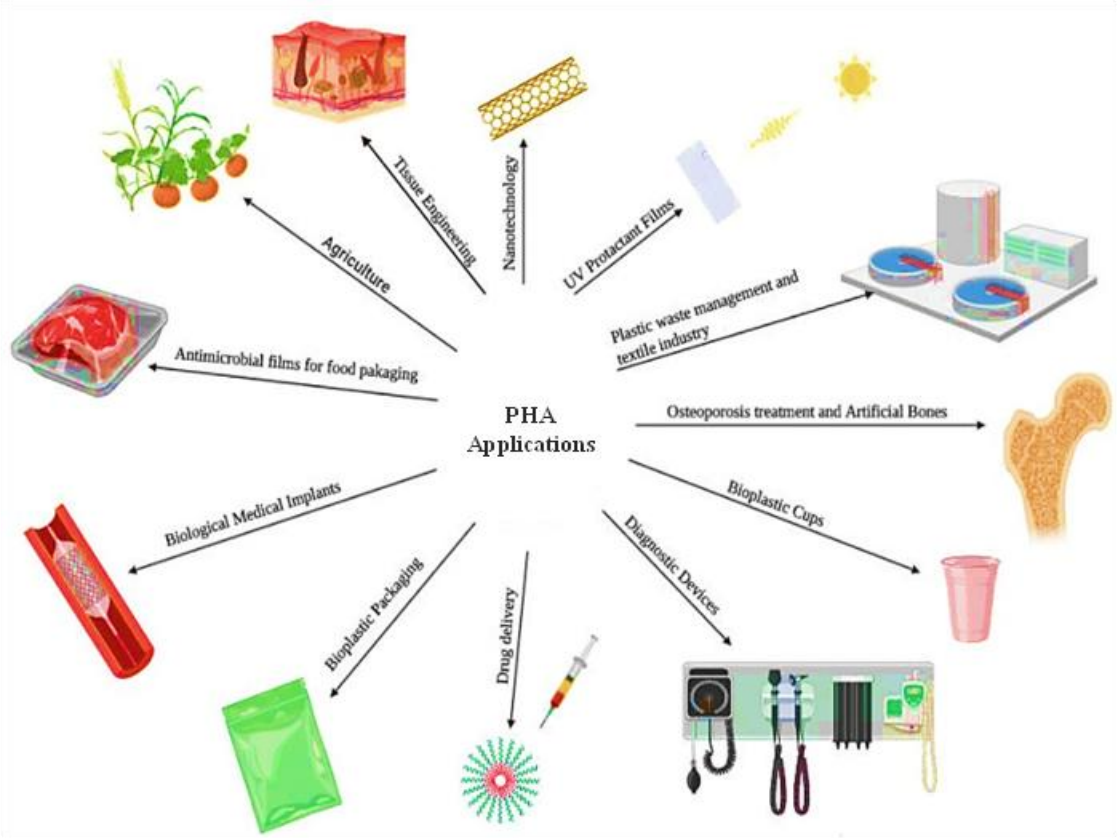

Figure I. 6 - Various applications for PHAs (Adapted from Muneer et al., 2020).

- **PHA production**

PHA production was first investigated in 1926, by Maurice Lemoigne, who observed the accumulation of PHB by *Bacillus megaterium* (Lemoigne, 1926). Since then, over 90 microbial genera and 150 hydroxyalkanoate monomers have been identified (Raza et al., 2018; Shah & Kumar, 2020). These microbial systems include single cultures (Kacanski et al., 2023; Kiselev et al., 2022; Wendy et al., 2022), co-cultures (Khan et al., 2022; Rebocho et al., 2020; Saratale et al., 2022) and mixed microbial cultures (MMC) (Cruz et al., 2022; Fradinho et al., 2016; Ntaikou et al., 2014), presenting different strategies for optimizing production efficiency and cost-effectiveness (Colombo et al., 2017). PHA synthesis is generally promoted under metabolic stress, triggered by nutrient-limiting conditions (e.g., nitrogen, phosphorus, oxygen, or magnesium) combined with excess carbon sources for the different microbial sources (Silva et al., 2021).

The use of single cultures has been widely studied, including wild type bacteria, such as *Cupriavidus necator* (Nguyenhuynh et al., 2021), *Alcaligenes latus* (Silva et al., 2021), and *Haloferax mediterranei* (Khatami et al., 2021), as well as several recombinant microorganisms like *Escherichia coli*(Chen et al., 2018) and *Pseudomonas putida* (Hur et al., 2024). Additionally, cyanobacteria (Bhati & Mallick, 2015) and fungi (Thu et al., 2023), have demonstrated the ability to produce PHAs, though their application remains less developed.

While using single cultures, the microbial sources play a crucial role in determining the type of PHA synthesized (Rai et al., 2011). For example, *C. necator* mostly synthesizes PHB, while *H. mediterraneai* produces the co-polymer PHBV (Tan et al., 2014). Mcl-PHAs are typically produced by *Pseudomonas* species, such as *P. chlororaphis* (Pereira et al., 2021), *P. resinovorans* (Cruz et al., 2016) and *P. citronellolis* (Rebocho et al., 2019). Additionally, recombinant strains have enabled the production of copolyesters, such as poly(3-hydroxybutyrate-co-3-hydroxyvalerate-co-3-hydroxyhexanoate) (PHBHVHHx) by *C. necator* Re2133/pCB81 (Bhubalan et al., 2010), (PHBHHx) and poly(3-hydroxyhexanoate-co-3-hydroxydecanoate) P(3HHx-co-3HD) by *P. putida* KTQQ20 (Tripathi et al., 2012) and a scl-lcl-PHA was obtained from *P. aeruginosa* MTCC 7925 (Singh & Mallick, 2009).

For single cultures, the production process generally involves a biomass growth phase followed by an accumulation phase under nutritional stress redirecting excess carbon flux towards PHA synthesis (Koller & Braunegg, 2015). Some exceptions exists, as the cases of *Alcaligenes latus* and *Paracoccus denitrificans* which accumulate PHA during their growth phase without requiring growth-limiting conditions (Kourmentza et al., 2017; Kumar et al., 2020). These processes are carried out in bioreactors under controlled conditions (e.g., pH, dissolved oxygen, temperature), usually employing either batch or fed-batch cultivation strategies (Koller, 2018). In general, batch cultivations are simpler to operate and widely used for studying novel substrates or optimizing conditions (Kaur & Roy, 2015). However, it is limited by initial carbon and nitrogen concentrations, often leading to lower cell density and productivity (Koller, 2018). Fed-batch, is the most commonly used, allowing for scalability and higher efficiency by controlling nutrient feed in pulses or continuously to avoid substrate depletion, achieving higher cell densities and polymer accumulation (Kaur & Roy, 2015).

PHAs can also be produced by MMC under cultivation conditions designed to promote the enrichment of PHA-storing microorganisms based on natural selection and competition (Koller et al., 2017). In these systems, microbial consortia adapt to fluctuating nutrient availability, of the substrate or by varying the availability of an electron acceptor (Montiel-Jarillo et al., 2017; Salehizadeh & Van Loosdrecht, 2004). Microorganisms capable of rapidly storing the available carbon source and, during carbon scarcity, utilizing the accumulated polymer for biomass growth, gain a competitive advantage over those that lack this ability (Kourmentza et al., 2017). Within the transient conditions that influence polymer yield and cell concentration are carbon source concentration and type, nutrient availability, temperature, pH and sludge retention time (SRT), all crucial for optimizing culture selection (Dias et al., 2006).

Most of the MMC-based processes are carried out using sequencing batch reactors (SBR), operated with cycles of feeding, reaction, settling and withdrawal. These facilitate the enrichment in PHA-producers through dynamic feeding strategies that enhance PHA (Dias et al., 2006). SBRs are highly effective for culture selection due to their easy of control and process manipulation

during operation (Valentino et al., 2017). Normally, they are followed by subsequent PHA accumulation stage performed under pulse-wise or continuous feeding strategies (Chen et al., 2015).

Both single and mixed microbial cultures are widely used for PHA synthesis, each with distinct advantages and limitations. Single cultures are known for achieving higher PHA accumulation (80-90% of cell dry weight) and reaching high cell densities (100 and 200 g/L) (Chen, 2009). They also attain volumetric productivities around 5 g_{PHA}/(L h), offering a significant advantage in developing a cost-effective process (Chen, 2009). Additionally, these systems are more consistent and controllable, enabling reproducible production (Wongsirichot et al., 2024) and supporting broader variety of PHA types. This includes homopolymers like PHB (de Mello et al., 2023), mcl-PHA incorporating monomers such as 3HO, 3-hydroxydecanoate (3HD), 3- hydroxydodecanoate (3HDd)) (Hahn et al., 2024), as well as copolymers such as PHBHHx and PHBV (Koller et al., 2017). However, single cultures are costly to maintain (Wongsirichot et al., 2024), as they require sterile conditions to avoid contamination, significantly increasing production costs (Zhang et al., 2024).

Currently, studies optimizing PHA production with MMC have achieved biomass concentrations of up to 10 g/L (Kourmentza et al., 2017), with PHA accumulation ranging from 45 to 70% of the biomass content (Lorini et al., 2020; Valentino et al., 2014) and productivities between 1.25-6.09 g_{PHA}/L.day (Oliveira et al., 2017; Valentino et al., 2014), depending on the selection parameters applied.

Research on MMC has primarily focused on the production of scl-PHA, namely PHB and the co-polymer PHBV, with 3HV ratios varying from 8 to 72 % (Wei & Fang, 2022). The monomer composition of PHA can be tailored by supplying specific precursors and leveraging the diverse metabolic pathways of different microorganisms (Carvalheira et al., 2022; Laycock et al., 2014). Additionally, MMC have been reported to synthesize scl-mcl-PHAs copolymers, with diverse monomeric compositions, including PHBHHx (Chen, 2009) and PHBHVHHx (Silva et al., 2022). Some copolymers exhibited an even broader monomeric composition, incorporating PHB, and monomers such as 3HO, 3HD and 3HDd (Tamang & Nogueira, 2021).

MMC are capable of robust integration into wastewater and biological treatment processes (Morgan-Sagastume, 2016). They exhibited versatility and flexibility to rapid changing conditions and substrate tolerance, while operating efficiently under non-sterile conditions (Bosco et al., 2021). However, their use in industrial production is still dependent by the effectiveness of the selection of PHA-accumulating bacteria, as poor selection can negatively impact production (Mannina et al., 2020). The inherent variability of MMC may introduce irreversible changes to microbial community, affecting both the process stability and PHA consistency, including its composition, molecular mass distribution and properties (Laycock et al., 2014; Mannina et al., 2020). To enhance MMC's global productivity, achieving high and stable PHA storage ability, as

well as high cell densities is crucial to improve PHA yields and making MMC-based PHA production more competitive (Reis et al., 2011; Serafim et al., 2008).

As a more sustainable and cost-effective approach to PHA production, there is an increasing interest in using low-cost feedstocks, including industrial byproducts, waste fats and oils (Argiz et al., 2021; Ingram et al., 2022), lignocellulosic raw materials (de Souza et al., 2020), agricultural and domestic waste (Amir et al., 2024; Zhou et al., 2023), and wastewater (Argiz et al., 2020). However, these substrates often require the need for pretreatment due to their complexity (e.g., lignocellulosic biomass), and the presence of contaminants resulting from this that hinder microbial growth, metabolism and overall production yield (George et al., 2021; Li et al., 2016; Li & Wilkins, 2020; Wang et al., 2023). Both microbial systems have demonstrated the ability to utilize cost-effective renewable carbon sources, significantly lowering PHA production expenses (Laycock et al., 2014; Sabapathy et al., 2020).

I.1.4. PET upcycling into value-added products: closing the loop cycle

Despite the non-biodegradable nature of PET, several enzymes and microorganisms have been reported for the breakdown of PET into its oligomers (BHET and MHET) and/or monomers (TPA, EG, and DMT) (Ru et al., 2020; Taniguchi et al., 2019; Yoshida et al., 2016). These microorganisms have been mostly isolated from natural environments, such as plastic contaminated water and soils, plastic landfills, and hydrocarbon polluted sites (Ali et al., 2021; Ru et al., 2020), namely from the genera *Pseudomonas*, *Bacillus, Comamonas* and, most recently, the bacterium *Ideonella sakaiensis* (Maheswaran et al., 2023; Ru et al., 2020).

Moreover, the discovery of PET-degrading enzymes, such as PETase and MHETase, expressed by bacteria (e.g., *Thermobifida fusca*, *Ideonella sakaiensis*) and fungi (e.g., *Fusarium solani, Thermomyces insolens*) (Herrera et al., 2023; Salvador et al., 2019; Yoshida et al., 2016) offer a promising solution for degrading PET. Mixed microbial consortium (composed of bacteria, protozoa and yeast) isolated from sediments near a PET recycling plant demonstrated potential for complete PET degradation or monomer recycling (Taniguchi et al., 2019).

Despite the ongoing development of engineered enzymes, the current biological processes still face efficiency challenges in PET waste management (Maurya et al., 2020). Microbial PET biodegradation is still limited due to factors like PET's crystallinity and impurities in waste streams which affect considerably the efficiency of microorganisms and their enzymes (PETase and MHETase) (Soong et al., 2022). To overcome these limitations and improve efficiency in degradation, chemical methods for depolymerization of PET waste into TPA and EG have been investigated, that when combined with microorganisms able to metabolize them into valuable products, offer a more robust approach for PET upcycling (Lomwongsopon & Varrone, 2022b; Mudondo et al., 2023). Microorganisms from different genera, namely C*omamonas sp.* E6 (Sasoh et al.,

2006), *R. jostii RHA*1 (Hara et al., 2007) and *P. putida* JM37 (Mückschel et al., 2012) have been identified for their capacity to metabolize PET degradation products like TPA and EG, as carbon and energy sources (Gao et al., 2022). Under aerobic conditions, TPA is transported into microbial cells via specific TPA transporters, and subsequently converted into protocatechuate (PCA), a key metabolic intermediate for central metabolism (Fig. I. 7) (Gao et al., 2022). This conversion is facilitated through Tph dioxygenases, with Tph genes that have been identified across microorganisms from the *Comamonas*, *Ideonella*, *Pseudomonas*, *Ramlibacter*, *Delftia* and *Rhodococcus* genera (Dissanayake & Jayakody, 2021; Satta et al., 2024). PCA then enters either the β-carboxymuconate or the catechol pathway, before reaching central metabolism (Gao et al., 2022). Meanwhile, EG is metabolized into glycolate and subsequently converted into glyoxylate, a crucial intermediate that is further processed in the tricarboxylic acid (TCA) cycle for degradation (Fig. I. 7) (Gao et al., 2022). So far, the EG metabolic pathway in *Pseudomonas putida* KT2440 has been mapped using omics-based systems biology, providing insights into its degradation mechanisms (Dissanayake & Jayakody, 2021).

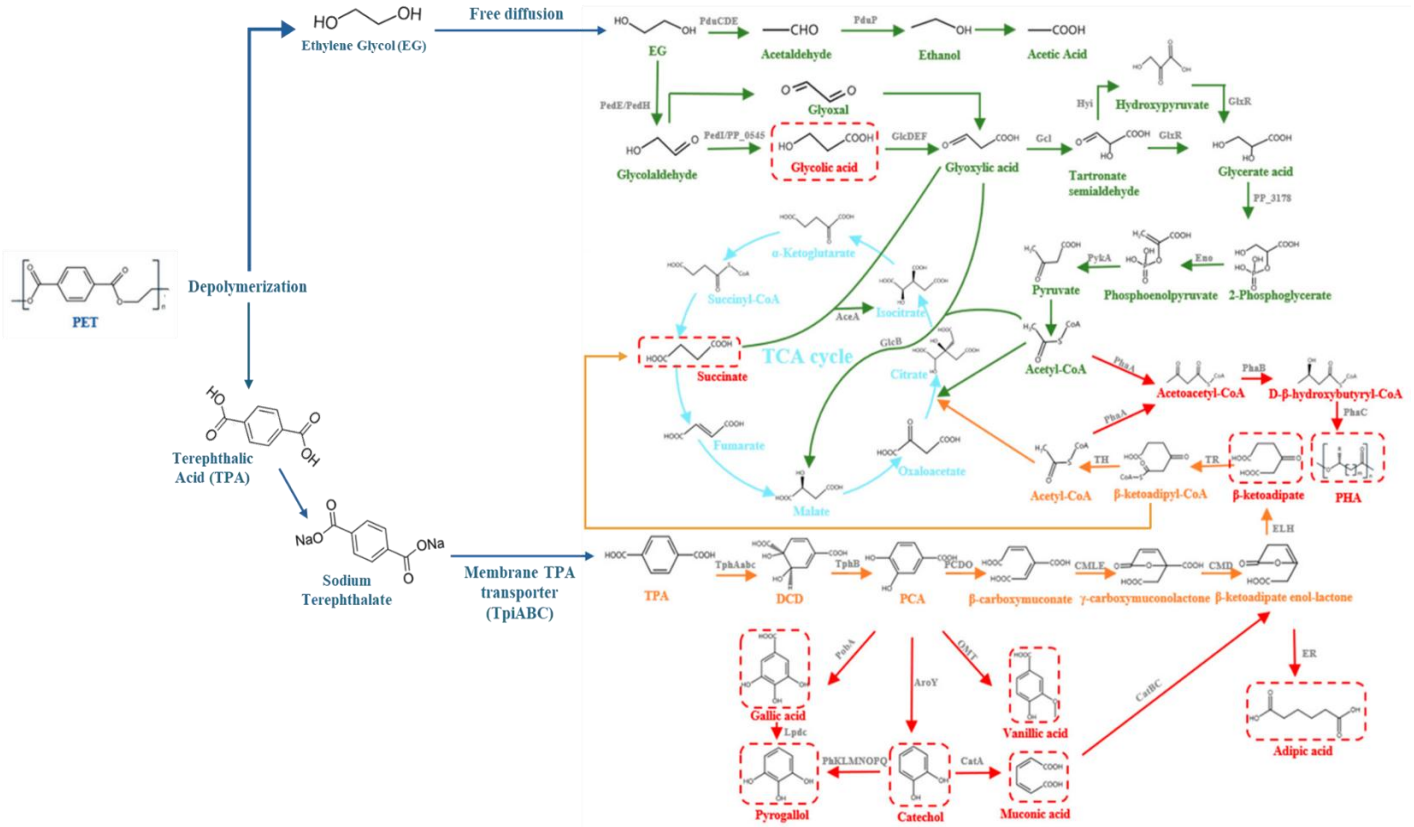

Figure I. 7 - Overview of PET depolymerization products (blue line), metabolic pathways for TPA (orange line), EG (green line), TCA cycle (light blue line) and conversion of high value compounds synthesis (red line). (Adapted from Qi et al., 2022)

These metabolic pathways show the possibility for TPA and EG bioconversion into high-value compounds, presenting the opportunity for biological recycling PET waste.

Interestingly, several studies report the production of high-value compounds resulting from feeding microorganisms with PET degradation products, namely TPA and/or EG. Examples of value-added compounds are depicted in Table I. 1, which include PHA (Kenny et al., 2012a), hydroxyalkanoyloxy-alkanoates (HAAs) (Tiso et al., 2021), bacterial cellulose (Esmail et al., 2022) and muconic acid, vanillic acid , gallic acid , pyrogallol (Kim et al., 2019).

Table I 1. High-value products obtained from PET degrading products upcycling: microbial sources, depolymerization strategies and substrates.

High-value product	Microbial source	Depolymerization strategy	Substrate	Reference
mcl-PHA	*Pseudomonas putida* GO16, GO19 and GO23	Hydrolytic pyrolysis	Mixture of TPA, oligomers, benzoic acid, and others.	Kenny et al., 2008, 2012a
	Pseudomonas umsongensis GO16 KS3	Enzymatic degradation	Hydrolysed TPA and EG	Tiso et al., 2021
	Pseudomonas putida MFL185	-	EG	Franden et al., 2018
	E. coli BL21 (DE3) *Pseudomonas putida KT2440-ΔRDt-ΔZP46C-M*	Enzymatic hydrolysis	TPA and EG	Liu et al., 2023
PHB	*Ideonella sakaiensis* 201-F6	Biological degradation	PET yielding a mixture of MHET, BHET, TPA and EG	Fujiwara et al., 2021
	Yarrowia lipolytica Po1f *(PETase)* *Pseudomonas stutzeri* TPA3P	Enzymatic hydrolysis	TPA and EG	Liu et al., 2021
Hydroxyalkanoyloxy-alka-noate (HAA)	*Pseudomonas umsongensis* GO16 KS3	Enzymatic degradation	Hydrolysed TPA and EG	Tiso et al., 2021
Glycolic acid (GLA)	*Gluconobacter oxydans* KCCM 40109	Microwave radiation	EG	Kim et al., 2019
	Pichia naganishii AKU 4267	-	EG	Kataoka et al., 2001
	Rhodotorula sp. 3Pr-126			
Vanillin	*E. coli* RARE_pVanX	Enzymatic hydrolysis	PET hydrolysate yielding TPA	Sadler & Wallace, 2021

Table I 1. High-value products obtained from PET degrading products upcycling: microbial sources, depolymerization strategies and substrates (cont.).

High-value product	Microbial source	Depolymerization strategy	Substrate	Reference
Bacterial Cellulose	*Komagataeibacter xylinus* DSM2004 and DSM 46604	-	TPA and EG	Esmail et al., 2022
Acetate and Ethanol	*Acetobacterium woodii*	-	EG	Trifunović et al., 2016
Gallic acid	*E. coli* strain PCA-1 and HBH-2	Microwave radiation	TPA	Kim et al., 2019
Pyrogallol	*E. coli* strain PG-1a			
Muconic Acid (MA	*E. coli strain CTL-1* and *MA-1*			
Vanillic acid	*E. coli strain PCA-1* and *OMT-2^{His}*			
Protocatechuic acid (PCA)	*E. coli PCA-1*	Chemocatalytic glycolysis and enzymatic hydrolysis	TPA	Kim et al., 2019
Catechol	*Bacillus subtilis* esterase (Bs2Est) and engineered *E. coli* expressing pKE112TphBaroY and pKM212TphAabc	Chemocatalytic glycolysis and enzymatic hydrolysis	Mixture of BHET, MHET, and PET oligomers	Kim et al., 2021
β-ketoadipate (βKA)	*Pseudomonas putida* KT2440	Chemocatalytical glycolysis	BHET	Werner et al., 2021
Lycopene	*Rhodococcus jostii* RPET	Alkaline Hydrolysis	TPA and EG	Diao et al., 2023

I.2. Motivation and objectives

The persistent accumulation of plastic waste, particularly PET, has significantly contributed to the continuous pollution of oceans and other natural ecosystems due to their inherent resistance to degradation. Current strategies for managing PET waste streams are insufficient to address this growing problem. Moreover, the need for sustainable alternatives to conventional synthetic plastics, which rely on fossil resources, has driven the search for more environmentally friendly plastics.

PHAs represent an alternative to petrochemical-based plastics because they are biodegradable, biocompatible, and can be produced from renewable sources. Their chemical, thermal and mechanical properties render them suitable for replacing many conventional petrochemical-based plastics in several applications, thus minimizing their adverse impact in the environment (Kumar et al., 2020). However, despite these advantages, the high production cost of PHAs limit their widespread commercial use. Nonetheless, global PHA production is expected to increase in the coming years (Naser et al., 2021).

A promising solution to both reducing PET waste and to obtain a feasible feedstock for bioplastics production is through the depolymerization of PET waste into its constituent monomers, such as TPA, which can then serve as carbon source for microorganisms to convert into PHA. This strategy enables the upcycling of PET degradation products into valuable biopolymers, integrating PET waste management strategy with sustainable bioplastic production. This approach will help reducing the environmental impact of plastic waste, tackling PET waste streams, while providing a sustainable alternative to non-biodegradable fossil-based plastics, aligning with EU bio-based policies and advancing the circular economy.

This thesis aims to tackle the challenge of heterogeneous PET waste contamination by developing and optimizing bioprocesses that use microbial systems capable to efficiently convert PET monomers (specifically TPA) into PHAs. Therefore, the research began with the characterization of depolymerized post-consumer PET (pcPET) material, which was assessed prior to its use as the sole carbon source in microbial cultivations. Subsequently, investigation was carried out for different microbial systems, including both single and MMC cultures, which were evaluated for their ability to produce PHA using the processed depolymerized pcPET waste as feedstock. The objective was to obtain effective microbial systems for PHA production for the upcycling of depolymerized pcPET waste. Additionally, the biopolymers produced during the cultivations, as well as other value-added products, were recovered and characterized. Furthermore, PHA films were developed, envisaging their potential future applications.

I.3. Thesis outline

The work developed during this PhD project is presented in 4 chapters. The first chapter presents a brief outline of the state-of-the-art, while the second and third chapters describe the experimental work performed and the results obtained during this PhD project, with each chapter comprising an introduction, the materials and methods section, the discussion of the results and the main conclusions. Finally, the last chapter presents the general conclusions of this thesis and suggestions for future work.

A summary of the content of each chapter is described below:

Chapter I – Background and Motivation – introduces a state-of-the-art overview on plastic waste general problematic, emphasizing on PET waste. It approaches the current management strategies to deal with this problem, its limitations and the efforts being put into PET recycling to complement the methods established, focusing on recent biological approaches. Additionally, this chapter also provides some insights on the motivation of this PhD thesis.

Chapter II – Microbial upcycling of post-consumer PET waste: Single cultures systems – describes the investigation of two novel bacterial isolates for their ability to use depolymerized pcPET waste sample for cellular growth and production of value-added compounds. Additionally, from this screening, a bacterial strain was selected for bioreactor process development, in which the selected strain was able produce PHA, as well as accumulating triacylglycerols (TAGs) as an intracellular storage compound. The bioproducts composition was characterized.

Chapter III – Post-consumer PET waste upcycling into bioplastics: unlocking the power of a natural microbiome – describes the development of a PHA production process using a MMC, selected from a natural microbiome, using depolymerized pcPET waste as sole feedstock. Culture selection was performed by the feast and famine regime. Additionally, the produced PHA was characterized regarding its physical and thermal properties, followed by the preparation of films which were evaluated for their mechanical and barrier properties.

Chapter IV – Conclusions and future work – reviews the main outputs of this work and proposes suggestions for future research.

II.

MICROBIAL UPCYCLING OF DEPOLYMERIZED POST-CONSUMER PET WASTE: SINGLE CULTURES SYSTEMS

The results presented in this chapter, namely those of section II.3.3., were published in the paper:

Rebocho, A. T., Torres, C.A.V., Konnickx, H., Stragier, L., Attallah, O. A., Mojicevic, M., Tas, C. E., Fournet, M.B., Reis, M.A., & Freitas, F. (2025). Upcycling depolymerized PET waste into polyhydroxyalkanoates and triacylglycerols by a newly isolated *Rhodococcus* sp. strain. *Biotechnology for the Environment*, *2*(5). https://doi.org/10.1186/s44314-025-00019-4

The depolymerized pcPET used in this study was kindly provided by the Materials Research Institute of the Technological University of the Shannon Midlands Midwest (TUS) (Ireland), in the scope of the PanEuropean project BioICEP (https://www.bioicep.eu/). The bacterial strains used in this study were kindly provided by Avecom NV (Belgium), under a material transfer agreement (MTA) agreement, in the scope of the PanEuropean Project BioICEP.

This page was intentionally left blank

Summary

Depolymerized pcPET waste (REX-PET) obtained through the reactive extrusion of a mixture of PET waste materials, was used for the cultivation of two bacterial isolates, *Delftia* sp. Ave5 and *Rhodococcus* sp. Ave7, for evaluating their ability to grow and produce PHA. Using TPA from REX-PET as the sole carbon source, optimal concentrations of TPA and ammonium were determined for each strain, towards maximum cell growth and PHA accumulation, by response surface methodology (RSM). *Delftia* sp. Ave5 and *Rhodococcus* sp. Ave7 showed the best results for high concentrations of TPA (10.00-11.66 g/L) and ammonium (0.17-0.50 g/L). These isolates achieved significant cell growth, with *Delftia* sp. Ave5 reaching 2.12 g/L, and *Rhodococcus* sp. Ave7 reaching 5.09 g/L. Additionally, they accumulated PHA, with *Delftia* sp. Ave5 accumulating 7.9wt.% and *Rhodococcus* sp. Ave7 accumulating 22.5wt.%. Interestingly, *Rhodococcus* sp. Ave7 also accumulated 19.2wt.% TAGs when grown on 10 g/L REX-TPA and 0.17 g/L ammonium. Given these findings, *Rhodococcus* sp. Ave7 was selected as the most promising strain for developing and optimizing the production of PHA and TAG in bioreactor cultivation assays. Aiming to improve both bioproducts' production, different reactor strategies were conducted. In batch mode, with initial concentrations of 12 g/L TPA and 0.3 g/L ammonium, the culture reached 2.67 ± 0.06 g/L of biomass with a 13.45 ± 0.69wt.% TAG content and 4.22 ± 0.03wt.% of PHA. Under fed-batch mode, with a 20 g/L TPA pulse feeding, the TAG content increased to 16.26 ± 0.12wt.% with only 3.05 ± 0.05wt.% of PHA, while continuous feeding with a 20 g/L REX-TPA solution resulted in higher a biomass production of 3.85 ± 0.09 g/L, with improved PHA and TAG contents of 15.01 ± 0.68wt% and 15.40 ± 0.29wt.%, respectively. The produced PHA was mainly composed of 3HV monomers (>90wt.%), while the TAGs presented a fatty acids profile rich in octadecenoic acid ($C_{18:1}$; 52wt.%), hexadecanoic acid ($C_{16:0}$; 32wt.%) and octadecanoic acid ($C_{18:0}$; 12wt.%). Overall, *Rhodococcus* sp. Ave7 demonstrated a high capacity for TPA removal (30.46 ± 0.25 g), converting it into cell biomass (0.24 ± 0.04 g_X/g_{TPA}), PHA (0.051 ± 0.003 g_{PHA}/g_{TPA}) and TAGs (0.052 ± 0.000 g_{TAG}/g_{TPA}), thus rendering this bioprocess a promising solution to help reducing the PET waste burden, in a circular and sustainable approach, by converting it into value-added bioproducts, including a bioplastic.

Keywords

Plastic upcycling; Biodegradation; *Rhodococcus*; Polyethylene terephthalate; Polyhydroxyalkanoates; Poly(3-hydroxybutyrate-co-3-hydroxyvalerate); Triacylglycerols

II.1. Introduction

The bioconversion of PET waste degradation products (e.g. TPA and EG) into high value products is an emerging approach to recycle PET waste, by using the monomers resulting from the depolymerization of PET as carbon source for microbial growth (Qi et al., 2022). TPA and EG are obtained from the depolymerization of PET and there are a few studies reporting attempts to transform them into valuable compounds, including, among other bioproducts, PHAs. For example, TPA derived from the pyrolysis of PET has been successfully used by bacterial strains, namely *Pseudomonas umsongensis* GO16 KS3, *P. putida* GO19, and *P. frederiksbergensis* GO23, for the accumulation of an mcl-PHA up to 23–27% of cell dry weight (CDW) (Kenny et al., 2008). The cultivation conditions were later optimized to improve polymer production by co-feeding TPA with waste glycerol (Kenny et al., 2012a). Several microorganisms, such as *Rhodococcus eryhthropolis* MTCC3951 and *R. pyridinivorans* P23, have been isolated based on their TPA degradation capacity and ability to produce PHA (Guo & Shao, 2020; Maurya et al., 2023). Additionally, the combination of PET enzymatic hydrolysis followed by TPA and EG bioconversion has also been tested. *Ideonella sakaiensis* 201-F6 and *P. umsongensis* GO16 KS3 produced PHB (48.5% of CDW) and mcl-PHA (7% of CDW), respectively, while *P. umsongensis* GO16 KS3 was also able to synthesize HAA from TPA (Fujiwara et al., 2021; Tiso et al., 2021).

The bioconversion of PET into PHA was also obtained when recurring to engineered microorganisms. Researchers have successfully engineered the fungi *Yarrowia lipolytica* Po1f *(PETase)* and the bacterium *Escherichia. coli* BL21 (DE3) to hydrolyse PET into TPA and EG, which were subsequently used to obtain PHB and mcl-PHA by *P. stutzeri* TPA3P and *P. putida KT2440,* respectively (Liu et al., 2021, 2023).

Delftia and *Rhodococcus* genera are widely distributed in different ecosystems, such as soil (Gilan et al., 2004; Wedulo et al., 2014), marine habitats (Guo et al., 2023), wastewater (Shigematsu et al., 2003) and municipal waste (Kumar et al., 2020), and have been reported for their ability to degrade a variety of recalcitrant compounds, including crude oil (Lenchi et al., 2020), HDPE, LDPE, PE (Fontanella et al., 2010; Peixoto et al., 2017) and PET (Guo et al., 2023). For example, *Delftia tsuruhatensis* $T7^T$ and *Delftia* sp.WL-3 were isolated for their terephthalate-assimilating ability and reported to degrade PET from activated sludge, respectively (Liu et al., 2018; Shigematsu et al., 2003). Similarly, *R.* jostii RHA1 and *Rhodococcus* sp. SSM1 were reported to degrade TPA (Hara et al., 2007; Kumar et al., 2020), whilst *Rhodococcus* sp. DK17 and *R. erythropolis* PR4 are able to degrade aromatic and alicyclic rings, and alkanes, respectively(Kim et al., 2018).

Moreover, many of these microorganisms can produce valuable compounds. For instance, *D. acidovorans* MM01 and *D. tsuruhatensis* Bet002 were reported to produce PHB and PHBV (Razaif-Mazinah et al., 2016; Smith et al., 2014). Additionally, several *Rhodococcus* species can produce many

valuable compounds, including biosurfactants and carotenoids (Cappelletti et al., 2020), PHA (Altaee et al., 2017), wax esters and TAGs (Alvarez & Steinbüchel, 2002; Castro et al., 2016), some of which are accumulated intracellularly. For example, *R. aetherivorans* IAR1 was reported to convert toluene into PHA and TAG (Hori et al., 2009).

By exploring microbial metabolic pathways and optimizing their bioconversion capabilities, significant steps can be made towards the mitigation of PET waste impact by combining it with the production of valuable and sustainable materials (Balola et al., 2024; Qi et al., 2022). Therefore, this study aimed at investigating two microbial isolates, namely *Delftia* sp. Ave5 and *Rhodococcus* sp. Ave7, for their ability to grow and produce PHA using depolymerized pcPET waste containing TPA as the sole feedstock. RSM was used to select the most suitable strain and determine the optimal concentration ranges of TPA and ammonium for developing a bioreactor process. The study assessed the performance of the chosen isolate under different cultivation modes, to evaluate its performance. Further, the produced bioproducts were extracted from the bacterial cells and characterized.

II.2. Materials and Methods

II.2.1. Feedstock processing and characterization

II.2.1.1. Chemical depolymerization of post-consumer PET waste

A sample of pcPET waste (Fig. II. 1A), containing approximately 2-5% PE, 1-2% pigments, metallic ingredients, and carbon black additives, was supplied by Novelplast (Ireland). Depolymerization experiments via reactive extrusion (REX) were conducted at TUS (Ireland) using a bench-top PrismTM twin-screw extruder (Thermo Electron GmbH, Karlsruhe, Germany) following a modified procedure from Fournet et al., 2022. The pcPET waste was mixed with solid NaOH at a 2:1 (wt%/wt%) ratio. The well-mixed depolymerization reaction mixture was then dispensed through the main shaft into the barrel, which was maintained at a constant temperature of 250 °C, while the screw rotational speed was set at 20 rpm. The resulting REX product was named REX-PET (Fig. II. 1B).

Figure II. 1 - pcPET waste (A), REX-PET chemical depolymerized sample obtained from reactive extrusion of pcPET waste (B) and REX-TPA aqueous solution obtained from REX-PET material used for the bioreactor cultivation runs (C).

II.2.1.2. Characterization of REX-PET

- **Moisture and Inorganic content**

For the moisture content determination, REX-PET (~50 mg) was subjected to a temperature of 100 °C until a constant weight was achieved. Afterwards, the dried sample was placed at a temperature of 550 °C for 24 h, and the inorganic salts content was determined gravimetrically by weighing the resulting ashes. All measurements were done in triplicate.

- **Elemental analysis**

Elemental analysis was performed in an elemental analyser (Thermo Finnigan-CE Instruments, Flash EA 1112 CHNS series, Italy). The samples are subjected to a flash combustion in an oxygen environment and the resulting gases (N_2, CO_2, H_2O and SO_2) were separated by gas chromatography (GC). Finally, the contents in nitrogen, carbon, hydrogen, and sulphur were calculated using a thermal conductivity detector.

- **Fourier Transform Infrared spectroscopy**

The REX-PET samples were characterized via Fourier-Transform Infrared (FT-IR) spectroscopy with a spectrum two spectrometer (Perkin-Elmer, Waltham, MA, USA) equipped with the attenuated total reflectance (ATR) accessory. The spectra were recovered based on five scans between a resolution of 4000 and 400 cm^{-1}, at room temperature.

II.2.1.3. REX-PET processing and characterization

For the bacterial cultivation experiments, REX-PET was processed into an aqueous solution (named REX-TPA), which was obtained by preparing a 3.33% (w/v) mixture of REX-PET (5 g) (Fig. II. 1B) in deionized water (150 mL), followed by homogenization by magnetic stirring at 600 rpm during 1 h. Then, the mixture was filtered (using paper filters with a pore size of 20 µm) followed by pH 7 normalization by HCl 5 M addition. The final solution contained approximately 20 g/L of TPA, representing a recovery of 60% (Fig. II. 1C). The REX-TPA solution was assessed for its pH, inorganic content, inductively coupled plasma (ICP-AES), total carbon and TPA quantification.

- **Inorganic salts content**

The inorganic salts content of REX-TPA (~5 mL) was determined as described above.

- **Inductively Coupled Plasma - Atomic Emission Spectroscopy**

REX-TPA samples (~5 mL) were filtered (0.2 µm nylon, Whatman) and analysed by ICP-AES (Horiba Jobin-Yvon, France, Ultima, equipped with a 40.68 MHz RF generator, Czerny-Turner monochromator with 1.00 m (sequential) and autosampler AS500).

- **Total Carbon**

The total carbon was determined in a TOC-VCSH Analyser (Shimadzu) with a combustion catalytic oxidation at a temperature of 680 °C. High purity air served as carrier gas at a flow rate of 150 mL/min.

- **TPA concentration**

TPA concentration was determined by high performance liquid chromatography (HPLC) using an Agilent Eclipse C18 250×4.6 mm, coupled to a UV detector. The analysis was performed at 50 °C, with samples eluted in isocratic mode using methanol (Fisher Chemical, HPLC grade) and 0.1% formic acid (Sigma-Aldrich, HPLC grade) solution (1:1, v/v). The flow rate was set to1 mL/min, and the injection volume 5 µL (Yang, 2013) . TPA detection was obtained at 240 nm. A TPA stock solution (1 g/L) (Merck Millipore, 98%) was prepared in a phosphate buffer (containing per liter: $(NH_4)_2HPO_4$, 1.1 g (PanReac AppliChem, 99%); K_2HPO_4, 5.8 g (PanReac AppliChem, 99%); KH_2PO_4, 3.7 g (ChemLab, 99.5%)) and adjusted to pH 7. From this stock solution, TPA standards were prepared by serial dilution with a water–methanol mixture (10% methanol, Fisher Chemical, HPLC grade) to achieve TPA

concentrations ranging from 4 to 400 mg/L.TPA standards and samples were prepared by diluting in 10% methanol (Fisher Chemical, HPLC grade). All measurements were done in triplicate.

II.2.2. Cultures' isolation

Two bacterial strains (Figure II. 2) were isolated by AVECOM (Belgium) from landfill soil, by serially diluting and cultivating a sample on selective plates of mineral salt media (MSM), containing commercial TPA (Merck Millipore, 98%) as carbon source.

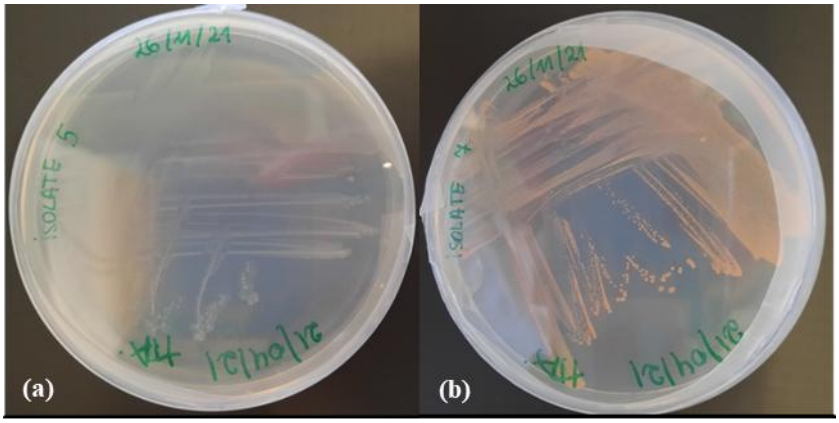

Figure II. 2 - Bacterial strains isolated by AVECOM and identified as *Delftia* sp. Ave5 (a) and *Rhodococcus* sp. Ave7 (b).

MSM had the following composition: 8.86 g/L K_2HPO_4 (PanReac AppliChem, 99%), 2.80 g/L KH_2PO_4 (ChemLab, 99.5%), 0.50 g/L NaCl (PanReac AppliChem, 99.5%), 0.10 g/L $MgSO_4 \cdot 7H_2O$ (Biochem Chemopharma, 99.5%), and 0.10 g/L NH_4Cl (PanReacAppliChem, 99.5%). The micronutrients' solution was added to the medium at a concentration of 10 mL/L. The micronutrients solution contained (per liter): $FeSO_4 \cdot 7H_2O$, 1.83 g; $MnSO_4 \cdot 1H_2O$, 0.56 g; $ZnSO_4 \cdot 7H_2O$, 1.35 g; $CaCl_2 \cdot 2H_2O$, 0.067 g; $CoSO_4$ $7H_2O$, 0.036 g; $CuSO_4$ $5H_2O$, 0.036 g; H_3BO_3, 0.65 g; EDTA dissodium $\cdot 2H_2O$, 1.104 g. TPA (Merck Millipore, 98%) was added to the medium at a concentration of 0.5 g/L. The culture media containing TPA was sonicated in an ultrasonic bath (Bandelin Sonorex Digitec Berlin) for 30 min, followed by pH adjustment to 7.0 by addition of 5 M NaOH to ensure TPA solubilization. All solutions were autoclaved separately (20 minutes at 121 °C, 1 bar) and mixed after cooling to avoid precipitation.

The isolation procedure involved inoculating the landfill soil samples in solid MSM (containing 15 g/L agar), and incubating, during 72 h at 30 °C. Single isolated colonies were collected and inoculated in MSM media containing TPA as sole carbon source. The cultures were incubated between 48 to 72 h at 30 °C and cryopreserved at -80 °C in glycerol (25%, v/v). Single isolated colonies of each isolate

were used for the amplification of the 16S rRNA gene via colony PCR using a T100 Thermal Cycler (Bio-Rad). The amplified 16S rRNA genes were then sent to Macrogen Europe (The Netherlands) for Sanger sequencing.

II.2.3. Cultures' selection

II.2.3.1. Media

MSM media, prepared as described in section II.2.2, was used for all experiments. For inocula preparation, MSM was supplemented with commercial TPA (Merck Millipore, 98%) as carbon source at a concentration of 0.5 g/L and NH_4Cl (PanReacAppliChem, 99.5%) as the nitrogen source (0.10 g/L). For the cultivation experiments, MSM was supplemented with REX-TPA solution (prepared as described in section II.2.1.3) to achieve the desired TPA concentration for each experiment. The media's pH was adjusted to 7 by addition of HCl 1M and NaOH 1M, and all media were sterilized by autoclaving at 121 °C and 1 bar, for 30 min.

II.2.3.2. Inocula preparation

The inoculum for each strain was prepared by inoculating a cryovial (1 mL) in a 500 mL baffled shake flask containing 200 mL MSM medium, prepared as described in section II.2.2. The cultures were incubated in a shaker incubator (200 rpm), at 30 ºC, during 48 h.

II.2.3.3. Cultivation experiments

The cultivation experiments were conducted with MSM supplemented with REX-TPA as carbon source, in 500 mL baffled shake flasks containing 200 mL of medium. The concentration of TPA and ammonium was set according to the design of experiments (Table II. 1). The flasks were inoculated with 10% (v/v) of inoculum, prepared as described above, and incubated at 30 ºC in an orbital shaker at 200 rpm, during 48 h. At the end of the experiments, the cultivation broth was collected for CDW, TPA, ammonium and storage compounds (PHA and TAGs) quantification.

II.2.3.4. Experimental design

RSM was used to evaluate the influence of nutrients' concentration using as experimental variables (X_i): TPA concentration (X_1, g/L) and ammonium (X_2, g /L), on the observed responses (Y_i): cellular growth, represented by CDW (Y_1, g/L) and PHA (Y_2, wt.%); for *Rhodococcus* sp.Ave7 the intracellular accumulation of TAG (Y_3, wt.%) was also evaluated as a response. A central composite rotatable design

(CCRD), with two independent variables was applied, composed of eleven runs, with four factorial design experiments at levels ±1; four axial experiments at level α = ±1.414; and a central point with three replicas (Table II. 1) which allowed the determination of both the experimental error and the reproducibility of the data (Lundstedt et al., 1998; Torres et al., 2012).

Table II. 1. Independent variables and their levels used in the response surface design.

Independent variables	Coded Variable	Factor Level				
		- α	-1	0	1	α
TPA (g/L)	X_1	0.34	2.00	6.00	10.00	11.66
Ammonium (g/L)	X_2	0.03	0.17	0.5	0.84	0.98

The mathematical relationship between the independent variables can be approximated by the second-order polynomial for two independent variables model equation (II.2.3.1):

$$Y_P = b_0 + b_1X_1 + b_2X_2 + b_{11}X_1^2 + b_{22}X_2^2 + b_{12}X_1X_2 \qquad \text{Eq. (II.2.3.1)}$$

In equation (II.2.3.1), Y_P corresponds to the predicted responses, and X_1 and X_2 are the coded values of the independent variables, namely TPA and ammonium concentrations. b_0, b_i, b_j, b_{ij} (i, j = 1, 2) are the coefficient estimates, b_0 being the interception, b_1 and b_2 the linear terms, b_{11} and b_{22} the quadratic terms, and the b_{12} the interaction term.

II.2.3.5. Statistical analysis

The significance of each source of variation was obtained from the statistical analysis of variance (ANOVA) provided by the statistical software (Design of Experiment 13, Design-Expert® software package from Stat-Ease Inc.). ANOVA was used to assess the fit of each model, which was considered an accurate prediction tool when it met the following criteria: a good correlation value ($R^2 > 0.7$, acceptable for biological samples with statistical meaning (p-value < 0.05, for a 95% confidence level) and with no lack of fit (p-value > 0.05, for 95% confidence level), meaning the model error was in the same range as the pure error (Lundstedt et al., 1998; Torres et al., 2012). The three-dimensional surface plots analysis provides information regarding to the best range for TPA and ammonium influence on CDW, PHA and TAG content.

II.2.4. Bioreactor cultivation

II.2.4.1. Inocula preparation

The inocula for the bioreactor assays were prepared by inoculating 1 mL of the cryopreserved culture into 200 mL MSM, prepared as described above, in a 500 mL baffled shake flask. The flasks were incubated in a rotary shaker (200 rpm), at 30 °C, for 48 h.

II.2.4.2. Media

For the bioreactor assays, a growth medium consisting of MSM supplemented with REX-TPA (prepared as described above) and ammonium concentrations of 12 and 0.3 g/L, respectively, was prepared as described above in section II.2.1.3. After sterilization in an autoclave at 121 °C, 1 bar, for 30 min.

II.2.4.3. Bioreactor assays

Three bioreactor experiments were performed under different modes of cultivation: batch (Assay A) and fed-batch with pulse feeding (Assay B) or continuous feeding (Assay C), for *Rhodococcus* sp. Ave7. In all assays, the bioreactor was inoculated with 200 mL of the prepared bacterial culture to initiate the experiments. The initial pH was set to 7 and monitored but not controlled during the cultivation. The temperature was controlled at 30 ± 0.1 °C. An aeration rate of 2 SLPM (Standard Liters per Minute) was kept during the experiments. The dissolved oxygen (DO) concentration was controlled at 20% of the air saturation, by automatically adjusting the stirring rate between 300 and 1000 rpm. Foam formation was automatically suppressed by addition of Antifoam 204 (Sigma-Aldrich).

Assay A, conducted under batch mode, was done in a 3 L bioreactor (Jupiter 3, Solaris, Italy), with initial working volume of 2 L. Assay B was performed in a 5 L bioreactor (Jupiter 6.0, Solaris, Italy) with an initial working volume of 2 L. After initial TPA depletion, signalled by an abrupt increase of the DO concentration, a REX-TPA pulse (1 L) containing 20 g/L TPA was fed to the bioreactor. Assay C was performed in a 3 L bioreactor (Bionet F1, Spain), with an initial working volume of 1.5 L. A continuous feeding of a REX-TPA solution containing 20 g/L TPA and 0.01 g/L of ammonium, was fed to the bioreactor at a 0.1 L/h flow rate, for 15 h.

Samples (10 - 20 mL) were taken from the bioreactor for quantification of the CDW, TPA, ammonium, PHA and TAG.

II.2.5. Analytical methods

II.2.5.1. CDW Quantification

For determination of the CDW, the culture broth samples were centrifuged (20 min, 18 516×*g*, 4 °C) to separate the cell pellet from the cell-free supernatant. The cell pellet was washed twice with deionized water and lyophilized (ScanVac CoolSafeTM, LaboGene, Lillerød, Denmark) for 48 h. The CDW was determined gravimetrically by weighing the dried cell pellets. All measurements were done in triplicate.

II.2.5.2. Quantification of TPA and ammonium

Determination of TPA concentration in the cell-free supernatant samples was performed by HPLC, as described in section II.2.1.3, diluted in the same 10% methanol aqueous solution to ensure consistency of the standards and samples matrix for the HPLC analysis. Ammonium concentration was determined by colorimetry using a flow segmented analyser (Skalar 5100, Skalar Analytical, Netherlands). NH_4Cl (PanReacAppliChem, 99.5%) samples at concentrations ranging from 2 to 20 mg/L were used as standards. All measurements were done in triplicate.

II.2.5.3. PHA and TAG quantification

Storage compounds content in the biomass, namely PHA and TAGs, and their composition were determined by GC analysis after acidic methanolysis of freeze-dried cells' samples. Freeze dried samples (3 to 5 mg) were mixed with 2 mL 20% (v/v) sulphuric acid (Honeywell Fluka, HPLC grade) in methanol (Fisher Chemical, HPLC grade) and 2 mL benzoic acid in chloroform (0.5 g/L) (Fisher Chemical, HPLC grade) and heated at 100 °C, for 4 h. Benzoic acid (Sigma-Aldrich, ≥99.5 %) acted as internal standard. The calibration curve for PHA quantification was prepared using a standard solution of PHBHV (Sigma-Aldrich) with a 3HV content of 14 mol% . For TAGs quantification, a mixture of fatty acid methyl esters (FAME) composed of C_{14}-C_{22} (Sigma-Aldrich) at concentrations ranging from 0.1 to 1.0 g/L, was used. The methyl esters obtained from the methanolysis, derived simultaneously from both PHA and TAGs, were analysed in a single run using a Trace 1300 GC apparatus (Thermo Fisher Scientific, US) equipped with a flame ionization detector (FID) (Thermo Fisher Scientific, US) and a Restek column (Crossbond, Stabilwax). The system operated at constant pressure (96 kPa) using helium as carrier gas. The oven temperature program was the following: 20 °C/min until 100 °C; 3 °C/min until 155 °C and, finally, 20 °C/min until 230 °C with a holding time of 30 min. All measurements were done in triplicate.

II.2.5.4. Glycogen Analysis

Glycogen content was assessed following the protocol described by (Lanham et al., 2012). The previously weighed freeze-dried biomass was treated with 2 mL of a dilute solution of HCl. The tubes were incubated at 100 °C for 3 h. The samples were filtered (filter with 0.2 µm pore size, Whatman) and analysed by HPLC using a chromatograph equipped with an Aminex HPX-87H HPLC column (Bio-Rad, USA). A solution of 0.01 N of H_2SO_4 was used as a mobile phase with a flow rate of 0.5 mL/min and a 30 °C operating temperature. The detection wavelength was set at 210 nm. Glucose (Scharlau, Barcelona, Spain) was used as standard ranging from 0.06 to 1 g/L. Samples were analysed in triplicate.

II.2.5.5. Polyphosphate staining

For staining polyphosphate inclusions, the samples were fixed with gentle heat on glass microscopic slides and exposed to Loeffler's methylene-blue staining followed by light washing in distilled water (Hernández et al., 2008).

II.2.5.6. Calculations

The maximum specific cell growth rate (μ_{max}, h^{-1}) was calculated by determining the linear regression slope of the exponential phase of Ln X_t/X_0 versus time curve, where X_t/X_0 (g/L) is the active biomass concentration at time t (h) and at the beginning of the run (t_0), respectively.

The active cell biomass (*X*, g/L) (without PHA and TAG) used for yield calculations, at time *t*, was determined by equation (II.2.5.1)

$$X_t = CDW_t - (PHA_t + TAG_t) \quad \text{Eq. (II.2.5.1)}$$

where CDW_t (g/L), PHA_t (g/L) and TAG_t (g/L) represent the CDW and the concentrations of PHA and TAG at time t(h), respectively.

The overall volumetric productivity (r_P, g/ L.(day)), where P is indicative of PHA or TAG, were determined by equation (II.2.5.2):

$$r_P = \frac{\Delta P}{\Delta t} \quad \text{Eq. (II.2.5.2)}$$

where ΔP (g/L) is the product (PHA or TAG) produced in time interval Δt (h).

The yields of active biomass ($Y_{X/S}$, g_X/g_{TPA}) and the products (P) on substrate basis ($Y_{P/S}$, g_P/g_{TPA}) were determined by equation (II.2.5.3) and (II.2.5.4):

$$Y_{X/S} = \frac{\Delta X}{\Delta S} \quad \text{Eq. (II.2.5.3)}$$

$$Y_{P/S} = \frac{\Delta P}{\Delta S} \quad \text{Eq. (II.2.5.4)}$$

where ΔX and ΔP are the active biomass and the PHA and/or TAG produced (g/L), respectively, and ΔS (g/L) is the concentration of TPA from REX-TPA residue consumed during the same time range of the cultivation run.

II.2.5.7. Statistical Analysis

The statistical differences for the mean and standard deviation of the kinetic and stoichiometric parameters obtained from the three assays performed by *Rhodococcus* sp. Ave7 using REX-TPA, were assessed using one-way ANOVA followed by Bonferroni's Multiple Comparison Tests in GraphPad Prism 5 with the criteria for statistical significance set at $p < 0.05$.

II.2.6. Bioproducts extraction and characterization

II.2.6.1. PHA and TAG extraction from *Rhodococcus* sp. Ave7 biomass

The cultivation broth was centrifuged (10,350 *g*, 20 min, 4 °C) and the obtained cell pellets were freeze-dried and milled. The bioproducts were extracted from the freeze-dried biomass by Soxhlet extraction with chloroform (Fisher Chemical, HPLC grade), at 80 °C, for 48 h. The PHA was precipitated in ice-cold ethanol (1:10, v/v), under vigorous stirring, and dried in a fume hood at room temperature (Rebocho et al., 2020). The ethanol used for PHA precipitation was collected and allowed to evaporate at room temperature in a fume hood, to recover the produced TAGs.

For further purifying the PHA from the ethanol precipitated extract, the sample was mixed with 1-butanol (≥ 99.5%, PanReac AppliChem) at a concentration of 0.3% (w/v), and heated to 75 °C for 2 h, under constant stirring, to dissolve the TAGs fraction. The solvent was removed while still hot and the insoluble PHA was recovered and left to dry at room temperature in a fume hood.

II.2.6.2. FT-IR

The recovered TAGs and PHA samples were characterized via FT-IR, as described in section II.2.1.2.

II.2.6.3. Thermal Properties

Differential Scanning Calorimetry (DSC) was carried out with a DSC Q2000 instrument (TA Instruments, New Castle, FL, USA). Hermetic aluminium pans were used to place the samples, and the analysis was performed with a heating and cooling rate of 10 ºC/min over a temperature range of -90 ºC to 180 ºC, through three heating cycles. The endotherm peak's temperature and area of the first heating

cycle were used to determine melting temperatures (T_m) and melting enthalpies (ΔH_m), respectively, while the glass transition temperature (T_g, °C) was taken as the midpoint of the heat flux step. The crystallinity (X_C, %) was estimated as the ratio between the obtained melting enthalpy and the melting enthalpy of 100% crystalline PHB, estimated as 146 J/g (Esmail et al., 2021).

Thermogravimetric Analysis (TGA) was performed using a thermogravimetric Analyzer Labsys EVO (Setaram, France), with weighing precision of +/- 0.01%. Samples were placed in aluminium crucibles and analysed in argon atmosphere with temperature range between 25 and 800 °C, at a rate of 10 °C/min. The maximum thermal degradation temperature (T_{deg}, °C) corresponds to the temperature value obtained for the maximum decreasing peak of the sample mass.

II.2.6.4. Molecular mass distribution

Size-exclusion chromatography (SE-HPLC) was performed to determine the number average molecular weight (M_n), weight average molecular weight (M_w), and polydispersity index ($PDI=M_w/M_n$) of the PHA. Monodisperse polystyrene standards (370–2520,000 Da) and the biopolymer were prepared at a concentration of 0.2% (w/v) in chloroform. Analysis was conducted using a KNAUER Smartline SE-HPLC system (Berlin, Germany) equipped with a Phenomenex Phenogel Linear Liquid Chromatographic Column (300 × 7.8 mm; Torrance, CA, USA), operated at 30 °C with a 1 mL/min chloroform flow rate as the mobile phase, using a Waters2414 refractive index detector (RID) (Milford, CT, USA).

II.3. Results and Discussion

II.3.1. Feedstock characterization

The material obtained from the depolymerization of pcPET waste, named REX-PET, was a uniform dark powder (Fig. II. 1B). The material mostly comprised particles in the 1000–2000 µm size range (46 ± 2.0wt.%), followed by particles larger than 2000 µm (28 ± 5.7wt.%) and those at 500-1000 µm (16 ± 1.4wt.%) (Fig. II. 3). Smaller particles (<500 µm) collectively accounted for less than 12 ± 1.1wt.%. This particle size distribution indicates that the material was predominantly granular, with larger size fractions dominating the sample.

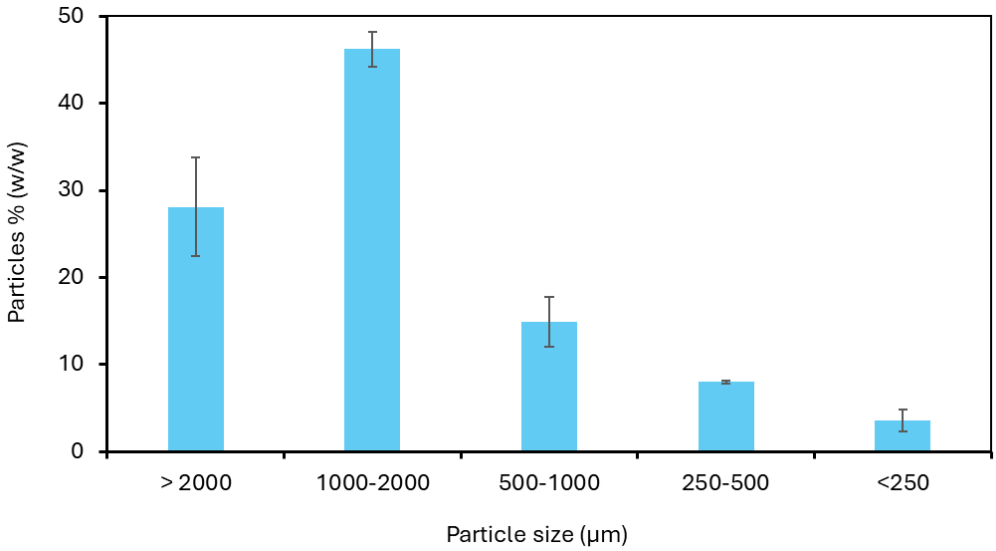

Figure II. 3 - Particle size distribution for REX-PET.

As shown in Table II. 2, REX-PET presented a low moisture content (11.66 ± 2.62). It had a high inorganic salts content (46.46 ± 4.69wt.%), which is probably related to the use of NaOH as catalyst for the depolymerization of the pcPET waste, forming a sodium salt of TPA (Abedsoltan, 2023). The main advantage of using this type of depolymerization conditions is its suitability for complex PET waste streams, containing multilayer PET or which often contain significant amounts of pigments as the mixture is not viscous and insoluble colour pigments can be separated from the TPA (Barredo et al., 2023; Sinha et al., 2010). The elemental analysis (Table II. 2) revealed that REX-PET was mainly composed of carbon (44.21 ± 2.4%), with traces of nitrogen (0.04 ± 0.02%), while no sulphur was detected.

Table II 2. Characterization of REX-PET feedstock (n.d. not detected).

Parameter	**REX-PET**
Moisture (wt.%)	11.66 ± 2.62
Organic content (wt.%)	52.47 ± 4.92
Inorganic salts (wt.%)	46.46 ± 4.69
Elemental analysis (%):	
C	44.21 ± 2.4
H	2.97 ± 0.39
N	0.04 ± 0.02
S	n.d.

As shown in Fig. II. 4, the spectral peaks of all analysed REX-PET batches exhibited high similarity among them, although they differed from those reported for commercial TPA. The carboxylic group (-OH) stretching peak appears around 3000-2800 cm^{-1}, but it is less intense in the REX-PET samples, suggesting a lower concentration of free carboxylic acid groups compared to pure TPA (Azeem et al., 2022). The peaks between 1718 and 1270 cm^{-1} correspond to the C=O and C=C bonds of the benzene ring in TPA, with intense peaks at 1557 and 1391 cm^{-1} indicative of the acidic carbonyl group (-C=O) and aromatic ring vibrations (Azeem et al., 2022; Liu et al., 2020; Wang et al., 2019). Notably, this region shows considerable differences from commercial TPA, as the peaks correspond to the formation of TPA disodium salt, a product of the depolymerization process (Štrukil, 2021). This is evidenced by the absence of -O-H bending bond in REX-PET, at 940 cm^{-1} attributed to the presence of disodium terephthalate (Wang et al., 2016), and the disappearance of the carboxylic acid groups (-COOH) at 1625 and 1423 cm^{-1} (Deng et al., 2017). Moreover, peaks displayed at 1088 and 1023 cm^{-1} can be attributed to the =C-H bending vibrations of the aromatic ring (Wang et al., 2019). The FT-IR spectra of the three REX-PET samples in Fig. II.4 show strong similarity among the batches, indicating consistent chemical structures with no significant variations in peaks or intensities, reflecting a stable and reproducible depolymerization process.

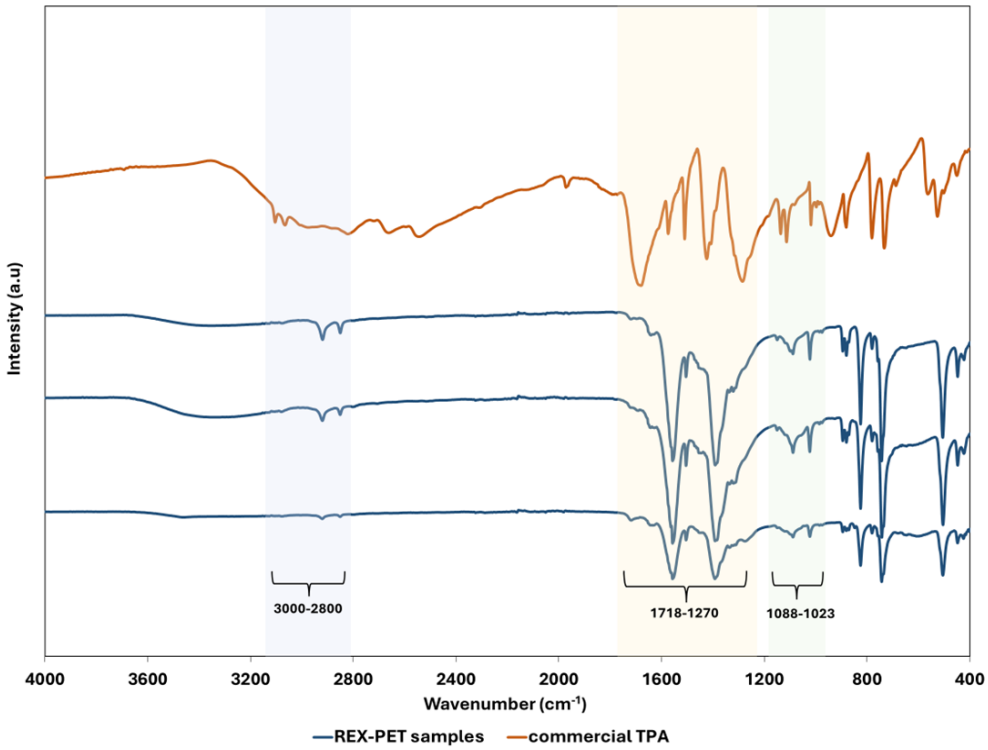

Figure II. 4 - Fourier-transform infrared (FT-IR) spectra of three batches of REX-PET samples derived from PET waste depolymerization under similar conditions, and of commercial TPA (Merck Millipore, 98%) .

The REX-TPA aqueous solution obtained from REX-PET presented a dark colour and was translucid without any visible suspended particles, as can be observed in Fig. II. 1C. Its pH was 11.05 ± 0.86 (Table II. 3), which correlates with the dry REX depolymerization process that follows the hydrolysis method under alkaline conditions provided by the presence of NaOH. This pH value is comparable to that obtained for a solution containing depolymerized PET upon relatable alkaline hydrolysis also using NaOH (Lee et al., 2021). The REX-TPA solution had a total carbon content of 12.06 ± 0.24 g/L (as determined by the TOC-VCSH Analysis) and a TPA concentration of 19.69 ± 0.09 g/L (as determined by the HPLC analysis). This TPA concentration accounts for a carbon content of 11.39 g/L which shows that the solution predominantly comprised TPA, with only a minor content of other carbonaceous compounds.

Table II. 3. Characterization of REX-TPA solution used in bioreactor media cultivation as feedstock.

Parameter	**REX-TPA**
pH	11.05 ± 0.86
Conductivity (mS/cm)	23.76 ± 4.71
Total carbon (g/L)	12.06 ± 0.24
[TPA] (g/L)	19.69 ± 0.09
Inorganic salts (wt.%)	2.21 ± 0.13
Element (mg/L)	
Na	461.12 ± 71.71
K	9.30 ± 3.91
Fe	8.84 ± 2.45
Ti	4.16 ± 1.48
Sb	3.82 ± 1.23
P	3.74 ± 0.98
Mg	3.11 ± 0.86
Ca	2.15 ± 0.36
Si	2.12 ± 0.84
Cr	0.51 ± 0.28
Cu	0.29 ± 0.03
Al	0.27 ± 0.09
Zn	0.25 ± 0.18
W	0.25 ± 0.06
Mo	0.13 ± 0.06

The inorganic salts content of the REX-TPA solution was 2.21 ± 0.13wt.% (Table II. 3). As expected, REX-TPA showed a high content of Na (461.12 ± 71.71 mg/L) (Table II. 3), which can be attributed to the depolymerization procedure in the presence of NaOH. Other elements found in the REX-TPA solution were Fe (8.84 ± 2.45 mg/L), Ti (4.16 ± 1.48 mg/L), Sb (3.82 ± 1.23 mg/L), Si (2.12 ± 0.84 mg/L), and traces of Cr, Al, Zn, W and Mo (<0.5 mg/L) (Table II. 3). This wide range of components reveals the high heterogeneity of additives that can be found in mixed plastic waste samples (Klöckner et al., 2021).

II.3.2. Bacterial cultivation on REX-TPA as sole carbon source: isolates' screening and selection

This section is focused on testing the microbial strains, namely *Delftia* sp. Ave5 and *Rhodococcus* sp. Ave7, that were isolated based on their ability to grow using TPA as the sole carbon source.

Statistical experimental design models, such as RSM, are valuable tools for identifying the relationship between multiple variables simultaneously and their response values, whilst using their relationship to generate the predicted yields of the run (Liu et al., 2024; Rao et al., 2019). Hence, aiming to identify the most promising microorganism and understand the best range of concentrations for TPA and ammonium that would enhance cell growth and PHA storage, a two-variable CCRD was employed. This approach allowed to understand the influence of REX-TPA, ammonium concentrations and the interactive effects of these parameters for the isolated microbial strains, *Delftia* sp. Ave5 and *Rhodococcus* sp. Ave7.

For each culture, TPA concentrations between 0.34 and 11.6 g/L and ammonium concentrations between 0.03 and 0.98 g/L were tested. These ranges were selected based on literature, since TPA concentrations usually range from 1 to 10 g/L in growth media, as higher levels might impair microbial metabolism (Suwanawat et al., 2019; Zhang et al., 2013). Due to the low solubility of TPA (~0.075 g/L), disodium terephthalate is a more soluble alternative (~130 g/L) that can be recovered from PET depolymerization under alkaline conditions (Fournet et al., 2022) and is commonly used in microbial media (Müller et al., 2023). Similarly, the ammonium concentration range was chosen to ensure an appropriate nitrogen balance, which is essential for cell growth and the production of specific metabolites (García-Torreiro et al., 2016).

A total of 11 assays were conducted for each culture under the conditions outlined in Table II. 1. The responses evaluated included CDW and intracellular storage compound content, providing insights into microbial performance under different TPA and ammonium conditions.

II.3.2.1. *Delftia* sp. Ave 5

Response analysis

The isolate *Delftia* sp. Ave5 demonstrated the ability to grow under all tested conditions, utilizing REX-TPA as the sole carbon source. The responses varied depending on the concentrations of REX-TPA and ammonium provided, which influenced both cell growth and PHA accumulation. The highest CDW values, 2.05 and 2.12 g/L (Table II. 4) were achieved in runs 1 and 8, respectively, which were conducted at high concentrations of TPA (10.00 and 11.66 g/L, respectively) and ammonium (0.84 and 0.50 g/L, respectively). The central points (runs 5, 6 and 7) (Table II. 4) resulted in CDW values of 1.44 – 1.53 g/L, for similar ammonium concentration (0.50 g/L) and 6.00 g/L of TPA, values lower than those obtained with higher concentrations of TPA, hence a higher availability of the feedstock promoted cell growth for run 8.

On the other hand, for run 3, a high TPA concentration of 10.00 g/L resulted in lower biomass production (1.20 g/L), since in this run the culture had available 0.17 g/L of ammonium. Still, the bacteria were able to accumulate 7.9wt.% PHA, suggesting that polymer synthesis was promoted by the higher TPA availability concomitant with ammonium limitation. As expected, the lowest CDW was observed for runs 9 and 11 (0.49 and 0.59 g/L, respectively), in which the concentrations of TPA (0.34 and 6 g/L, respectively) and ammonium (0.50 and 0.03 g/L, respectively) were limiting.

Table II. 4. Experimental design and result of central composite rotatable design (CCRD) with two independent variable, X_1 (REX-TPA concentration, g/L) and X_2 (Ammonium g/L) and the response Y_1 (CDW, g/L) and Y_2 (PHA, wt.%) for *Delftia* sp. Ave5.

	Run Number	Coded level (X_1)	X_1 TPA (g/L)	Coded level (X_2)	X_2 Ammonium (g/L)	Y_1 CDW (g/L)	Y_2 PHA (wt.%)
Factorial design	1	+1	10	+1	0.84	2.05	1.4
	2	-1	2	+1	0.84	1.06	1.7
	3	+1	10	-1	0.17	1.20	7.9
	4	-1	2	-1	0.17	0.83	1.5
Central Point	5	0	6	0	0.50	1.44	1.2
	6	0	6	0	0.50	1.52	1.4
	7	0	6	0	0.50	1.53	1.3
Axial Points	8	1.414	11.66	0	0.50	2.12	3.1
	9	-1.414	0.34	0	0.50	0.49	1.2
	10	0	6	1.414	0.98	1.51	1.3
	11	0	6	-1.414	0.03	0.59	5.7

Apparently, the conditions of run 11 (i.e., low ammonium concentration, 0.03 g/L, with high availability of TPA, 6 g/L), despite the low observed CDW (0.59 g/L), favoured PHA accumulation (5.7wt.%) (Table II. 4). A PHA content of 3.1wt.% was reached in run 8, in which the high TPA availability, together with limiting ammonium, seems to have also favoured polymer synthesis. For the remaining runs, low polymer contents in the biomass were obtained (<2wt.%) (Table II. 4).

The experiments performed demonstrated the ability of the *Delftia* sp. Ave5 to consume REX-TPA as sole carbon source, growing and accumulating PHA. These results are in line with previous studies for *Delftia tsuruhantensis* strain $T7^T$ isolated from a wastewater treatment plant that grew on TPA as sole carbon source , in a basal salt medium containing 1 g/L of sodium terephthalate (Shigematsu et al., 2003), although data was not reported regarding the strain's ability to produce PHA using TPA as substrate.

RSM modelling

RSM was applied to evaluate the influence of REX-TPA and ammonium concentration as variables on the culture's cell growth and PHA accumulation, as well as the combined effect of both of variables. The quadratic model was evaluated by ANOVA (Table II. 5) to assess the working ranges for each variable resulting in the highest CDW and PHA accumulation.

The ANOVA analysis (Table II. 5) shows that the proposed model is adequate since the quadratic model was found to be significant (F-value = 14.64 and *p*-value = 0.0111), and it was supported by a non-significant lack-of-fit (*p*-value= 0.2118) (Baptista et al., 2022), towards the response (CDW).

Table II. 5. ANOVA of the second order model for CDW (g/L) and PHA (wt.%) for *Delftia* sp. Ave5. (SS)—Sum of Squares shows the variance of values; (MS)—Mean Square is the arithmetic mean of the squared differences; *p*-value < 0.05 indicate model terms are significant.

Source	CDW				PHA			
	SS	MS	F-value	*p*-value	SS	MS	F-value	*p*-value
Model	2.65	0.5304	14.64	0.0111	47.14	9.43	22.75	0.0049
X_1 - REX-TPA	1.68	1.68	46.34	0.0024	9.61	9.61	23.19	0.0085
X_2 - Ammonium	0.7087	0.7087	19.56	0.0115	19.87	19.87	47.95	0.0023
$X_1 X_2$	0.0961	0.0961	2.65	0.1787	11.06	11.06	26.68	0.0067
X_1^2	0.0182	0.0182	0.5027	0.5174	1.25	1.25	3.00	0.1581
X_2^2	0.1661	0.1661	4.58	0.0990	6.60	6.60	15.93	0.0162
Lack of fit*	0.1409	0.0470	11.60	0.2118*	1.65	0.5515	172.35	0.0559

* Calculated for 10 experimental runs (without one replicate of the central point)

There is only a 1.11% chance that an F-value this large could occur due to noise, hence a model F-value of 14.64 implies the model is significant, since the greater F-value explains the variation of the data around its mean (Sachan et al., 2024). The lack of fit of the model was found not to be significant whilst calculated for 10 runs, excluding one replica, which initially introduced a significant lack of fit (p-value <0.05). Indicating the suitability of the model for describing the discrepancy between the actual and the predicted values, effectively fitting the experimental data (Mazaheri et al., 2017). The determination coefficient R^2 (0.9482) showed reasonable agreement with the adjusted R^2 (0.8834), indicating that 88.34% of the variability in the response could be explained by the model, which is also high to advocate for a high significance of the model. Furthermore, the observed precision of 10.2515 indicates an adequate signal, since a ratio greater than 4 is desirable. Hence, the quadratic model is an accurate representation of the actual relationships between the CDW and the variables.

Statistical analysis (Table II. 5) was also used to evaluate the impact of REX-TPA and ammonium on the quadratic model for the intracellular accumulation of PHA. The model was found to be significant (F-value=22.75 and p-value=0.0049), indicating only a 0.49% chance that a high F-value could occur from noise. This was supported by a non-significant lack-of-fit (p-value= 0.0559) (Baptista et al., 2022), for PHA content in the biomass, and similar to the previous response, a replica of the central point was removed since it was providing the model with an artificial lack of fit (p-value <0.05). Additionally, ANOVA of the second order model confirmed a strong fit (R^2 = 0.966), indicating that 96.6% of the variability in the response could be explained by the model (Lundstedt et al., 1998). The value of the adjusted R^2 (0.9236) is also high to advocate for a high significance of the model.

Effect of REX-TPA and ammonium concentrations on cell growth

The cell growth response in the RSM analysis was represented using a three-dimensional surface graph and contour plot (Fig. II. 5). The results suggest that, for the range tested, TPA and ammonium concentrations above 10.00 and 0.5 g/L, respectively, promoted cell growth, obtaining CDW values above 2.12 g/L. Fig. II. 5 shows that the increase in the concentration of TPA and ammonium were directly proportional to the increase of CDW. This is due to the CDW concentration for *Delftia* sp. Ave5 being affected by the linear term of TPA concentration (X_1) (p-value=0.0024), as well as linear term of ammonium also affected the response (p-value = 0.0115) (Table II. 5).

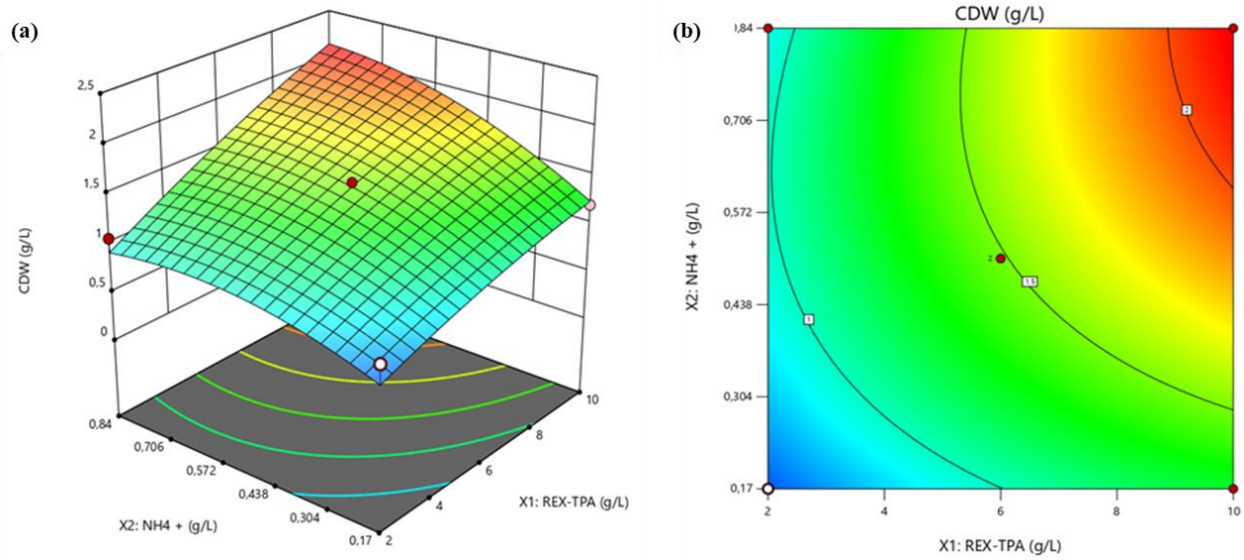

Figure II. 5 -Three-dimensional response surface (a) and contour plot (b) show the interactive effects of different concentrations of ammonium and REX-TPA on CDW (g/L) for *Delftia* sp. Ave5.

These results clearly confirm that increasing the concentration of REX-TPA and ammonium enhances higher cell growth. However, high PHA yield is obtained with lower ammonium availability, despite the decrease in biomass production. *Delftia acidovorans* JCM 10181 have demonstrated CDW values close to those obtained in this study when testing 10g/L of several carbon sources, including fructose (1.6 g/L), lactose (1.7 g/L), sucrose (1.8 g/L), 3-hydroxybutyric acid (2.1 g/L), acetate (2.1 g/L), maltose (2.1 g/) and glucose (2.4 g/L) for PHB production (Lee et al., 2004).

A study by (Razaif-Mazinah et al., 2016) investigated the strain *Delftia tsuruhatensis* Bet002, isolated from palm oil mill effluent, cultivated in shake flasks over 48 hours using a nitrogen-limited medium (0.46 g/L). The strain was tested with various carbon sources, including 0.5-0.7% w/v n-carboxylic acids and 1% w/v sugars and glycerol. The results showed that the CDW values range from 0.1 to 3.6 g/L when different even-chain fatty acids were tested. For odd-chain fatty acids, the CDW ranged from 0.7 to 3.7 g/L. When sugars such as glucose, fructose, lactose, and sucrose were used, the CDW ranged from 0.7 to 1.8 g/L, while glycerol resulted in a CDW of 1.5 g/L. The CDW values observed for *Delftia* sp. Ave5 in this study are comparable to those obtained for other *Delftia* strains, indicating its potential for robust growth under varying nutrient conditions.

Effect of TPA and ammonium concentrations on PHA accumulation

The response of the RSM for PHA content in the biomass is displayed in the three-dimensional surface graphs and contour plot (Fig. II. 6). It demonstrates that the model shifts significantly towards the second response (Y_2, PHA wt.%), with an inversely proportional interaction between TPA and

ammonium, whereby PHA production increases with the increase of TPA (10 g/L) and decrease in ammonium concentration. In this case, linear (X_2: ammonium) and interaction (X_1X_2) are significant model terms that affected the PHA accumulation by *Delftia* sp. Ave5, including a positive linear effect (*p*-value = 0.0023) of ammonium (Table II. 5).

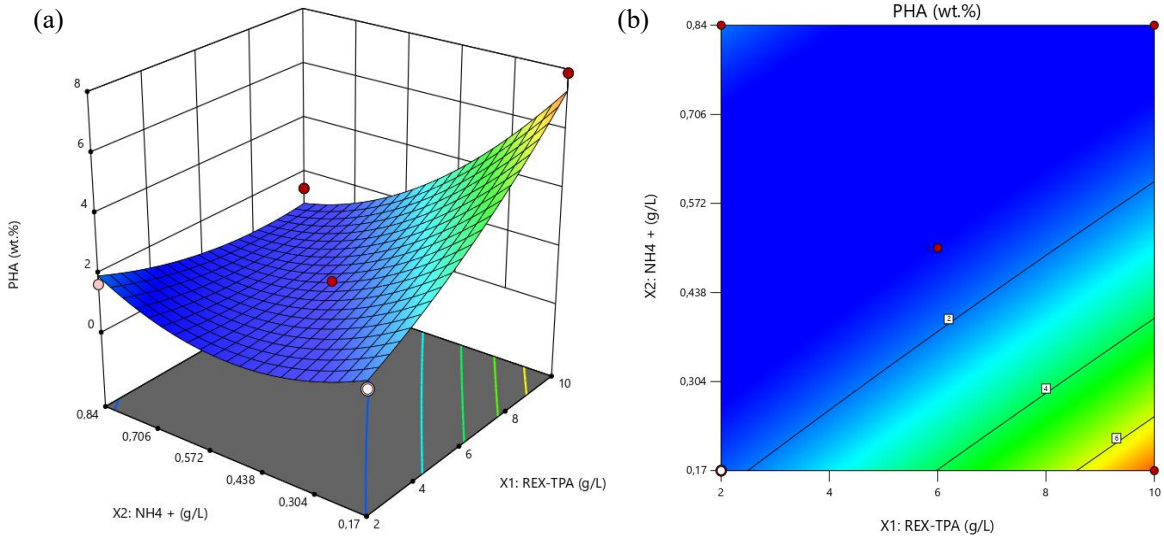

Figure II. 6 - Three-dimensional response surface (a) and contour plot (b) show the interactive effects of different concentrations of ammonium and REX-TPA on PHA (wt.%) for *Delftia* sp. Ave5.

D. acidovorans JCM 10181 was reported to accumulate 53wt.% PHA in the biomass when cultivated with 10g/L of glucose as the carbon source (Lee et al., 2004). Additionally, PHA production was observed in a nitrogen free mineral medium, where 10 g/L of sodium valerate was used as the carbon source, resulting in the production of 33wt% PHBV at pH 7 (Loo & Sudesh, 2007). The concentration of carbon source reported is aligned with the concentrations demonstrated by the model for *Delftia* sp. Ave5, although a lower concentration of ammonium promoted PHA accumulation in the present study and at lower values than those reported.

Moreover, *D. tsuruhatensis BET002* reported a wide range of PHA content depending on the substrate used (Razaif-Mazinah et al., 2016). For instance, when grown in fatty acids, the strain reached 46.2 and 28.2wt.% of PHA, when using pentadecanoic and myristic acid, respectively. The strain also accumulated PHA at lower contents—6.5wt.% for octanoic acid, 2.1wt.% for palmitic acid, and 0.4wt.% for stearic acid. In contrast, when grown on sugars and glycerol, PHA accumulation was below 5wt.% (Razaif-Mazinah et al., 2016), values similar to what was observed for *Delftia* sp. Ave5.

The profile observed for *Delftia* sp. Ave5, where polymer storage is enhanced under ammonium limiting conditions, shifting the metabolic focus from cellular growth to polymer storage under nitrogen

stress, is similar to that reported for *D. acidovorans* JCM 10181. Both strains exhibit a metabolic shift under nitrogen-limited conditions, favouring the polymer accumulation as the nitrogen availability decreases, even though the associated reduction cellular growth. This suggests that *Delftia* sp. Ave5 may not be the most promising culture for achieving high PHA yields while using TPA as sole carbon source.

II.3.2.2. *Rhodococcus* sp. Ave7

Response analysis

Rhodococcus sp. Ave7 grew under all tested conditions using REX-TPA as the sole carbon source. Biomass production and intracellular storage compound accumulation varied significantly depending on the concentrations of TPA and ammonium. In addition to PHA, the culture was also observed to produce TAGs as a value-added product, emphasizing its potential for upcycling REX-TPA into diverse storage compounds. Consequently, after verifying the culture's capacity to store this compound under the tested conditions, the response related to TAG accumulation was incorporated into the matrix of the central composite rotatable design. As previously reported, the genus *Rhodococcus* is known to synthesize and accumulate a variety of intracellular compounds, such as PHA and TAGs (Cappelletti et al., 2020). During the cultivations, TAG accumulation was consistently observed, further supporting its inclusion in the proposed model.

The CDW production of *Rhodococcus* sp. Ave7 indicates that higher REX-TPA concentrations resulted in increased biomass yield. The highest values of CDW obtained were 5.09 and 4.91 g/L (Table II. 6), namely for run 1 (10 and 0.84 g/L of REX-TPA and ammonium, respectively) and run 8 (11.66 and 0.5 g/L of REX-TPA and ammonium, respectively). For the central point conditions (run 5, 6 and 7), the values of CDW attained were between 2.95 to 3.17 g/L (Table II. 6). Under the remaining conditions, CDW was significantly lower, except for run 10 (6 and 0.98 g/L for REX-TPA and ammonium, respectively) achieved a biomass production, of 3.05 g/L, comparable to the central point runs. In contrast, run 9, where REX-TPA was in an extreme low concentration (0.34 g/L), resulted in minimal CDW production (0.24 g/L).

Table II 6. Experimental design and result of central composite rotatable design (CCRD) with two independent variable, X_1 (REX-TPA concentration, g/L) and X_2 (ammonium concentration, g/L) and the response Y_1 (CDW, g/L), Y_2 (PHA wt.%) and Y_3 (TAG, wt.%) for *Rhodococcus* sp. Ave7.

	Run Number	Coded level	X_1 TPA (g/L)	Coded level	X_2 Ammonium (g/L)	Y_1 CDW (g/L)	Y_2 PHA (wt.%)	Y_3 TAG (wt.%)
Factorial design	1	+1	10	+1	0.84	4.91	6.8	3.7
	2	-1	2	+1	0.84	1.09	0.3	3.8
	3	+1	10	-1	0.17	1.26	11.2	19.2
	4	-1	2	-1	0.17	0.96	0.1	4.3
Central Point	5	0	6	0	0.5	2.95	1.6	4.1
	6	0	6	0	0.5	3.17	2.3	3.9
	7	0	6	0	0.5	3.02	1.8	3.9
Axial Points	8	1.414	11.66	0	0.5	5.09	22.5	8.2
	9	-1.414	0.34	0	0.5	0.24	0.3	3.4
	10	0	6	1.414	0.98	3.05	1.9	4.8
	11	0	6	-1.414	0.03	0.52	2.0	19.9

Concerning the PHA accumulation by *Rhodococcus* sp. Ave7, it is possible to observe in Table II. 6 the highest polymer accumulation (22.5wt.%) was observed in run 8 (11.66 and 0.5 g/L of TPA and ammonium, respectively). In run 3, the culture achieved 11.2wt.% of polymer storage with high concentrations of TPA (10 g/L) and a lower ammonium concentration, 0.17 g/L. Moreover, for run 1, (10 g/L of REX-TPA with 0.84 g/L of ammonium), the culture attained 6.8wt.% of PHA accumulation. For the experiments 2, 4 and 9, where TPA concentrations were lower (between 2.00 and 0.34 g/L), resulted in minimal PHA accumulation (0.33, 0.14 and 0.32wt.%) (Table II. 6). The remaining conditions tested resulted in PHA accumulations ranging from 1.6 – 2.0wt.%, presenting low polymer content in the biomass.

As shown in Table II. 6, the highest TAG accumulation (19.2 and 19.9wt.%) was observed in runs 3 and 11, where high TPA concentrations (6-10 g/L) and low of ammonium concentration, between 0.03-0.17 g/L, were tested. Additionally, in run 8, the bacterium attained an intermediate TAG accumulation, of 8.2wt.% (Table II. 6). For the remaining conditions, TAG content remained lower, ranging from 3.4 to 4.8wt.%.

These results suggested that to increase *Rhodococcus* sp. Ave7 PHA and TAG accumulations, a high C/N ratio condition must be provided, as high availability in TPA apparently promotes their production. Regarding PHA, the highest PHA accumulation (22.5wt.%) and a significant TAG storage (8.2wt.%) in run 8 were observed at a high REX-TPA concentration. Similarly, the highest TAG accumulations (19.2 - 19.9wt.%) in runs 3 and 11 occurred with very low ammonium (0.03-0.17 g/L) and high TPA concentration (6-10 g/L) concentration, further reinforcing the impact of high C/N ratio on promoting the culture polymer and lipid storage.

On the contrary, when the C/N ratio was lower, either due to more balanced concentrations of TPA and ammonium, or a higher ammonium concentration, as the case of run 1, PHA and TAG were significantly lower, 6.8 and 3.8wt.%, respectively. Thus, a lower C/N ratio resulted in higher cell growth, while a higher C/N ratio availability strongly promotes the accumulation of both these intracellular compounds. This is in accordance with study performed with *Rhodococcus jostii* RHA1, reported to accumulate storage compounds simultaneously, such as PHA and TAG, where is shown that when the bacteria is exposed to nitrogen-limited conditions, uses the substrate for intracellular reserves (e.g., such as PHA and TAG) rather than using it for cellular growth (Tajparast & Frigon, 2015).

RSM modelling

The quadratic model applied for the optimization of TPA and ammonium concentration was evaluated using ANOVA for its impact on production of CDW and accumulation of PHA and TAG for *Rhodococcus* (Table II. 7). The model was found to be significant for CDW production, with a *p*-value of 0.0054 (Table II. 7). The ANOVA analysis of the second order model showed a good fit ($R^2 = 0.9641$), indicating that 96.41% of the variability in the response could be explained by the model. Additionally, the adjusted R^2 (0.9192) was high, indicative for a high significance of the model (Torres et al., 2012). The *p*-value of the lack of fit was found to non-significant (0.1340) (Table II. 7), suggesting that the model adequately describes the experiment data without significant deviation due to pure error. Also, the model's adequate precision (signal to noise ratio = 12.6102) indicates an adequate signal (value > 4 is desirable) in the model suitability for the navigation of the design space (Aghaie et al., 2009; Körbahti & Rauf, 2008).

Table II 7. ANOVA of the second order model for CDW (g/L), PHA (wt.%) and TAG (wt.%) for *Rhodococcus* sp. Ave7. (SS)—Sum of Squares shows the variance of values; (MS)—Mean Square is the arithmetic mean of the squared differences; *p*-value < 0.05 indicate model terms are significant.

Source	CDW				PHA				TAG			
	SS	MS	F-value	*p*-value	SS	MS	F-value	*p*-value	SS	MS	F-value	*p*-value
Model	27.17	5.43	21.48	0.0054	419.12	83.82	9.64	0.0238	354.07	70.81	16.82	0.0086
X_1-REX-TPA	15.07	15.07	59.56	0.0015	300.35	300.35	34.53	0.004	58.44	58.44	13.88	0.0204
X_2-NH_4^+	6.77	6.77	26.75	0.007	2.38	2.38	0.2731	0.629	137.06	137.06	32.55	0.0047
X_1X_2	3.10	3.10	12.25	0.025	5.38	5.38	0.6188	0.476	55.73	55.73	13.23	0.0220
X_1^2	0.303	0.303	1.20	0.335	79.73	79.73	9.17	0.039	0.8875	0.8875	0.2108	0.6700
X_2^2	2.22	2.22	8.79	0.041	1.50	1.50	0.1730	0.699	90.75	90.75	21.55	0.0097
Lack of fit*	1.00	0.25	29.65	0.134	34.62	11.54	66.29	0.090	16.84	5.61	4491.50	0.0110

* Calculated for 10 experimental runs (without one replicate of the central point)

ANOVA was used to determine the best range of concentration range for PHA accumulation by *Rhodococcus* sp. Ave7. The statistical analysis (Table II. 7) shows that the proposed model was found to be significant (F-value = 9.64 and *p*-value = 0.0238). Additionally, the model showed no significant lack of fit (*p*-value = 0.0900) for PHA production. The model F-value of 9.64 implies the model is significant, with only a 2.38% probability that such a large F-value could occur due to random variation (noise). The lack of fit was not found to be non-significant, with an F-value = 66.29, implying a 9.00% chance that this result is due to noise. However, for PHA, for certain terms there was evidence of lack of fit ($p < 0.05$), meaning that the model prediction error was above the error of the replicas which might be explained by the pure error (calculated from the central point), which were low values (1.6- 2.3wt.%), providing a sense of a model with lack of fit.

Moreover, $R^2 = 0.9234$ was the determination coefficient obtained for the model. Hence, it holds 92.34% of the variability in the dependent variable (response), with 7.66% influenced by other factors. Whilst adjusted R^2 (0.8275), considers the sample size and number of terms (Zhang et al., 2012). The high R^2 imply the model holds more influential and it presents better response prediction (Aghaie et al., 2009).

Considering TAG content in the biomass (Y_3) for *Rhodococcus* sp. Ave7, statistical analysis of the quadratic model indicated that the model was significant, with a *p*-value=0.0086 (Table II. 7). The model

F-value of 16.82 further supports this, with only a 0.86% chance that this result is due to noise. In this case, linear terms (X_1 and X_2), interaction (X_1X_2) and quadratic term (X_2^2) are significant model terms on TAG content in biomass. However, the model exhibited a significant lack of fit (*p*-value=0.0110), indicating a 1.10% probability that a lack of fit (F-value = 4491.50) this large could occur due to noise.

The lack of fit found, reflects data variation around the fitted model, an essential measure of model adequacy in representing the experimental results (Mazaheri et al., 2017). This suggests that the model does not fully capture the data trends within the tested experimental region. This indicates that higher-order terms might have to be included in the regression model to eliminate the lack of fit (Oh et al., 1995).

Effect of REX-TPA and ammonium concentrations on cell growth

Fig. II. 7 displays the 3D response plots for CDW, illustrating the optimization of TPA and ammonium concentrations for *Rhodococcus* sp. Ave7 cultivation. Regarding CDW, the response surface (Fig. II. 7) indicates that biomass production increased with higher concentrations of TPA and ammonium, a trend similar to that observed for *Delftia* sp. Ave5. This behaviour, presented by *Rhodococcus* sp. Ave7, aligns with previous reported for *Rhodococcus opacus* PD630, where a high cell density cultivation was achieved using sugar beet molasses and sucrose as sole carbon sources in a fed-batch mode (Voss & Steinbüchel, 2001).

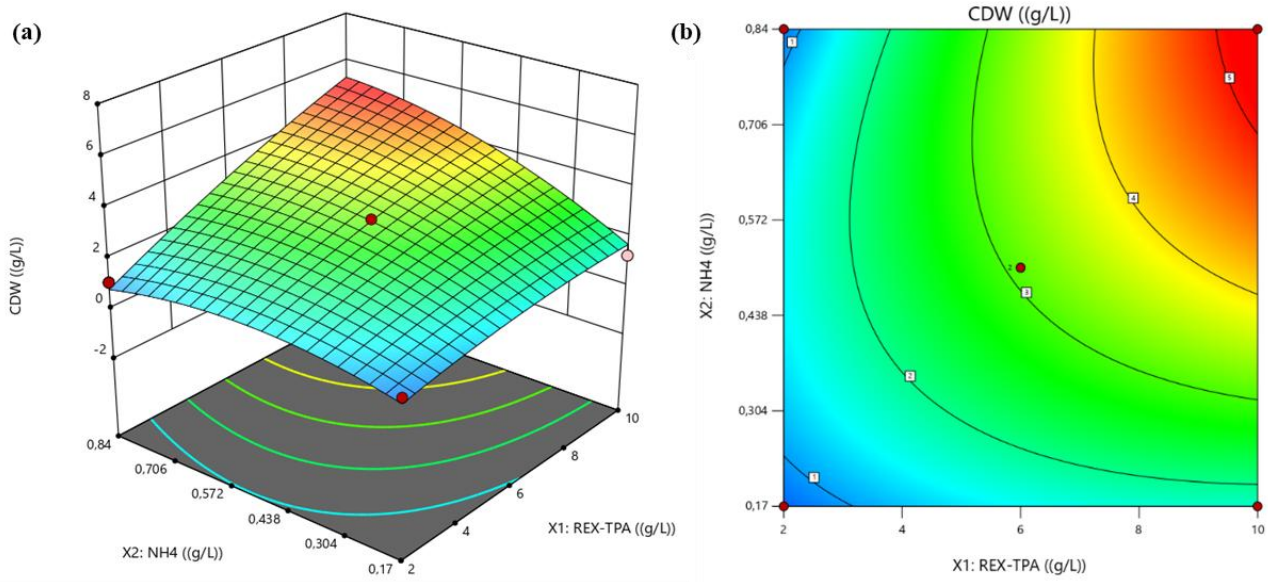

Figure II. 7 - Three-dimensional response surface (a) and contour plot (b) show the interactive effects of different concentrations of ammonium and REX-TPA on CDW (g/L) for *Rhodococcus* sp. Ave7.

For CDW production, the linear (X_1 and X_2), interaction (X_1X_2) and quadratic (X_2^2) model terms are significant, as shown in Table II. 7. The strongest effects were observed for the linear terms, with F-values of 59.56 and 26.75 for TPA and ammonium, respectively. Since the quadratic ammonium term (X_2^2) affected the response (F-value of 8.79) (Table II. 7), combined with the effect of the interaction (X_1X_2) resulted in the curvature found in 3D surface graphs (Fig. II. 7a).

Effect of REX-TPA and ammonium concentrations on PHA and TAG accumulation

Based on Fig. II. 8, the model predicted that *Rhodococcus* sp. Ave7 resulted in higher accumulation of products when TPA concentration exceed above 10 g/L. In the proposed quadratic proposed model, PHA accumulation was affected by the linear and quadratic terms of REX-TPA concentration (*p*-value<0.05) (Table II. 7). Regarding ammonium concentration, results suggest that lower concentrations seem to promote higher PHA accumulations (Fig. II. 8a).

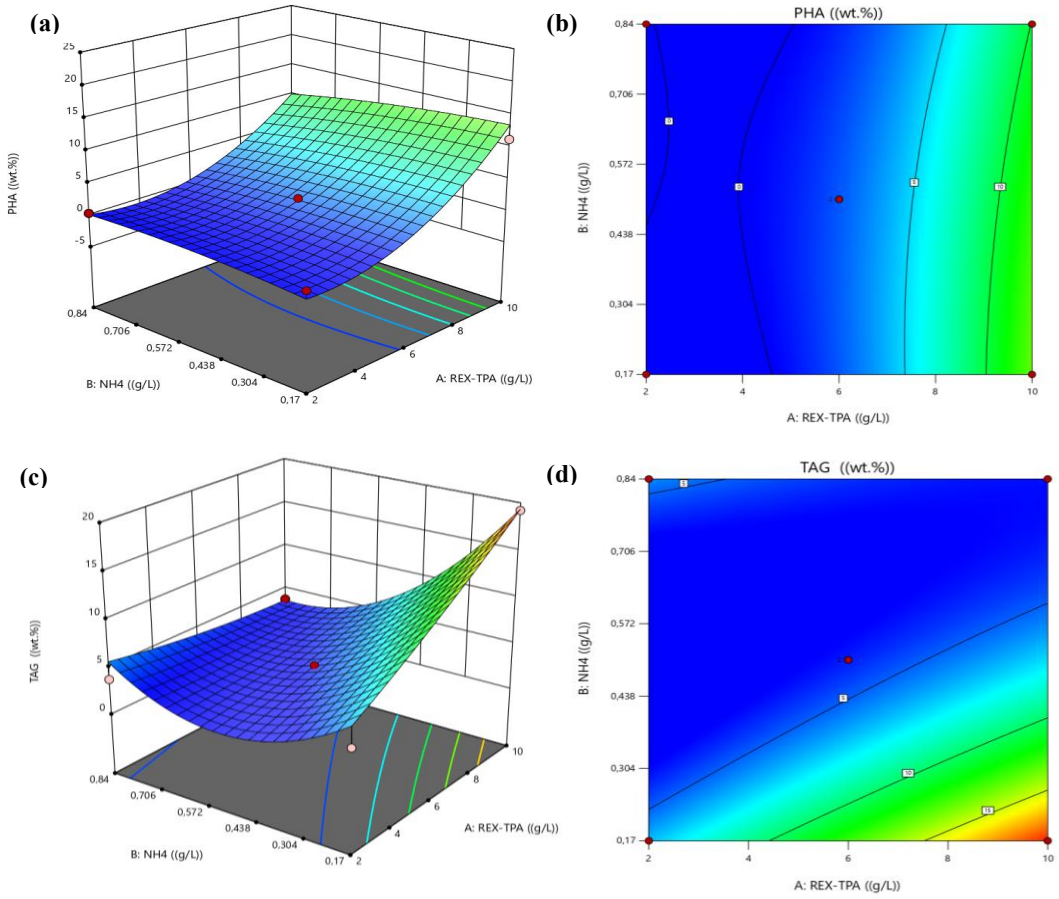

Figure II. 8 Three-dimensional response surface (a and c) and contour plots (b and d) show the interactive effects of different concentrations of ammonium and REX-TPA on PHA and TAG (wt.%) for *Rhodococcus* sp. Ave7.

Very few RSM studies for *Rhodococcus* cultivation experiments have been reported that focused on the optimization of the medium, which is crucial concerning cell growth and polymer production. A study for *R. pyridinivorans* BSRT1-1, reported the combined effects for concentrations of carbon (fructose) and nitrogen source (KNO_3), and trace element solution impacted the PHA production in shake flask, reporting that upon the conditions tested, cellular growth was achieved for higher concentrations of fructose and KNO_3 and trace element was not excessive. On the other hand, taking into consideration both cell growth and polymer accumulation, a reduced concentration of nitrogen (< 0.3 g/L), showed lower cell growth but increase in polymer content. Upon applying RSM optimized medium (fructose, 33.6 g/L, KNO_3, 0.3 g/L, and 1.0 mL/L of TE solution) the strain attained 43.1wt% PHB for 3.60 g/L of biomass (Trakunjae et al., 2021). In comparison with *Rhodococcus* sp. Ave7, a similar response for biomass production was obtained, whereas PHA accumulation was significantly enhanced under nitrogen-limiting conditions with excess TPA. *R. pyridinivorans* BSRT1-1, showed optimal PHA production under moderate nitrogen levels. Both strains promoted PHA accumulation under nitrogen limitation, although *Rhodococcus* sp. Ave7 requires a higher C/N ratio when compared to *R. pyridinivorans* BSRT1-1.

Concerning TAG accumulation, Fig.II. 8c shows that increasing REX-TPA concentration while maintaining a low ammonium concentration leads to higher TAG production. This is related to the presence of excess carbon and limitation of ammonium that triggers TAG biosynthesis and accumulation (Alvarez & Steinbüchel, 2002; Voss & Steinbüchel, 2001).

Between the bacteria tested, the isolated *Rhodococcus* sp. Ave7 presented the highest cellular growth and achieved the highest PHA content, while also accumulating TAG as a second value-added storage compound that hold market interest (Pinto-Ibieta et al., 2021). Thus, *Rhodococcus* sp. Ave7 emerges as a candidate towards the upcycling of depolymerized pcPET waste, within the region tested under the optimum conditions, more precisely for concentrations of REX-TPA above 10 g/L, whilst maintaining a lower concentration of ammonium (of 0.3 g/L) in order to trigger intracellular storage compounds of interest. Therefore, the isolate *Rhodococcus* sp. Ave7 was selected for the subsequent bioreactor process development.

II.3.3. Bioreactor process for *Rhodococcus* sp. Ave7

II.3.3.1. Batch Bioreactor Cultivation

Rhodococcus sp. Ave7 was cultivated under batch mode using an initial TPA concentration of 12 g/L as sole carbon source, under a controlled temperature of 30 ºC and an initial pH of 7 (Fig. II. 9a).

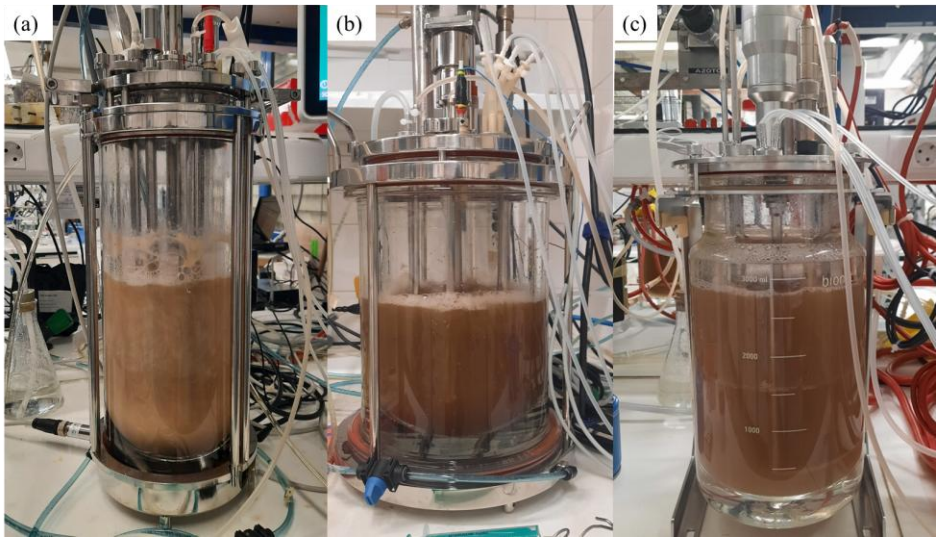

Figure II. 9 - Experimental set-up used in the bioreactor cultivation in batch (a) and fed batch with pulse (b) and continuous feeding (c) of *Rhodococcus* sp. Ave7 using REX-TPA as feedstock.

After a 10 h lag phase, *Rhodococcus* sp. Ave7 entered an exponential phase, reaching a maximum specific cell growth rate of 0.18 ± 0.05 h^{-1} and a CDW of 1.78 ± 0.08 g/L at 20 h of cultivation, when ammonium was exhausted (Fig. II. 10 (A1)). A final CDW of 2.67 ± 0.06 g/L was reached at the end of the assay. This value is slightly higher than the 2.3 g/L of CDW reported for *Pseudomonas umsongensis* G016 KS3 grew in a batch reactor, with similar duration, using as carbon source TPA and EG monomers obtained by enzymatic PET hydrolysis (Tiso et al., 2021).

PHA accumulation started during the exponential cell growth phase, at 13 h of cultivation, and continued (Fig. II. 10 (A2)) until the end of the assay, reaching a maximum PHA content in the biomass of 4.22 ± 0.03wt.%, corresponding to a PHA concentration of 0.11 ± 0.02 g/L (Table II. 8). Slightly higher values were reported for *P. umsongensis* G016 KS3 (7wt.%), corresponding to 0.15 g/L of PHA (Tiso et al., 2021).

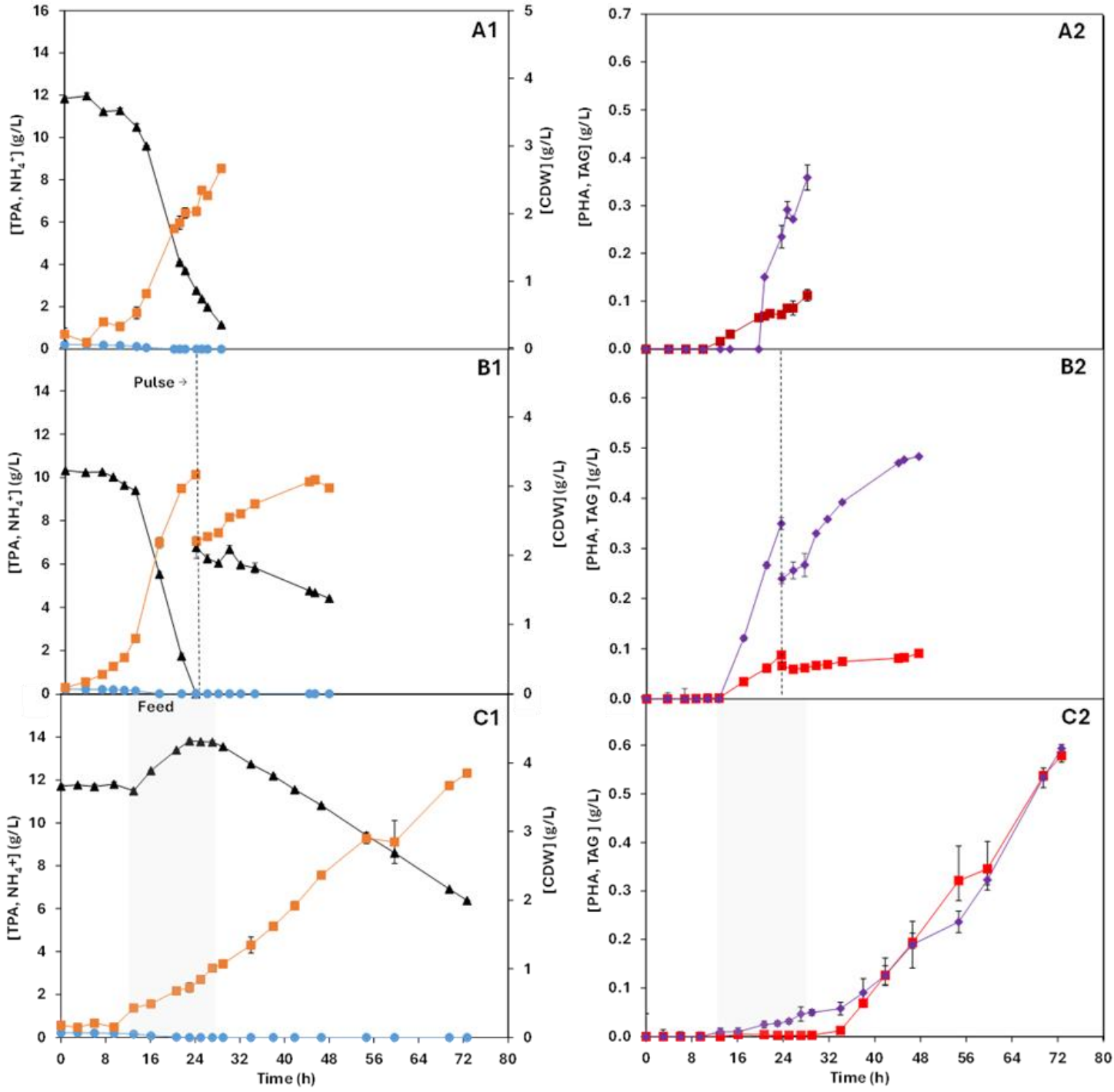

Figure II. 10 - Cultivation profiles for batch (A), fed-batch with pulse feed (the dashed line denotes the time the REX-TPA pulse was given) (B) and fed-batch with continuous feed (the grey area denotes the time REX-TPA was fed to the bioreactor, at a rate of 0.1 L/h) (C) of *Rhodococcus* sp. Ave7 using REX-TPA as feedstock (▲, TPA (g/L); ●, NH_4^+ (g/L); ■, CDW (g/L); ■, PHA (g/L); ◆, TAG (g /L)). Error bars correspond to triplicate measurements.

Table II. 8. Kinetic and stoichiometric parameters of the three assays performed by *Rhodococcus* sp. Ave7 using REX-TPA (μ_{max}, maximum specific cell growth; CDW, cell dry weight; r_{PHA}, PHA volumetric productivity; r_{TAG}, TAG volumetric productivity; $Y_{PHA/TPA}$, polymer yield on TPA basis; $Y_{TAG/TPA}$, TAG yield on TPA basis; n.s. (not significant), $p > 0.05$;*, $p < 0.05$ **, $p \leq 0.01$; ***, $p \leq 0.001$).

Parameter	Cultivation			
	A	B	C	*p-value*
μ_{max} (h^{-1})	0.18 ± 0.05	0.18 ± 0.02	0.17 ± 0.01	n.s.
CDW (g/L)	2.67 ± 0.06	2.97 ± 0.05	3.85 ± 0.09	***
PHA (wt.%)	4.22 ± 0.03	3.05 ± 0.05	15.01 ± 0.68	***
PHA (g/L)	0.11 ± 0.02	0.09 ± 0.00	0.58 ± 0.02	***
TAG (wt.%)	13.45 ± 0.69	16.26 ± 0.12	15.40 ± 0.29	***
TAG (g/L)	0.36 ± 0.05	0.48 ± 0.04	0.59 ± 0.04	**
r_{PHA} (g/(L.day)	0.096 ± 0.000	0.062 ± 0.000	0.245 ± 0.001	***
r_{TAG} (g/(L.day)	0.305 ± 0.001	0.331 ± 0.001	0.252 ± 0.021	***
$Y_{X/TPA}$ (g_X/g_{TPA})	0.19 ± 0.02	0.40 ± 0.03	0.24 ± 0.04	***
$Y_{PHA/TPA}$ (g_{PHA}/g_{TPA})	0.011 ± 0.00	0.015 ± 0.001	0.051 ± 0.003	***
$Y_{TAG/TPA}$ (g_{TAG}/g_{TPA})	0.031 ± 0.002	0.081±0.001	0.052 ± 0.000	***

TAGs synthesis was initiated later, at around 21 h of cultivation **(**Fig. II. 10 (A2)), reaching an intracellular content of 13.45 ± 0.69wt.% and a concentration of 0.15 g/L by 21 h of cultivation (Table II. 8). This corresponds to an overall volumetric productivity of 0.305 g/(L.day). During the first 21 h the bacterial strain consumed 7.74 g of TPA, for both cellular growth and PHA accumulation, resulting in growth yield of 0.19 g_X/g_{TPA}. After ammonium depletion, the culture used the available TPA for PHA and TAG accumulation. The PHA yield was 0.011 ± 0.00 g_{PHA}/g_{TPA}, while a higher yield was reached for TAGs (0.031 ± 0.002 g_{TAG}/g_{TPA}). An overall consumption of 10.7 g/L of TPA was achieved over 28 h. Similar values were obtained for *P. umsongensis* GO16 KS3 cultivated in TPA and EG obtained by enzymatic PET hydrolysis, (0.21 $g_{CDW}/g_{substrate}$ and 0.014 $g_{PHA}/g_{substrate}$, respectively) (Tiso et al., 2021).

II.3.3.2. Fed-batch cultivation with pulse feeding

In Assay B (Fig. II. 9b), *Rhodococcus* sp. Ave7 entered the exponential growth phase after 9 h of cultivation, presenting a maximum specific growth rate of 0.18 ± 0.02 h^{-1} (Fig. II. 10 (B1)), which was not significantly different ($p > 0.05$) from Assay A (0.18 ± 0.05 h^{-1}). Ammonium depletion was observed after 17 h of cultivation, resulting in a CDW of 2.18 ± 0.13 g/L. By 24 h, the culture achieved a maximum CDW of 3.17 ± 0.03 g/L (Fig. II. 10 (B1)), with PHA and TAGs contents of 2.77 ± 0.01wt.% and 11.03 ± 0.36wt.%, respectively. At this moment, dissolved oxygen concentration started to increase (data not shown), indicating depletion of the carbon source. Therefore, a 1 L REX-TPA pulse (containing 20 g/L TPA) was fed to the culture, rising the TPA concentration to 6.76 ± 0.87 g/L.

During the first 24 h, *Rhodococcus* sp. Ave7 produced 0.09 ± 0.00 g/L of PHA (Fig. II. 10 (B2)). Despite the subsequent feeding of a TPA pulse, no further increase in PHA concentration was observed until the end of the assay, resulting in a final polymer content in the cells of 3.05 ± 0.05wt.%, a significant statistical decrease from the previous assay, corresponding to an overall volumetric productivity of 0.062 g/(L.day) (Table II. 8). This PHA accumulation is comparable to that achieved by engineered *P. stutzeri* TPA3P (3.66wt.%) whilst using BHET as carbon source that yielded 3.54 g/L of biomass (Liu et al., 2021).

Regarding TAG accumulation, *Rhodococcus* sp. Ave7 achieved a biomass content of 11.03 wt.%, corresponding to a concentration of 0.35 ± 0.04 g/L (Fig. II. 10 (B2)), within the first 24 h of cultivation. After the TPA pulse provided at 24 h, under ammonium-limited conditions, TAG content continued to increase, reaching 0.48 ± 0.04 g/L (Fig. II. 10 (B2)) by the end of the cultivation. This represented a final TAG content in the biomass of 16.26 ± 0.12wt.%, corresponding to an overall volumetric productivity of 0.331 g/(L.day) (Table II. 8).

The TPA pulse conditions tested in Assay B resulted in a statistically significant increase in TAG content to 16.3 ± 0.1wt.% compared to the value obtained in Assay A under batch mode (13.45 ± 0.69wt.%) (Table II. 8). Previous studies with different *Rhodococcus* strains reported PHA and TAG accumulation capabilities. For instance, *R. jostii* RHA1, when grown on glucose or gluconate, accumulated PHA contents ranging from 2 to 7.6wt.% and TAGs content representing 56wt.% of the CDW (Hernández et al., 2008). Moreover, R. *aetherivorans* IAR1, grown on acetate or toluene, accumulated 10–12wt.% PHA and 24wt.% TAG of the CDW (Table II. 9) (Hori et al., 2009). Although *Rhodococcus* sp. Ave7 did not reach comparable TAG contents in this study, its PHA accumulation, using REX-TPA as the sole carbon source, was comparable to that of the reported strains.

The initial TPA (10.30 ± 0.01 g/L) available in the bioreactor was depleted within 24 h of cultivation, while further 2.34 g/L were consumed after the pulse, corresponding to an overall uptake of 12.67 ± 0.03 g/L. Moreover, a growth yield of 0.40 g_X/g_{TPA} was obtained, while the products' yields were 0.015 g_{PHA}/g_{TPA} and 0.081 g_{TAG}/ g_{TPA} (Table II. 8).

Table II. 9. Assessment of PHA, TAG and bioproducts from PET degradation products and pollutants feedstocks from various microbial strains. (EG, ethylene glycol; HAAs, hydroxyalkanoyloxy-alkanoates monomers; BHET, commercial bis(2-hydroxyethyl) TPA; BTEXS, benzene, toluene, ethylbenzene, p-xylene; n.a. not available; tr, traces).

Microbial Strain	Substrate	Cultivation mode	Time (h)	Biomass (g/L)	PHA (wt. %)	TAG (wt. %)	Bioproducts	Reference
Rhodococcus sp. Ave7	REX-TPA	Bioreactor	28-73	2.67-3.85	3.05-15.0	13.45-16.26	PHBV TAG	This study
R. pyridinivorans P23	TPA	Erlenmeyer	24-96	2.14	15	n.a.	PHBV	Guo & Shao, 2020
	Disodium terephthalate			2.65	23.8	n.a.		
Rhodococcus sp. A5	Hexadecane	Erlenmeyer	48	n.a.	Tr.	1.3-1.9 32	PHA TAG	Bequer Urbano et al., 2013
R. aetherivorans IAR1	Toluene	Erlenmeyer	80	2.5	10	24	PHBV TAG	Hori et al., 2009
R. jostii RHA 1	Hexadecane	Erlenmeyer	n.a.	n.a.	Tr.	30.4	PHBV TAG	Hernández et al., 2008
	Hexadecane + Hexadecanol		n.a.	n.a.	Tr.	7.0		
R. opacus PD630	Petroleum wastewater supplemented with molasses	Bioreactor	96	5.91	n.a.	52.5	Lipids	Saisriyoot et al., 2016
				7.24	n.a.	54.4		
Rhodococcus sp. 602	n-hexadecane	Erlenmeyer	48	n.a.	n.a.	22.3	PHA TAG	Silva et al., 2010
	Benzoate			n.a.	8.2	64.9		
Priesta sp.	REX-TPA	Shake Flask	n.a.	1.06	4.14	n.a.	PHA	Herrera et al., 2023
Streptomyces sp.			n.a.	1.39	0.32	n.a.		

Table II. 9. Assessment of PHA, TAG and bioproducts from PET degradation products and pollutants feedstocks from various microbial strains. (EG, ethylene glycol; HAAs, hydroxyalkanoyloxy-alkanoates monomers; BHET, commercial bis(2-hydroxyethyl) TPA; BTEXS, benzene, toluene, ethylbenzene, p-xylene; n.a. not available; tr, traces) (cont.).

Microbial Strain	Substrate	Cultivation mode	Time (h)	Biomass (g/L)	PHA (wt. %)	TAG (wt. %)	Bioproducts	Reference
Pseudomonas umsongensis GO16 KS3	Sodium terephthalate	Shake Flask	48	3.5	27	n.a.	mcl-PHA	Kenny et al., 2008
Pseudomonas putida GO19				3.5	23	n.a.		
Pseudomonas frederiks-bergensis GO23				4	14	n.a.		
Pseudomonas umsongensis GO16 KS3	Hydrolyzed PET	Bioreactor	28	2.3	7	n.a.	mcl-PHA HAAs	Tiso et al., 2021
Pseudomonas umsongensis GO16 KS3	Sodium terephthalate	Fed-batch Bioreator	48	8.7	30	n.a.	mcl-PHA	Kenny et al., 2012a
	Sodium terephthalate supplemented with waste glycerol	Fed-batch Bioreator	48	14.3	36	n.a.	mcl-PHA	
				15.1	35	n.a.		
				14.1	35	n.a.		
				11.7	36	n.a.		
Pseudomonas putida F1	Benzene	Shake flask	48	0.34	22	n.a.	mcl-PHA	Nikodinovic et al., 2008
	Toluene			0.72	15	n.a.		
	Ethylbenzene			0.67	14	n.a.		

Table II. 9. Assessment of PHA, TAG and bioproducts from PET degradation products and pollutants feedstocks from various microbial strains. (EG, ethylene glycol; HAAs, hydroxyalkanoyloxy-alkanoates monomers; BHET, commercial bis(2-hydroxyethyl) TPA; BTEXS, benzene, toluene, ethylbenzene, p-xylene; n.a. not available; tr, traces) (cont.).

Microbial Strain	Substrate	Cultivation mode	Time (h)	Biomass (g/L)	PHA (wt.%)	TAG (wt.%)	Bioproducts	Reference
Pseudomonas putida MT-2	Toluene	Shake flask	48	0.37	22	n.a.	mcl-PHA	Nikodinovic et al., 2008
	Xylene			0.53	26	n.a.		
Consortium of *Pseudomonas putida* (F1 +mt-2 + CA-3)	BTEXS mixture	Batch Bioreactor	48	1.03	24	n.a.		
Engineered Pseudomonas putida AW165	BHET	Bioreactor	96	n.a	n.a.	n.a.	β-ketoadipic acid	Werner et al., 2021
Engineered Pseudomonas stutzeri TPA3P	BHET	Erlenmeyer	54	3.54	3.66	n.a.	PHB	Liu et al., 2021

II.3.3.3. Fed-batch cultivation with continuous feeding

Aiming to further enhance PHA and TAG, Assay C was conducted under fed-batch mode with continuous feeding (Fig. II. 9c) that was initiated after 13 h of cultivation. The culture presented a lag phase of approximately 10 h (Fig. II. 10 (C1)) observed in Assays A and B. Afterwards, the bacterium entered an exponential phase with a maximum cell growth rate of 0.17 ± 0.01 h^{-1} (Table II. 8). TPA consumption remained low during the lag phase of the cultivation (of 0.22 g/L). At the start of the exponential phase, a continuous REX-TPA feed was initiated at a rate of 0.1 L/h, which lasted 15 h. As shown in Fig. II. 10 (C1), TPA concentration in the bioreactor increased between 13 and 21 h, reaching 13.8 g/L of TPA, which coincided with the onset of cell growth in the cultivation.

By the end of the experiment (73 h), the culture reached a maximum CDW of 3.58 ± 0.09 g/L (Table II. 8), which was significantly higher ($p \leq 0.001$) than the values obtained in assay A and B. TAG production started around 13 h (Fig. II. 10 (C1)), representing 15.40 ± 0.29wt.% of the CDW, with a final concentration of 0.59 ± 0.04 g/L (Fig. II. 10 (C2)), corresponding to a volumetric productivity of 0.252 ± 0.021 g/(L.day) (Table II. 8). These values are slightly lower than those obtained in Assay A and B (0.305 ± 0.001g/L and 0.331 ± 0.001 g/(L.day), respectively).

Interestingly, PHA synthesis was initiated around the same time of TAG, but it continued until the end of the assay, reaching a polymer content of 15.01±0.68wt.% (0.58 g/L), Fig. II. 10 (C2). PHA concentration was significantly higher than that observed for Assays A and B, leading to an overall volumetric productivity of 0.245 ± 0.001 g/(L.day) (Table II. 8). These results are close to those reported and patented for *Rhodococcus pyridinivorans* P23*,* a bacterium isolated from a PET film, which achieved similar levels of PHA accumulation when cultivated with commercial TPA (15wt.%) or disodium terephthalate (23.8wt.%) (Table II. 9) as substrates (Guo & Shao, 2020). Moreover, *R. aetherivorans* IAR1, grown under batch mode using acetate or in fed-batch mode with toluene as sole carbon sources, displayed a similar production profile to the one obtained in this experiment and synthesizing simultaneously both products during bacterial exponential phase. However, a lower PHA accumulation was reached (between 10 and 12wt.%) (Table II. 9) (Hori et al., 2009).

Nonetheless, the results showed that under the conditions of assays A and B, TAG accumulation (13.45 and 16.30wt.%) was favoured over PHA synthesis (4.22 and 3.05wt.%). On the other hand, in assay C, under continuous feeding, after ammonium depletion and with higher TPA availability, the TAG content remained comparable (15.40wt.%) to previous experiments, while PHA accumulation showed a statical significantly increased (from 3.05wt.% to 15wt.%) ($p \leq 0.001$). These findings suggest that higher TPA availability during continuous feeding of the carbon source apparently enhanced the flux towards PHA synthesis in *Rhodococcus* sp. Ave7, when ammonium became limiting.

In assay C, under continuous feeding conditions, a total of approximately 16.5 g/L of TPA were consumed, surpassing the consumption observed in Assay B. A growth yield of 0.24 g_X/g_{TPA} was

achieved, along with products' yields of 0.051 g_{PHA}/g_{TPA} and 0.052 g_{TAG}/g_{TPA} for PHA and TAG (Table II. 8), respectively, demonstrating significant improvement ($p \leq 0.001$) when compared to Assays A and B. Statistical analysis (Appendix A, Table A.1.) confirmed that continuous feeding significantly enhanced PHA accumulation compared to pulse feeding, while TAG accumulation remained statistically similar between Assays B and C. These findings underscore the metabolic flexibility of *Rhodococcus* sp. Ave7 under different feeding strategies and reinforce its potential for biotechnological applications. Additionally, the yields obtained in Assay C are higher than those reported for *P. umsongensis* GO16 KS3 (0.21 $g_{CDW}/g_{substrate}$ and 0.014 $g_{PHA}/g_{substrate}$), although this study was carried out in batch reactor (Tiso et al., 2021).

According to several literature reports, some *Rhodococcus* strains can accumulate intracellular reserves of glycogen or PolyP (Tajparast & Frigon, 2015). However, no glycogen nor PolyP were detected for *Rhodococcus* sp. Ave7 in any of the assays.

Overall, the bioreactor assays demonstrated that *Rhodococcus* sp. Ave7 possesses a high capacity for TPA degradation, consuming 30.46 ± 0.25 g in 73 h while yielding two value-added bioproducts. Biomass concentrations up to 3.85 g/L were reached, which is higher than the values reported, for example, for *R. pyridinivorans* P23 (2.14 -2.65 g/L) and *P. umsongensis* G016 KS3 (2.3 g/L), grown on similar feedstocks, including TPA and TPA derived from PET depolymerization (Table II. 9) (Guo & Shao, 2020; Tiso et al., 2021).

Additionally, *Rhodococcus* sp. Ave7 was able to accumulate PHA and TAGs as the main intracellular products, conducted under REX-TPA excess and an ammonium-limiting strategy. The values obtained for PHA accumulation with *Rhodococcus* sp. Ave7 are in accordance with those reported in literature for other bacteria tested on PET degradation products. Microorganism from different genera have been reported to utilize REX-TPA as substrate, however these cultivations were conducted under shake flask conditions, with strains such as *Priesta* sp. and *Streptomyces* sp. yielding polymer content of 4.14wt.% and 0.32wt.%, respectively (Table II. 9) (Herrera et al., 2023).

The PHA content in *Rhodococcus* sp. Ave7 biomass in assay C was significantly higher than the values reported for other *Rhodococcus* species. For instance, for *R. jostii* RHA1 grown on a mixture hexadecane and hexadecanol, only traces of PHA were detected (Hernández et al., 2008). Similarly, *Rhodococcus* sp. 602, which was grown on benzoate, accumulated 8.2wt.% of PHA (Silva et al., 2010). On the other hand, TAG production by *Rhodococcus* sp. Ave7 reached values similar to those reported by *R. jostii* when using mixtures of hexadecane and hexadecanol (7.0 %) (Hernández et al., 2008). However, it was lower than the 54.4% produced by *R. opacus* PD630 grown on petroleum wastewater supplemented with molasses (Table II. 9) (Saisriyoot et al., 2016).

II.3.3.4. Extraction and characterization of intracellular storage compounds

The biomass produced by *Rhodococcus* sp. Ave7, in Assay C, was recovered and the bioproducts were characterized. Soxhlet extraction with chloroform was used to extract both PHBV and TAGs were produced as intracellular storage reserve during cultivation. This solvent-based extraction method is commonly used for its high yields in extracting PHA and lipids, as well as its ability to achieve high polymer purity (Pérez-Rivero et al., 2019; Saini et al., 2021). After extraction, the polymer was precipitated by adding ethanol, a low molecular weight alcohol usually used for PHA recovery at laboratory scale (Koller et al., 2013; Mannina et al., 2020).

The PHBV recovered from the ethanol was dried at room temperature, revealing a low purity (29.5 ± 2.2%). As shown in Fig. II. 11, the recovered sample presented an oily appearance due to the significant amounts of TAGs precipitating together with PHBV (Fig. II. 11b), indicating that ethanol was not effective for separating these compounds. This occurred because the ethanol, used to separate the polymer from non-PHA compounds coextracted by chloroform, was placed at -20 ºC, causing the crystallization and precipitation of TAGs (Nielsen & Shukla, 2004).

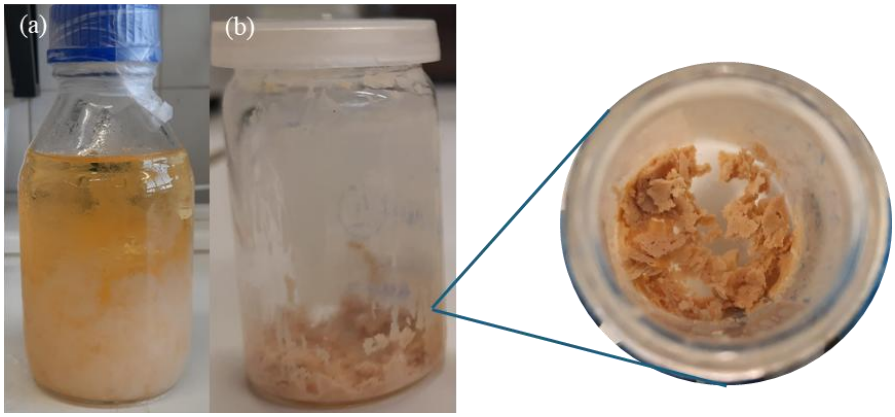

Figure II. 11- Images of the extraction from *Rhodococcus* sp. Ave7 biomass precipitated in cold ethanol (a) and the dried sample recovered (b).

PHBV and TAGs are difficult to separate due to their similar polarity, with PHBV being semi-polar (Vermeer et al., 2022) and TAGs non-polar and water-insoluble (Alvarez et al., 2017; Zarrinmehr et al., 2022). Using highly polar or non-polar solvents, namely alcohols or alkanes, to precipitate PHBV often results in TAGs precipitating as well, due to PHBV's low solubility in these solvents (Vermeer et al., 2022). Additionally, the polymer's high 3HV content and the precipitation temperature are key factors in solvent selection (Werker et al., 2015).

1-Butanol was selected for the second polymer precipitation at a higher temperature, based on studies showing its effectiveness in recovering PHA from biomass (Werker et al., 2015) and recently for its use

as antisolvent to purify PHBV with 50% 3HV content to 98.0 ± 0.1% purity (de Souza Reis et al., 2020). After this second precipitation, the recovered sample had a much whiter, opaque appearance (Fig. II. 12), in contrast to the ethanol-purified sample (Fig. II. 11). This appearance is consistent with other studies where PHBV purified with 1-butanol also showed a whiter colour (de Souza Reis et al., 2020).

Figure II. 12 – Image of the dried PHBV sample recovered from the PHBV+TAGs extract after precipitation in 1-butanol.

Overall, the 1-butanol precipitation allowed to increase the polymer's purity to 55.7 ± 3.8% of purity. Although the quantity of TAGs was reduced, $C_{18:1}$, $C_{16:0}$ and $C_{18:0}$ acids produced by *Rhodococcus* sp. Ave7 were still found in the sample recovered. The procedure was able to dissolve a significant part of the TAGs under the conditions used, as 1-butanol is known to facilitate the transesterification of TAGs into biodiesel (Wahlen et al., 2011). However, it did not completely separate the two bioproducts, as evidence by the lack of homogeneity in the sample shown in Fig. II. 12. After heating, the butanol was allowed to cool to room temperature to remove the butanol fraction containing dissolved TAGs from the precipitated polymer. However, the decrease in temperature may have caused some TAGs to precipitate along with the polymer since fatty acids such as $C_{18:1}$, $C_{16:0}$, and $C_{18:0}$, found in TAGs produced by *Rhodococcus* sp. Ave7, were still present in the recovered sample.

II.3.3.5. Characterization of TAGs

Composition

Cis-9-octadecenoic acid ($C_{18:1}$) (43.3-50.8wt.%) and hexadecanoic acid ($C_{16:0}$) (32.1-38.9wt.%) were the predominant fatty acids in the TAG produced in all assays, with lower contents of octadecanoic acid ($C_{18:0}$) (8.5 -8.7wt.%) (Fig. II. 13). Moreover, in assays A and B, 3.1-3.2wt.% of cis,cis,cis-9,12,15-octadecatrionic acid ($C_{18:3}$), a polyunsaturated fatty acid was also detected, together with other minor

fatty acids fractions, such as tetradecanoic acid ($C_{14:0}$) (2.3-3.0wt.%) and docosanoic acid ($C_{22:0}$) (1.2 - 2.9wt.%).

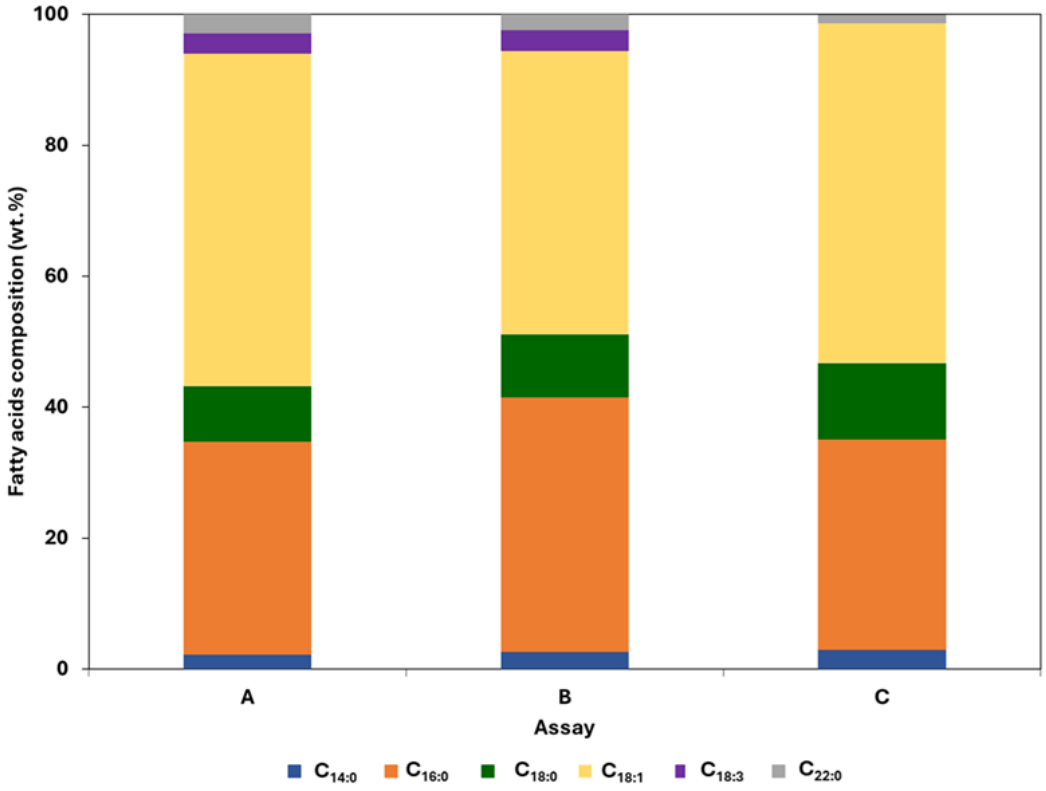

Figure II. 13 - Fatty acids composition of the TAGs produced by *Rhodococcus sp.* Ave7 attained in biomass obtained at the end of the cultivation assays.

Similar fatty acids compositions were detected for *R. pyridinivorans* CCZU-B16 and *R. aetherivorans* IAR1, although their relative contents were significantly different. *R. pyridinivorans* CCZU-B16 TAG presented a fatty acids profile rich in $C_{16:0}$ (22.4%), $C_{16:1}$ (21.1%), $C_{18:0}$ (16.2%) $C_{18:1}$ (23.1%) (Chong et al., 2018). Furthermore, *R. aetherivorans* IAR1 was also reported as TAGs producer from toluene, showing a profile in fatty acids mainly comprising $C_{16:0}$ (~ 50%), followed by $C_{18:1}$ (25%), with fatty acids such as $C_{18:0}$, $C_{17:0}$, $C_{16:1}$ and $C_{14:0}$ also being detected (Hori et al., 2009). *Rhodococcus* sp. Ave7 cultivated in REX-TPA represents a source of TAGs rich in fatty acids, comparable to the species *R. rhodochrous*, which produced TAG composed mostly of $C_{16:0}$ (35%) and $C_{18:1}$ (42 %) (Shields-Menard et al., 2015). zx

The predominance of $C_{18:1}$ and $C_{16:0}$ fatty acids, commonly found in soybean oil and palm oil, renders *Rhodococcus* sp. Ave7 TAGs as potential candidates, for example, for biodiesel as oxidative stabilizer, cetane number and balancing cold flow properties (Shields-Menard et al., 2015). These findings suggest

the possibility of using the produced fatty acids as a complementary and renewable source alongside these oils, whilst valorising a PET waste through a more sustainable approach (Ahmad et al., 2019).

FTIR

The FT-IR spectra for TAGs produced in assay C (Fig. II. 14a) show a band around 2853 and 2922 cm^{-1} are related to the asymmetric and symmetric stretching vibrations of the C-H bonds in the alkane hydrocarbon chains of fatty acids in TAGs (Chaturvedi et al., 2023).

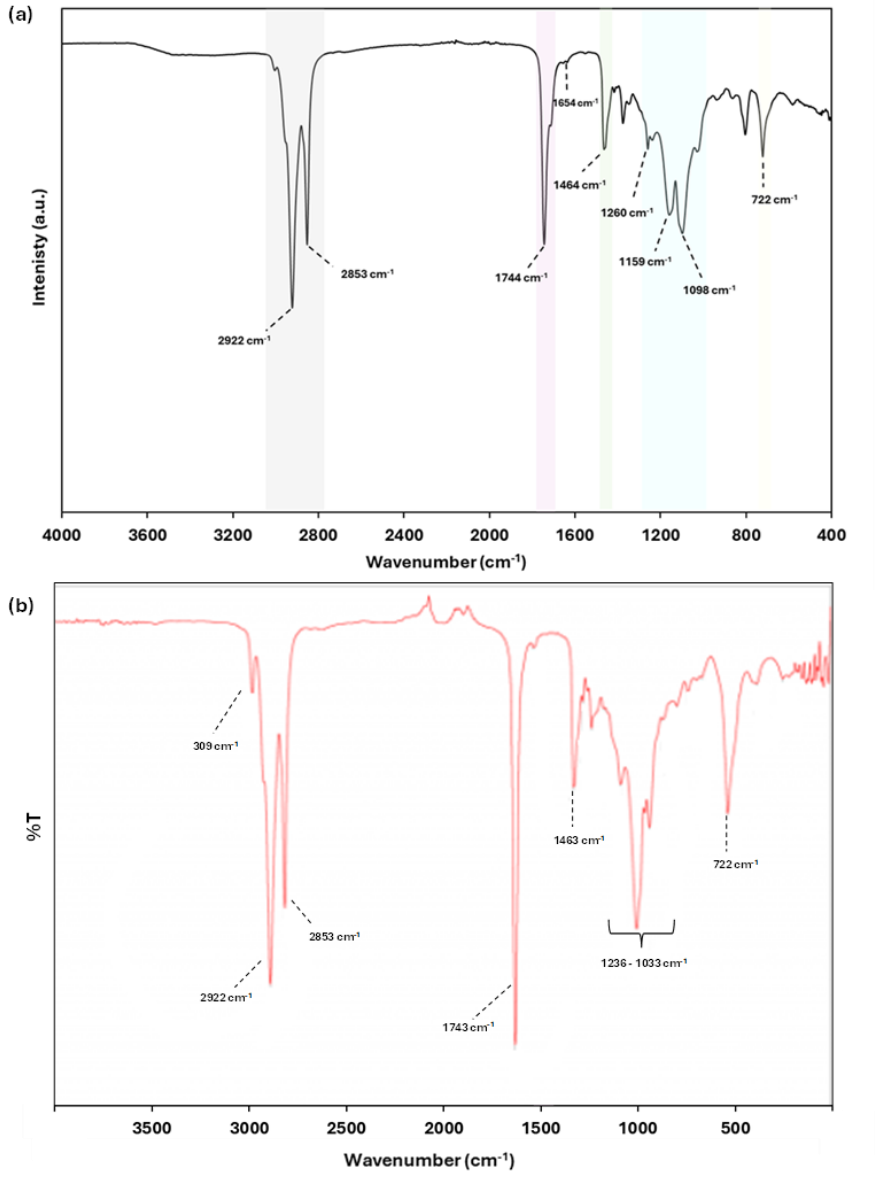

Figure II. 14 - FT-IR spectra for (a) TAGs produced by *Rhodococcus* sp. Ave7 during fed-batch with continuous feed conditions and (b) soybean oil (adapted from Vahur et al., 2025).

The intense peak at 1744 cm^{-1} is related to C=O stretching vibration in ester groups of TAGs (Suri et al., 2019). Moreover, a weaker peak at 1654 cm^{-1} associated with C=C stretching vibrations were detected, indicating the presence of unsaturated bonds in $C_{18:1}$ structure, one of the main fatty acids that compose TAGs produced by *Rhodococcus* sp. Ave7 (Nosal et al., 2020). Additionally, the bands observed between 1098-1158 cm^{-1} correspond to the stretching vibration of C-O bond in TAGs ester groups. The band at 1464 cm^{-1} is related with the deforming vibration of C-H bonds in aliphatic groups of TAGs (Suri et al., 2019). A band at 722 cm^{-1} appear due to the vibration of the -CH_2 groups present in $C_{18:1}$ structure (Chaturvedi et al., 2023).

When compared to the FT-IR spectra of a soybean oil (Fig. II 14b), a relevant reference due to its similar composition to the TAGs produced by *Rhodococcus* sp. Ave7, particularly the presence of $C_{18:1}$, $C_{18:0}$ and $C_{16:0}$ fatty acids, both spectra share similar features, such as the intense 1743 cm^{-1} peak for C=O stretching and the 2922 and 2853 cm^{-1} peaks for C-H vibrations, indicating a comparable TAG structure. However, variations in peak intensity or position, such as those observed for the 1159 cm^{-1} band in soybean oil, reflect differences in the composition of unsaturated fatty acids and potential variations in the degree of saturation or chain length of fatty acids (Poiana et al., 2015). These differences likely result from the distinct cultivation conditions of *Rhodococcus* sp. Ave7 and TAGs recovery methods used.

II.3.3.6. Characterization of PHA

Composition

The PHA produced by *Rhodococcus sp.* Ave7, in all assays, was a co-polymer of 3-hydroxybutyrate (3HB) and 3-hydroxyvalerate (3HV) monomers, namely PHBV. As shown in Table II. 10**,** 3HV is the main monomer in all assays, accounting for 60.5 ± 0.2wt.% of the biopolymer produced in Assay A under batch conditions, while under fed-batch mode, it increased, representing 88.1 ± 0.3wt.% and 92.0 ± 0.1wt.% in Assays B and C, respectively (Table II. 10).

Table II. 10. Monomeric composition of PHA produced by *Rhodococcus sp.* Ave7 in biomass attained at the end of the cultivation assays using REX-TPA as feedstock (n.d. not detected; 3HB, 3-hydroxybutyrate; 3HV, 3-hydroxyvalerate).

Assay	**PHA composition (wt.%)**	
	3 HB	3 HV
A	39.5 ± 0.2	60.5 ± 0.2
B	11.9 ± 0.3	88.1 ± 0.3
C	8.1 ± 0.1	92.0 ± 0.1

Similar composition, namely high 3HV contents, was reported for PHBV synthesized by different *Rhodococcus* sp. For instance, *R. ruber* NCIM 40126 grown on different substrates, such as acetate, fructose, glucose, presented 3HV as the main monomer, at contents ranging from 69-84mol%, whilst *R. rhodochrous* ATCC19070 reached 3HV contents between 73-97 mol% while using the same substrate (Haywoodt et al., 1991). Additionally, *R. aetherivorans* IAR23 produced a PHA with 79 mol% of 3HV and 21 mol% of 3HB on acetate, increasing the 3HV fraction to 80mol% when grown on toluene (Hori et al., 2009). *R. pyridinivorans* P23 is reported to synthesize PHA with 3HV monomer content higher than 60 mol% using TPA as feedstock (Guo & Shao, 2020).

This study demonstrated that REX-TPA can be used as feedstock for the synthesis of high 3HV content PHBV by *Rhodococcus* sp. Ave7. This increased proportion in 3HV in the polyester presents the opportunity for tunning properties such as thermal features, which are crucial for the manipulation during processing of PHBV copolymers blends applications (Langford et al., 2019). It has been reported, for copolymers with 3HV contents similar to the one obtained in this study, melting temperatures (89-110 ºC) in the range of those reported for PHBV 50-80mol% with a variation regarding the crystallinity degree (54-62 %), which affects directly on the biodegradability of the material (Feng et al., 2004; Langford et al., 2019). Furthermore, the production of PHBV is highly priced when compared to fossil-fuel-derived plastics (Policastro et al., 2021), therefore, exploiting *Rhodococcus* sp. Ave7 upcycling of TPA from depolymerized non-recyclable PET waste establishes the opportunity to render a more environmental and circular economic process for plastics.

FTIR

The FT-IR spectra (Fig. II 15a) for PHBV produced by *Rhodococcus* sp. Ave7 shows an intense peak at 1723 cm^{-1}, corresponding to the stretching band of the carbonyl group (-C=O) (Ponjavic et al., 2023), characteristic of PHA spectra. Peaks between 2855 to 2964 cm^{-1} are associated with the C-H stretching vibrations of the methyl and the methylene groups in the polymer structure and side chain (Ponjavic et al., 2023), while the broad region between 969-1074 cm^{-1} corresponds to the C-C bonds (Ajmal et al., 2018). The peak at 1258 cm^{-1}, linked to the asymmetric stretching of saturated ester bond (C-O-C) (Ponjavic et al., 2023), is associated with the crystallinity of the biopolymer, suggesting that low crystallinity is expected for the PHBV produced by *Rhodococcus* sp. Ave7 (Esmail et al., 2021). In comparison to the PHBV with 11% 3HV content (Fig. II 15b), the spectra for PHBV produced by *Rhodococcus* sp. Ave7 (Fig. II 15a) exhibits notable differences, particularly in the intensity of this peak further suggesting the reduced crystallinity of the polymer attained by *Rhodococcus*. Additionally, the variations in the band at 1452 cm^{-1}, associated with CH_2 bending vibrations, highlight the influence of compositional differences in the polymer backbone.

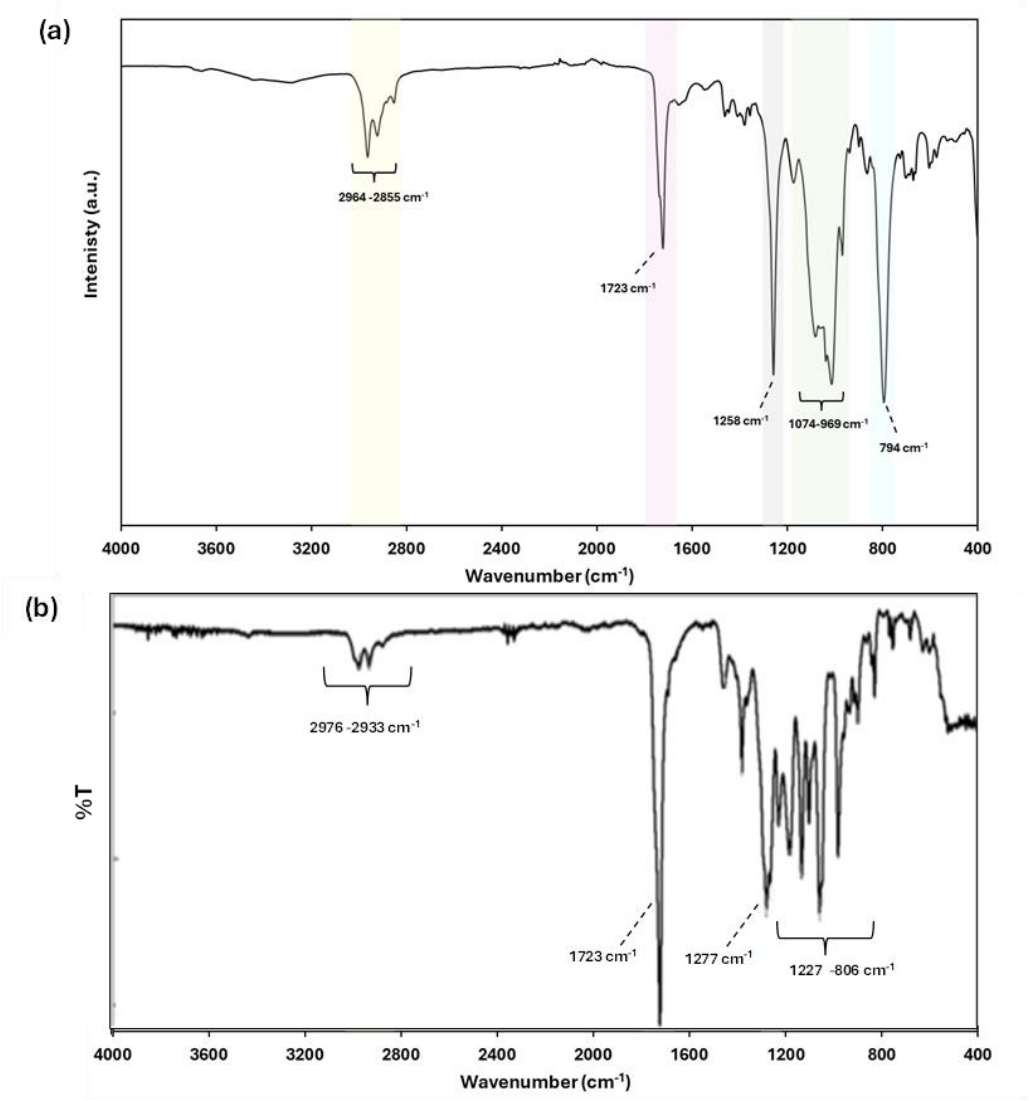

Figure II. 15 - FT-IR spectra of (a) PHBV produced by *Rhodococcus* sp. Ave7 during assay C, under fed-batch with continuous feed conditions, and (b) PHBV with 11% 3HV content (adapted from Chaber et al., 2022).

Molecular mass distribution

The PHBV produced had a M_w of 277 kDa and a PDI of 1.5 (Table II.11), falling within the typical range of M_w (250-820 kDa) and PDI (1.4 to 2.7) values reported for PHBV with high 3HV content (58 to 98mol%) (Feng et al., 2004). Moreover, the M_w and PDI obtained was also comparable to the PHBV, 260 kDa and PDI of 1.9, produced by mixed microbial cultures with 82mol% 3HV (Langford et al., 2019). Nevertheless, the M_w attained for *Rhodococcus* sp. Ave7 PHBV was low compared to the produced by *R. pyridinivorans* P23 (M_w of 600 kDa) using TPA, but still within the same order of magnitude (Guo & Shao, 2020).

The PDI of the PHBV attained in assay C suggests a good polymer uniformity, which may facilitate its processing and biodegradation rate (Elhami et al., 2022; Hong et al., 2013).

Table II. 11. Physical- chemical and thermal properties of PHBV produced in Assay C from *Rhodococcus* sp. Ave7 (M_w, molecular weight; PDI, polydispersity index; T_m, melting temperature; ΔH_m, melting temperature; T_{deg}, degradation temperature; X_c, crystallinity index).

Characterization	Value
M_w (k Da)	277
PDI	1.5
T_m (°C)	95.1
ΔH_m (J/g)	26.3
X_c (%)	18.0
T_g (°C)	-21.1
T_{deg} (°C)	270.0

Thermal properties

The biopolymer presented a T_m of 95.1 °C (Appendix A, Figure A.1) that is within the range of several PHBV with 3HV contents varying between 58 and 98 mol% (89.9 -109.4 °C) (Feng et al., 2004), and similar to the T_m (101 °C) reported for PHBV produced with TPA as feedstock (Guo & Shao, 2020). The high 3HV content in the copolymer lowers the T_m significantly, thus broadening its processability window, which facilitates the polymer processing in comparison to the homopolymer composed by 3HB, characterized by a T_m very close to the degradation temperature (Urtuvia et al., 2023).

The PHBV also exhibited a T_g of -21.1 °C (Table II. 11), which is significantly lower than the typical values reported for PHBV with 3HV contents of 82mol% (-13.2 °C) (Langford et al., 2019). The low T_g observed for PHBV may result from TAGs still present in the polymer matrix after 1-butanol precipitation, potentially acting as plasticizers that increase the free volume between PHBV chains and enhance their mobility at lower temperatures, as reported for PHBV and plasticizers blends (Nosal et al., 2020; Umemura & Felisberti, 2021).

The polymer presented a crystallinity of 18.0% (Table II. 11), indicating it was more amorphous than other 3HV-rich PHBV (40-50 mol % of 3HV) that present crystallinities within 50% (Feng et al., 2004). For copolymers where 3HV content was higher, a higher crystallinity was expected since it would mainly take the crystal structure of the P(3HV) homopolymer lattice (Wang et al., 2001). This decrease

in crystallinity may be related to the presence of remnants of TAGs that were not completely removed from the sample (Kaniuk et al., 2022), as previously detected in the biopolymer FT-IR spectrum. Nevertheless, the biopolymer's low crystallinity may provide more flexibility compared to other PHBV blends with lower 3HV content, making it suitable for applications that require softer, more flexible materials (Langford et al., 2019).

The biopolymer was thermally stable until 270 °C (Fig. II. 16), in concomitant with T_{deg} (279 °C) for other 3HV-rich PHBV, where it suffered a weight loss of 46% (Chan et al., 2019). Above this temperature, a second weight loss of 15.5%, was attained at 395.5 °C followed by a third observed at 503.6 °C for 33.8 % of weight loss. These later stages of degradation are attributed to the degradation of fatty acids, confirming the decomposition of TAGs monounsaturated and saturated fatty acids, mainly composed by $C_{18:1}$, $C_{16:0}$ and $C_{18:0}$ (Sanahuja et al., 2011).

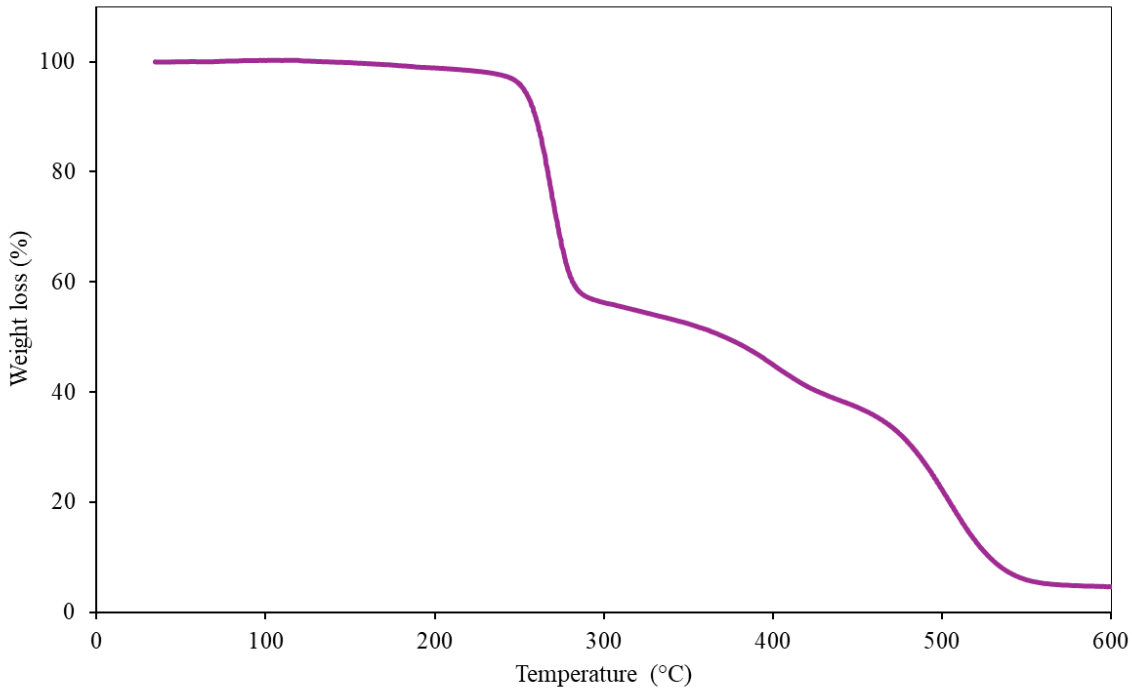

Figure II. 16 - Thermogravimetric curve of PHBV produced from *Rhodococcus* sp. Ave7 using REX-TPA as feedstock.

The presence of fatty acids significantly affected the thermal properties of the sample. The fatty acids within the polymer matrix exhibited higher T_{deg} than the individual oleic, stearic and palmitic methyl esters (210-229 °C for 5% weight loss) or their ethylene glycol esters (228-248 °C) tested as potential PHBV plasticizers (Nosal et al., 2020). This shows that the presence of TAGs-derived fatty acids in the polymer provide a higher window of thermal stability compared to previously PHBV composites with

similar fatty acids. This demonstrates that PHBV materials with high 3HV content can be tailored by adding natural fatty acids as plasticizers, enhancing the biopolymer's performance, particularly in the thermal stability for end-use applications (Nosal et al., 2020).

II.4. Conclusions

This chapter reports the use of chemical depolymerized pcPET waste (REX-PET) as feedstock for microbial upcycling experiments. REX-PET was processed into a TPA-containing solution (REX-TPA) that was used as sole substrate for bacterial cultivation experiments.

Bacteria isolated from contaminated sites, namely *Delftia* sp. Ave5 and *Rhodococcus* sp. Ave7, were tested for their ability to grow using REX-TPA. RSM was used to assess how the concentrations of REX-TPA and ammonium influenced cell growth and polymer storage by each strain. *Delftia* sp. Ave5 showed maximum CDW (2.12 g/L) for high REX-TPA (11.66 g/L) and ammonium (0.50g/L) concentrations. On the other hand, *Rhodococcus* sp. Ave7 revealed to be the strain able to produce higher CDW values (5.09 g/L) for similar REX-TPA and ammonium conditions as *Delftia* strain. Concerning PHA, *Delftia* sp. Ave5 and *Rhodococcus* sp. Ave7 were able to produce polymer under the experimental conditions assessed in the RSM, for 10-11.66 g/L and 0.17-0.5 g/L ranges of REX-TPA and ammonium, attaining 7.88 and 22.55wt.%, for *Delftia* sp. Ave5 and *Rhodococcus* sp. Ave7 respectively. Furthermore, during the experiments, it was possible to detected and quantify the accumulation of a second storage compound by *Rhodococcus* sp. Ave7, TAGs for 6-10 g/L of REX-TPA under limiting concentration of ammonium (0.03-0.17 g/L).

This work validated *Rhodococcus* sp. Ave7 as a promising microorganism for the bioremediation of PET waste, given its high capacity for TPA bioconversion. The culture efficiently upcycled depolymerized pcPET waste into biomass, PHA and TAGs. The biosynthesized TAGs, on the other hand, were enriched in $C_{18:1}$ and $C_{16:0}$, which might be of interest to pair with the existing production from vegetable oils sources. The produced co-polyester PHBV, with a 3HV content up to 90wt.%, exhibited potential for being used in PHBV copolymer blends. The recovered polymer demonstrated an impact on the sample thermal properties, related to the high content in 3HV and the presence of fatty acids, which contributed to a broader thermal stability range. This suggested a potential opportunity to develop PHBV with thermal properties improved by the presence of $C_{18:1}$, $C_{16:0}$ and $C_{18:0}$ fatty acids as potential plasticizers. Overall, the bioreactor process study demonstrated the potential of *Rhodococcus* sp. Ave7 for effective biodegradation of chemically depolymerized mixed PET waste into value-added bio-based products, thus contributing to reduce the impact of PET waste and valorising it into value-added products, within the circular economy concept.

III.

POST-CONSUMER PET WASTE UPCYCLING INTO BIO-PLASTICS: UNLOCKING THE POWER OF A NATURAL MICROBIOME

The results presented in this chapter, are part of the publication under preparation:

Rebocho, A. T., Almeida, B., Torres, C.A.V., Boer, T., Budin, C., Fournet, M.B., Reis, M.A., & Freitas, F. Post-consumer PET waste upcycling into bioplastics: unlocking the power of a natural microbiome.

The depolymerized pcPET waste used in this study was kindly provided by the Materials Research Institute of the Technological University of the Shannon Midlands Midwest (TUS) (Ireland), in the scope of the PanEuropean project BioICEP (https://www.bioicep.eu/).

The 16S rDNA community analysis was performed at Microlife Solutions (Amesterdam, Netherlands) by Dr. Tjalf de Boer and Clémence Budin, in the scope of the PanEuropean project BioICEP (https://www.bioicep.eu/).

This page was intentionally left blank

Summary

This study evaluated the upcycling of chemically depolymerizing pcPET waste (named REX-PET) into PHA, a natural biodegradable plastic. A microbiome collected from a river marshland was subjected to a cyclic (4 days) feast-and-famine (F/f) strategy for 113 days, with hydraulic (HRT) and solids retention times (SRT) of 40 days, in a controlled bioreactor fed with a terephthalic acid (TPA) rich solution prepared from REX-PET as sole feedstock. The prolonged HRT and SRT, coupled with a strategic cyclic 4-day F/f approach, allowed the system's stability over only one retention time, resulting in a consortium with a high PHA accumulation capacity using REX-TPA substrate, maintaining stability until the end of the assay (an additional two retention times). During that time, three production assays were conducted, in which the culture consumed up to 6.93 ± 0.03 g/L TPA in 29 h and reached PHA contents in the biomass of 71.32 ± 0.34wt.%. The microbial community obtained in the end of the selection was predominantly composed of *Gammaproteobacteria*, with *Halomonadaceae* and *Zoogloeaceae* families identified as key contributors, both known for their PHA-producing capabilities. These findings demonstrate for the first time the feasibility of converting a non-biodegradable petrochemical-based plastic (i.e., PET) into a natural biodegradable plastic (i.e., PHA) by a mixed microbial culture using depolymerized PET waste as sole feedstock. The results also highlight the critical role of long SRTs and cyclic F/f regimes in rapidly enhancing PHA production and establishing a robust microbial consortium for sustainable plastic upcycling.

Keywords

Polyethylene terephthalate; Biodegradation; Plastic upcycling; Microbiome; Polyhydroxyalkanoates

III.1. Introduction

Microbial communities are complex and diverse networks of microorganisms interacting with each other and their environment across diverse ecosystems (Zuñiga et al., 2017). Their adaptability is driven by their high enzyme diversity, robust protein expression, resilience to metabolic perturbations (e.g., nutrient availability, temperature, pH, tolerance to toxic compounds), as well as cooperative interactions, like division of labour, enabling them to thrive and remain robust in a wide range of environments (Lyu et al., 2024; Scarborough et al., 2022; Wu & Wang, 2024).

Due to these capabilities, microbial communities have been increasingly applied for bioremediation, sustainable waste valorisation and biomanufacturing (Lahel et al., 2016; Scarborough et al., 2022). They can degrade a wide range of complex substrates (Lyu et al., 2024) including lignocellulosic (Wongfaed et al., 2023) and recalcitrant compounds such as petroleum wastewater (Ghosh & Chakraborty, 2020), phenol (Zhang et al., 2018), chlorinated solvents (Amanat et al., 2022), mixed plastic waste and polystyrene (Marzulli et al., 2023). Thus, mixed microbial cultures (MMCs) have been increasingly used to convert these feedstocks into high-value bioproducts, such as renewable energy (Campanari et al., 2017), biochemicals (Zhou et al., 2017) and bioplastics (Silva et al., 2022), offering a sustainable alternative to fossil fuel-based production processes (Lyu et al., 2024).

MMC-based technologies are commonly derived from natural microbial consortia in which a selective pressure is applied under controlled conditions to guide the microbial community and activity toward a specific function, namely the production of key catabolic products (Lin et al., 2011; Lyu et al., 2024). For instance, selective enrichment of PHA-storing microorganisms through efficient conversion of complex substrates into bioplastics. An example of this is the use of an acclimatized sludge for phenol degradation, by varying parameters such as pH, dissolved oxygen levels and C/N ratio, the culture achieved a maximum PHA% production rate of 1.15% min^{-1} under 500 mg/L of phenol (Zhang et al., 2018).

During PHA production from feedstocks, MMC process typically involves three stages: (i) conversion of wastes into organic acids through acidogenic fermentation; (ii) a selection reactor, in which a microbial community is enriched with PHA-storing organisms by feeding with the organic acids produced in the acidogenic reactor, which are the precursors for PHA synthesis; (iii) an accumulation reactor, where the enriched culture is fed with the organic acids up to the culture's maximum capacity (Reis et al., 2011).

The selection stage is a central part of process, where the culture is subjected to an aerobic dynamic feeding (ADF) strategy, also known as the feast-and-famine (F/f) strategy (Chen et al., 2017). This approach alternates between periods of carbon availability (feast phase), which promote polymer storage, followed by periods of carbon starvation (famine phase) during which stored PHA is consumed as

carbon and energy source for cellular viability maintenance. Although the long famine period limits RNA and enzymes levels, required for cell growth, the PHA synthase remains active, enabling a rapid metabolic response at the start of a new feast phase, for PHA storage metabolism and its subsequent use for growth during starvation (Moretto et al., 2020; Reis et al., 2011). Microorganisms' incapable of producing PHA during the feast, do not survive the famine phase and are eliminated from the reactor (Nguyenhuynh et al., 2021; Pakalapati et al., 2018). The F/f strategy imposes a strong selective pressure, favouring PHA-storing microorganism and enhancing their physiological adaptation to PHA synthesis in the feast phase (Villano et al., 2014). Research on MMC technology has focuses on activated sludge utilizing agro-industrial feedstocks, including municipal solid waste (Moretto et al., 2020), fruit waste (Silva et al., 2022), and brewery spent grain (Guarda et al., 2024) aiming to enhance cost-effectiveness (Zhou et al., 2023). More recently natural sediments, from soil sediments, coastal wetlands and river estuarine have showed their potential as MMC for PHA production although using defined substrates (Chen et al., 2017; Cui et al., 2016; Ntaikou et al., 2018).

Estuaries are coastal wetlands where the transition of sediments between marine and fluvial environments occurs, often acting as sinks for sediments (Moreira et al., 2009). The marshes affected by tidal processes are dynamic habitats, characterized by cyclical fluctuations (dissolved oxygen, temperature, and salinity) due to diurnal tides (Weinstein et al., 2020). In the Tagus Estuary, intertidal areas have been contaminated from several human activities (maritime, aquaculture, agriculture, etc.), turning these ecosystems vulnerable to accumulate plastic debris and pollution, that has been associated with urban wetlands (Khuyen et al., 2021; Martins et al., 2023; Townsend et al., 2019). In these ecosystems, microorganisms play a crucial role for bioremediation of pollutants such as plastic debris and petroleum hydrocarbons, in which recently isolated bacteria from mangrove sediments have demonstrated ability to degrade PET (Afianti et al., 2024; Rawte et al., 2002).

MMCs have been evaluated for their ability to degrade TPA using active sludge (Aksu et al., 2021; Ma et al., 2020) and natural microbiomes, such as mangrove sediments that showed potential to biodegrade synthetic plastic like PET and PS (Auta et al., 2022). Although PHAs can be produced from PET degradation monomers such as TPA, through microbial cultivations, by single cultures (wild strain or engineered bacteria) (Liu et al., 2021; Maurya et al., 2023; Tiso et al., 2021), the production of PHA from TPA with MMC is still to be reported.

The objective of this study was to select a culture enriched in PHA-producing microorganisms of a natural microbiome from the Tagus River estuarine marshland (Corroios, Portugal) by applying a feast-and-famine (F/f) regime. The sole feedstock was a TPA-containing solution (REX-TPA) obtained from depolymerized pcPET waste (REX-PET), aiming to achieve the microbial valorisation of TPA. into PHAs. To the best of the authors' knowledge, this strategy has never been performed by a mixed

microbial culture (MMC). The produced bioplastic was characterized for its composition, molecular mass distribution, and thermal properties.

III.2. Materials and methods

III.2.1. Post-consumer PET waste depolymerization and feedstock preparation

The depolymerization and preparation of pcPET waste as feedstock for bioreactor cultivation was conducted as described in section II.2.1.

III.2.2. Microbial source

The natural microbiome was collected from Tagus River estuarine marshland (Fig. III. 1a), located at Corroios, Portugal (38°38'27.3"N 9°07'46.0"W), on June 6th, 2023, during the low tide (7:30 am), with an ambient temperature of around 20 ºC. Approximately 1 L of sediments were collected from the upper layer of a non-vegetated area and placed in a plastic bag (Fig. III. 1b). On the same day, the sediments were sieved to remove larger particles (above 2-3 mm) and homogenised by magnetic stirring (100-150 rpm) (Fig. III. 1c). A sample collected at 20 °C was taken to measure its pH and conductivity, as well as for elemental analysis and ICP-AES.

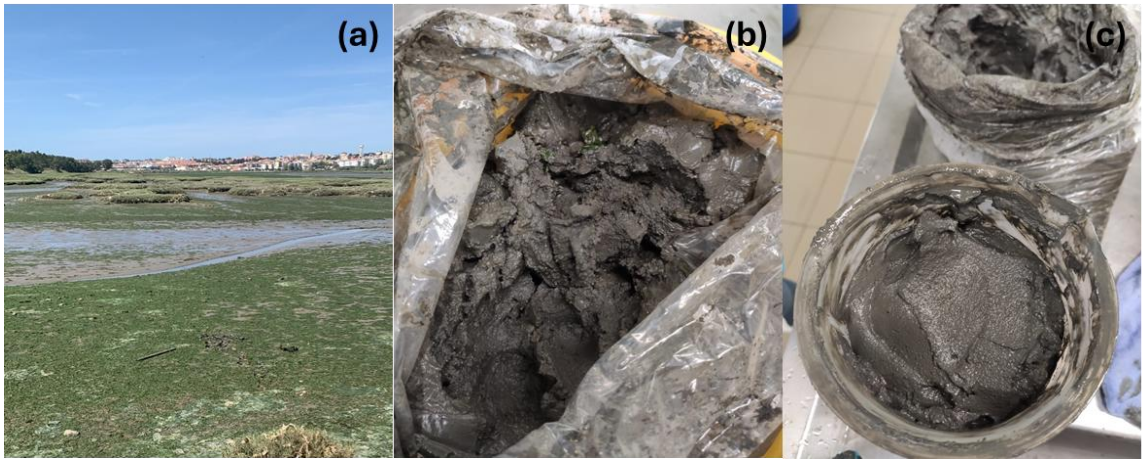

Figure III. 1 - Tagus River estuarine marshland at Corroios, Portugal, on June 6th, 2023, during the low-tide (a), where sediments were collected (b) and later sieved to be used as inoculum for the selection bioreactor (c).

III.2.3. Cultivation assays

III.2.3.1. Media

Mineral solution was used in all experiments. It was composed of (per liter): NH_4Cl, 0.4 g; $MgSO_4 \cdot 7H_2O$, 0.6 g; $CaCl_2 \cdot 2H_2O$, 0.07 g; EDTA, 0.1; K_2HPO_4, 0.92 g; KH_2PO_4, 0.45 g; micronutrients' solution, 1 mL. The micronutrients' solution comprised (per liter of 1N HCl): 1.5 g $FeCl_3 \cdot 6H_2O$; 0.15 g H_3BO_3; 0.03 g $CuSO_4 \cdot 5H_2O$; 0.03 g KI; 0.12 g $MnCl_2 \cdot 4H_2O$; 0.06 g $Na_2MoO_4 \cdot 2H_2O$; 0.12 g $ZnSO_4 \cdot 7H_2O$; 0.15 g $CoCl_2 \cdot 6H_2O$. The media was supplemented with REX-TPA to give a TPA concentration of approximately 20 g/L. Afterwards, it was autoclaved at 121 ºC and 1 bar, for 20 min. The phosphate solution was autoclaved separately and mixed with the rest of the medium after autoclaving and cooling at room temperature.

III.2.3.2. Selection bioreactor

A 2 L bioreactor (BioStat B-Plus, Sartorius, Germany) was operated with 4 days F/f cycles, comprising a feast phase initiated by feeding a pulse of fresh MSM (200 mL) supplemented with REX-TPA to reach a TPA concentration of 2 g/L in the bioreactor, followed by a famine phase (determined by the depletion of TPA). At the end of each cycle, 200 mL of cultivation broth were withdrawn, and the subsequent cycle was initiated by addition of fresh MSM (200 mL) containing REX-TPA. These operating conditions corresponded to a hydraulic and solids retention times (HRT and SRT, respectively) of 40 days. The bioreactor (Fig. III. 2) was inoculated with the marshland sediments (~600 mL), prepared as described above, and operated at controlled temperature (20 °C ± 0.1) and pH (8.00 ± 0.50). pH control was done through the automatic addition of 0.5 M HCl and 2 M NaOH. The air flow rate was kept at 1 SLPM and the stirring rate was kept at 300-400 rpm.

Reactor performance was monitored over time by collecting samples (20 mL) at the beginning and end of each cycle for the quantification of the total and the volatile suspended solid (TSS and VSS, respectively), TPA, ammonium and PHA. The nutrients' concentration and PHA content profiles were further monitored throughout the 4 days of cycles 4, 9. 15 and 26. Samples were also taken for 16s rRNA analysis.

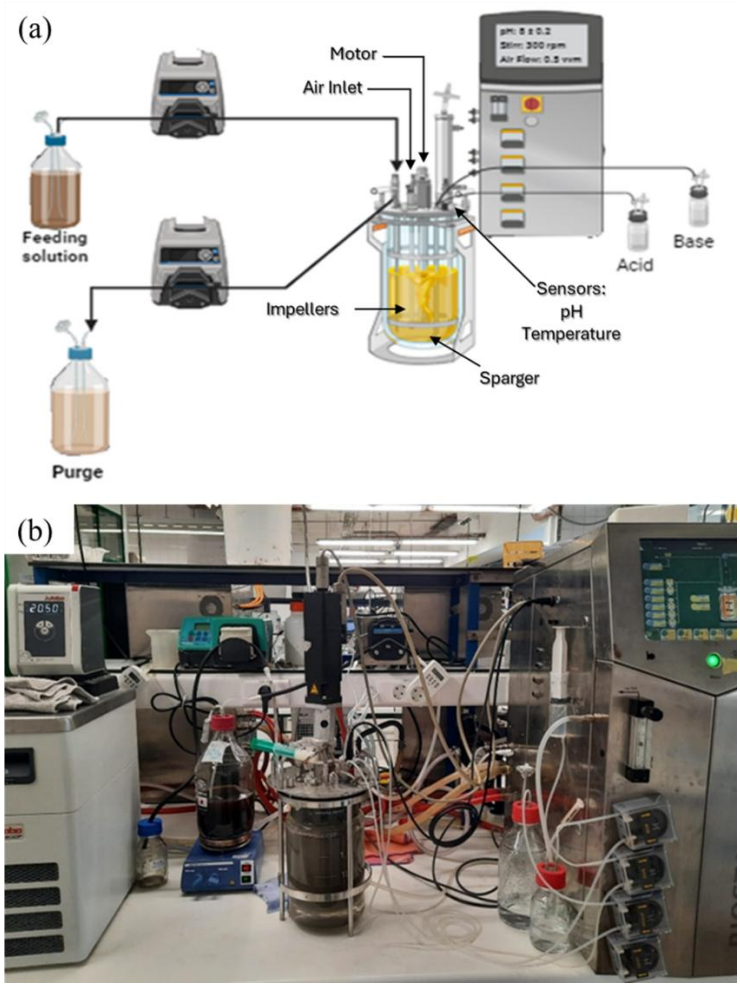

Figure III. 2 - Schematic representation of bioreactor (a) and experimental set-up used for 2 L (b) selection bioreactor for marshland microbiome using REXTPA as feedstock.

III.2.3.3. Production bioreactor

Fed-batch assays were carried out in a New Brunswick™ BioFlo®/CelliGen® 115 system (Eppendorf AG, Germany) with a working volume of 0.8 L, operated at controlled temperature (20 ± 0.1 ºC), pH (8.00 ± 0.50), aeration (1 SLPM) and stirring rate (300 rpm). In each assay, the bioreactor was inoculated with 200 mL of cultivation broth collected from the selection bioreactor at the end of the famine phase of cycles 17, 22 and 28. The dissolved oxygen (DO) concentration was not controlled, but it was continuously monitored because the abrupt increase on DO concentration signalled the exhaustion of TPA. At that point, a pulse (80 mL) of REX-TPA solution (20 g/L) was fed to provide a TPA concentration in the reactor of 2 g/L. A total of four pulses were provided to the culture during each assay. Samples (12 mL) were collected throughout the assays, and used to quantify TSS, VSS, TPA, ammonium and PHA. At the end of the assays, the broth was collected for PHA extraction.

III.2.4. Analytical methods

TSS and VSS were measured according to the standard methods (APHA, 1998). For nutrients' and PHA quantification, the broth samples were centrifuged (7012×*g*, 5 min, at 4 °C) for separation of the pellet, which was freeze dried and used for PHA quantification, from the supernatant that was used for quantification of TPA and ammonium. The TPA concentration was determined by HPLC as described in section II.2.1.3. The ammonium concentration was quantified by Skalar as previously explained in section II.2.5.2.

The freeze-dried pellets (3 mg) were used for PHA quantification by GC, after acidic methanolysis at 100 °C, for 4 h, with benzoic acid (Sigma-Aldrich, ≥99.5 %) as internal standard, as described by Rebocho et al., 2020. The obtained methyl esters were analysed in a GC-FID apparatus (Trace 1300, Thermo Fisher Scientific, US) and a Restek column (Crossbond, Stabilwax), at constant pressure (96 kPa) using helium as carrier gas. The heating ramp comprised: 20 °C/min until 100 °C, 3 °C/min until 155 °C, and 20 °C/min until 220 °C. P(HB-co-HV) (88:12%mol, 3HB:3HV) (Sigma-Aldrich) was used to construct a calibration curve with standards concentration ranging from 0.1 to 1.0 g/L. Replicate measurements were done for all analyses.

The culture broth samples were stained with Nile Blue following the procedure described by Carvalheira et al., 2022 and visualized under the microscope (Carl Zeiss Axio Imager D2) at a magnification of 100×, under contrast and fluorescent light.

III.2.5. Calculations

The F/f ratio was calculated by dividing the duration of the feast phase (h) by the duration of the famine phase (h). The overall specific TPA removal rate (q_{TPA}, ($g_{TPA}/(g_{VSS}.h)$) was calculated by dividing the amount of TPA consumed by initial VSS concentration and the production time. For PHA production experiments, TPA removal efficiency (%) was obtained by TPA consumed divided by the TPA supplied in all pulses.

The PHA overall volumetric productivity (r_{PHA}, $g_{PHA}/(L.day)$ was calculated by according to the equation:

$$r_{PHA} = \frac{\Delta PHA}{\Delta t} \quad \text{(III.2.5.1.)}$$

Where ΔPHA (g/L) represents the polymer produced by the time elapsed, Δt (h).

The polymer yield on a substrate basis ($Y_{PHA/TPA}$, g_{PHA}/g_{TPA}) was calculated on a substrate basis, where ΔPHA is the polymer produced (g/L) and ΔTPA (g/L) is the concentration of TPA consumed during the production:

$$Y_{\mathrm{PHA/TPA}} = \frac{\Delta PHA}{\Delta TPA} \quad \text{(III.2.5.2.)}$$

III.2.6. 16S rDNA community analysis

DNA was extracted and purified from lyophilized samples collected at the end of the cycle during the selection process, using the Quick-DNA Soil Microbe kit (Zymo Research, Irvine, CA, USA). Sequencing of the full-length 16S rDNA was conducted using the MinION next- generation sequencing platform (Oxford Nanopore Technology, UK) featuring a Flongle adapter and a R9.4.1 Flongle flow cell (Šaraba et al., 2023). The barcoded DNA libraries were prepared with Oxford Nanopore's 16S barcoding kit 1–24 (Oxford Nanopore Technology, UK) following the manufacturer's instructions, using 25ng of genomic DNA per sample and 30 PCR amplification samples. The final library consisted of equal proportions of each barcoded sample and was sequenced for 30 hours. Base calling was performed using the Guppy basecaller (v6.4.2) in high accuracy mode and reads were filtered by length to retain reads between 1,200 and 1,800 base pairs. The quality of the filtered reads was then assessed, and sequencing primers sequences trimmed using Porechop (v0.2.4). Taxonomic classification was achieved using KrakenUniq (Breitwieser et al., 2018). The visualization of taxonomic data was achieved using Pavian (Breitwieser & Salzberg, 2020) in combination with in-house analysis pipelines (MicroLife Solutions, the Netherlands).

III.2.7. PHA extraction and characterization

III.2.7.1. PHA extraction and composition

The cultivation broth was centrifuged (10,375×g, 15 min, at 4 °C) and freeze dried. The biopolymer was extracted from the dry pellet (~2 g) in a closed 100 mL shott flask, for extraction with chloroform (60 mL), with controlled temperature (80ºC), for 48 h, under constant stirring (150 rpm). Afterwards, the polymer was purified by precipitation in ice-cold ethanol (1:10, v/v) and left at room temperature until completely dry. Afterwards, PHA polymer samples (~1 mg) were used to determined monomeric composition by GC as described in section III.2.4.

III.2.7.2. Thermal properties

DSC was conducted as previously described in section II.2.6.3, with modification in heating and cooling rate of 10 ºC/min over a temperature range of -60 ºC to 180 ºC, through two heating cycles.

TGA analysis was performed as previously described in section II.2.6.3.

III.2.7.3. Molecular mass distribution

The number average molecular weight (M_n), weight average molecular weight (M_w), and the poly-dispersity index (M_w/M_n) of the biopolymers were determined by SE-HPLC as described in section II.2.6.4.

III.2.8. PHB films: preparation and characterization

III.2.8.1. Preparation of PHB films

Films were prepared by casting 15 mL of a 35 g/L biopolymer's solution in chloroform (Sigma-Aldrich, HPLC grade) in a glass plate with a casting knife (Elcometer 3580), adjusted to 150 µm of thickness. After solvent evaporation in the fume hood at room temperature, the film was peeled of the glass plate and kept at room temperature in a closed glass petri dish until use.

III.2.8.2. Characterization of PHB films

- **Morphology**

The apparent thickness of the membrane was determined by a digital micrometer (Mitutoyo, Andover, UK) in an average of 6 measurements at different points of the membrane. The morphology of the PHB films was assessed visually and by scanning electron microscopy (SEM). The samples were frozen in liquid nitrogen and fractured in small pieces, followed by coating with a layer of gold-palladium (60/40%) alloy (Q150T ES, Quorum Technologies, Ringmer, UK). The samples were analysed using a benchtop scanning electron microscope (TM3030 Plus, Hitachi, Tokyo, Japan) with an acceleration voltage of 15 kV. The obtained SEM images were processed by ImageJ.

- **Mechanical properties**

The films were cut into rectangular-shaped test pieces (~30×15 mm), and tensile tests were performed using a texture analyser (Food Technology Corporation, Wales, England), operated with a tensile rate of 100 mm/min until break, using a load cell of 250 N, at room temperature. The Young's Modulus (E, MPa) was determined as the initial slope of the curve, the tensile strength (σ, MPa) was taken at the highest point of the curve just before break, and the elongation at break (ε, %) was determined as the ratio of the length of the test piece at rupture point by its initial length. Five specimens were tested for each film.

- **Permeability to oxygen and carbon dioxide**

Gas permeation tests for pure CO_2 and O_2 were performed as described by (Neves et al., 2010) using a stainless-steel cell with a feed and permeate compartments, separated by the polymer films. The films' permeability (*P*, Barrer) for pure CO_2 and O_2 gases was calculated according to the following equation:

$$\frac{1}{\beta}\ln\frac{\Delta_{po}}{\Delta_p} = P\ \frac{t}{l} \quad \text{(III.2.8.1.)}$$

where Δ_p (bar) corresponds to the difference of the pressures in the feed and permeate compartments, *t* (s) is the time and *l* (m) is the film's thickness. β is a geometric parameter characteristic of the cell (m^{-1}), and was obtained using the equation:

$$\beta = A\left(\frac{1}{V_{feed}} + \frac{1}{V_{perm}}\right) \quad \text{(III.2.8.2.)}$$

where A is the film's area (1 cm^2) and V_{feed} and V_{perm} are the volumes (bar) of the feed and permeate compartments, respectively. The gas permeability *P* was obtained from the slope when representing $\frac{1}{\beta} ln\frac{\Delta_{po}}{\Delta_p}$ as a function of $\frac{t}{l}$.

- **Water vapour permeability**

Water vapor permeability (WVP) was measured using modifications of the ASTM E 96 Standard Method ('cup method') (CupMethod) at a relative humidity (RH%) of 51%, in a desiccator with a saturated Mg $(NO_3)_2 \cdot 6H_2O$ solution. Glass petri dishes (5 cm in diameter) were prepared with 5 mL of water and covered with the samples, which were sealed to the petri dish with silicone sealant The prepared petri dishes were weighted and placed in the desiccator at controlled temperature (30 °C). The samples were weighed each day until no mass variation occurred and the WVP flux (g $m^{-1}s^{-1}Pa^{-1}$) was calculated by the following equation:

$$WVP = \frac{N_w \times \delta}{\Delta P_{w,eff}} \quad \text{(III.2.8.3.)}$$

where N_w is the water vapour molar flux (g m^{-2} s^{-1}), δ (m) is the film thickness and $\Delta P_{w,eff}$ (Pa) is the effective driving force, calculated as the water vapour pressure difference between both sides of the film.

III.2.9. Statistical analysis

The average and standard deviation values for PHA production profiles, as well as the biopolymer's M_w, PDI, thermal properties, were analysed using a one-way ANOVA with Bonferroni's multiple comparison test in GraphPad Prism 5 (GraphPad Software Inc., La Jolla, California) with the criteria for statistical significance set at $p < 0.05$.

III.3. Results and Discussion

III.3.1. Marshland sediments: characterization and source of the microbiome

The estuarine marshland sediments sample was a dense and viscous, heterogeneous material (Fig. III. 1b) that contained large amounts of particles of different size. After sieving for removal of larger particles (above 2-3 mm), the sample was still dense but more homogeneous, rendering it more suitable for use as inoculum for the selection bioreactor (Fig. III. 1c).

The sample's pH (8.03 ± 0.04) (Table III. 1) aligns with typical pH values reported for similar estuarine environments, that from 7.5 to 9.0, as reported for the Tagus River estuary (Rodrigues et al., 2020) and is consistent with pH values observed in intertidal marsh sediments collected from the Douro River (7.9) (Magalhães et al., 2007) and shallow marshland sediments (7.1–8.0) (Blume & Müller-Thomsen, 2007; Du Laing et al., 2008). While slightly higher than the pH reported for Paio Pires salt marsh sediments (7.2) (Peres et al., 2016), the sample's pH falls within the natural daily summer fluctuations (7.0–8.5) (Koop-Jakobsen & Gutbrod, 2019), which corresponds to the season when the marshland sediments used in this study were collected. Additionally, the pH of the sediments is in accordance with those reported in bioreactors operated with F/f cycles for PHA-storing microbiome enrichment (Carvalheira et al., 2022; Villano et al., 2010), supporting the choice to set the selection bioreactor at pH 8.00.

The sediments had a conductivity of 1.5 ± 0.36 mS/cm, reflecting the low tide and warm conditions at the time of collection in a brackish environment, typical of locations with substantial river input (Burchard et al., 2019). This value is in accordance with studies indicating that estuarine sediments exhibit variable conductivity due to tidal cycles, which affect the balance of freshwater and saltwater (Burchard et al., 2019). In contrast, samples from the nearby River Coina salt marsh, showed higher conductivity values (7.2 to 18.5 dS/m) (Santos et al., 2017), highlighting the Corroios heterogenous sediment, shaped by the dynamic tidal interaction's characteristic of estuarine environments (Burchard et al., 2019).

The sediments collected had a TSS of 540.81 ± 22.78 g/L of which 56.78 ± 2.30 g/L were VSS. This low VSS/TSS ratio (10.50 ± 0.01%) is consistent with the characterization of Tagus estuary sediments mainly composed of sand, silt and clay with added organic matter (Silva et al., 2013). The sample's composition was confirmed by elemental analysis, which showed that its content in carbon was only 1.43±0.10% (Table III. 1), characteristic of mineral-rich sediments as those reported by low accumulation of organic matter (3.39 ± 1.83 mg cm^{-2} per year) for sediments collected from tidal estuaries (Wu et al., 2023).

Table III. 1 Characterization of the sediments collected from Corroios marshland (tr, traces).

Parameter	Value
Conductivity (mS/cm)	1.5 ± 0.36
pH	8.03 ± 0.04
TSS (g/L)	540.81 ± 22.78
VSS (g/L)	56.78 ± 2.30
VSS/TSS (%)	10.50 ± 0.01
Elemental analysis (%)	
Carbon	1.43 ± 0.10
Sulphur	0.82 ± 0.20
Hydrogen	0.46 ± 0.03
Nitrogen	0.17 ± 0.02
Element (mg/L)	
Na	147.51
Mg	45.10
Ca	17.16
B	1.61
Si	1.38
K	0.23
Li	0.15
P, Cu, Mo, Mn	tr

The sediments primarily contained Na (147.51 mg/L) and Mg (45.10 mg/L) (Table III. 1), consistent with the predominant water-soluble cations found in marshland soils and estuarine sediments influenced by tidal seawater mixing (Wang et al., 2011; Zhao et al., 2017). The abundance Na in estuary seawater (Adesina & Ogunseiju, 2017), demonstrates the tidal influence on Corroios Marshland environment. Lower concentrations of Ca (17.16 mg/L), B (1.61 mg/L), Si (0.80 ± 0.81 mg/L) and K (0.23 mg/L) were detected. The relatively low Ca levels obtained may also result from ion exchange processes, where Mg and Na displace Ca and K on clay minerals, contributing to nutrient retention in estuary sediments (Adesina & Ogunseiju, 2017). Furthermore, traces of P, Cu, Mo, Mn (<0.05 mg/L) were also detected, suggesting that Corroios marshland sediments may act as a sink for dissolved minerals and trace elements (Cui et al., 2016; Peres et al., 2016).

The potential of aquatic sediments as source of microorganisms for bioprocess development has been previously demonstrated in other studies. For instance, lake sediments were tested for degrading PET-derived compounds (e.g. TPA) (Schaerer et al., 2023), while river sediments have been utilized to screen for microbes capable of degrading aromatic pollutants (e.g., benzene, biphenyl, naphthalene) (Narancic

et al., 2012), further highlighting the versatility of these microbial communities. Particularly, the Corroios marshland sediments' characteristics render it suitable candidate microbiome for developing a bioprocess for production of PHA due to their diverse microbial community and adaptability to variable estuarine conditions (e.g. pollutants accumulation, salinity, nutrient availability) (Li et al., 2019). This adaptation is reflected in the sediment's physicochemical properties and makes these microbiomes promising for PHA production, as wetland microorganisms often produce PHA as an energy reserve under stress (Grey et al., 2023). Although the VSS content in marshland sediments may be low, authors have reported 0.345 g/L of VSS from estuarine sediments used as inoculum in a saline wastewater treatment reactor (Cui et al., 2014). To enhance the proliferation of PHA-storing microorganisms within such microbiomes, enrichment techniques such as F/f regime were successfully applied (Cui et al., 2016).

III.3.2. Culture selection: the feast and famine strategy for enrichment in PHA storing organisms

A selection reactor was operated under F/f regime with 4-day cycle, fed with REX-TPA as sole carbon source, operated for 113 days. The REX-TPA solution was prepared as previously described in section II.2.1.3. Monitoring cycles were conducted for a few cycles to verify the culture's evolution. Upon its stabilization, production assays were performed, in which successive pulses of TPA were provided for PHA production

Cell Growth

To select a consortium able to use REX-TPA and produce PHA, the marshland microbiome was subjected to a selective pressure that consisted in applying cyclic feast/famine (F/f) conditions. This selection process was carried out in a 2 L bioreactor over a period of time of 113 days, with each F/f cycle lasting 4 days (except the first cycle that comprised 5 days). At the beginning of each cycle, a REX-TPA solution supplemented with ammonium was supplied to the bioreactor obtaining approximately concentrations of 1.68 ± 0.20 and 0.11 ± 0.05 g/L, respectively, during the selection process.

As shown in Fig. III. 3, at the beginning of the assay, organic matter (VSS) in the bioreactor represented a small fraction (17.0 ± 0.7 g/L), representing 10.5wt% of the total solids (TSS) (162.2 ± 6.8 g/L). However, within the first SRT, there was a significant reduction in inorganic material content, with the VSS (3.1 ± 0.4 g/L) representing 26.3wt% of the TSS (11.6 ± 0.9 g/L). This increase in the VSS/TSS ratio indicates a rapid organic fraction enrichment occurred, enabled by the extended SRT with a more gradual yet effective removal of inorganic particles.

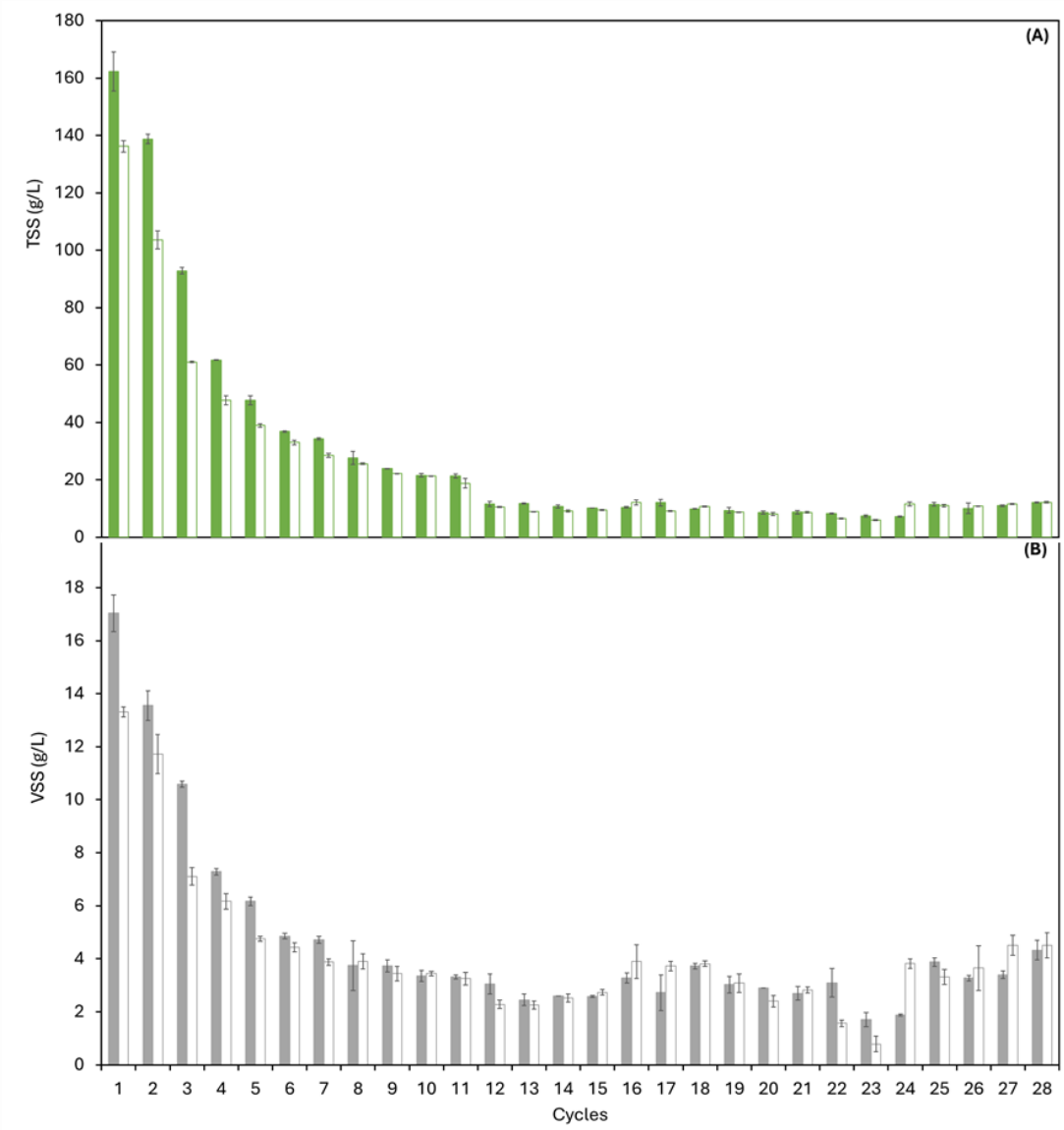

Figure III. 3 - TSS (A) and VSS (B) concentrations at the beginning (full bars) and at the end (open bars) of the F/f cycles throughout the operation of the selection bioreactor.

The decrease in VSS from 17.0 g/L to 3.1 g/L, likely resulted from the removal of non-PHA-producing microorganisms' and the slow growth of PHA-storing bacteria during continuous REX-TPA feeding (Zhou et al., 2023a). During the second SRT and until the end of operation, both VSS and TSS stabilized (Fig. III. 3), with VSS varying between 3.1 ± 0.4 g/L and 4.3 ± 0.4 g/L, representing 36wt.% of the total solids at the end of selection reactor operation, thus showing the system had reached a stable VSS concentration with a SRT of 40 days and successive feeding of REX-TPA as sole feedstock.

Similar trends have been reported for other MMC systems, in which higher biomass content was attained with an SRT of 8 days rather than 2 days, using fermented agriculture wastes (Zhou et al.,

2023a). Comparable VSS concentrations (1.5-3.4 g/L) were also observed for an MMC system fed with acidified hardwood spent sulphite liquor, operated at an SRT of 5 days and an HRT of 1-2 days (Pereira et al., 2020). Similarly, the MMC system fed with bio-oil from chicken beds fast pyrolysis, tested at SRT of 5 days and HRT of 1 day, reached a VSS of 3.8 g/L (Fidalgo et al., 2014).

MMC systems typically operate with SRT values (1-10 days) higher than their HRT (24 h) (Jayakrishnan et al., 2020; Moretto et al., 2020; Queirós et al., 2015) and were reported to require at least 3 SRTs to achieve stability (Colombo et al., 2017). In the present study, despite the longer and equal HRT and SRT (40 days) applied in the F/f cycles, the Corroios marshland microbiome reached stable operation with one SRT/HRT, as demonstrated by the VSS and TSS values observed afterwards (Fig. III. 3). These findings highlight the microbiome's adaptability and capacity to efficiently utilize a complex substrate as REX-TPA. Furthermore, the long retention times may have facilitated the establishment of a well-adapted microbial community capable of efficiently metabolize REX-TPA, ultimately leading to process stability. The visual evolution of the selection bioreactor (Fig. III. 4) reflects the progressive adaptation to REX-TPA substrate. Initially, in cycle 1, the culture appeared dark and dense due to the high inorganic content of the marshland microbiome. As selection progressed, the decrease in TSS and stabilization of VSS led to a gradual clarification of the medium (cycles 9 to 17), indicating the removal of a non-PHA accumulating microorganisms. By cycle 28, the reactor exhibited a lighter and more homogenous appearance (Fig. III. 4d) similar to cycle 17, keeping a more stable selection in the second SRT to the end of the selection.

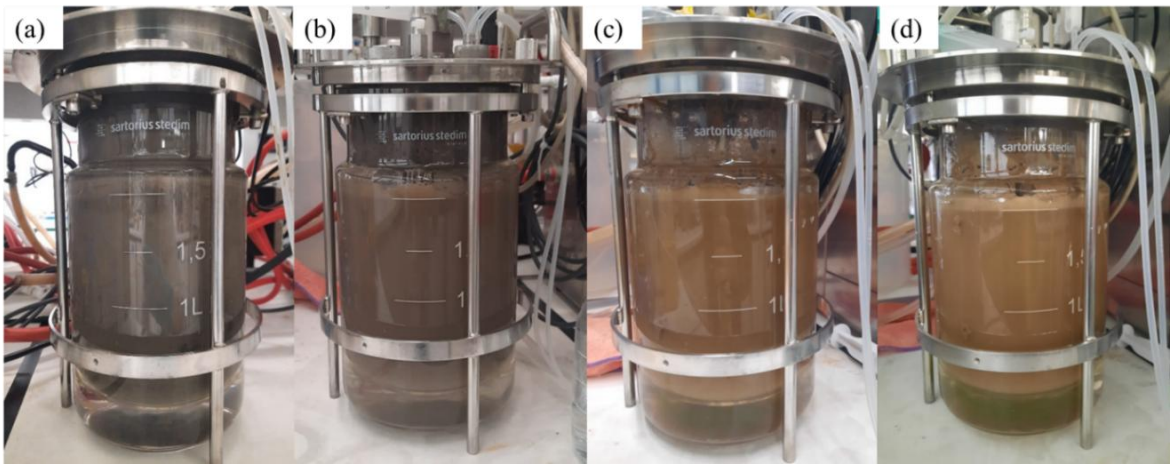

Figure III. 4 - Selection bioreactor for marshland microbiome in cycles 1 (a), 9 (b), 17 (c) and 28 (d) during selection stage using REX-TPA as feedstock.

Nutrients' removal

The culture successfully depleted TPA in all cycles, with an overall average consumption of 1.68 ± 0.03 g/L (Fig. III. 5a), demonstrating its adaptation to using TPA as carbon source. Regarding ammonium, there was a build-up of this nutrient during the first selection cycles, namely from 1 to 9, due to its incomplete consumption within the 4 days' cycles (Fig. III. 5b). Nevertheless, the culture demonstrated increasing ammonium consumption over the cycles, reaching complete consumption after cycle 9. This may be attributed to the variation observed for VSS concentration during the first SRT, with VSS gradually increasing from 3.44 g/L to 3.90 g/L between cycles 9 and 16 (Fig. III. 3b).

These results demonstrate the effectiveness of applying F/f conditions for TPA uptake as a carbon source by the MMC derived from marshland microbiome. This novel approach achieved 100% TPA removal efficiency at a stable rate of 0.23 g_{TPA}/h after the first SRT, as evidenced by the monitored cycles 15 and 26 (Fig. III. 6). This efficiency was maintained until the end of the selection, using an average TPA concentration of 2 g/L per cycle. Interestingly, the removal efficiency for such substrate concentrations is higher than that reported for other biological systems, although those studies tested lower TPA concentrations as carbon and energy sources.

The reported studies are mostly focused on continuous anaerobic/aerobic systems for TPA removal in wastewater treatments. As far as the authors are aware, this study is the first to apply an F/f strategy for selecting a microbial consortium enriched in PHA producers using TPA as carbon source.

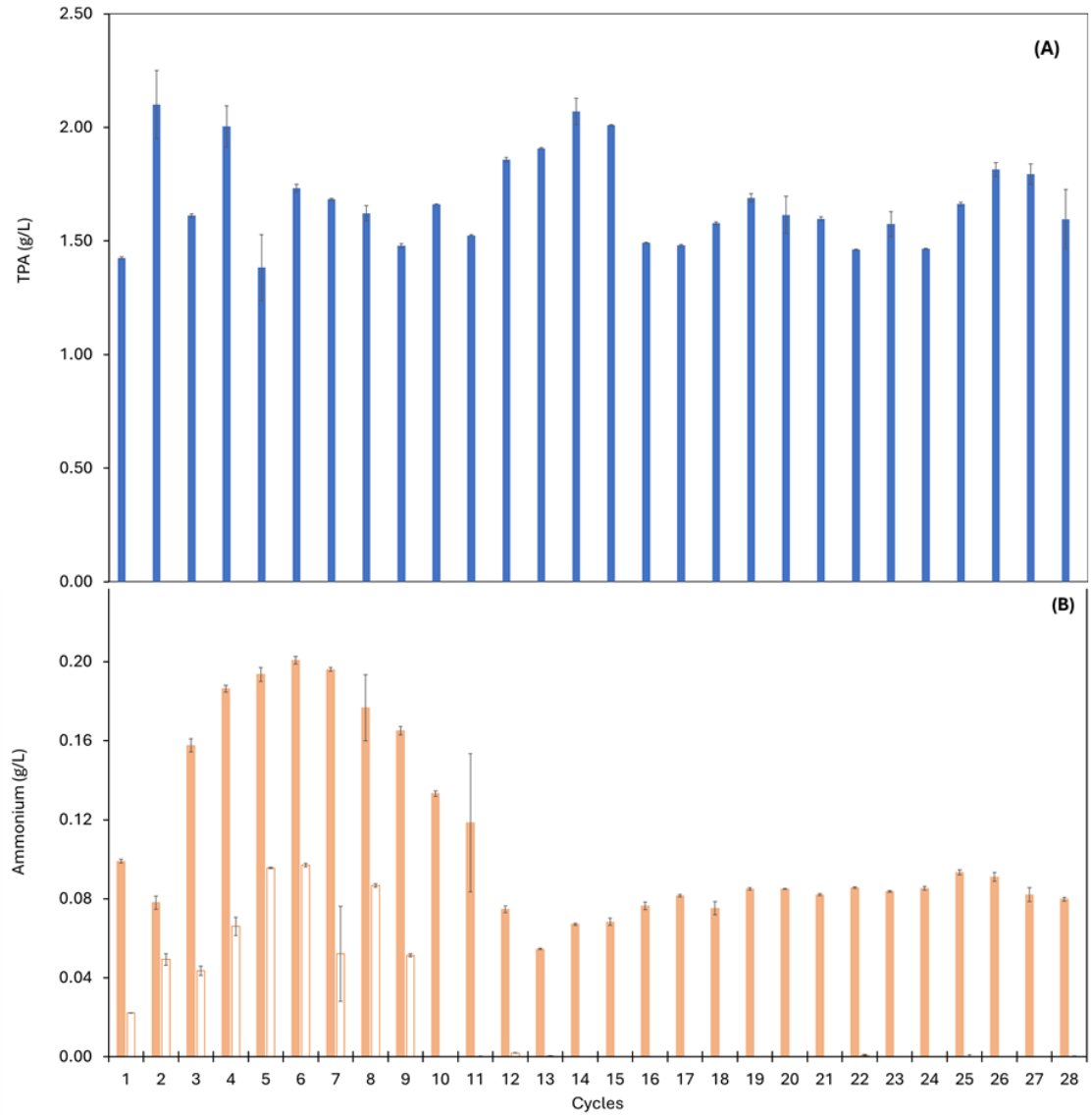

Figure III. 5 - TPA (A) and ammonium (B) concentrations at the beginning (full bars) and at the end (open bars) of the F/f cycles throughout the operation of the selection bioreactor.

Other studies describing the assimilation of TPA by MMC systems include, for example, that of Aksu et al., 2021 which achieved an 85.8% TPA removal (corresponding to a removal rate of 0.379 mg_{TPA}/h) using a bioaugmented continuously stirred tank reactor (CSTR) with pre-selected TPA-degrading bacteria from activated sludge of a petrochemical wastewater treatment plant, with 50 mg/L of commercial TPA. Similarly, Vural et al., 2020 used a CSTR with activated sludge bioaugmented with hydrocarbon-degrading strains to treat a feed containing 372.6 mg/L TPA, achieving a removal efficiency of 97.9%. Both studies achieved lower removal efficiencies and rates than the present study (100% removal efficiency and 0.23 g_{TPA}/h removal rate achieved), while operating at lower feed concentrations compared to the 2 g/L of REX-TPA used in this study. Yang et al., 2014 achieved 98.2%

TPA removal in a polyester wastewater treatment system combining an anoxic hydrolysis-acidification reactor (HABR) and an aerobic hybrid membrane reactor (HMBR), treating 150–600 mg/L TPA. Liu et al., 2019 achieved 76–78% TPA removal in a moving-bed biofilm reactor (MBBR) inoculated with *Delftia sp.* strain WL-3, testing 500–1750 mg/L TPA with HRTs of 24–36 hours. In contrast, the selected marshland MMC demonstrated superior performance with complete TPA removal at higher feed concentrations without applying bioaugmentation approach.

Several microorganisms have been evaluated for TPA degradation under different conditions. *Rhodococcus erythropolis* MTCC 3951 is reported to degrade 20 g/L in 84 h, corresponding to a TPA removal rate of $0.23 g_{TPA}/h$, which is similar to the selected marshland MMC during stable feast phases (Maurya et al., 2023). Furthermore, *Pseudomonas umsongensis* GO16 which is an isolated bacteria from a PET bottle processing plant (Kenny et al., 2008), has been studied due to its metabolic versatility to use a wide range of substrate including PET-derived products, has reported higher rate of 1.88 g_{TPA}/h, degrading 90 g of TPA obtained from the pyrolysis of PET, in 48 h under optimized fed-batch conditions for mcl-PHA production (Kenny et al., 2012a). While single cultures may achieve higher TPA consumption rates, the selected MMC from the marshland microbiome presents the benefit of lower operational costs due to reduced sterility requirements (Chen et al., 2017).

PHA synthesis

The culture's capacity for PHA synthesis was evaluated throughout the selection reactor operation, by monitoring the profiles for the nutrients' concentrations, namely TPA and ammonium, and PHA content in the biomass, in cycles 4, 9, 15 and 26. During the first HRT, the monitoring profiles for cycles 4 (Fig. III. 6A) and 9 (Fig. III. 6B) showed a significant variation in the duration of the feast phase (determined by TPA exhaustion). In cycle 4, the feast phase had a duration of 18.5 h, which decreased to 11.4 h in cycle 9, lowering the F/f ratio from 0.24 to 0.13 (Table III. 2). However, no PHA accumulation was detected in either cycle (Table III. 2), despite the extended famine period, which is a key factor in applying physiological selective pressure to promote polymer storage when ammonium and carbon are fed simultaneously (Reis et al., 2011). Additionally, the significant reduction in the duration of the feast phase that shows the faster TPA consumption by the culture, coincided with the decrease in VSS concentration, from 7.28 ± 0.12 in cycle 4 to 3.73 ± 0.24 in cycle 9. This indicates there was a selection of microorganisms able to thrive on TPA as sole carbon source, while those that could not grow on TPA were eliminated.

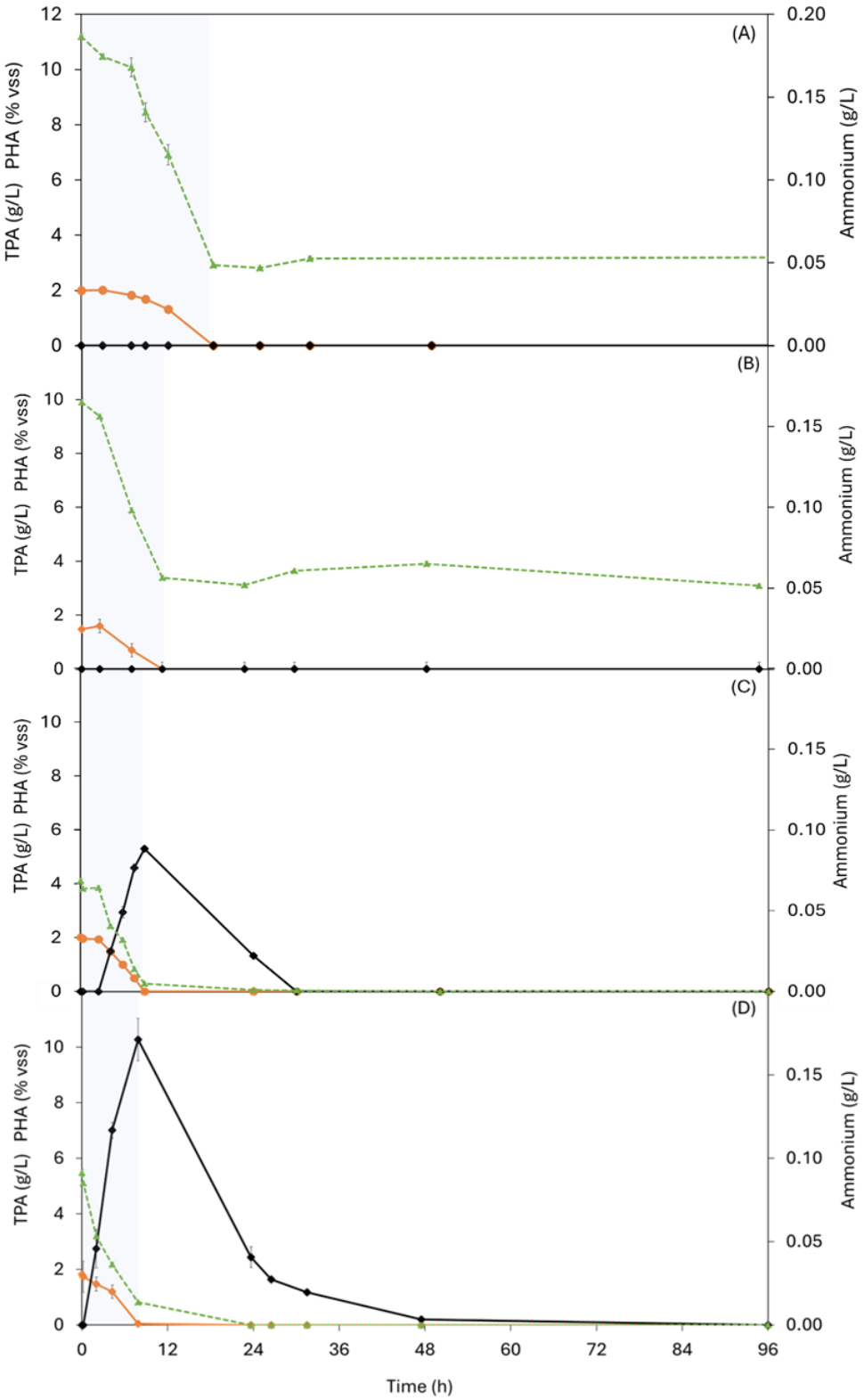

Figure III. 6 - Selection bioreactor monitoring: profiles obtained for cycles 4 (A), 9 (B), 15 (C) and 26 (D). (●, TPA (g/L); X, Ammonium (g/L); ◆, PHA (%VSS)).

After cycle 9, the culture was able to deplete the ammonium during the famine phase (Fig. III. 6C). A further decrease in the F/f ratio was observed (0.10 and 0.09, for cycles 15 and 26, respectively), with the feast phase duration being reduced to only 8.9 h and 7.8 h, for cycles 15 and 26, respectively, indicating that the selective pressure become more effective, resulting in a culture able to consume TPA at a higher rate. During this period, the biomass reached PHA contents of 5.29 ± 0.11% (cycle 15) and 10.27 ± 0.76% (cycle 16) (Table III. 2). The reduction of the feast phase duration, alongside with the observed increased specific TPA removal rates (0.088 ± 0.001 and 0.071 ± 0.002 $g_{TPA}/(g_{VSS}.h)$) and complete consumption of ammonium, favoured the enrichment of the microbiome in PHA-storing microorganisms (Reddy & Mohan, 2012) (Fig. III. 6).

Table III. 2 Cycles' monitoring performance of the culture during the selection reactor operation. The values represented are mean ± standard deviation. (F, feast; f, famine; F/f, Feast to famine ratio; n.d. not detected).

Cycle		4	9	15	26
Day of operation		13	33	57	101
Feast phase	Duration (h)	18.5	11.4	8.9	7.8
	VSS (g/L)	7.28 ± 0.12	3.73 ± 0.24	2.58 ± 0.04	3.28 ± 0.11
	TPA (g/L)	2.00 ± 0.09	1.48 ± 0.01	2.01 ± 0.00	1.81 ± 0.03
	Specific TPA removal rate ($g_{TPA}/(g_{VSS}.h)$)	0.015 ± 0.001	0.035 ± 0.002	0.088 ± 0.001	0.071 ± 0.002
	Ammonium (g/L)	0.19 ± 0.00	0.17 ± 0.00	0.07 ± 0.00	0.09 ± 0.00
	Ammonium consumed (g/L)	0.14 ± 0.00	0.11 ± 0.00	0.06 ± 0.00	0.08 ± 0.00
	PHA (%) *	n.d	n.d.	5.29 ± 0.11	10.27 ± 0.76
Famine phase	Duration (h)	79.0	83.5	87.1	88.2
F/f ratio		0.24	0.13	0.10	0.09

* Calculated on a VSS basis

The profiles shown in Fig. III. 6 indicate that the F/f regime imposed a significant selective pressure, effectively enriching the marshland MMC in PHA-accumulating bacteria, using a complex feedstock such as REX-TPA. The culture TPA removal rate increased over time, leading to shorter feast phases and correspondingly longer famine periods. This shift in F/f dynamics, with ratios consistently below 0.2, aligns with the recommended values for effective internal limitation, towards PHA storage and ensuring selection stability (Queirós et al., 2015), indicating a well-conducted selection process in favouring PHA-accumulating microorganisms. Although the commonly recommended F/f value for

enriching MMC in microorganisms able to accumulate PHA are within 0.2 and 0.3 (Albuquerque et al., 2010; Colombo et al., 2016; Dionisi et al., 2006), several studies have reported lower F/f ratios, ranging from 0.05 ± 0.01 to 0.08 (Guarda et al., 2024; Johnson et al., 2009), while achieving good PHA accumulation in the biomass (24-53%). This suggest that a lower F/f ratio can support effective selection of PHA accumulating organisms.

As stated above, the long SRT and HRT values applied to the marshland microbiome (40 days) were also relevant in assuring the evolution of the culture towards improved PHA storing capacity, which was established after just one SRT/HRT. While the culture exhibited a slightly lower PHA accumulation content when compared to other MMC selections with shorter SRTs, between 1 and 10 days (Cui et al., 2016; Jayakrishnan et al., 2020; Valentino et al., 2017), commonly applied in F/f systems for culture enrichment in PHA accumulating organisms, longer SRTs (within 20-25 days) (Basset et al., 2016; Wang & Cui, 2024) have also been reported to achieve stable PHA producing cultures within a lower number of applied SRTs (~1.5).

As demonstrated for the marshland microbiome, the use of long SRT/HRT was successful in establishing a stable MMC with the capacity to accumulate PHA after only one SRT, thus representing a relatively rapid culture adaptation to the tested REX-TPA substrate.

III.3.3. Microbial composition dynamics during the selection process

There was a clear evolution of the microbiome's composition across the selection bioreactor under the selective pressure applied through the cyclic F/f strategy (Fig. III. 7). It was not possible to analyse the initial marshland microbiome sample since it had a very low organic fraction, which resulted in low read counts for microbial identification.

The microbial community showed a highly diverse composition during the first SRT. At Class-level (Fig. III. 7a), during cycle 5, the reactor was dominated by *Proteobacteria* specifically, *Betaproteobacteria* (32.5%), *Gammaproteobacteria* (23.0%) and *Alphaproteobacteria* (18.6%), which are commonly found in coastal freshwater wetlands (Zhao et al., 2020) (Mellado & Vera, 2021). In this phase, members of *Alcaligenaceae* (31.2%), *Xanthomonadaceae* (17.8%) and *Rhodobacteraceae* (12.4%) families were the primary contributors to the diversity of the early-stage microbial community. The predominant genera included *Paenalcaligenes, Lysobacter*, and *Pseudorhodobacter* which have been identified in various soil bacterial communities, including coastal and wetland soils (Sun et al., 2022; Zheng et al., 2024), crude-oil polluted soils (Omenna et al., 2023) and plastic-contaminated soils (Meng et al., 2024; Mitzscherling et al., 2022).

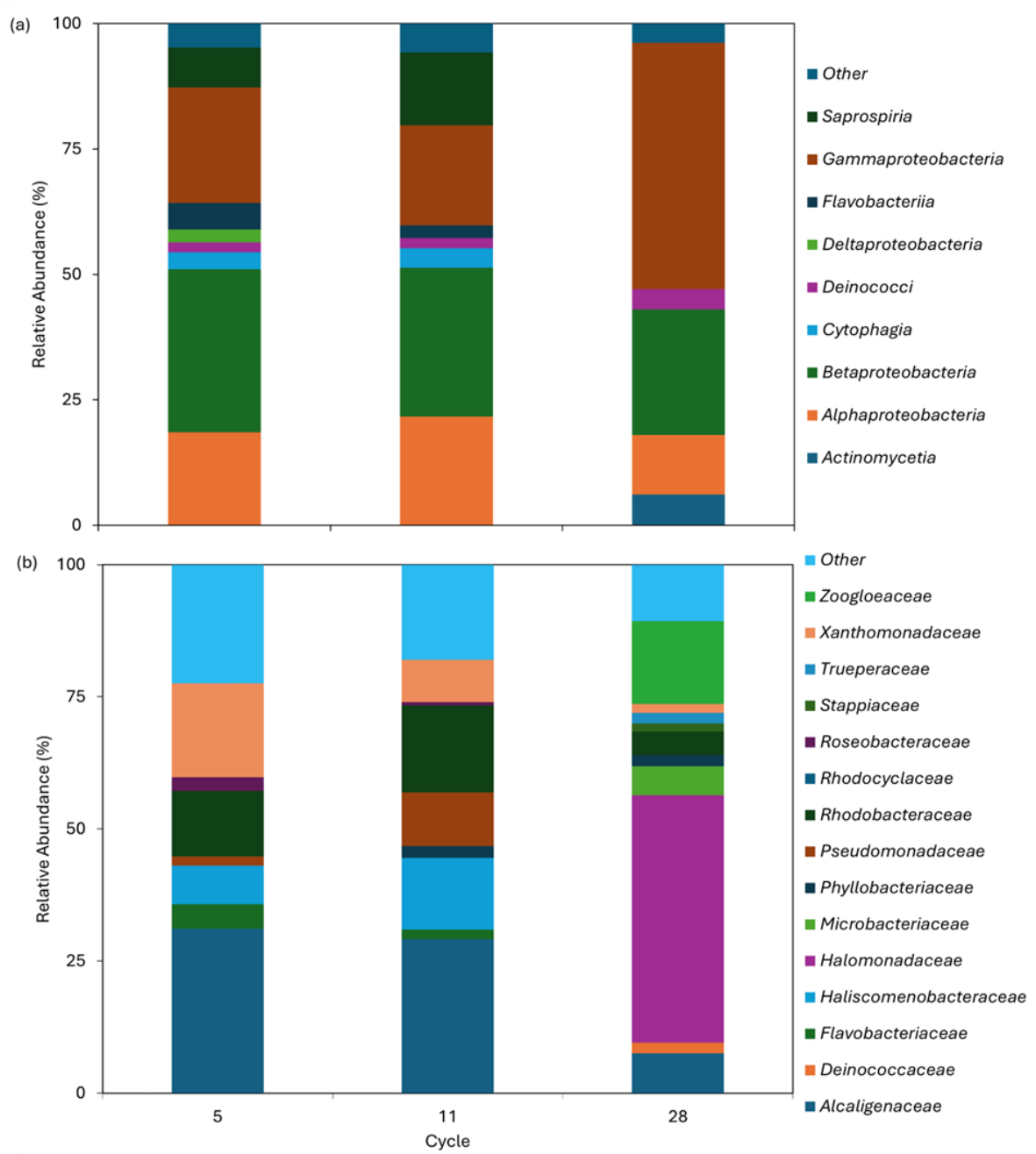

Figure III. 7 -Taxonomic composition of the bacterial community achieved during the reactor selection of the marshland microbiome using REX-TPA as feedstock. Relative abundance (cut-off 2%) of bacterial communities at the class (a) and family (b) level on different selection cycles.

This community structure remained stable until cycle 11 (Fig. III. 7), marking the completion of the first SRT, with the predominant classes, *Betaproteobacteria*, *Gammaproteobacteria* and *Alphaproteobacteria* reported as a source of microorganisms capable of degrading aliphatic and aromatic hydrocarbons (Brzeszcz & Kaszycki, 2018; Crisafi et al., 2022; Sierra-García et al., 2014). From this stage until

cycle 28, there was a notable shift in the microbiome composition (Fig. III. 7). *Gammaproteobacteria* became dominant (49.1%), indicative of its competitive advantage under the reactor's operational conditions, during the second SRT, using TPA as substrate. This dominance suggests that these microorganisms adapted to the F/f regime and were able to withstand the famine phase, by utilizing PHA storage, according with previous studies on MMC cultures seeded with estuary sediments (Cui et al., 2016).

The presence of *Alcaligenaceae* (7.5%), *Rhodobacteraceae* (4.4%) and *Xanthomonadaceae* (1.7%) at low abundance until the end of the operation suggests their role as core bacteria, contributing to the stability and function of the microbiome. Particularly, *Rhodobacteraceae* and *Xanthomonadaceae*, known producers of biofilm and extracellular polymeric substances (EPS), likely playing a key role in maintaining long-term biomass stability (Paulo et al., 2021). Additionally, the presence of *Deinococci* class, particularly the *Deinococcus* genus, known for degrading synthetic polymers, including PET (Makryniotis et al., 2023), further indicates the establishment of TPA degraders within the microbiome.

By cycle 28, the most abundant families were *Halomonadaceae* (46.8%) and *Zoogloeaceae* (15.7%) (Fig. III. 7b). These families were associated with *Halomonas* and *Thauera* genera identified in microbiome. *Halomonas* presence is reported within microbial communities that efficiently degrade plastics in contaminated sites (Niu et al., 2021) including PET and PE films (Gao & Sun, 2021). Meanwhile, *Thauera* is reported for its role as organic compounds degraders (e.g. polycyclic aromatic hydrocarbons) (Huang et al., 2021). Both genera are described as PHA producers (Sruamsiri et al., 2020; Wang & Cui, 2024). Nevertheless, to the best of our knowledge there are no reports confirming their ability to upcycle TPA into PHA.

The establishment of PHA-storing microbes under the selective pressure applied (F/f ratio of 0.1) with a SRT of 40 days suggests a positive effect on the bacterial community, aligning with previous studies on similar operating conditions (Frison et al., 2021).

III.3.4. Polymer production: pulse feeding for enhanced PHA accumulation by the selected microbiome

Three polymer production assays were performed to evaluate the culture's performance under permanent feast conditions, by supplying three REX-TPA pulses. Those assays were conducted using biomass collected from the selection bioreactor at the end of the famine phase, in days 69 (assay A), 89 (assay B) and 113 (assay C). All assays were initiated with a TPA concentration of 2 g/L and an ammonium concentration of 0.1 g/L. Subsequently, after TPA exhaustion, three REX-TPA pulses were supplied to the culture, to give a TPA concentration in the bioreactor of 2 g/L TPA. No further ammonium

was supplied to the culture to impose growth limiting conditions to the culture, which are known to favour PHA accumulation by the cells (Ntaikou et al., 2019).

Fig. III. 8 shows the profile obtained in Assay C, which is representative of the 3 production assays conducted. In this assay, the initial TPA (1.93 ± 0.01 g/L) was nearly exhausted within 8 h, corresponding to an overall consumption rate of 0.22 g_{TPA}/(L.h). Subsequently, a REX-TPA pulse was provided to the culture at 8 h to guarantee carbon availability for PHA production. During this first REX-TPA pulse, a VSS of 0.84 ± 0.56 g/L was produced (Table III. 3) and the available ammonium (0.11 g/L) was exhausted at 14 h of cultivation. An increased TPA consumption rate of 0.27 g_{TPA}/(L.h) was also observed. In the second pulse, provided at 15 h, the TPA consumption rate increased further to 0.31 g_{TPA}/(L.h), a maximum obtained during the assay, decreasing to 0.19 g_{TPA}/(L.h) after the last pulse. The culture's performance demonstrates the selected microbiome's ability to increase TPA consumption rate from pulse to pulse, which is a typical trend observed during PHA production assays with pulse-wise feeding (Cui et al., 2016).

Table III. 3**.** Kinetic and stoichiometric parameters of the PHA production assays (VSS, volatile suspended solids; r_{PHA}, PHA volumetric productivity; $Y_{PHA/TPA}$, PHA yield on TPA basis).

Assay	A	B	C	Average
Cultivation time in the selection bioreactor (days)	69	89	113	
VSS produced (g/L)	0.87 ± 0.29	0.55 ± 0.14	0.84 ± 0.56	0.75 ± 0.18
Overall TPA consumption (g/L)	5.65 ± 0.04	5.07 ± 0.03	6.93 ± 0.03	5.88 ± 0.95
TPA removal efficiency (%)	86.34 ± 0.01	74.71 ± 0.01	92.87 ± 0.01	84.64 ± 9.20
PHA (wt.%) *	63.44 ± 0.07	60.65 ± 1.49	71.32 ± 0.34	65.14 ± 5.37
PHA (g/L)	1.26 ± 0.06	1.16 ± 0.03	1.29 ± 0.01	1.24 ± 0.07
r_{PHA} (g_{PHA}/(L.day)	1.35 ± 0.07	0.60 ± 0.06	1.07 ± 0.01	1.01 ± 0.38
Overall $Y_{PHA/TPA}$ (g_{PHA}/g_{TPA})	0.22 ± 0.05	0.23 ± 0.03	0.19 ± 0.00	0.21 ± 0.02

* on a VSS basis.

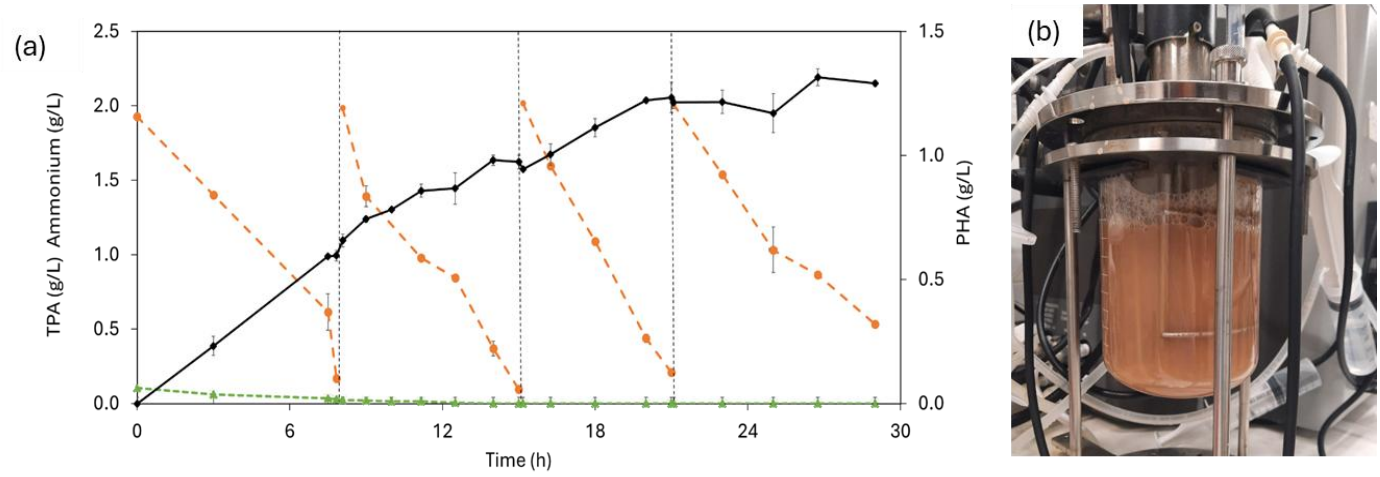

Figure III. 8 - Profile of TPA and ammonium concentration and PHA content in the biomass over time for assay C (a), in which the production bioreactor was inoculated with biomass collected from the selection bioreactor in day 113 (●, TPA (g/L); X, Ammonium (g/L); ◆, PHA (g/L)) and experimental set-up for PHA production (b).

PHA synthesis was initiated during the cell growth phase, as shown by Nile Blue staining (Fig. III. 9), attaining 0.97 ± 0.03 g_{PHA}/L by the end of the first pulse (around 15 h) (Fig. III. 8), corresponding to a polymer content in the biomass of 54.8 ± 0.26wt.%. During the second pulse, PHA production increased further, reaching 1.23 ± 0.06 g_{PHA}/L by 21 h, representing 69.4 ± 3.06wt.% of polymer content of the biomass. This increase was supported by the maximum TPA consumption rate observed during this period of the assay. From this moment until the end, polymer synthesis continued, attaining a maximum production of 1.32 ± 0.03 g_{PHA}/L at around 27 h (Fig. III. 8), with a polymer content of 71.32 ± 0.34wt.% (Table III. 3). The decrease in TPA consumption rate during the final pulse suggests a decline in the culture's metabolic activity to convert TPA into PHA, likely due to the microorganisms reaching PHA storage saturation as a result of continuous polymer accumulation (Tamang et al., 2019). These findings indicate that the selected microbiome fed with REX-TPA solution was able to achieve high polymer contents, sustaining its high efficiency in upcycling TPA into PHA, which was established after just one SRT.

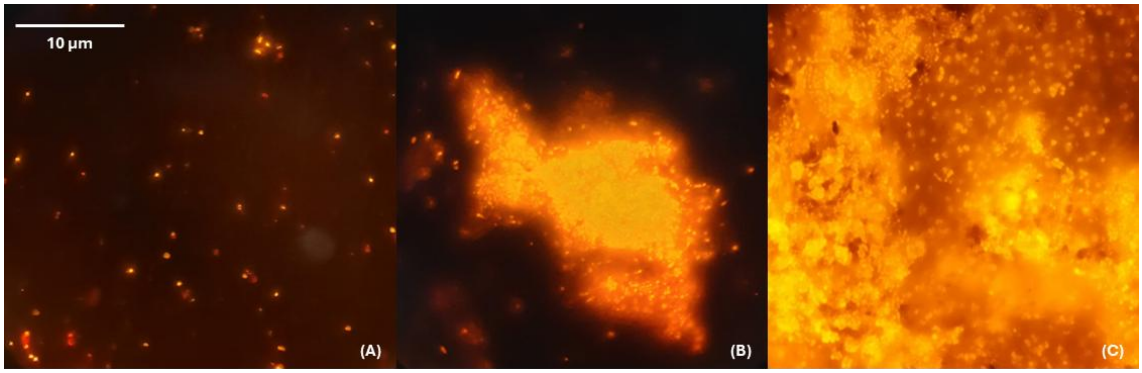

Figure III. 9 - Microscopic observations under fluorescent light, with 100× magnification, of biomass samples stained with Nile blue. Samples collected from the PHA production assay performed at the end of the culture selection, at 3 h (A), 12 h (B) and 29 h (C).

There was an average VSS production of 0.75 ± 0.18 g/L, concomitant with an average PHA accumulation of 65.14 ± 5.37wt.% (Table III. 3). Concerning substrate consumption, the culture exhibited high TPA removal efficiency (84.64 ± 9.20%) during the polymer productions. The lower TPA removal efficiency observed for assay B (74.71 ± 0.01%) is probably related with the lower concentration of VSS produced in the assay. Additionally, the overall polymer yield was 0.21 ± 0.02g_{PHA}/g_{TPA}, reinforcing that the selected microbiome ability to convert TPA into PHA efficiently remained stable.

The results obtained in assays A, B and C show the overall performance of the selection bioreactor remained relatively stable between days 69 and 113. For instance, the TPA removal efficiency remained high across all assays, with an average of 84.64 ± 9.20%, despite slight variations between 86.34 ± 0.01% and 74.71 ± 0.01% (Table III. 3). Similarly, PHA content showed consistency, averaging 65.14 ± 5.37wt.%, with values ranging from 60.65 ± 1.49wt.% to 71.32 ± 0.34wt.% (Table III. 3).

The slight differences among the average kinetic and stoichiometric parameters of the production assays were not statistically significant (Appendix B, Table B.1). These results show that, overall, the performance of the MMC selected from the marshland microbiome had consistent and comparable performance, indicating a stable and reliable culture.

Although no similar PHA production bioprocess has been reported for MMC utilizing PET-degrading products as feedstock, polymer production by the selected microbiome was comparable to those achieved for MMC systems selected from other natural microbiomes, like river sediments, using acetate (64.7wt.%) and glucose (60.5wt.%), and were notably higher than those observed with starch (27.3wt.%) (Cui et al., 2016). This indicates that the selected microbiome exhibited superior PHA storage efficiency with TPA compared to MMCs relying on more defined carbon sources. Furthermore, the PHA accumulation attained by the culture selected from marshland microbiome using REX-TPA was similar to or even exceeded values reported in the literature for MMCs using various feedstocks,

including sugar cane molasses (74.6wt.%) (Albuquerque et al., 2010), cheese whey (43wt.%) (Oliveira et al., 2018), lignocellulosic-based hydrolysate (27wt.%) (Dai et al., 2015) and confectionary industry effluents rich in ethanol and lactate (52.6 - 59.1wt.%) (Rangel et al., 2023). Nevertheless, the overall polymer yield was $0.21 \pm 0.02 g_{PHA}/g_{TPA}$, is still lower compared to that reported for wood hydrolysates ($0.32\ g_{PHB}/g_{sugars}$) (Dai et al., 2015) from lignocellulosic feedstock.

The microbial uptake of TPA is more complex due to its size and charge, requiring specific transporters to enter the cell (Hosaka et al., 2013; Kincannon et al., 2022), as it cannot diffuse freely across the cell membrane such as acetate (Pinhal et al., 2019). Consequently, substrates that require active transport, such as TPA are associated with higher oxygen demand for PHA storage , while conditions favouring passive diffusion (e.g., acetate) require less (Werker et al., 2022). Once internalized, TPA undergoes a multi-step metabolic pathway, where it is activated by TPA-dioxygenase, then subjected to ring cleavage before entering central metabolic pathways, a process that demands significant enzymatic activity (Gautom et al., 2021; Kincannon et al., 2022).

Furthermore, similar polymer yields ($0.17\ g_{PHA}/g_{TPA}$) have been attained by single cultures using disodium terephthalate obtained from PET-degradation, given its higher solubility (Kenny et al., 2012a). Previous studies have reported that Na^+ accumulation in cultivations can limit biomass production by reducing the specific uptake, ultimately hindering the maximization of polymer yield (Beagan et al., 2020).

III.3.5. PHA characterization

III.3.5.1. Composition

The MMC selected from the marshland microbiome produced a homopolymer of 3-HB (PHB) (Table III. 4). This monomeric composition aligns with that of PHA-producing microorganisms from the class *Gammaproteobacteria*, which dominated the culture during polymer production. Notably, members of the *Halomonas* genus (Crisafi et al., 2022) and microbial families, such as *Halomonadaceae* (Angra et al., 2023; Mitra et al., 2020) and *Zoogloeaceae* (Jiang et al., 2011) are known PHB producers and were present in the microbial community at the end of the selection process. Similarly, an MMC developed from river sediments under F/f regime during 350 cycles using acetate as substrate exhibited *Gammaproteobacteria* dominance and PHB production (Zhao et al., 2021).

Hence, the production of PHB suggest that TPA may have served as precursor for the 3-HB monomer. Nonetheless, the conversion of PET depolymerization monomers into PHA by MMC remains largely unexplored. Previous studies with monocultures that successfully upcycled TPA into PHA, reported TPA is typically metabolized into protocatechuate, which via ortho-cleavage pathway, is converted to β-carboxymuconate and ultimately acetyl-CoA, entering the TCA cycle (Qi et al., 2022). For example, *Ideonella sakaiensis* 201-F6 has been showed to convert acetyl-CoA into PHB from PET

hydrolytic products such as TPA (Fujiwara et al., 2021) due to a PHA synthase similar to the class I PhaC, which is capable of incorporating 3-hydroxybutyrate monomers (Tan et al., 2022).

Table III. 4 Molecular mass distribution and thermal properties of the PHB produced by different microbial sources (M_w, molecular weight; PDI, polydispersity index; T_m, melting temperature; ΔH_m, melting enthalpy**;** $T_{5\%}$, degradation temperature at 5% weight loss; T_{max}, maximum degradation temperature; X_c, crystallinity index; n.a., not available).

Microbial source	Assay	Feedstock	M_w (kDa)	PDI	T_m (ºC)	ΔH_m (J/g)	X_c (%)	$T_{5\%}$ (ºC)	T_{max} (ºC)	Reference
Marshland microbiome	A	REX-TPA	239	1.68	173	82.5	56.5	220.4	249.7	This study
	B		378	1.9	174	81.5	55.8	233.6	256.0	
	C		440	1.98	176	102.3	70.0	231.1	252.0	
	Average		352	1.85	174	88.7	61	228.4	252.6	
Petroleum refinery sludge	-	synthetic wastewater with sodium acetate	430	1.5	168	n.a.	50.4	258	289	Jayakrishnan et al., 2020
Brewery sludge	-		430	1.7	165	n.a.	53.3	268	293	
Soil sediments	-	Waste glycerol	1490	2.0	171.2	59.6	41.1	n.a.	n.a.	Ntaikou et al., 2018
Activated sludge from wastewater plant	-	Crude glycerol waste	200-380	1.2-1.7	158-171	n.a.	62-66	n.a.	n.a.	Hu et al., 2013
	-	Fermented candy wastewater	430	1.88	165.4	n.a.	n.a.	n.a.	293.6	Rangel et al., 2023

III.3.5.2. Molecular mass distribution

The PHB produced by the selected culture exhibited M_w values between 239 and 440 kDa, with their PDI varying from 1.68 to 1.98 (Table III. 4), with no statistical differences observed (p >0.05) among the samples obtained in assays A, B and C (Appendix B, Table B.2). These results are consistent with the M_w values reported for PHB synthesized by other microbial sources (Table III. 4). For instance, the PHB produced by activated sludge cultivated on crude glycerol waste exhibited M_w in the range of 200 and 380 kDa (Hu et al., 2013), while upon cultivation on fermented candy wastewater (430 kDa) (Rangel et al., 2023), brewery sludge (430 kDa), and petroleum refinery sludge cultivated on synthetic wastewater with sodium acetate (430 kDa) (Jayakrishnan et al., 2020) yielded similar M_w and PDI values of those obtained in this study. However, PHB with significantly higher M_w values, such as 1490 kDa, has been reported for an enriched MMC derived from soil sediments using waste glycerol as feedstock (Ntaikou et al., 2018). Additionally, single-culture systems, such as *Ideonella sakaiensis* 201-F6 and *Rhodococcus pyridinivorans* P23, using PET and TPA as substrates, achieved higher M_w values between 600 and 800 kDa (Fujiwara et al., 2021; Guo & Shao, 2020).

III.3.5.3. Thermal properties

The DSC curves (Appendix B, Figure B.1) of the biopolymer samples exhibited a T_m varying from 173 to 176 °C (Table III. 4). These values are in accordance with the typical range reported for PHB (173 -180 ºC) (Czerniecka-Kubicka et al., 2017), but slightly higher than those reported for PHB synthesized by other MMC, including those derived from petroleum refinery sludge (168 °C) and brewery sludge (Jayakrishnan et al., 2020), as well as from fermented candy wastewater (165.4 °C) (Rangel et al., 2023) (Table III. 4).

Additionally, the biopolymers also presented melting enthalpies between 81.5 and 102.3 J/g with crystallinities ranging from 55.8 to 70.0%. These values surpass those reported for PHB produced from various feedstocks, which typically range from 41.1% to 66% (Table III. 4). The higher crystallinity observed for PHB produced by the selected microbiome is comparable to that synthesized from waste-derived glycerol (Hu et al., 2013), suggesting the production of a stiffer and stronger material (McAdam et al., 2020).

The TGA curves (Figure III. 10) demonstrated the homopolymer's thermal stability up to approximately 220.4 to 233.6 ºC, suffering a weight loss of 5% within this range. The maximum degradation rate (T_{max}) for all biopolymer samples was observed between 249.7 and 256 ºC, where the biopolymer suffered a fast degradation in single-step process. Furthermore, there were no significant statistical differences among the PHB produced in assays A, B and C (Appendix B, Table B.2).

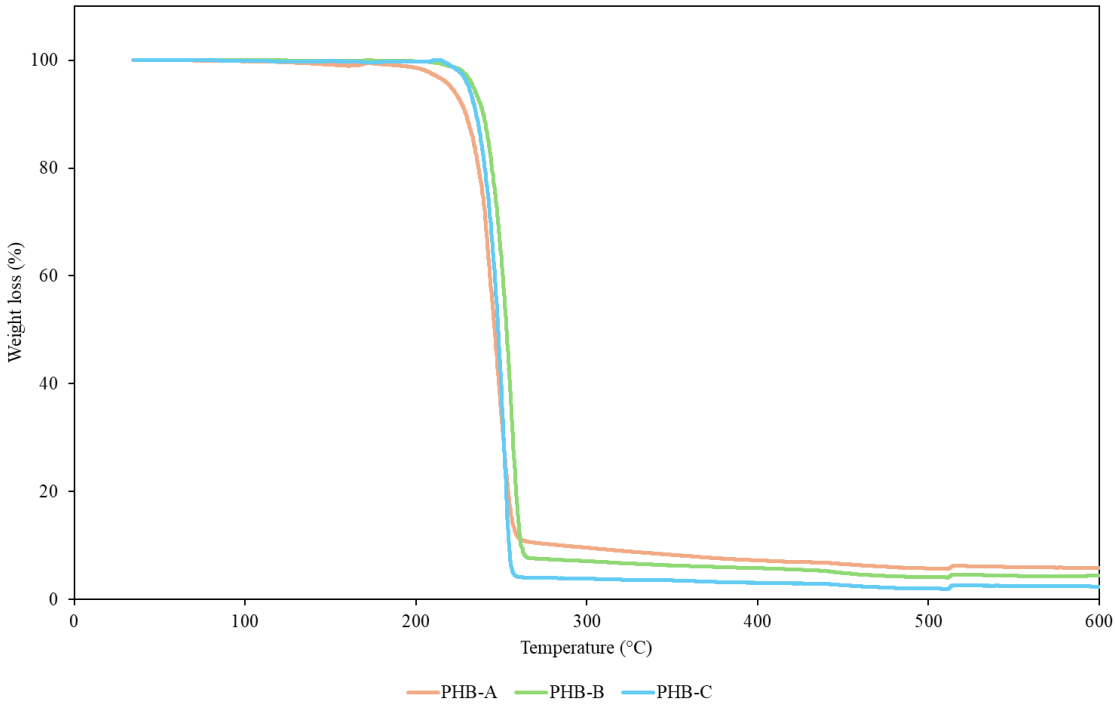

Figure III. 10 - Thermogravimetric curves of PHB produced of the three production assays with the selected marshland microbiome using REX-TPA as feedstock.

This thermal degradation profile is consistent with those reported for other PHB homopolymers (238-293 ºC) (Esmail et al., 2021; Montiel-Jarillo et al., 2022; Rebocho et al., 2020). However, the $T_{5\%}$ and T_{max} values (228 and 253°C, respectively) are slightly lower than those observed for PHB derived from petroleum refinery and brewery sludge (258-268°C and 289-293°C) (Jayakrishnan et al., 2020). This variation highlights the differences in thermal properties among PHB produced by various microbial systems.

The PHB produced by the selected marshland microbiome exhibited characteristics comparable to those of commercial PHB. For instance, Sigma-Aldrich PHB powder has a M_w of 550 kDa and a T_{max} of 277 ºC, while Biomer PHB extruded strand (with unknow additives) has a lower M_w of 280 kDa and T_{max} of 268 ºC (Morgan-Sagastume et al., 2015). Additionally, Biomer PHB powder shows a higher Mw of 660 kDa and T_{max} of 290 ºC (Morgan-Sagastume et al., 2015). In terms of thermal properties, Enmat Y3000 PHB powder and PHAlife™-PB3000 powder both have a melting temperature of 175 ºC, with the latter also reporting crystallinity index of 55–65% (https://shop.helianpolymers.com/, accessed on 30 January 2025).

III.3.6. PHB Films

III.3.6.1. Morphological characterization

The PHB was used to prepared films by solution casting and solvent evaporation. The films obtained were white and opaque, when visualized macroscopically (Fig. III. 11a).

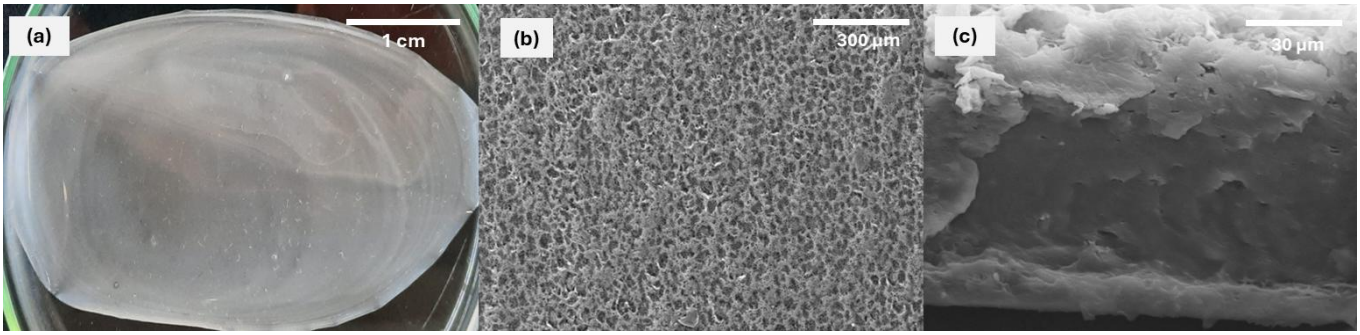

Figure III. 11 - PHB film (a). SEM images from the surface (b) and cross section (c), amplified 250× and 2500×, respectively.

SEM analysis of the films showed a very irregular and fractured surface (Fig. III. 11b), which could be the result from the rapid solvent evaporation rate imposed during the casting method (Rodrigues et al., 2024). The films' cross-section revealed a compact but irregular structure (Fig. III. 11c), with no visible porosity.

III.3.6.2. Mechanical properties

The biopolymer rendered films with average tensile strength ranging from 18.8 ± 1.9 MPa, an elongation at break between 8.01 ± 5.5 and 14.3 ± 0.9% and a Young's Modulus within 422.5 ± 142.3 MPa (Table III. 5).

Table III. 5. Mechanical properties of PHA films produced by polymer from marshland microbiome using REX-TPA as feedstock. (PHB, polyhydroxybutyrate; PET; polyethylene terephthalate; PP, polypropylene; HDPE, High-density Polypropylene; LDPE, Low density Polypropylene; PS, Polystyrene; PLA, polylactic acid; n.a., data not available).

Material	Thickness (µm)	σ (MPa)	ε (%)	E (MPa)	Reference
PHB	47 ± 9.1	18.8 ± 1.9	8.0 ± 5.5	422.5 ± 142.3	This study
PHB	70-300	14-40	1-15	283-3500	Adorna et al., 2022; Aydemir & Gardner, 2020; Bossu et al., 2021; McAdam et al., 2020; Rebocho et al., 2020; Zhao et al., 2003
PET	n.a.	45-62	230-7300	610-9350	McAdam et al., 2020; Sangroniz et al., 2019
PP	n.a.	27-98	200-1000	1180	Bastarrachea et al., 2011
HDPE	50	30–40	500–770	500-1100	McAdam 2020; Chrissafis 2009
LDPE	n.a.	12-30	200–600	88.4-500	McAdam et al., 2020; Sangroniz et al., 2019
PS	n.a.	50	n.a.	3100	Bastarrachea et al., 2011
PLA	n.a.	59	7	1280	Farah et al., 2016

The high tensile strength and Young's modulus of PHB suggests greater resistance to breaking under tension, as well as stiffness and resistance to deformation, which is associated with the material's crystallinity (X_c varying from 55.8 to 60.0%) (McAdam et al., 2020). The results align with those reported in literature for PHB films, confirming that the homopolymer produced was brittle and rigid (Adorna et al., 2022; Aydemir & Gardner, 2020; Bossu et al., 2021; McAdam et al., 2020; Rebocho et al., 2020; Zhao et al., 2003).

Comparing to commonly used packaging plastics such as PET, HDPE, and LDPE, the Young's modulus of the PHB films (260-525 MPa) was within values reported for LDPE (88.4-500 MPa) (McAdam et al., 2020; Sangroniz et al., 2019). However, PET (610-9350 MPa) (McAdam et al., 2020; Sangroniz et al., 2019), PP (1180 MPa) and PS (3100 MPa) (Bastarrachea et al., 2011) exhibit significantly higher stiffness than PHB. Moreover, PHB films present a lower tensile strength than PET (45-62 MPa), PP (27-98 MPa), HDPE (30–40 MPa), PS (50 MPa) and PLA (59 MPa), but fall within those reported for LDPE (12-30 MPa) (Table III. 5). Regarding elongation at break, PHB films exhibited low ductility (8.0 ± 5.5%), compared to LDPE (200-600%), HDPE (500-700%), and PP (200-1000%), which highlights

PHB's inherent brittleness. This aligns with previous findings on the homopolymer's limited flexibility (El-Hadi et al., 2002).

III.3.6.3. Barrier properties

The films prepared with PHB exhibited O_2 and CO_2 permeabilities of 8.68 ± 1.20 and 8.97 ± 1.25 Barrer, respectively (Table III. 6). These values align with previously reported permeability ranges for PHB (0.01–34.05 Barrer for O_2 and 0.33–26 Barrer for CO_2) (Beukelaer et al., 2022; Chaos et al., 2019; Follain et al., 2014; Rebocho et al., 2020). The observed variations in permeability are primarily related to biopolymer properties, namely M_w, and crystallinity. Additionally, film processing conditions, particularly the solvent casting method, play a significant role in performance. This technique often introduces variability due to challenges in achieving uniform film morphology, as factors such as solvent evaporation rates and polymer concentration directly impact film structural integrity (Alkandari & Castro-Dominguez, 2024; Perez-Martinez et al., 2024). Consequently, these inconsistencies can, in turn, impact the uniformity of the film's barrier and mechanical properties, as observed.

From a packaging perspective, low O_2 permeability is highly desirable, especially for applications that require protection against oxygen-sensitive spoilage, quality degradation, and moisture exposure (Mujtaba et al., 2022). The PHB films in this study demonstrated significantly lower O_2 permeability than PBAT (94.94 – 5550 Barrer) (Calderaro et al., 2020; Wu et al., 2021), which is widely used in flexible biodegradable packaging but provides poor gas barrier properties (Qin et al., 2021). The O_2 permeability values of the PHB films are higher to those of PET, which has an O_2 permeability range of 0.09 to 3.55 Barrer (Sangroniz et al., 2019; Wu et al., 2021), suggesting that PHB could be a viable alternative for oxygen-sensitive packaging. Similarly, PHB displayed a CO_2 permeability of 8.97 ± 1.25 Barrer, that fell within PET's values, reinforcing its potential as a sustainable alternative for packaging applications (Sangroniz et al., 2019; Wu et al., 2021). Furthermore, the PHB films in this study (Table III. 6) are within the range of permeability for O_2 (5.42 – 2513.70 Barrer) and CO_2 (6.3 Barrer) to those of LDPE films, widely used for packaging (Fiallos-Núñez et al., 2024). When compared to PP (97.21-116.72 Barrer) and PS (156.81 Barrer) (Wu et al., 2021), which have significantly higher O_2 permeability, PHB demonstrates superior gas barrier performance.

Table III. 6. Permeability values for oxygen, carbon dioxide and water vapour of PHA films and for different natural and synthetic materials for both gases (PHB, Poly(3-hydroxybutyrate); PBAT, Polybutylene adipate terephthalate; PLA, Polylactic acid; PET, polyethylene terephthalate; LDPE, low density polyethyelene; PP, Polypropylene; PS, Polystyrene; n.a., data not available).

Material	O_2 (Barrer)	CO_2 (Barrer)	WVP (g m^{-1} s^{-1} Pa^{-1})	Reference
PHB	8.68 ± 1.20	8.97 ± 1.25	$4.86\times10^{-16} \pm 1.41\times10^{-17}$	This study
PHB	0.01 – 34.05	0.33-26	$3.30\times10^{-15} – 6.28\times10^{-07}$	Beukelaer et al., 2022; Chaos et al., 2019; Follain et al., 2014; Rebocho et al., 2020
PBAT	94.94 - 5550	n.a.	$3.80 – 40.6\times10^{-11}$	Calderaro et al., 2020; Wu et al., 2021
PLA	5.14 – 22.96	n.a.	$1.85 – 10.10\times10^{-11}$	Drieskens et al., 2009; Wu et al., 2021
PET	0.09 – 3.55	0.50 - 11.20	$4.41 – 5.88\times10^{-12}$	Sangroniz et al., 2019; Wu et al., 2021
LDPE	5.42 – 2513.70	6.3	$8.14 – 17.71\times10^{-11}$	Sangroniz et al., 2019;Wu et al., 2021
PP	97.21- 116.72	n.a.	$1.47\text{-}2.94\times10^{-12}$	Wu et al., 2021
PS	156.81	n.a.	3.88×10^{-11}	Wu et al., 2021

This further highlights its suitability for applications requiring protection of oxygen-sensitive products. These findings indicate that PHB films are a promising alternative to synthetic plastics in packaging applications, reinforcing their potential as a sustainable packaging material. This aligns with the growing demand for biobased and biodegradable polyesters in the packaging industry (Mujtaba et al., 2022).

The PHB films exhibited WVP value of $4.86\times10^{-16} \pm 1.41\times10^{-17}$ g m^{-1} s^{-1} Pa^{-1} (Table III.6). These values are orders of magnitude lower than literature than those previously reported for PHB in literature ($5.73–3300\times10^{-11}$ g m^{-1} s^{-1} Pa^{-1}) (Beukelaer et al., 2022; Chaos et al., 2019; Follain et al., 2014; Rebocho et al., 2020). Moreover, these PHB films demonstrate better WVP properties compared to other biodegradable polymers, such as PBAT ($3.80–40.6\times10^{-11}$ $gm^{-1}s^{-1}Pa^{-1}$) and PLA ($1.85–10.10\times10^{-11}$ $gm^{-1}s^{-1}Pa^{-1}$) (Calderaro et al., 2020; Drieskens et al., 2009; Wu et al., 2021) but also to petroleum-based plastics in the packaging sector, such as PET ($4.41–5.88\times10^{-12}$ g m^{-1} s^{-1} Pa^{-1}), LDPE ($8.14–17.71\times10^{-11}$ g m^{-1} s^{-1} Pa^{-1}), PP ($1.47\text{-}2.94\times10^{-12}$ g m^{-1} s^{-1} Pa^{-1}) and PS (3.88×10^{-11} g m^{-1} s^{-1} Pa^{-1}). These results confirm that PHB

films prepared exhibited higher moisture barrier performance, making it an attractive candidate for applications where reduced water vapor transmission is essential, particularly in biodegradable mulch films and packaging applications (Anjana et al., 2024; Zhong et al., 2020).

It is noteworthy that film-preparation methodology and morphology—specifically the crystallinity of PHB (varied between 55.8 to 70.0%) along with the film's thickness may have played a role in influencing the films' permeability characteristics (Mujtaba et al., 2022). The high crystallinity of PHB creates an ordered molecular structure with fewer diffusion pathways for oxygen and moisture diffusion. Consequently, PHB has been utilized as coating material to enhance the barrier performance of materials such as paper and other biopolymers like poly(vinyl alcohol) (Anjana et al., 2024; Garcia-Garcia et al., 2022). Coupled with the interesting mechanical properties above demonstrated, these PHB films show potential for further development and incorporation into applications demanding low moisture permeability (Garcia-Garcia et al., 2022).

III.4. Conclusions

In this study, a natural microbiome collected from Tagus River estuarine marshland was subjected to the F/f strategy to select for a MMC enriched in PHA-storing organisms using depolymerized PET waste as sole feedstock. Applying the F/f strategy and keeping a 40-day SRT, the microbiome evolved into a PHA-storing MMC, comprising a community dominated by *Gammaproteobacteria*, a well-known class of PHA producers. Remarkably, the culture achieved 65.14±5.37wt% of PHA accumulation, representing the first study to report such high PHA storage for an MMC using TPA from PET waste as the sole substrate. This robust PHA production during the fed-batch cultivations demonstrates the feasibility of the culture selection process.

The PHB produced by the selected microbiome exhibited properties similar to those of commercial and previously reported PHB homopolymers, reinforcing its potential as a sustainable biopolymer with features suitable for commercialization, which could serve as a promising alternative to petroleum-based plastics. Furthermore, the PHB films exhibited good mechanical properties, with high tensile strength and stiffness, due to the PHB high crystallinity. However, their low deformation confirms their brittleness and rigidity, consistent with reported PHB characteristics. Regarding barrier performance, PHB films exhibited notable O_2 and CO_2 permeability, significantly better than PBAT, and synthetic plastics such as LDPE, PS, and PP, reinforcing PHB's potential as a competitive barrier material, making them particularly suitable for oxygen-sensitive packaging. Additionally, PHB demonstrated superior moisture resistance, outperforming PBAT, PLA as well as PET, PP, LDPE and PS. These findings highlight

PHB's potential as a sustainable alternative for biodegradable packaging and coatings, particularly in applications demanding low moisture and gas permeability.

Ultimately, this study introduces a novel approach for PET waste upcycling using natural microbial consortia, simultaneously producing a biodegradable alternative to synthetic plastics and contributing to the transformation of PET waste into a valuable resource, thus supporting circular economy, promoting sustainable plastic waste management and bio-based material development with industrial relevance.

IV.

CONCLUSIONS AND FUTURE WORK

This page was intentionally left blank

IV.1. General conclusions

This PhD thesis aimed to address the accumulation of PET waste by exploring additional biological upcycling strategies, through different microbial sources, capable of utilizing PET depolymerization products. Thus, the research focused on the microbial conversion of depolymerized pcPET waste into valuable bioproducts, particularly biodegradable plastics, aligning with market demand for sustainable bioplastics.

The research started with the characterization of a depolymerized pcPET waste (named REX-PET) and its processing to obtain REX-TPA, a heterogeneous substrate used as the sole carbon source for microbial conversion. REX-TPA presented a high Na content, due to the alkaline depolymerization process used to prepare REX-PET. The feedstock was primarily composed by TPA (19.69 ± 0.09 g/L), but also contain minor elements, such as Fe, Ti, Sb and Si, reflecting the heterogeneity of additives commonly found in mixed PET waste streams.

Isolated bacteria, namely *Delftia* sp. Ave5 and *Rhodococcus* sp. Ave7, were evaluated for their ability to utilize REX-TPA to grow and accumulate value-added intracellular storage compounds. Although the two bacteria were able to grow on REX-TPA, *Rhodococcus* sp. Ave7 demonstrated to be the microorganism with higher efficiency for upcycling REX-TPA into biomass, achieving a CDW of 5.09 g/L. It also demonstrated superior accumulation of intracellular storage compounds, reaching contents of 22.55 ± 0.02wt.% and 19.9 ± 1.51wt.% of PHA and TAGs, respectively. Specifically, it showed optimal conversion efficiency under conditions where TPA concentrations exceeded 10 g/L and ammonium levels were maintained at 0.3 g/L, a strategy designed to stimulate the production of intracellular storage compounds. These results unveiled *Rhodococcus* sp. Ave7 potential for high TPA degradation and the biosynthesis of value-added compounds with commercial relevance. Hence, the isolate was chosen as the most promising candidate for further bioreactor process development.

Rhodococcus sp. Ave7 was cultivated under different mode strategies. It was observed that, under batch and fed-batch with pulse feed, TAG synthesis was enhanced over PHA. Whereas, during the fed-batch process with continuous feeding, REX-TPA in excess was crucial to attain a final PHA and TAG synthesis of 0.58 and 0.59 g/L, respectively. The findings suggest that the higher availability of carbon source for the culture enhanced the flux towards PHA accumulation under ammonium-limiting conditions. *Rhodococcus* sp. Ave7 presented an overall high capacity for TPA consumption while yielding two value-added bioproducts, showcasing the potential for the isolate for upcycling pcPET waste. Furthermore, the characterization of both bioproducts revealed that *Rhodococcus* sp. Ave7 produced a PHBV copolyester with a high 3HV monomeric content, making it a promising candidate for copolymer blending. Additionally, the TAGs were mainly enriched in $C_{18:1}$ and $C_{16:0}$, highlighting their potential as complementary and renewable sources.

Additionally, this thesis explored, for the first time, the potential of a natural microbiome collected from a marshland to upcycle REX-TPA as sole feedstock, operating under an F/f strategy, to obtain an MMC enriched in PHA-storing organisms. During the first SRT, stabilizing the VSS concentration was crucial to ensure complete ammonium consumption from each cycle. The shorter feast phase resulted in the stabilization of F/f around 0.1, which is a strong indicator of a successful selection for PHA accumulation capacity. As a result, after the first SRT, PHA content in the VSS increased from 5.29% to 10.27% in the last SRT. The applied 4-day cycle and 40-day SRT conditions created strong selective pressure to obtain a stable and effective culture, mainly composed by *Gammaproteobacteria*, demonstrating its ability to upcycle REX-TPA into PHA.

The culture was able to maintain reproducible PHA content, reaching 65.14±5.37wt% at the end of the selection. Hence, reflecting the successful adaptation of the microbial community towards enhanced polymer storage capabilities over the selection process under the F/f strategy which led to a robust culture capable of consistent PHA accumulation. The produced biopolymer, namely PHB, presented intrinsic features which were consistent during the production and comparable to those of commercial PHB, since maintaining stable polymer composition properties is essential for future industrial applications.

Furthermore, the PHB films prepared demonstrating brittleness and rigidity, alongside promising barrier properties, with water vapor permeability lower than other biodegradable polymers as well as oxygen and carbon dioxide permeabilities comparable to synthetic plastics, namely such as LDPE, PS, and PP. These characteristics position PHB films as potential candidate for further optimization as strong candidate for sustainable packaging applications, offering a viable alternative to PET-based packaging.

Overall, this thesis demonstrated different biological approaches to address plastic waste accumulation through microbial upcycling of a depolymerized pc PET waste. The thesis successfully converted the processed depolymerized pcPET waste into different valuable compounds, namely PHA with different monomeric composition and TAGs, using both isolated single cultures and an MMC.

The research presents key results for upcycling approaches, more specifically a new strategy using an MMC, focusing on converting TPA obtained from PET waste into sustainable alternatives to conventional plastics. These processes not only promote a circular economy by integrating PET waste management with bioplastic production but also contribute to the development of eco-friendly materials, supporting efforts to mitigate plastic pollution and align with bio-based sustainability initiatives.

IV.2. Future Work

The results obtained in this PhD presented different biological upcycling strategies to valorise a depolymerized pcPET waste, using an MMC for the first time, as well as a single culture, to produce valuable compounds. Based on the findings, several suggestions for future work and improvements are to be considered.

The second chapter investigated different bacterial strains isolated from landfill soil, regarding their ability to use REX-TPA as a sole carbon source. Despite *Rhodococcus* sp. Ave7 presenting the highest biomass production and storage compounds synthesis, *Delftia* sp. Ave5 was also able to grow although at lower levels. Thus, it would be important to investigate further into substrate and nitrogen concentrations for optimizing biomass production and PHA yield, including testing various nitrogen sources (e.g., ammonium sulphate, ammonium nitrate, or urea) for the strain that presented potential for mixed PET waste upcycling.

Chapter II provided novel insights into using pcPET waste as feedstock for producing PHBV and TAGs with *Rhodococcus* sp. Ave7. However, challenges remain, particularly in improving yield and productivity, as continuous feeding assay results are still relatively low for economic feasibility at larger scales. The prolonged lag phase observed in *Rhodococcus* sp. Ave7 cultivations, a common issue for TPA-degrading bacteria, which could be addressed by optimizing inoculum preparation with a pre-inoculum or an additional carbon source for biomass growth, as well as gradually increasing REX-TPA concentrations over generations.

Despite the strain's high capacity to consume TPA, the conversion to desired products remained low, indicating that a significant portion of the substrate is not being converted to the target bioproducts. Thus, understanding the metabolic pathways and gene expression involved in PHA and TAG production would be crucial. Using metabolic engineering approaches to optimize carbon flux towards product synthesis could improve yields and productivity, making the process more viable for industrial applications.

Although a CDW comparable to other strains using plastic feedstocks was achieved, it remains insufficient for industrial applications, largely due to TPA's low solubility in aqueous media (approximately 0.017 g/L at 25 °C) (Kenny et al., 2012b). Most processes convert TPA to sodium terephthalate, which has a much higher solubility of approximately 130 g/L (Müller et al., 2023). Nevertheless, this requires larger volumes of REX-TPA feed to provide similar concentrations used in other processes. The use of a more readily metabolizable co-substrate (e.g. waste oils and waste glycerol) alongside REX-TPA could increase biomass growth and product productivity.

Lastly, the recovery and purification of PHBV from *Rhodococcus* biomass containing TAGs posed challenges due to their similar polarity and solubility in the solvents used during the purification step.

Thus, to improve purity and minimize losses, effective separation methods should be further assessed by exploring differences in thermal properties and solubility. For example, biomass pre-treatment, using sonication or supercritical CO_2 extraction might an alternative to separate TAGs prior to the extraction of PHBV from cells avoiding hazardous solvents. Adjusting the conditions of solvent extraction for butanol and temperature would be important to enhance the solubility of one of the bioproducts.

In Chapter III, the upcycling strategy developed for the marshland microbiome with REX-TPA revealed novel findings. However, future optimization could be performed during the culture selection to enhance global PHA productivity. One key factor was the operation in 4-day cycles using an F/f strategy, alongside an equal HRT and SRT of 40 days. This approach created a strong selective pressure on the MMC, directly influencing its overall PHA storage capacity.

To further refine the process, varying HRT and SRT during culture selection would be essential to better understand their impact on culture competitiveness, particularly in maintaining high PHA storage capacity while sustaining growth. Additionally, the prolonged famine phase acted as a physiological selective pressure, prompting the MMC to prioritize polymer storage over microbial growth in the following feast period. Another critical aspect during the selection stage was the stabilization of VSS, which played a fundamental role in enabling efficient ammonium consumption by the end of each cycle. However, VSS production remained low during selection stage. To address this, increasing biomass production by testing different REX-TPA and ammonium concentrations as well as tuning the F/f ratio and cycle length, could improve global PHA productivity, to maintain an appropriate selection pressure but also increase the concentration of biomass during the feast phase to sustain a highly enriched PHA-accumulating culture, ultimately enhancing process efficiency and yield.

Additionally, the use of real-time monitoring methods for biological processes during the culture selection to help predict REX-TPA consumption and monitoring intracellular PHA content in order to enhance process control for instance, evaluating operating conditions with REX-TPA feedstock. Further investigations could focus on optimizing productivity during PHA production assays. One key aspect would be controlling DO levels while maintaining a continuous feed of REX-TPA could help determine whether the constant availability of a carbon source prevents polymer consumption between pulses, which may occur with a pulse-feeding strategy in a way to avoid substrate inhibition.

Regarding the downstream process, in the study a chlorinated solvent was employed to recover the PHA produced, applying more sustainable approaches for PHA recovery from microbial biomass, namely non-halogenated solvent extraction or mechanical separation, would be important to improve economic and sustainable viability of PHA production using REX-TPA as feedstock. In addition, studying methods such as hot-press technique or extrusion would be interesting to prepare PHB films with more controlled uniformity.

Future studies should assess the metabolic capacity of the microbial sources tested throughout this work, both isolated strains and marshland microbiome, to upcycle the depolymerize pc PET waste.

Exploring their enzymatic machinery for degrading PET and metabolizing its by-products will highlight our understanding of biotechnological processes for PET upcycling and allowing to tackle different plastic from various waste sources. Combining these microbial pathways with complementary recycling techniques (enzymatic, thermal or chemical) can lead to new bioprocesses for the valorisation of complex PET waste for PHA production.

Furthermore, performing a techno-economic analysis to assess the costs and savings of the process would be of importance, to evaluate the competitiveness of the different design processes for single and mixed culture systems tested in this thesis and their different demands in terms of energy and materials. On the other hand, a life cycle assessment would be crucial to assess economic feasibility and environmental impact, providing a comprehensive understanding of the viability of the biological upcycling strategies presented for single and mixed cultures considering the already established recycling methods used for mixed PET waste. The analysis would help determine their potential contribution to a circular economy by quantifying resource efficiency, waste reduction, and the overall sustainability of the processes investigated in this thesis.

Addressing the identified limitations and proposed improvements would contribute to developing a more robust and scalable process, enhancing the technology presented in this thesis. By optimizing the upcycling of recalcitrant mixed PET waste into renewable, high-value products, this work aligns with circular economy principles and supports the transition toward more sustainable biomanufacturing strategies.

BIBLIOGRAPHY

Abang, S., Wong, F., Sarbatly, R., Sariau, J., Baini, R., & Besar, N. A. (2023). Bioplastic classifications and innovations in antibacterial, antifungal, and antioxidant applications. *Journal of Bioresources and Bioproducts*, *8*(4), 361–387. https://doi.org/10.1016/j.jobab.2023.06.005

Abedsoltan, H. (2023). A focused review on recycling and hydrolysis techniques of polyethylene terephthalate. *Polymer Engineering Science*, *63*(9), 2651–2674. https://doi.org/10.1002/pen.26406

Acharjee, S. A., Bharali, P., Gogoi, B., Sorhie, V., Walling, B., & Alemtoshi. (2023). PHA-Based Bioplastic: a Potential Alternative to Address Microplastic Pollution. *Water, Air, and Soil Pollution*, *234*(21). https://doi.org/10.1007/s11270-022-06029-2

Adesina, R. B., & Ogunseiju, P. (2017). An Assessment of Bathymetry, Hydrochemistry and Trace Metals in Sediments of Awoye Estuary in Ilaje Area, Southwestern Nigeria. *Journal of Geosciences and Geomatics*, *5*(2), 78–86. https://doi.org/10.12691/jgg-5-2-4

Adorna, J. A., Ruby, R. L., Dang, V. D., Doong, R. A., & S. Ventura, J. R. (2022). Biodegradable polyhydroxybutyrate/cellulose/calcium carbonate bioplastic composites prepared by heat-assisted solution casting method. *Journal of Applied Polymer Science*, *139*(7). https://doi.org/10.1002/app.51645

Afianti, N. F., Febrianti, F. K., Hatmanti, A., Endrotjahyo, E., Manik, H., & Sutiknowati, L. I. (2024). Identification and Screening of Biofilm-Forming Bacteria Isolated from Mangrove Sediment for Plastic Degradation. *Journal of Ecological Engineering*, *25*(8), 357–366. https://doi.org/10.12911/22998993/189541

Aghaie, E., Pazouki, M., Hosseini, M. R., Ranjbar, M., & Ghavipanjeh, F. (2009). Response surface methodology (RSM) analysis of organic acid production for Kaolin beneficiation by Aspergillus niger. *Chemical Engineering Journal*, *147*(2–3), 245–251. https://doi.org/10.1016/j.cej.2008.07.008

Aguado, A., Martínez, L., Becerra, L., Arieta-araunabeña, M., Arnaiz, S., Asueta, A., & Robertson, I. (2014). Chemical depolymerisation of PET complex waste: Hydrolysis vs. glycolysis. *Journal of Material Cycles and Waste Management*, *16*(2), 201–210. https://doi.org/10.1007/s10163-013-0177-y

Ahmad, F. B., Zhang, Z., Doherty, W. O. S., & O'Hara, I. M. (2019). The prospect of microbial oil production and applications from oil palm biomass. *Biochemical Engineering Journal*, *143*, 9–23. https://doi.org/10.1016/j.bej.2018.12.003

Ajmal, A. W., Masood, F., & Yasin, T. (2018). Influence of sepiolite on thermal, mechanical and biodegradation properties of poly-3-hydroxybutyrate-co-3-hydroxyvalerate nanocomposites. *Applied Clay Science*, *156*, 11–19. https://doi.org/10.1016/j.clay.2018.01.010

Aksu, D., Vural, C., Karabey, B., & Ozdemir, G. (2021). Biodegradation of Terephthalic Acid by Isolated Active Sludge Microorganisms and Monitoring of Bacteria in a Continuous Stirred Tank Reactor. *Brazilian Archives of Biology and Technology*, *64*, 1–10. https://doi.org/10.1590/1678-4324-2021200002

Albuquerque, M. G. E., Torres, C. A. V., & Reis, M. A. M. (2010). Polyhydroxyalkanoate (PHA) production by a mixed microbial culture using sugar molasses: Effect of the influent substrate concentration on culture selection. *Water Research*, *44*(11), 3419–3433. https://doi.org/10.1016/j.watres.2010.03.021

Ali, S. S., Elsamahy, T., Koutra, E., Kornaros, M., El-Sheekh, M., Abdelkarim, E. A., Zhu, D., & Sun, J. (2021). Degradation of conventional plastic wastes in the environment: A review on current status of knowledge and future perspectives of disposal. *Science of the Total Environment*, *771*. https://doi.org/10.1016/j.scitotenv.2020.144719

Alkandari, S. H., & Castro-Dominguez, B. (2024). Advanced and sustainable manufacturing methods of polymer-based membranes for gas separation: a review. *Frontiers in Membrane Science and Technology*, *3*. https://doi.org/10.3389/frmst.2024.1390599

Al-Maaded, M., Madi, N. K., Kahraman, R., Hodzic, A., & Ozerkan, N. G. (2012). An Overview of Solid Waste Management and Plastic Recycling in Qatar. *Journal of Polymers and the Environment*, *20*(1), 186–194. https://doi.org/10.1007/s10924-011-0332-2

Al-Salem, S. M., Lettieri, P., & Baeyens, J. (2009). Recycling and recovery routes of plastic solid waste (PSW): A review. *Waste Management*, *29*(10), 2625–2643. https://doi.org/10.1016/j.wasman.2009.06.004

Altaee, N., El-Hiti, G. A., Fahdil, A., Sudesh, K., & Yousif, E. (2017). Screening and Evaluation of Poly(3-hydroxybutyrate) with Rhodococcus equi Using Different Carbon Sources. *Arabian Journal for Science and Engineering*, *42*(6), 2371–2379. https://doi.org/10.1007/s13369-016-2327-8

Alvarez, H. M., Herrero, O. M., Lanfranconi, M. P., Silva, R. A., & Villalba, M. S. (2017). Biotechnological production and significance of triacylglycerols and wax esters. In Springer (Ed.), *Consequences of Microbial Interactions with Hydrocarbons, Oils, and Lipids: Production of Fuels and Chemicals. Handbook of Hydrocarbon and Lipid Microbiology.* (Sang Yup Lee, Vol. 1). Springer International Publishing AG, part of Springer Nature. https://doi.org/10.1007/978-3-319-50436-0_222

Alvarez, H. M., & Steinbüchel, A. (2002). Triacylglycerols in prokaryotic microorganisms. *Applied Microbiology and Biotechnology*, *60*(4), 367–376. https://doi.org/10.1007/s00253-002-1135-0

Amanat, N., Matturro, B., Villano, M., Lorini, L., Rossi, M. M., Zeppilli, M., Rossetti, S., & Petrangeli Papini, M. (2022). Enhancing the biological reductive dechlorination of trichloroethylene with PHA from mixed microbial cultures (MMC). *Journal of Environmental Chemical Engineering*, *10*(2). https://doi.org/10.1016/j.jece.2021.107047

Amir, M., Rizvi, S. F., Asif, M., Ahmad, A., Alshammari, M. B., Gupta, A., Zaheer, M. R., & Roohi, R. (2024). Polyhydroxybutyrate (PHB) bioplastic characterization from the isolate Pseudomonas stutzeri PSB1 synthesized using potato peel feedstock to combat solid waste management. *Biocatalysis and Agricultural Biotechnology*, *57*. https://doi.org/10.1016/j.bcab.2024.103097

Andrady, A. L., & Neal, M. A. (2009). Applications and societal benefits of plastics. *Philosophical Transactions of the Royal Society B: Biological Sciences*, *364*(1526), 1977–1984. https://doi.org/10.1098/rstb.2008.0304

Angra, V., Sehgal, R., & Gupta, R. (2023). Trends in PHA Production by Microbially Diverse and Functionally Distinct Communities. *Environmental Microbiology*, *85*, 572–585. https://doi.org/10.1007/s00248-022-01995-w

Anjana, N., Rawat, S., & Goswami, S. (2024). Development of a Biodegradable Ternary Blend of Poly(vinyl alcohol) and Polyhydroxybutyrate Functionalized with Triacetin for Agricultural Mulch Applications. *ACS Omega*, *9*(28), 30169–30182. https://doi.org/10.1021/acsomega.3c10027

Anjum, A., Zuber, M., Zia, K. M., Noreen, A., Anjum, M. N., & Tabasum, S. (2016). Microbial production of polyhydroxyalkanoates (PHAs) and its copolymers: A review of recent advancements. *International Journal of Biological Macromolecules*, *89*, 161–174. https://doi.org/10.1016/j.ijbiomac.2016.04.069

APHA. (1998). Standard Methods for the Examination of Water and Wastewater. In L. Clesceri & A. Greenberg (Eds.), *American Public Health Association (APHA)* (20th ed.). American Public Health Association (APHA).

Argiz, L., Fra-Vázquez, A., del Río, Á. V., & Mosquera-Corral, A. (2020). Optimization of an enriched mixed culture to increase PHA accumulation using industrial saline complex wastewater as a substrate. *Chemosphere*, *247*. https://doi.org/10.1016/j.chemosphere.2020.125873

Argiz, L., González-Cabaleiro, R., Val del Río, Á., González-López, J., & Mosquera-Corral, A. (2021). A novel strategy for triacylglycerides and polyhydroxyalkanoates production using waste lipids. *Science of the Total Environment*, *763*. https://doi.org/10.1016/j.scitotenv.2020.142944

Atiwesh, G., Mikhael, A., Parrish, C. C., Banoub, J., & Le, T. A. T. (2021). Environmental impact of bioplastic use: A review. *Heliyon*, *7*(9), e07918. https://doi.org/10.1016/j.heliyon.2021.e07918

Auta, H. S., Abioye, O. P., Aransiola, S. A., Bala, J. D., Chukwuemeka, V. I., Hassan, A., Aziz, A., & Fauziah, S. H. (2022). Enhanced microbial degradation of PET and PS microplastics under natural conditions in mangrove environment. *Journal of Environmental Management*, *304*. https://doi.org/10.1016/j.jenvman.2021.114273

Aydemir, D., & Gardner, D. J. (2020). The effects of cellulosic fillers on the mechanical, morphological, thermal, viscoelastic, and rheological properties of polyhydroxybutyrate biopolymers. *Polymer Composites*, *41*(9), 3842–3856. https://doi.org/10.1002/pc.25681

Azeem, M., Fournet, M. B., & Attallah, O. A. (2022). Ultrafast 99% Polyethylene terephthalate depolymerization into value added monomers using sequential glycolysis-hydrolysis under microwave irradiation. *Arabian Journal of Chemistry*, *15*(7). https://doi.org/10.1016/j.arabjc.2022.103903

Balola, A., Ferreira, S., & Rocha, I. (2024). From plastic waste to bioprocesses: Using ethylene glycol from polyethylene terephthalate biodegradation to fuel Escherichia coli metabolism and produce value-added compounds. *Metabolic Engineering Communications*, *19*. https://doi.org/10.1016/j.mec.2024.e00254

Baptista, S., Pereira, J. R., Gil, C. V., Torres, C. A. V., Reis, M. A. M., & Freitas, F. (2022). Development of Olive Oil and α-Tocopherol Containing Emulsions Stabilized by FucoPol: Rheological and Textural Analyses. *Polymers*, *14*(12). https://doi.org/10.3390/polym14122349

Barredo, A., Asueta, A., Amundarain, I., Leivar, J., Miguel-Fernández, R., Arnaiz, S., Epelde, E., López-Fonseca, R., & Gutiérrez-Ortiz, J. I. (2023). Chemical recycling of monolayer PET tray waste by alkaline hydrolysis. *Journal of Environmental Chemical Engineering*, *11*(3). https://doi.org/10.1016/j.jece.2023.109823

Basset, N., Katsou, E., Frison, N., Malamis, S., Dosta, J., & Fatone, F. (2016). Integrating the selection of PHA storing biomass and nitrogen removal via nitrite in the main wastewater treatment line. *Bioresource Technology*, *200*, 820–829. https://doi.org/10.1016/j.biortech.2015.10.063

Bastarrachea, L., Dhawan, S., & Sablani, S. S. (2011). Engineering Properties of Polymeric-Based Antimicrobial Films for Food Packaging. *Food Engineering Reviews*, *3*(2), 79–93. https://doi.org/10.1007/s12393-011-9034-8

Beagan, N., O'Connor, K. E., & Del Val, I. J. (2020). Model-based operational optimisation of a microbial bioprocess converting terephthalic acid to biomass. *Biochemical Engineering Journal*, *158*. https://doi.org/10.1016/j.bej.2020.107576

Bequer Urbano, S., Albarracín, V. H., Ordoñez, O. F., Farías, M. E., & Alvarez, H. M. (2013). Lipid storage in high-altitude Andean Lakes extremophiles and its mobilization under stress conditions in Rhodococcus sp. A5, a UV-resistant actinobacterium. *Extremophiles*, *17*(2), 217–227. https://doi.org/10.1007/s00792-012-0508-2

Beukelaer, H. de, Hilhorst, M., Workala, Y., Maaskant, E., & Post, W. (2022). Overview of the mechanical, thermal and barrier properties of biobased and/or biodegradable thermoplastic materials. *Polymer Testing*, *116*. https://doi.org/10.1016/j.polymertesting.2022.107803

Bhati, R., & Mallick, N. (2015). Poly(3-hydroxybutyrate-co-3-hydroxyvalerate) copolymer production by the diazotrophic cyanobacterium Nostoc muscorum Agardh: Process optimization and polymer characterization. *Algal Research*, *7*, 78–85. https://doi.org/10.1016/j.algal.2014.12.003

Bhola, S., Arora, K., Kulshrestha, S., Mehariya, S., Bhatia, R. K., Kaur, P., & Kumar, P. (2021). Established and Emerging Producers of PHA: Redefining the Possibility. *Applied Biochemistry and Biotechnology*, *193*(11), 3812–3854. https://doi.org/10.1007/s12010-021-03626-5

Bhubalan, K., Rathi, D. N., Abe, H., Iwata, T., & Sudesh, K. (2010). Improved synthesis of P(3HB-co-3HV-co-3HHx) terpolymers by mutant Cupriavidus necator using the PHA synthase gene of Chromobacterium sp. USM2 with high affinity towards 3HV. *Polymer Degradation and Stability*, *95*(8), 1436–1442. https://doi.org/10.1016/j.polymdegradstab.2009.12.018

Biermann, L., Brepohl, E., Eichert, C., Paschetag, M., Watts, M., & Scholl, S. (2021). Development of a continuous PET depolymerization process as a basis for a back-to-monomer recycling method. *Green Processing and Synthesis*, *10*(1), 361–373. https://doi.org/10.1515/gps-2021-0036

Blume, H. P., & Müller-Thomsen, U. (2007). A field experiment on the influence of the postulated global climatic change on coastal marshland soils. *Journal of Plant Nutrition and Soil Science*, *170*(1), 145–156. https://doi.org/10.1002/jpln.200521892

Bosco, F., Cirrincione, S., Carletto, R., Marmo, L., Chiesa, F., Mazzoli, R., & Pessione, E. (2021). Pha production from cheese whey and "scotta": Comparison between a consortium and a pure culture of leuconostoc mesenteroides. *Microorganisms*, *9*(12). https://doi.org/10.3390/microorganisms9122426

Bossu, J., Le Moigne, N., Dieudonné-George, P., Dumazert, L., Guillard, V., & Angellier-Coussy, H. (2021). Impact of the processing temperature on the crystallization behavior and mechanical properties of poly[R-3-hydroxybutyrate-co-(R-3-hydroxyvalerate)]. *Polymer*, *229*. https://doi.org/10.1016/j.polymer.2021.123987

Breitwieser, F. P., Baker, D. N., & Salzberg, S. L. (2018). KrakenUniq: Confident and fast metagenomics classification using unique k-mer counts. *Genome Biology*, *19*(1). https://doi.org/10.1186/s13059-018-1568-0

Breitwieser, F. P., & Salzberg, S. L. (2020). Pavian: Interactive analysis of metagenomics data for microbiome studies and pathogen identification. *Bioinformatics*, *36*(4), 1303–1304. https://doi.org/10.1093/bioinformatics/btz715

Brzeszcz, J., & Kaszycki, P. (2018). Aerobic bacteria degrading both n-alkanes and aromatic hydrocarbons: an undervalued strategy for metabolic diversity and flexibility. *Biodegradation*, *29*(4), 359–407. https://doi.org/10.1007/s10532-018-9837-x

Bugnicourt, E., Cinelli, P., Lazzeri, A., & Alvarez, V. (2014). Polyhydroxyalkanoate (PHA): Review of synthesis, characteristics, processing and potential applications in packaging. *Express Polymer Letters*, *8*(11), 791–808. https://doi.org/10.3144/expresspolymlett.2014.82

Burchard, H., Lange, X., Klingbeil, K., & Maccready, P. (2019). Mixing estimates for estuaries. *Journal of Physical Oceanography*, *49*(2), 631–648. https://doi.org/10.1175/JPO-D-18-0147.1

Calderaro, M. P., de Luca Sarantopóulos, C. I. G., Sanchez, E. M. S., & Morales, A. R. (2020). PBAT/hybrid nanofillers composites—Part 1: Oxygen and water vapor permeabilities, UV barrier and mechanical properties. *Journal of Applied Polymer Science*, *137*(46), 1–12. https://doi.org/10.1002/app.49522

Campanari, S., Augelletti, F., Rossetti, S., Sciubba, F., Villano, M., & Majone, M. (2017). Enhancing a multi-stage process for olive oil mill wastewater valorization towards polyhydroxyalkanoates and

biogas production. *Chemical Engineering Journal*, *317*, 280–289. https://doi.org/10.1016/j.cej.2017.02.094

Cantor, K. M., & Watts, P. (2011). Plastics Materials. In William Andrew Publishing (Ed.), *Applied Plastics Engineering Handbook: Processing and Materials*. Elsevier. https://doi.org/10.1016/B978-1-4377-3514-7.10001-

Cao, F., Wang, L., Zheng, R., Guo, L., Chen, Y., & Qian, X. (2022). Research and progress of chemical depolymerization of waste PET and high-value application of its depolymerization products. *RSC Advances*, *12*(49), 31564–31576. https://doi.org/10.1039/d2ra06499e

Cappelletti, M., Presentato, A., Piacenza, E., Firrincieli, A., Turner, R. J., & Zannoni, D. (2020). Biotechnology of Rhodococcus for the production of valuable compounds. *Applied Microbiology and Biotechnology*, *104*, 8567–8594. https://doi.org/10.1007/s00253-020-10861-z

Carr, C. M., Clarke, D. J., & Dobson, A. D. W. (2020). Microbial Polyethylene Terephthalate Hydrolases: Current and Future Perspectives. *Frontiers in Microbiology*, *11*, 1–23. https://doi.org/10.3389/fmicb.2020.571265

Carvalheira, M., Amorim, C. L., Oliveira, A. C., Guarda, E. C., Costa, E., Ribau Teixeira, M., Castro, P. M. L., Duque, A. F., & Reis, M. A. M. (2022). Valorization of Brewery Waste through Polyhydroxyalkanoates Production Supported by a Metabolic Specialized Microbiome. *Life*, *12*(9), 1–14. https://doi.org/10.3390/life12091347

Carvalheira, M., Hilliou, L., Oliveira, C. S. S., Guarda, E. C., & Reis, M. A. M. (2022). Polyhydroxyalkanoates from industrial cheese whey: Production and characterization of polymers with differing hydroxyvalerate content. *Current Research in Biotechnology*, *4*, 211–220. https://doi.org/10.1016/j.crbiot.2022.03.004

Castro, A. R., Rocha, I., Alves, M. M., & Pereira, M. A. (2016). Rhodococcus opacus B4: a promising bacterium for production of biofuels and biobased chemicals. *AMB Express*, *6*(1). https://doi.org/10.1186/s13568-016-0207-y

Chaber, P., Tylko, G., Włodarczyk, J., Nitschke, P., Hercog, A., Jurczyk, S., Rech, J., Kubacki, J., & Adamus, G. (2022). Surface Modification of PHBV Fibrous Scaffold via Lithium Borohydride Reduction. *Materials*, *15*(21). https://doi.org/10.3390/ma15217494

Chamas, A., Moon, H., Zheng, J., Qiu, Y., Tabassum, T., Jang, J. H., Abu-Omar, M., Scott, S. L., & Suh, S. (2020). Degradation Rates of Plastics in the Environment. *ACS Sustainable Chemistry and Engineering*, *8*(9), 3494–3511. https://doi.org/10.1021/acssuschemeng.9b06635

Chan, C. M., Vandi, L. J., Pratt, S., Halley, P., Ma, Y., Chen, G. Q., Richardson, D., Werker, A., & Laycock, B. (2019). Understanding the effect of copolymer content on the processability and mechanical properties of polyhydroxyalkanoate (PHA)/wood composites. *Composites Part A: Applied Science and Manufacturing*, *124*. https://doi.org/10.1016/j.compositesa.2019.05.005

Chang, S. H. (2023). Plastic waste as pyrolysis feedstock for plastic oil production: A review. *Science of the Total Environment*, *877*. https://doi.org/10.1016/j.scitotenv.2023.162719

Chaos, A., Sangroniz, A., Gonzalez, A., Iriarte, M., Sarasua, J. R., del Río, J., & Etxeberria, A. (2019). Tributyl citrate as an effective plasticizer for biodegradable polymers: effect of plasticizer on free

volume and transport and mechanical properties. *Polymer International*, *68*(1), 125–133. https://doi.org/10.1002/pi.5705

Chaturvedi, D., Bharti, D., Dhal, S., Sahu, D., Behera, H., Sahoo, M., Kim, D., Jarzębski, M., Anis, A., Mohanty, B., Sagiri, S. S., & Pal, K. (2023). Role of Stearic Acid as the Crystal Habit Modifier in Candelilla Wax-Groundnut Oil Oleogels. *ChemEngineering*, *7*(5). https://doi.org/10.3390/chemengineering7050096

Chen, G. Q. (2009). A microbial polyhydroxyalkanoates (PHA) based bio- and materials industry. *Chemical Society Reviews*, *38*(8), 2434–2446. https://doi.org/10.1039/b812677c

Chen, J., Li, W., Zhang, Z. Z., Tan, T. W., & Li, Z. J. (2018). Metabolic engineering of Escherichia coli for the synthesis of polyhydroxyalkanoates using acetate as a main carbon source. *Microbial Cell Factories*, *17*(102). https://doi.org/10.1186/s12934-018-0949-0

Chen, Y., Kumar, A., Wei, F., Tan, Q., & Li, J. (2021). Single-use plastics: Production, usage, disposal, and adverse impacts. *Science of the Total Environment*, *752*. https://doi.org/10.1016/j.scitotenv.2020.141772

Chen, Z., Huang, L., Wen, Q., & Guo, Z. (2015). Efficient polyhydroxyalkanoate (PHA) accumulation by a new continuous feeding mode in three-stage mixed microbial culture (MMC) PHA production process. *Journal of Biotechnology*, *209*, 68–75. https://doi.org/10.1016/j.jbiotec.2015.06.382

Chen, Z., Huang, L., Wen, Q., Zhang, H., & Guo, Z. (2017). Effects of sludge retention time, carbon and initial biomass concentrations on selection process: From activated sludge to polyhydroxyalkanoate accumulating cultures. *Journal of Environmental Sciences*, *52*, 76–84. https://doi.org/10.1016/j.jes.2016.03.014

Cheng, F., Cheng, J., Nan, Y., Xie, Y., Yang, T., Cheng, D., Zhu, J., & Xu, H. (2022). Enhancing oxidative hydration of ethylene towards ethylene glycol over metal-modified titanosilicate catalysts. *Applied Catalysis A: General*, *643*. https://doi.org/10.1016/j.apcata.2022.118752

Chong, G. G., Huang, X. J., Di, J. H., Xu, D. Z., He, Y. C., Pei, Y. N., Tang, Y. J., & Ma, C. L. (2018). Biodegradation of alkali lignin by a newly isolated Rhodococcus pyridinivorans CCZU-B16. *Bioprocess and Biosystems Engineering*, *41*(4), 501–510. https://doi.org/10.1007/s00449-017-1884-x

Colombo, B., Favini, F., Scaglia, B., Sciarria, T. P., D'Imporzano, G., Pognani, M., Alekseeva, A., Eisele, G., Cosentino, C., & Adani, F. (2017). Enhanced polyhydroxyalkanoate (PHA) production from the organic fraction of municipal solid waste by using mixed microbial culture. *Biotechnology for Biofuels*, *10*(1), 1–15. https://doi.org/10.1186/s13068-017-0888-8

Colombo, B., Sciarria, T. P., Reis, M., Scaglia, B., & Adani, F. (2016). Polyhydroxyalkanoates (PHAs) production from fermented cheese whey by using a mixed microbial culture. *Bioresource Technology*, *218*, 692–699. https://doi.org/10.1016/j.biortech.2016.07.024

Crisafi, F., Valentino, F., Micolucci, F., & Denaro, R. (2022). From Organic Wastes and Hydrocarbons Pollutants to Polyhydroxyalkanoates: Bioconversion by Terrestrial and Marine Bacteria. *Sustainability*, *14*. https://doi.org/10.3390/su14148241

Cruz, R. A. P., Oehmen, A., & Reis, M. A. M. (2022). The impact of biomass withdrawal strategy on the biomass selection and polyhydroxyalkanoates accumulation of mixed microbial cultures. *New Biotechnology*, *66*, 8–15. https://doi.org/10.1016/j.nbt.2021.08.004

Cruz, M. V., Araújo, D., Alves, V. D., Freitas, F., & Reis, M. A. M. (2016). Characterization of medium chain length polyhydroxyalkanoate produced from olive oil deodorizer distillate. *International Journal of Biological Macromolecules*, *82*, 243–248. https://doi.org/10.1016/j.ijbiomac.2015.10.043

Cui, Y. W., Ding, J. R., Ji, S. Y., & Peng, Y. Z. (2014). Start-up of halophilic nitrogen removal via nitrite from hypersaline wastewater by estuarine sediments in sequencing batch reactor. *International Journal of Environmental Science and Technology*, *11*(2), 281–292. https://doi.org/10.1007/s13762-013-0190-7

Cui, Y. W., Zhang, H. Y., Lu, P. F., & Peng, Y. Z. (2016). Effects of carbon sources on the enrichment of halophilic polyhydroxyalkanoate-storing mixed microbial culture in an aerobic dynamic feeding process. *Scientific Reports*, *6*. https://doi.org/10.1038/srep30766

Czerniecka-Kubicka, A., Frącz, W., Jasiorski, M., Błażejewski, W., Pilch-Pitera, B., Pyda, M., & Zarzyka, I. (2017). Thermal properties of poly(3-hydroxybutyrate) modified by nanoclay. *Journal of Thermal Analysis and Calorimetry*, *128*(3), 1513–1526. https://doi.org/10.1007/s10973-016-6039-9

Dai, J., Gliniewicz, K., Settles, M. L., Coats, E. R., & McDonald, A. G. (2015). Influence of organic loading rate and solid retention time on polyhydroxybutyrate production from hybrid poplar hydrolysates using mixed microbial cultures. *Bioresource Technology*, *175*, 23–33. https://doi.org/10.1016/j.biortech.2014.10.049

Damayanti, & Wu, H. S. (2021). Strategic possibility routes of recycled pet. *Polymers*, *13*, 1–37. https://doi.org/10.3390/polym13091475

Danso, D., Chow, J., & Streita, W. R. (2019). Plastics: Environmental and biotechnological perspectives on microbial degradation. *Applied and Environmental Microbiology*, *85*(e01095-19). https://doi.org/10.1128/AEM.01095-19

de Mello, A. F. M., Vandenberghe, L. P. de S., Machado, C. M. B., Valladares-Diestra, K. K., de Carvalho, J. C., & Soccol, C. R. (2023). Polyhydroxybutyrate production by Cupriavidus necator in a corn biorefinery concept. *Bioresource Technology*, *370*. https://doi.org/10.1016/j.biortech.2022.128537

de Souza, L., Manasa, Y., & Shivakumar, S. (2020). Bioconversion of lignocellulosic substrates for the production of polyhydroxyalkanoates. *Biocatalysis and Agricultural Biotechnology*, *28*. https://doi.org/10.1016/j.bcab.2020.101754

de Souza Reis, G. A., Michels, M. H. A., Fajardo, G. L., Lamot, I., & de Best, J. H. (2020). Optimization of green extraction and purification of PHA produced by mixed microbial cultures from sludge. *Water*, *12*(4). https://doi.org/10.3390/W12041185

Deng, Q., Wang, Y., Zhao, Y., & Li, J. (2017). Disodium terephthalate/multiwall-carbon nanotube nanocomposite as advanced anode material for Li-ion batteries. *Ionics*, *23*(10), 2613–2619. https://doi.org/10.1007/s11581-016-1951-3

Dhaka, V., Singh, S., Anil, A. G., Sunil Kumar Naik, T. S., Garg, S., Samuel, J., Kumar, M., Ramamurthy, P. C., & Singh, J. (2022). Occurrence, toxicity and remediation of polyethylene terephthalate plastics. A review. *Environmental Chemistry Letters*, *20*(3), 1777–1800. https://doi.org/10.1007/s10311-021-01384-8

Diankristanti, P. A., Lin, Y. C., Yi, Y. C., & Ng, I. S. (2024). Polyhydroxyalkanoates bioproduction from bench to industry: Thirty years of development towards sustainability. *Bioresource Technology*, *393*, 130149. https://doi.org/10.1016/j.biortech.2023.130149

Diao, J., Hu, Y., Tian, Y., Carr, R., & Moon, T. S. (2023). Upcycling of poly(ethylene terephthalate) to produce high-value bio-products. *Cell Reports*, *42*(1). https://doi.org/10.1016/j.celrep.2022.111908

Dias, J. M. L., Lemos, P. C., Serafim, L. S., Oliveira, C., Eiroa, M., Albuquerque, M. G. E., Ramos, A. M., Oliveira, R., & Reis, M. A. M. (2006). Recent advances in polyhydroxyalkanoate production by mixed aerobic cultures: From the substrate to the final product. *Macromolecular Bioscience*, *6*(11), 885–906. https://doi.org/10.1002/mabi.200600112

Ding, Q., & Zhu, H. (2023). The Key to Solving Plastic Packaging Wastes: Design for Recycling and Recycling Technology. *Polymers*, *15*(16, 1485), 1–22. https://doi.org/10.3390/polym15061485

Diniz, M. S. da F., Mourão, M. M., Xavier, L. P., & Santos, A. V. (2023). Recent Biotechnological Applications of Polyhydroxyalkanoates (PHA) in the Biomedical Sector—A Review. *Polymers*, *15*(22), 4405. https://doi.org/10.3390/polym15224405

Dionisi, D., Majone, M., Vallini, G., Di Gregorio, S., & Beccari, M. (2006). Effect of the applied organic load rate on biodegradable polymer production by mixed microbial cultures in a sequencing batch reactor. *Biotechnology and Bioengineering*, *93*(1), 76–88. https://doi.org/10.1002/bit.20683

Dissanayake, L., & Jayakody, L. N. (2021). Engineering Microbes to Bio-Upcycle Polyethylene Terephthalate. *Frontiers in Bioengineering and Biotechnology*, *9*. https://doi.org/10.3389/fbioe.2021.656465

Drieskens, M., Peeters, R., Mullens, J., Franco, D., Iemstra, P. J., & Hristova-Bogaerds, D. G. (2009). Structure versus properties relationship of poly(lactic acid). I. effect of crystallinity on barrier properties. *Journal of Polymer Science, Part B: Polymer Physics*, *47*(22), 2247–2258. https://doi.org/10.1002/polb.21822

Du Laing, G., De Meyer, B., Meers, E., Lesage, E., Van de Moortel, A., G Tack, F. M., & Verloo, M. G. (2008). Metal accumulation in intertidal marshes: role of sulphide precipitation. *Wetlands*, *28*(3), 735–746. https://doi.org/10.1672/07-103.1

El-Hadi, A., Schnabel, R., Straube, E., Müller, G., & Henning, S. (2002). Correlation between degree of crystallinity, morphology, glass temperature, mechanical properties and biodegradation of poly (3-hydroxyalkanoate) PHAs and their blends. *Polymer Testing*, *21*(6), 665–674. https://doi.org/10.1016/S0142-9418(01)00142-8

Elhami, V., van de Beek, N., Wang, L., Picken, S. J., Tamis, J., Sousa, J. A. B., Hempenius, M. A., & Schuur, B. (2022). Extraction of low molecular weight polyhydroxyalkanoates from mixed microbial cultures using bio-based solvents. *Separation and Purification Technology*, *299*. https://doi.org/10.1016/j.seppur.2022.121773

Eriksen, M. K., Pivnenko, K., Olsson, M. E., & Astrup, T. F. (2018). Contamination in plastic recycling: Influence of metals on the quality of reprocessed plastic. *Waste Management*, *79*, 595–606. https://doi.org/10.1016/j.wasman.2018.08.007

Esmail, A., Pereira, J. R., Sevrin, C., Grandfils, C., Menda, U. D., Fortunato, E., Oliva, A., & Freitas, F. (2021). Preparation and characterization of porous scaffolds based on poly(3-hydroxybutyrate) and poly(3-hydroxybutyrate-co-3-hydroxyvalerate). *Life*, *11*(9). https://doi.org/10.3390/life11090935

Esmail, A., Rebocho, A. T., Marques, A. C., Silvestre, S., Gonçalves, A., Fortunato, E., Torres, C. A. V., Reis, M. A. M., & Freitas, F. (2022). Bioconversion of Terephthalic Acid and Ethylene Glycol Into Bacterial Cellulose by *Komagataeibacter xylinus* DSM 2004 and DSM 46604. *Frontiers in Bioengineering and Biotechnology*, *10*. https://doi.org/10.3389/fbioe.2022.853322

Farah, S., Anderson, D. G., & Langer, R. (2016). Physical and mechanical properties of PLA, and their functions in widespread applications — A comprehensive review. *Advanced Drug Delivery Reviews*, *107*, 367–392. https://doi.org/10.1016/j.addr.2016.06.012

Faust, K., Denifl, P., & Hapke, M. (2023). Recent Advances in Catalytic Chemical Recycling of Polyolefins. *ChemCatChem*, *15*(13). https://doi.org/10.1002/cctc.202300310

Feng, L., Wang, Y., Inagawa, Y., Kasuya, K., Saito, T., Doi, Y., & Inoue, Y. (2004). Enzymatic degradation behavior of comonomer compositionally fractionated bacterial poly(3-hydroxybutyrate-co-3-hydroxyvalerate)s by poly(3-hydroxyalkanoate) depolymerases isolated from *Ralstonia pickettii* T1 and *Acidovorax* sp. TP4. *Polymer Degradation and Stability*, *84*(1), 95–104. https://doi.org/10.1016/j.polymdegradstab.2003.09.016

Fiallos-Núñez, J., Cardero, Y., Cabrera-Barjas, G., García-Herrera, C. M., Inostroza, M., Estevez, M., España-Sánchez, B. L., & Valenzuela, L. M. (2024). Eco-Friendly Design of Chitosan-Based Films with Biodegradable Properties as an Alternative to Low-Density Polyethylene Packaging. *Polymers*, *16*(17). https://doi.org/10.3390/polym16172471

Fidalgo, R. M., Ortigueira, J., Freches, A., Pelica, J., Gonçalves, M., Mendes, B., & Lemos, P. C. (2014). Bio-oil upgrading strategies to improve PHA production from selected aerobic mixed cultures. *New Biotechnology*, *31*(4), 297–307. https://doi.org/10.1016/j.nbt.2013.10.009

Follain, N., Chappey, C., Dargent, E., Chivrac, F., Crétois, R., & Marais, S. (2014). Structure and barrier properties of biodegradable polyhydroxyalkanoate films. *Journal of Physical Chemistry C*, *118*(12), 6165–6177. https://doi.org/10.1021/jp408150k

Fontanella, S., Bonhomme, S., Koutny, M., Husarova, L., Brusson, J. M., Courdavault, J. P., Pitteri, S., Samuel, G., Pichon, G., Lemaire, J., & Delort, A. M. (2010). Comparison of the biodegradability of various polyethylene films containing pro-oxidant additives. *Polymer Degradation and Stability*, *95*(6), 1011–1021. https://doi.org/10.1016/j.polymdegradstab.2010.03.009

Fournet, M. B., Attallah, O. A., Mojicevic, M., Chen, Y., & Major, I. (2022). *High Throughput Mechanochemical Depolymerisation and Purification of Polyethylene Terephthalate and Related Polymer.* WO2023088946A1.

Fradinho, J. C., Reis, M. A. M., & Oehmen, A. (2016). Beyond feast and famine: Selecting a PHA accumulating photosynthetic mixed culture in a permanent feast regime. *Water Research*, *105*, 421–428. http://dx.doi.org/10.1016/j.watres.2016.09.022

Francis, R. (2016). Methods of Recycling. In R. Francis (Ed.), *Recycling of polymers : methods, characterization and applications* (pp. 55–114). Wiley-VCH Verlag GmbH & Co. KGaA. John Wiley & Sons. https://doi.org/10.1002/9783527689002.ch3

Franden, M. A., Jayakody, L. N., Li, W. J., Wagner, N. J., Cleveland, N. S., Michener, W. E., Hauer, B., Blank, L. M., Wierckx, N., Klebensberger, J., & Beckham, G. T. (2018). Engineering *Pseudomonas putida* KT2440 for efficient ethylene glycol utilization. *Metabolic Engineering*, *48*, 197–207. https://doi.org/10.1016/j.ymben.2018.06.003

Fredi, G., & Dorigato, A. (2022). Recycling of bioplastic waste: A review. *Advanced Industrial and Engineering Polymer Research*, *4*(3), 159–177. https://doi.org/10.1016/j.aiepr.2021.06.006

Frison, N., Andreolli, M., Botturi, A., Lampis, S., & Fatone, F. (2021). Effects of the Sludge Retention Time and Carbon Source on Polyhydroxyalkanoate-Storing Biomass Selection under Aerobic-Feast and Anoxic-Famine Conditions. *ACS Sustainable Chemistry and Engineering*, *9*(28), 9455–9464. https://doi.org/10.1021/acssuschemeng.1c02973

Fujiwara, R., Sanuki, R., Ajiro, H., Fukui, T., & Yoshida, S. (2021). Direct fermentative conversion of poly(ethylene terephthalate) into poly(hydroxyalkanoate) by *Ideonella sakaiensis*. *Scientific Reports*, *11*(1). https://doi.org/10.1038/s41598-021-99528-x

Gao, R., Pan, H., Kai, L., Han, K., & Lian, J. (2022). Microbial degradation and valorization of poly(ethylene terephthalate) (PET) monomers. *World Journal of Microbiology and Biotechnology*, *38*(5). https://doi.org/10.1007/s11274-022-03270-z

Gao, R., & Sun, C. (2021). A marine bacterial community capable of degrading poly(ethylene terephthalate) and polyethylene. *Journal of Hazardous Materials*, *416*. https://doi.org/10.1016/j.jhazmat.2021.125928

Garcia-Garcia, D., Quiles-Carrillo, L., Balart, R., Torres-Giner, S., & Arrieta, M. P. (2022). Innovative solutions and challenges to increase the use of Poly(3-hydroxybutyrate) in food packaging and disposables. *European Polymer Journal*, *178*. https://doi.org/10.1016/j.eurpolymj.2022.111505

García-Torreiro, M., Lu-Chau, T. A., & Lema, J. M. (2016). Effect of nitrogen and/or oxygen concentration on poly(3-hydroxybutyrate) accumulation by *Halomonas boliviensis*. *Bioprocess and Biosystems Engineering*, *39*(9), 1365–1374. https://doi.org/10.1007/s00449-016-1612-y

Gautom, T., Dheeman, D., Levy, C., Butterfield, T., Alvarez Gonzalez, G., Le Roy, P., Caiger, L., Fisher, K., Johannissen, L., & Dixon, N. (2021). Structural basis of terephthalate recognition by solute binding protein TphC. *Nature Communications*, *12*(1), 1–12. https://doi.org/10.1038/s41467-021-26508-0

George, N., Debroy, A., Bhat, S., Singh, S., & Bindal, S. (2021). Biowaste to bioplastics: An ecofriendly approach for a sustainable future. *Journal of Applied Biotechnology Reports*, *8*(3), 221–233. https://doi.org/10.30491/jabr.2021.259403.1318

Geyer, R. (2020). Production, use, and fate of synthetic polymers. In Trevor M. Letcher (Ed.), *Plastic Waste and Recycling. Environmental Impact, Society Issues, Prevention, and Solutions* (pp. 13–32). Academic Press Inc. https://doi.org/10.1016/B978-0-12-817880-5.00002-5

Geyer, R., Jambeck, J. R., & Law, K. L. (2017). Production, use, and fate of all plastics ever made. *Science Advances*, *3*(7), 25–29. https://doi.org/10.1126/sciadv.1700782op

Ghosh, S., & Chakraborty, S. (2020). Production of polyhydroxyalkanoates (PHA) from aerobic granules of refinery sludge and Micrococcus aloeverae strain SG002 cultivated in oily wastewater. *International Biodeterioration and Biodegradation*, *155*. https://doi.org/10.1016/j.ibiod.2020.105091

Gibb, B. C. (2019). Plastics are forever. *Nature Chemistry*, *11*(5), 394–395. https://doi.org/10.1038/s41557-019-0260-7

Gilan, I., Hadar, Y., & Sivan, A. (2004). Colonization, biofilm formation and biodegradation of polyethylene by a strain of *Rhodococcus ruber*. *Applied Microbiology and Biotechnology*, *65*(1), 97–104. https://doi.org/10.1007/s00253-004-1584-8

Goel, V., Luthra, P., Kapur, G. S., & Ramakumar, S. S. V. (2021). Biodegradable/Bio-plastics: Myths and Realities. *Journal of Polymers and the Environment*, *29*(10), 3079–3104. https://doi.org/10.1007/s10924-021-02099-1

Grey, A., Costeira, R., Lorenzo, E., O'Kane, S., McCaul, M. V., McCarthy, T., Jordan, S. F., Allen, C. C. R., & Kelleher, B. P. (2023). Biogeochemical properties of blue carbon sediments influence the distribution and monomer composition of bacterial polyhydroxyalkanoates (PHA). *Biogeochemistry*, *162*(3), 359–380. https://doi.org/10.1007/s10533-022-01008-5

Grigore, M. E. (2017). Methods of recycling, properties and applications of recycled thermoplastic polymers. *Recycling*, *2*(24), 1–11. https://doi.org/10.3390/recycling2040024

Guarda, E. C., Amorim, C. L., Pasculli, G., Castro, P. M. L., Galinha, C. F., Duque, A. F., & Reis, M. A. M. (2024). Polyhydroxyalkanoates production from a waste-derived feedstock driven by the reactor operating conditions: The role of biomass microbiome and its reactivation capacity. *Journal of Cleaner Production*, *451*. https://doi.org/10.1016/j.jclepro.2024.141810

Guo, W., Duan, J., Shi, Z., Yu, X., & Shao, Z. (2023). Biodegradation of PET by the membrane-anchored PET esterase from the marine bacterium *Rhodococcus pyridinivorans* P23. *Communications Biology*, *6*(1). https://doi.org/10.1038/s42003-023-05470-1

Guo, W., & Shao, Z. (2020). *Rhodococcus pyridinivorans and application thereof in production of PHBV*. CN112063567A.

Hahn, T., Alzate, M. O., Leonhardt, S., Tamang, P., & Zibek, S. (2024). Current trends in medium-chain-length polyhydroxyalkanoates: Microbial production, purification, and characterization. *Engineering in Life Sciences*, *24*(6), 1–22. https://doi.org/10.1002/elsc.202300211

Hara, H., Eltis, L. D., Davies, J. E., & Mohn, W. W. (2007). Transcriptomic analysis reveals a bifurcated terephthalate degradation pathway in Rhodococcus sp. strain RHA1. *Journal of Bacteriology*, *189*(5), 1641–1647. https://doi.org/10.1128/JB.01322-06

Haywoodt, G. W., Anderson, A. J., Williams, D. R., Dawes, E. A., & Ewing, D. F. (1991). Accumulation of a poly(hydroxyalkanoate) copolymer containing primarily 3-hydroxyvalerate from simple carbohydrate substrates by *Rhodococcus* sp. NCIMB 40126. *International Journal of Biological Macromolecules*, *13*(2), 83–88. https://doi.org/10.1016/0141-8130(91)90053-W

Hernández, M. A., Mohn, W. W., Martínez, E., Rost, E., Alvarez, A. F., & Alvarez, H. M. (2008). Biosynthesis of storage compounds by *Rhodococcus jostii* RHA1 and global identification of genes involved in their metabolism. *BMC Genomics*, *9*. https://doi.org/10.1186/1471-2164-9-600

Herrera, D. A. G., Mojicevic, M., Pantelic, B., Joshi, A., Collins, C., Batista, M., Torres, C., Freitas, F., Murray, P., Nikodinovic-Runic, J., & Brennan Fournet, M. (2023). Exploring Microorganisms from Plastic-Polluted Sites: Unveiling Plastic Degradation and PHA Production Potential. *Microorganisms*, *11*(12). https://doi.org/10.3390/microorganisms11122914

Hong, S. G., Hsu, H. W., & Ye, M. T. (2013). Thermal properties and applications of low molecular weight polyhydroxybutyrate. *Journal of Thermal Analysis and Calorimetry*, *111*(2), 1243–1250. https://doi.org/10.1007/s10973-012-2503-3

Hori, K., Abe, M., & Unno, H. (2009). Production of triacylglycerol and poly(3-hydroxybutyrate-co-3-hydroxyvalerate) by the toluene-degrading bacterium *Rhodococcus aetherivorans* IAR1. *Journal of Bioscience and Bioengineering*, *108*(4), 319–324. https://doi.org/10.1016/j.jbiosc.2009.04.020

Hosaka, M., Kamimura, N., Toribami, S., Mori, K., Kasai, D., Fukuda, M., & Masai, E. (2013). Novel tripartite aromatic acid transporter essential for terephthalate uptake in *Comamonas* sp. strain e6. *Applied and Environmental Microbiology*, *79*(19), 6148–6155. https://doi.org/10.1128/AEM.01600-13

Hu, S., McDonald, A. G., & Coats, E. R. (2013). Characterization of polyhydroxybutyrate biosynthesized from crude glycerol waste using mixed microbial consortia. *Journal of Applied Polymer Science*, *129*(3), 1314–1321. https://doi.org/10.1002/app.38820

Huang, S., Wang, H., Ahmad, W., Ahmad, A., Vatin, N. I., Mohamed, A. M., Deifalla, A. F., & Mehmood, I. (2022). Plastic Waste Management Strategies and Their Environmental Aspects: A Scientometric Analysis and Comprehensive Review. In *International Journal of Environmental Research and Public Health 19* (8), 1-31. https://doi.org/10.3390/ijerph19084556

Huang, Z., Liu, R., Chen, F., Lai, Q., Oren, A., & Shao, Z. (2021). *Nitrogeniibacter aestuarii* sp. nov., a Novel Nitrogen-Fixing Bacterium Affiliated to the Family *Zoogloeaceae* and Phylogeny of the Family *Zoogloeaceae* Revisited. *Frontiers in Microbiology*, *12*. https://doi.org/10.3389/fmicb.2021.755908

Hur, D. H., Lee, J., Park, S. J., & Jeong, K. J. (2024). Engineering of Pseudomonas putida to produce medium-chain-length polyhydroxyalkanoate from crude glycerol. *International Journal of Biological Macromolecules*, *281*, 136411. https://doi.org/10.1016/j.ijbiomac.2024.136411

Ingram, H. R., Martin, R. J., & Winterburn, J. B. (2022). Optimized cell growth and poly(3-hydroxybutyrate) synthesis from saponified spent coffee grounds oil. *Applied Microbiology and Biotechnology*, *106*(18), 6033–6045. https://doi.org/10.1007/s00253-022-12093-9

Jabłońska, B. (2018). Water consumption management in polyethylene terephthalate (PET) bottles washing process via wastewater pretreatment and reuse. *Journal of Environmental Management*, *224*, 215–224. https://doi.org/10.1016/j.jenvman.2018.07.054

Jabłonska, B., Kiełbasa, P., Korenko, M., & Drózdz, T. (2019). Physical and chemical properties of waste from pET bottles washing as a component of solid fuels. *Energies*, *12*(11 (2197)), 1–17. https://doi.org/10.3390/en12112197

Jaffur, N., Jeetah, P., & Kumar, G. (2021). A review on enzymes and pathways for manufacturing polyhydroxybutyrate from lignocellulosic materials. *3 Biotech*, *11* (483), 1–24. https://doi.org/10.1007/s13205-021-03009-x

Jansen, J. A. (2016). Plastics - It's all about molecular structure. *Plastics Engineering*, *72*(8), 44–49. https://doi.org/10.1002/j.1941-9635.2016.tb01587.x

Jayakrishnan, U., Deka, D., & Das, G. (2020). Influence of inoculum variation and nutrient availability on polyhydroxybutyrate production from activated sludge. *International Journal of Biological Macromolecules*, *163*, 2032–2047. https://doi.org/10.1016/j.ijbiomac.2020.09.061

Jiang, Y., Marang, L., Kleerebezem, R., Muyzer, G., & Van Loosdrecht, M. C. M. (2011). Effect of temperature and cycle length on microbial competition in PHB-producing sequencing batch reactor. *ISME Journal*, *5*(5), 896–907. https://doi.org/10.1038/ismej.2010.174

Johnson, K., Jiang, Y., Kleerebezem, R., Muyzer, G., & Van Loosdrecht, M. C. M. (2009). Enrichment of a mixed bacterial culture with a high polyhydroxyalkanoate storage capacity. *Biomacromolecules*, *10*(4), 670–676. https://doi.org/10.1021/bm8013796

Joo, S., Cho, I. J., Seo, H., Son, H. F., Sagong, H. Y., Shin, T. J., Choi, S. Y., Lee, S. Y., & Kim, K. J. (2018). Structural insight into molecular mechanism of poly(ethylene terephthalate) degradation. *Nature Communications*, *9*(382). https://doi.org/10.1038/s41467-018-02881-1

Joseph, T. M., Azat, S., Ahmadi, Z., Jazani, O. M., Esmaeili, A., Kianfar, E., Haponiuk, J., & Thomas, S. (2024). Polyethylene terephthalate (PET) recycling: A review. *Case Studies in Chemical and Environmental Engineering*, *9*. https://doi.org/10.1016/j.cscee.2024.100673

Kacanski, M., Stelzer, F., Walsh, M., Kenny, S., O'Connor, K., & Neureiter, M. (2023). Pilot-scale production of mcl-PHA by Pseudomonas citronellolis using acetic acid as the sole carbon source. *New Biotechnology*, *78*, 68–75. https://doi.org/10.1016/j.nbt.2023.10.003

Kalia, V. C., Patel, S. K. S., & Lee, J.-K. (2023). Exploiting Polyhydroxyalkanoates for Biomedical Applications. *Polymers*, *15*(8). https://doi.org/ 10.3390/polym15081937

Kaniuk, Ł., Podborska, A., & Stachewicz, U. (2022). Enhanced mechanical performance and wettability of PHBV fiber blends with evening primrose oil for skin patches improving hydration and comfort. *Journal of Materials Chemistry B*, *10*(11), 1763–1774. https://doi.org/10.1039/d1tb02805g

Kataoka, M., Sasaki, M., Hidalgo, A. R. G. D., Nakano, M., & Shimizu, S. (2001). Glycolic acid production using ethylene glycol-oxidizing microorganisms. *Bioscience, Biotechnology and Biochemistry*, *65*(10), 2265–2270. https://doi.org/10.1271/bbb.65.2265

Kaur, G., & Roy, I. (2015). Lipopolystrategies for large-scale production of Polyhydroxyalkanoates. *Chemical and Biochemical Engineering Quarterly*, *29*(2), 157–172. https://doi.org/10.15255/CABEQ.2014.2255

Kenny, S. T., Runic, J. N., Kaminsky, W., Woods, T., Babu, R. P., Keely, C. M., Blau, W., & O'Connor, K. E. (2008). Up-cycling of PET (Polyethylene Terephthalate) to the biodegradable plastic PHA (Polyhydroxyalkanoate). *Environmental Science and Technology*, *42*(20), 7696–7701. https://doi.org/10.1021/es801010e

Kenny, S. T., Runic, J. N., Kaminsky, W., Woods, T., Babu, R. P., & O'Connor, K. E. (2012a). Development of a bioprocess to convert PET derived terephthalic acid and biodiesel derived glycerol to medium chain length polyhydroxyalkanoate. *Applied Microbiology and Biotechnology*, *95*(3), 623–633. https://doi.org/10.1007/s00253-012-4058-4

Kenny, S. T., Runic, J. N., Kaminsky, W., Woods, T., Babu, R. P., & O'Connor, K. E. (2012b). Development of a bioprocess to convert PET derived terephthalic acid and biodiesel derived glycerol to medium chain length polyhydroxyalkanoate. *Applied Microbiology Biotechnology*, *95*(3), 623–633. https://doi.org/10.1007/s00253-012-4058-4

Keshavarz, T., & Roy, I. (2010). Polyhydroxyalkanoates: bioplastics with a green agenda. *Current Opinion in Microbiology*, *13*(3), 321–326. https://doi.org/10.1016/j.mib.2010.02.006

Keskin, G., Klzll, G., Bechelany, M., Pochat-Bohatier, C., & Öner, M. (2017). Potential of polyhydroxyalkanoate (PHA) polymers family as substitutes of petroleum based polymers for packaging applications and solutions brought by their composites to form barrier materials. *Pure and Applied Chemistry*, *89*(12), 1841–1848. https://doi.org/https://doi.org/10.1515/pac-2017-0401

Khan, N., Ali, I., Mazhar, S., Munir, S., Batool, R., & Jamil, N. (2022). Co-Culture of Halotolerant Bacteria to Produce Poly(3-hydroxybutyrate-co-3-hydroxyvalerate) Using Sewage Wastewater Substrate. *Polymers*, *14*(22). https://doi.org/10.3390/ polym14224963

Khanna, S., & Srivastava, A. K. (2005). Recent advances in microbial polyhydroxyalkanoates. *Process Biochemistry*, *40*(2), 607–619. https://doi.org/10.1016/j.procbio.2004.01.053

Khatami, K., Perez-Zabaleta, M., Owusu-Agyeman, I., & Cetecioglu, Z. (2021). Waste to bioplastics: How close are we to sustainable polyhydroxyalkanoates production? *Waste Management*, *119*, 374–388. https://doi.org/10.1016/j.wasman.2020.10.008

Khuyen, V. T. K., Le, D. V., Fischer, A. R., & Dornack, C. (2021). Comparison of Microplastic Pollution in Beach Sediment and Seawater at UNESCO Can Gio Mangrove Biosphere Reserve. *Global Challenges*, *5*(11). https://doi.org/10.1002/gch2.202100044

Kibria, M. G., Masuk, N. I., Safayet, R., Nguyen, H. Q., & Mourshed, M. (2023). Plastic Waste: Challenges and Opportunities to Mitigate Pollution and Effective Management. *International Journal of Environmental Research 17* (20). https://doi.org/10.1007/s41742-023-00507-z

Kim, D., Choi, K. Y., Yoo, M., Zylstra, G. J., & Kim, E. (2018). Biotechnological potential of rhodococcus biodegradative pathways. *Journal of Microbiology and Biotechnology*, *28*(7), 1037–1051. https://doi.org/10.4014/jmb.1712.12017

Kim, H. T., Hee Ryu, M., Jung, Y. J., Lim, S., Song, H. M., Park, J., Hwang, S. Y., Lee, H. S., Yeon, Y. J., Sung, B. H., Bornscheuer, U. T., Park, S. J., Joo, J. C., & Oh, D. X. (2021). Chemo-Biological Upcycling of Poly(ethylene terephthalate) to Multifunctional Coating Materials. *ChemSusChem*, *14*(19), 4251–4259. https://doi.org/10.1002/cssc.202100909

Kim, H. T., Kim, J. K., Cha, H. G., Kang, M. J., Lee, H. S., Khang, T. U., Yun, E. J., Lee, D. H., Song, B. K., Park, S. J., Joo, J. C., & Kim, K. H. (2019). Biological Valorization of Poly(ethylene terephthalate) Monomers for Upcycling Waste PET. *ACS Sustainable Chemistry and Engineering*, *7*(24), 19396–19406. https://doi.org/10.1021/acssuschemeng.9b03908

Kim, N. K., Lee, S. H., & Park, H. D. (2022). Current biotechnologies on depolymerization of polyethylene terephthalate (PET) and repolymerization of reclaimed monomers from PET for bio-upcycling: A critical review. *Bioresource Technology*, *363*. https://doi.org/10.1016/j.biortech.2022.127931

Kincannon, W. M., Zahn, M., Clare, R., Beech, J. L., Romberg, A., Larson, J., Bothner, B., Beckham, G. T., McGeehan, J. E., & DuBois, J. L. (2022). Biochemical and structural characterization of an aromatic ring–hydroxylating dioxygenase for terephthalic acid catabolism. *Proceedings of the National Academy of Sciences of the United States of America*, *119*(13). https://doi.org/10.1073/pnas.2121426119

Kiselev, E. G., Demidenko, A. V., Zhila, N. O., Shishatskaya, E. I., & Volova, T. G. (2022). Sugar Beet Molasses as a Potential C-Substrate for PHA Production by Cupriavidus necator. *Bioengineering*, *9*(4). https://doi.org/10.3390/ bioengineering9040154

Klöckner, P., Reemtsma, T., & Wagner, S. (2021). The diverse metal composition of plastic items and its implications. *Science of the Total Environment*, *764*. https://doi.org/10.1016/j.scitotenv.2020.142870

Koller, M. (2018). A review on established and emerging fermentation schemes for microbial production of polyhydroxyalkanoate (PHA) biopolyesters. *Fermentation*, *4*(2). https://doi.org/10.3390/fermentation4020030

Koller, M., & Braunegg, G. (2015). Potential and prospects of continuous polyhydroxyalkanoate (PHA) production. *Bioengineering*, *2*(2), 94–121. https://doi.org/10.3390/bioengineering2020094

Koller, M., & Braunegg, G. (2018). Advanced approaches to produce polyhydroxyalkanoate (PHA) biopolyesters in a sustainable and economic fashion. *The EuroBiotech Journal*, *2*(2), 89–103. https://doi.org/10.2478/ebtj-2018-0013

Koller, M., Maršálek, L., de Sousa Dias, M. M., & Braunegg, G. (2017). Producing microbial polyhydroxyalkanoate (PHA) biopolyesters in a sustainable manner. *New Biotechnology*, *37*, 24–38. https://doi.org/10.1016/j.nbt.2016.05.001

Koller, M., Niebelschütz, H., & Braunegg, G. (2013). Strategies for recovery and purification of poly[(R)-3-hydroxyalkanoates] (PHA) biopolyesters from surrounding biomass. *Engineering in Life Sciences*, *13*(6), 549–562. https://doi.org/10.1002/elsc.201300021

Koop-Jakobsen, K., & Gutbrod, M. S. (2019). Shallow Salt Marsh Tidal Ponds–An Environment With Extreme Oxygen Dynamics. *Frontiers in Environmental Science*, *7*. https://doi.org/10.3389/fenvs.2019.00137

Koppala, B. C. N., Povari, S., Alam, S., Rao, V. V. B., Nakka, L., & Chenna, S. (2024). Comparative assessment on thermo-chemical conversion of different waste plastics to value added syngas: thermodynamic investigation. *Environment, Development and Sustainability*, *0123456789*. https://doi.org/10.1007/s10668-024-04811-2

Körbahti, B. K., & Rauf, M. A. (2008). Response surface methodology (RSM) analysis of photoinduced decoloration of toludine blue. *Chemical Engineering Journal*, *136*(1), 25–30. https://doi.org/10.1016/j.cej.2007.03.007

Koshti, R., Mehta, L., & Samarth, N. (2018). Biological Recycling of Polyethylene Terephthalate: A Mini-Review. *Journal of Polymers and the Environment*, *26*(8), 3520–3529. https://doi.org/10.1002/pen.26017

Kourmentza, C., Plácido, J., Venetsaneas, N., Burniol-Figols, A., Varrone, C., Gavala, H. N., & Reis, M. A. M. (2017). Recent advances and challenges towards sustainable polyhydroxyalkanoate (PHA) production. *Bioengineering*, *4*(2), 1–43. https://doi.org/10.3390/bioengineering4020055

Kumar, M., Bolan, S., Padhye, L. P., Konarova, M., Foong, S. Y., Lam, S. S., Wagland, S., Cao, R., Li, Y., Batalha, N., Ahmed, M., Pandey, A., Siddique, K. H. M., Wang, H., Rinklebe, J., & Bolan, N. (2023). Retrieving back plastic wastes for conversion to value added petrochemicals: opportunities, challenges and outlooks. *Applied Energy*, *345*(121307). https://doi.org/10.1016/j.apenergy.2023.121307

Kumar, M., Rathour, R., Singh, R., Sun, Y., Pandey, A., Gnansounou, E., Andrew Lin, K. Y., Tsang, D. C. W., & Thakur, I. S. (2020). Bacterial polyhydroxyalkanoates: Opportunities, challenges, and prospects. *Journal of Cleaner Production, 263*. https://doi.org/10.1016/j.jclepro.2020.121500

Kumar, R., Verma, A., Shome, A., Sinha, R., Sinha, S., Jha, P. K., Kumar, R., Kumar, P., Shubham, Das, S., Sharma, P., & Prasad, P. V. V. (2021). Impacts of plastic pollution on ecosystem services, sustainable development goals, and need to focus on circular economy and policy interventions. *Sustainability*, *13*(17). https:// doi.org/10.3390/su13179963

Kumar, V., Maitra, S. S., Singh, R., & Burnwal, D. K. (2020). Acclimatization of a newly isolated bacteria in monomer terephthalic acid (TPA) may enable it to attack the polymer poly-ethylene tere-phthalate(PET). *Journal of Environmental Chemical Engineering*, *8*(4). https://doi.org/10.1016/j.jece.2020.103977

Kunwar, B., Cheng, H. N., Chandrashekaran, S. R., & Sharma, B. K. (2016). Plastics to fuel: a review. *Renewable and Sustainable Energy Reviews*, *54*, 421–428. http://dx.doi.org/10.1016/j.rser.2015.10.015

Kusenberg, M., Eschenbacher, A., Delva, L., De Meester, S., Delikonstantis, E., Stefanidis, G. D., Ragaert, K., & Van Geem, K. M. (2022). Towards high-quality petrochemical feedstocks from mixed plastic packaging waste via advanced recycling: The past, present and future. *Fuel Processing Technology*, *238*. https://doi.org/10.1016/j.fuproc.2022.107474

Lahel, A., Fanta, A. B., Sergienko, N., Shakya, M., López, M. E., Behera, S. K., Rene, E. R., & Park, H. S. (2016). Effect of process parameters on the bioremediation of diesel contaminated soil by mixed microbial consortia. *International Biodeterioration and Biodegradation*, *113*, 375–385. https://doi.org/10.1016/j.ibiod.2016.05.005

Langford, A., Chan, C. M., Pratt, S., Garvey, C. J., & Laycock, B. (2019). The morphology of crystallisation of PHBV/PHBV copolymer blends. *European Polymer Journal*, *112*, 104–119. https://doi.org/10.1016/j.eurpolymj.2018.12.022

Lanham, A. B., Ricardo, A. R., Coma, M., Fradinho, J., Carvalheira, M., Oehmen, A., Carvalho, G., & Reis, M. A. M. (2012). Optimisation of glycogen quantification in mixed microbial cultures. *Bioresource Technology*, *118*, 518–525. https://doi.org/10.1016/j.biortech.2012.05.087

Lapa, H. M., & Martins, L. M. D. R. S. (2023). p-Xylene Oxidation to Terephthalic Acid: New Trends. *Molecules*, *28*(4), 1922. https:// doi.org/10.3390/molecules28041922

Laycock, B., Halley, P., Pratt, S., Werker, A., & Lant, P. (2014). The chemomechanical properties of microbial polyhydroxyalkanoates. *Progress in Polymer Science*, *39*(2), 397–442. https://doi.org/10.1016/j.progpolymsci.2013.06.008

Lebreton, L., & Andrady, A. (2019). Future scenarios of global plastic waste generation and disposal. *Palgrave Communications*, *5*(6), 1–11. https://doi.org/10.1057/s41599-018-0212-7

Lee, H. L., Chiu, C. W., & Lee, T. (2021). Engineering terephthalic acid product from recycling of PET bottles waste for downstream operations. *Chemical Engineering Journal Advances*, *5*. https://doi.org/10.1016/j.ceja.2020.100079

Lee, W. H., Azizan, M. N. M., & Sudesh, K. (2004). Effects of culture conditions on the composition of poly(3-hydroxybutyrate-co-4-hydroxybutyrate) synthesized by *Comamonas acidovorans*. *Polymer Degradation and Stability*, *84*(1), 129–134. https://doi.org/10.1016/j.polymdegradstab.2003.10.003

Lemoigne, M. (1926). Produits de déshydration et de polymerisation de l'acide boxybutyrique. *Bull. Soc. Chim. Biol*, *8*, 770–782.

Lenchi, N., Kebbouche-Gana, S., Servais, P., Gana, M. L., & Llirós, M. (2020). Diesel Biodegradation Capacities and Biosurfactant Production in Saline-Alkaline Conditions by *Delftia* sp NL1, Isolated from an Algerian Oilfield. *Geomicrobiology Journal*, *37*(5), 454–466. https://doi.org/10.1080/01490451.2020.1722769

Li, C., Aston, J. E., Lacey, J. A., Thompson, V. S., & Thompson, D. N. (2016). Impact of feedstock quality and variation on biochemical and thermochemical conversion. *Renewable and Sustainable Energy Reviews*, *65*, 525–536. https://doi.org/10.1016/j.rser.2016.06.063

Li, H., Chi, Z., Li, J., Wu, H., & Yan, B. (2019). Bacterial community structure and function in soils from tidal freshwater wetlands in a Chinese delta: Potential impacts of salinity and nutrient. *Science of the Total Environment*, *696*. https://doi.org/10.1016/j.scitotenv.2019.134029

Li, M., & Wilkins, M. R. (2020). Recent advances in polyhydroxyalkanoate production: Feedstocks, strains and process developments. *International Journal of Biological Macromolecules*, *156*, 691–703. https://doi.org/10.1016/j.ijbiomac.2020.04.082

Lin, C. W., Wu, C. H., Tran, D. T., Shih, M. C., Li, W. H., & Wu, C. F. (2011). Mixed culture fermentation from lignocellulosic materials using thermophilic lignocellulose-degrading anaerobes. *Process Biochemistry*, *46*(2), 489–493. https://doi.org/10.1016/j.procbio.2010.09.024

Liu, J., Xu, G., Dong, W., Xu, N., Xin, F., Ma, J., Fang, Y., Zhou, J., & Jiang, M. (2018). Biodegradation of diethyl terephthalate and polyethylene terephthalate by a novel identified degrader Delftia sp. WL-3 and its proposed metabolic pathway. *Letters in Applied Microbiology*, *67*(3), 254–261. https://doi.org/10.1111/lam.13014

Liu, J., Zhou, J., Xu, N., He, A., Xin, F., Ma, J., Fang, Y., Zhang, W., Liu, S., Jiang, M., & Dong, W. (2019). Performance evaluation of a lab-scale moving bed biofilm reactor (MBBR) using polyethylene as support material in the treatment of wastewater contaminated with terephthalic acid. *Chemosphere*, *227*, 117–123. https://doi.org/10.1016/j.chemosphere.2019.03.186

Liu, P., Zhang, T., Zheng, Y., Li, Q., Su, T., & Qi, Q. (2021). Potential one-step strategy for PET degradation and PHB biosynthesis through co-cultivation of two engineered microorganisms. *Engineering Microbiology*, *1*. https://doi.org/10.1016/j.engmic.2021.100003

Liu, P., Zheng, Y., Yuan, Y., Han, Y., Su, T., & Qi, Q. (2023). Upcycling of PET oligomers from chemical recycling processes to PHA by microbial co-cultivation. *Waste Management*, *172*, 51–59. https://doi.org/10.1016/j.wasman.2023.08.048

Liu, S., Zhang, Y., Zhao, C., Li, H., Shen, X., Zhou, M., Daigger, G. T., Zhang, P., & Song, G. (2024). Effects of nitrogen and carbon source addition on biomass and protein production by Rhodopseudomonas via the RSM-CCD approach. *Desalination and Water Treatment*, *319*. https://doi.org/10.1016/j.dwt.2024.100438

Liu, Y., Yao, X., Yao, H., Zhou, Q., Xin, J., Lu, X., & Zhang, S. (2020). Degradation of poly(ethylene terephthalate) catalyzed by metal-free choline-based ionic liquids. *Green Chem*, *22*(10), 3122–3131. https://doi.org/10.1039/d0gc00327a

Lomwongsopon, P., & Varrone, C. (2022a). Contribution of Fermentation Technology to Building Blocks for Renewable Plastics. *Fermentation*, *8*(2). https://doi.org/10.3390/fermentation8020047

Lomwongsopon, P., & Varrone, C. (2022b). Critical Review on the Progress of Plastic Bioupcycling Technology as a Potential Solution for Sustainable Plastic Waste Management. *Polymers*, *14*(22). https://doi.org/10.3390/polym14224996

Loo, C. Y., & Sudesh, K. (2007). Biosynthesis and native granule characteristics of poly(3-hydroxybutyrate-co-3-hydroxyvalerate) in *Delftia acidovorans*. *International Journal of Biological Macromolecules*, *40*(5), 466–471. https://doi.org/10.1016/j.ijbiomac.2006.11.003

Lorini, L., di Re, F., Majone, M., & Valentino, F. (2020). High rate selection of PHA accumulating mixed cultures in sequencing batch reactors with uncoupled carbon and nitrogen feeding. *New Biotechnology*, *56*, 140–148. https://doi.org/10.1016/j.nbt.2020.01.006

Lundstedt, T., Seifert, E., Abramo, L., Thelin, B., Nystrom, A., Pettersen, J., & Bergmanä Bergman, R. (1998). Experimental design and optimization. *Chemometrics and Intelligent Laboratory Systems*, *42*(1–2), 3–40. https://doi.org/10.1016/S0169-7439(98)00065-3

Lv, S., Li, Y., Zhao, S., & Shao, Z. (2024). Biodegradation of Typical Plastics: From Microbial Diversity to Metabolic Mechanisms. *International Journal of Molecular Sciences*, *25*(1). https://doi.org/10.3390/ijms25010593

Lyu, X., Nuhu, M., Candry, P., Wolfanger, J., Betenbaugh, M., Saldivar, A., Zuniga, C., Wang, Y., & Shrestha, S. (2024). Top-down and bottom-up microbiome engineering approaches to enable bio-omanufacturing from waste biomass. *Journal of Industrial Microbiology and Biotechnology*, *51*. https://doi.org/10.1093/jimb/kuae025

Ma, K., Zhang, X., Shang, Y., Zhu, Z., Li, X., Li, X., & Li, X. (2020). Improved purified terephthalic acid wastewater treatment using combined UAFB-SBR system: At mesophilic and ambient temperature. *Chemosphere*, *247*. https://doi.org/10.1016/j.chemosphere.2019.125752

Magalhães, C., Costa, J., Teixeira, C., & Bordalo, A. A. (2007). Impact of trace metals on denitrification in estuarine sediments of the Douro River estuary, Portugal. *Marine Chemistry*, *107*(3), 332–341. https://doi.org/10.1016/j.marchem.2007.02.005

Maheswaran, B., Al-Ansari, M., Al-Humaid, L., Sebastin Raj, J., Kim, W., Karmegam, N., & Mohamed Rafi, K. (2023). In vivo degradation of polyethylene terephthalate using microbial isolates from plastic polluted environment. *Chemosphere*, *310*. https://doi.org/10.1016/j.chemosphere.2022.136757

Mai, J., Kockler, K., Parisi, E., Chan, C. M., Pratt, S., & Laycock, B. (2024). Synthesis and physical properties of polyhydroxyalkanoate (PHA)-based block copolymers: A review. *International Journal of Biological Macromolecules*, *263*. https://doi.org/10.1016/j.ijbiomac.2024.130204

Makryniotis, K., Nikolaivits, E., Gkountela, C., Vouyiouka, S., & Topakas, E. (2023). Discovery of a polyesterase from *Deinococcus maricopensis* and comparison to the benchmark LCC^{ICCG} suggests high potential for semi-crystalline post-consumer PET degradation. *Journal of Hazardous Materials*, *455*. https://doi.org/10.1016/j.jhazmat.2023.131574

Mannina, G., Presti, D., Montiel-Jarillo, G., Carrera, J., & Suárez-Ojeda, M. E. (2020). Recovery of polyhydroxyalkanoates (PHAs) from wastewater: A review. *Bioresource Technology*, *297*. https://doi.org/10.1016/j.biortech.2019.122478

Marczak, H. (2022). Energy Inputs on the Production of Plastic Products. *Journal of Ecological Engineering*, *23*(9), 146–156. https://doi.org/10.12911/22998993/151815

Martínez-Narro, G., Hassan, S., & Phan, A. N. (2024). Chemical recycling of plastic waste for sustainable polymer manufacturing – A critical review. *Journal of Environmental Chemical Engineering*, *12*(2). https://doi.org/10.1016/j.jece.2024.112323

Martins, D., Alves da Silva, A., Duarte, J., Canário, J., & Vieira, G. (2023). Changes in Vessel Traffic Disrupt Tidal Flats and Saltmarshes in the Tagus Estuary, Portugal. *Estuaries and Coasts*, *46*(5), 1141–1156. https://doi.org/10.1007/s12237-023-01198-7

Marzulli, F., Musivand, S., Arengi, M., De Caprariis, B., De Filippis, P., Marchetti, A., Majone, M., & Villano, M. (2023). Coupled Biological and Thermochemical Process for Plastic Waste Conversion into Biopolymers. *Chemical Engineering Transactions*, *100*, 469–474. https://doi.org/10.3303/CET23100079

Maurya, A., Bhattacharya, A., & Khare, S. K. (2020). Enzymatic Remediation of Polyethylene Terephthalate (PET)–Based Polymers for Effective Management of Plastic Wastes: An Overview. *Frontiers in Bioengineering and Biotechnology*, *8*, 602325. https://doi.org/10.3389/fbioe.2020.602325

Maurya, A. C., Bhattacharya, A., & Khare, S. K. (2023). Biodegradation of terephthalic acid using *Rhodococcus erythropolis* MTCC 3951: Insights into the degradation process, applications in wastewater treatment and polyhydroxyalkanoate production. *Environmental Science and Pollution Research*. https://doi.org/10.1007/s11356-023-30054-1

Mazaheri, H., Ghaedi, M., Ahmadi Azqhandi, M. H., & Asfaram, A. (2017). Application of machine/statistical learning, artificial intelligence and statistical experimental design for the modeling and optimization of methylene blue and Cd(ii) removal from a binary aqueous solution by natural walnut carbon. *Physical Chemistry Chemical Physics*, *19*(18), 11299–11317. https://doi.org/10.1039/c6cp08437k

McAdam, B., Fournet, M. B., McDonald, P., & Mojicevic, M. (2020). Production of polyhydroxybutyrate (PHB) and factors impacting its chemical and mechanical characteristics. *Polymers*, *12*(12), 1–20. https://doi.org/10.3390/polym12122908

Mellado, M., & Vera, J. (2021). Microorganisms that participate in biochemical cycles in wetlands. *Canadian Journal of Microbiology*, *67*(11), 771–788. https://doi.org/10.1139/cjm-2020-0336

Meneses, R. A. M., Cabrera-Papamija, G., Machuca-Martínez, F., Rodríguez, L. A., Diosa, J. E., & Mosquera-Vargas, E. (2022). Plastic recycling and their use as raw material for the synthesis of carbonaceous materials. *Heliyon*, *8*(3). https://doi.org/10.1016/j.heliyon.2022.e09028

Meng, L., Liang, L., Shi, Y., Yin, H., Li, L., Xiao, J., Huang, N., Zhao, A., Xia, Y., & Hou, J. (2024). Biofilms in plastisphere from freshwater wetlands: Biofilm formation, bacterial community assembly, and biogeochemical cycles. *Journal of Hazardous Materials*, *476*. https://doi.org/10.1016/j.jhazmat.2024.134930

Mezzolla, V., D'Urso, O. F., & Poltronieri, P. (2018). Role of PhaC type I and type II enzymes during PHA biosynthesis. *Polymers*, *10*, 1–12. https://doi.org/10.3390/polym10080910

Mitra, R., Xu, T., Xiang, H., & Han, J. (2020). Current developments on polyhydroxyalkanoates synthesis by using halophiles as a promising cell factory. *Microbial Cell Factories*, *19*(86). https://doi.org/10.1186/s12934-020-01342-z

Mitzscherling, J., Maclean, J., Lipus, D., Bartholomäus, A., Mangelsdorf, K., Lipski, A., Roddatis, V., Liebner, S., & Wagner, D. (2022). *Paenalcaligenes niemegkensis* sp. nov., a novel species of the

family Alcaligenaceae isolated from plastic waste. *International Journal of Systematic and Evolutionary Microbiology*, *72*(4). https://doi.org/10.1099/ijsem.0.005333

Montiel-Jarillo, G., Carrera, J., & Suárez-Ojeda, M. E. (2017). Enrichment of a mixed microbial culture for polyhydroxyalkanoates production: Effect of pH and N and P concentrations. *Science of the Total Environment*, *583*, 300–307. https://doi.org/10.1016/j.scitotenv.2017.01.069

Montiel-Jarillo, G., Morales-Urrea, D. A., Contreras, E. M., López-Córdoba, A., Gómez-Pachón, E. Y., Carrera, J., & Suárez-Ojeda, M. E. (2022). Improvement of the Polyhydroxyalkanoates Recovery from Mixed Microbial Cultures Using Sodium Hypochlorite Pre-Treatment Coupled with Solvent Extraction. *Polymers*, *14*(19). https://doi.org/10.3390/polym14193938

Moreira, S., Freitas, M. C., Araújo, M. F., Andrade, C., Munhá, J., & Fatela, F. (2009). Contamination of Intertidal Sediments-The Case of Sado Estuary (Portugal). *Cruces Source: Journal of Coastal Research*, *II*(56), 1380–1384.

Moretto, G., Lorini, L., Pavan, P., Crognale, S., Tonanzi, B., Rossetti, S., Majone, M., & Valentino, F. (2020). Biopolymers from urban organic waste: Influence of the solid retention time to cycle length ratio in the enrichment of a Mixed Microbial Culture (MMC). *ACS Sustainable Chemistry and Engineering*, *8*(38). https://doi.org/10.1021/acssuschemeng.0c04980

Morgan-Sagastume, F. (2016). Characterisation of open, mixed microbial cultures for polyhydroxyalkanoate (PHA) production. *Reviews in Environmental Science and Biotechnology*, *15*(4), 593–625. https://doi.org/10.1007/s11157-016-9411-0

Morgan-Sagastume, F., Hjort, M., Cirne, D., Gérardin, F., Lacroix, S., Gaval, G., Karabegovic, L., Alexandersson, T., Johansson, P., Karlsson, A., Bengtsson, S., Arcos-Hernández, M. V., Magnusson, P., & Werker, A. (2015). Integrated production of polyhydroxyalkanoates (PHAs) with municipal wastewater and sludge treatment at pilot scale. *Bioresource Technology*, *181*, 78–89. https://doi.org/10.1016/j.biortech.2015.01.046

Mückschel, B., Simon, O., Klebensberger, J., Graf, N., Rosche, B., Altenbuchner, J., Pfannstiel, J., Huber, A., & Hauer, B. (2012). Ethylene glycol metabolism by Pseudomonas putida. *Applied and Environmental Microbiology*, *78*(24), 8531–8539. https://doi.org/10.1128/AEM.02062-12

Mudondo, J., Lee, H. S., Jeong, Y., Kim, T. H., Kim, S., Sung, B. H., Park, S. H., Park, K., Cha, H. G., Yeon, Y. J., & Kim, H. T. (2023). Recent Advances in the Chemobiological Upcycling of Polyethylene Terephthalate (PET) into Value-Added Chemicals. *Journal of Microbiology and Biotechnology*, *33*(1), 1–14. https://doi.org/10.4014/jmb.2208.08048

Muhammadi, Shabina, Afzal, M., & Hameed, S. (2015). Bacterial polyhydroxyalkanoates-eco-friendly next generation plastic: Production, biocompatibility, biodegradation, physical properties and applications. *Green Chemistry Letters and Reviews*, *8*(3–4), 56–77. https://doi.org/10.1080/17518253.2015.1109715

Mujtaba, M., Lipponen, J., Ojanen, M., Puttonen, S., & Vaittinen, H. (2022). Trends and challenges in the development of bio-based barrier coating materials for paper/cardboard food packaging; a review. *Science of the Total Environment*, *851*. https://doi.org/10.1016/j.scitotenv.2022.158328

Müller, C., Heck, C. A., Stephan, L., Paschetag, M., & Scholl, S. (2023). Precipitation of Terephthalic Acid from Alkaline Solution: Influence of Temperature and Precipitation Acid. *Industrial and Engineering Chemistry Research*, *62*(30), 12029–12040. https://doi.org/10.1021/acs.iecr.2c04451

Muneer, F., Rasul, I., Azeem, F., Siddique, M. H., Zubair, M., & Nadeem, H. (2020). Microbial Polyhydroxyalkanoates (PHAs): Efficient Replacement of Synthetic Polymers. *Journal of Polymers and the Environment*, *28*(9), 2301–2323. https://doi.org/10.1007/s10924-020-01772-1

Narancic, T., Djokic, L., Kenny, S. T., O'Connor, K. E., Radulovic, V., Nikodinovic-Runic, J., & Vasiljevic, B. (2012). Metabolic versatility of Gram-positive microbial isolates from contaminated river sediments. *Journal of Hazardous Materials*, *215–216*, 243–251. https://doi.org/10.1016/j.jhazmat.2012.02.059

Naser, A. Z., Deiab, I., & Darras, B. M. (2021). Poly(lactic acid) (PLA) and polyhydroxyalkanoates (PHAs), green alternatives to petroleum-based plastics: a review. *RSC Advances, 11* (28), 17151–17196. https://doi.org/10.1039/d1ra02390j

Ncube, L. K., Ude, A. U., Ogunmuyiwa, E. N., Zulkifli, R., & Beas, I. N. (2021). An overview of plasticwaste generation and management in food packaging industries. *Recycling*, *6* (12), 1–25. https://doi.org/10.3390/recycling6010012

Neves, L. A., Crespo, J. G., & Coelhoso, I. M. (2010). Gas permeation studies in supported ionic liquid membranes. *Journal of Membrane Science*, *357*, 160–170. https://doi.org/10.1016/j.memsci.2010.04.016

Nguyenhuynh, T., Yoon, L. W., Chow, Y. H., & Chua, A. S. M. (2021). An insight into enrichment strategies for mixed culture in polyhydroxyalkanoate production: feedstocks, operating conditions and inherent challenges. *Chemical Engineering Journal*, *420*. https://doi.org/10.1016/j.cej.2021.130488

Nielsen, H., & Shukla, V. K. S. (2004). In situ solid phase extraction of lipids from spray-dried egg yolk by ethanol with subsequent removal of triacylglycerols by cold temperature crystallization. *LWT*, *37*(6), 613–618. https://doi.org/10.1016/j.lwt.2003.12.007

Nikodinovic, J., Kenny, S. T., Babu, R. P., Woods, T., Blau, W. J., & O'Connor, K. E. (2008). The conversion of BTEX compounds by single and defined mixed cultures to medium-chain-length polyhydroxyalkanoate. *Applied Microbiology and Biotechnology*, *80*(4), 665–673. https://doi.org/10.1007/s00253-008-1593-0

Nisticò, R. (2020). Polyethylene terephthalate (PET) in the packaging industry. *Polymer Testing*, *90*. https://doi.org/10.1016/j.polymertesting.2020.106707

Niu, L., Li, Y., Li, Y., Hu, Q., Wang, C., Hu, J., Zhang, W., Wang, L., Zhang, C., & Zhang, H. (2021). New insights into the vertical distribution and microbial degradation of microplastics in urban river sediments. *Water Research*, *188*. https://doi.org/10.1016/j.watres.2020.116449

Nosal, H., Moser, K., Warzała, M., Holzer, A., Stańczyk, D., & Sabura, E. (2020). Selected Fatty Acids Esters as Potential PHB-V Bioplasticizers: Effect on Mechanical Properties of the Polymer. *Journal of Polymers and the Environment*, *29*, 38–53. https://doi.org/10.1007/s10924-020-01841-5

Ntaikou, I., Koumelis, I., Kamilari, M., Iatridi, Z., Tsitsilianis, C., & Lyberatos, G. (2019). Effect of nitrogen limitation on polyhydroxyalkanoates production efficiency, properties and microbial dynamics using a soil-derived mixed continuous culture. *International Journal of Biobased Plastics*, *1*(1), 31–47. https://doi.org/10.1080/24759651.2019.1648016

Ntaikou, I., Koumelis, I., Tsitsilianis, C., Parthenios, J., & Lyberatos, G. (2018). Comparison of yields and properties of microbial polyhydroxyalkanoates generated from waste glycerol based substrates. *International Journal of Biological Macromolecules*, *112*, 273–283. https://doi.org/10.1016/j.ijbiomac.2018.01.175

Ntaikou, I., Valencia Peroni, C., Kourmentza, C., Ilieva, V. I., Morelli, A., Chiellini, E., & Lyberatos, G. (2014). Microbial bio-based plastics from olive-mill wastewater: Generation and properties of polyhydroxyalkanoates from mixed cultures in a two-stage pilot scale system. *Journal of Biotechnology*, *188*, 138–147. http://dx.doi.org/10.1016/j.jbiotec.2014.08.015

Obruca, S., Sedlacek, P., Mravec, F., Krzyzanek, V., Nebesarova, J., Samek, O., Kucera, D., Benesova, P., Hrubanova, K., Milerova, M., & Marova, I. (2017). The presence of PHB granules in cytoplasm protects non-halophilic bacterial cells against the harmful impact of hypertonic environments. *New Biotechnology*, *39*, 68–80. http://dx.doi.org/10.1016/j.nbt.2017.07.008

Oh, S., Rheem, S., Sim, J., Kim, S., & Baek, Y. (1995). Optimizing Conditions for the Growth of Lactobacillus casei YIT 9018 in Tryptone-Yeast Extract-Glucose Medium by Using Response Surface Methodology. *Applied and Environmental Microbiology, 61*(11), 3809–3814. https://doi.org/0099-2240/95/$04.00+0

Oliveira, C. S. S., Silva, C. E., Carvalho, G., & Reis, M. A. (2017). Strategies for efficiently selecting PHA producing mixed microbial cultures using complex feedstocks: Feast and famine regime and uncoupled carbon and nitrogen availabilities. *New Biotechnology*, *37*, 69–79. https://doi.org/10.1016/j.nbt.2016.10.008

Oliveira, C. S. S., Silva, M. O. D., Silva, C. E., Carvalho, G., & Reis, M. A. M. (2018). Assessment of protein-rich cheese whey waste stream as a nutrients source for low-cost mixed microbial PHA production. *Applied Sciences*, *8*(10). https://doi.org/10.3390/app8101817

Omenna, E. C., Omage, K., Ezaka, E., & Azeke, M. A. (2023). Tolerance, taxonomic and phylogenetic studies of some bacterial isolates involved in bioremediation of crude oil polluted soil in the southern region of Nigeria. *Heliyon*, *9*(4). https://doi.org/10.1016/j.heliyon.2023.e15639

Pakalapati, H., Chang, C. K., Show, P. L., Arumugasamy, S. K., & Lan, J. C. W. (2018). Development of polyhydroxyalkanoates production from waste feedstocks and applications. *Journal of Bioscience and Bioengineering*, *126*(3), 282–292. https://doi.org/10.1016/j.jbiosc.2018.03.016

Pandey, A., Adama, N., Adjallé, K., & Blais, J. F. (2022). Sustainable applications of polyhydroxyalkanoates in various fields: A critical review. *International Journal of Biological Macromolecules*, *221*, 1184–1201. https://doi.org/10.1016/j.ijbiomac.2022.09.098

Pascault, J.-P., & Williams, R. J. J. (2013). 28 Thermosetting Polymers. In E. Saldıvar-Guerra & E. Vivaldo-Lima (Eds.), *Handbook of Polymer Synthesis, Characterization, and Processing*. John Wiley & Sons, Inc.

Paulo, A. M. S., Amorim, C. L., Costa, J., Mesquita, D. P., Ferreira, E. C., & Castro, P. M. L. (2021). Long-term stability of a non-adapted aerobic granular sludge process treating fish canning wastewater associated to EPS producers in the core microbiome. *Science of the Total Environment*, *756*. https://doi.org/10.1016/j.scitotenv.2020.144007

Pavlovskyi, D., & Vorobyova, V. (2025). A Comprehensive Overview of Chemical Additives in Single-Use Polimeric Products: Functionality, Environmental Impact and the Analytical Greenness Assessment. *Water, Air, and Soil Pollution, 236* (3). https://doi.org/10.1007/s11270-025-07826-1

Peixoto, J., Silva, L. P., & Krüger, R. H. (2017). Brazilian Cerrado soil reveals an untapped microbial potential for unpretreated polyethylene biodegradation. *Journal of Hazardous Materials*, *324*, 634–644. https://doi.org/10.1016/j.jhazmat.2016.11.037

Pereira, J., Queirós, D., Lemos, P. C., Rossetti, S., & Serafim, L. S. (2020). Enrichment of a mixed microbial culture of PHA-storing microorganisms by using fermented hardwood spent sulfite liquor. *New Biotechnology*, *56*, 79–86. https://doi.org/10.1016/j.nbt.2019.12.003

Pereira, J. R., Araújo, D., Freitas, P., Marques, A. C., Alves, V. D., Sevrin, C., Grandfils, C., Fortunato, E., Reis, M. A. M., & Freitas, F. (2021). Production of medium-chain-length polyhydroxyalkanoates by *Pseudomonas chlororaphis* subsp. aurantiaca: Cultivation on fruit pulp waste and polymer characterization. *International Journal of Biological Macromolecules*, *167*, 85–92. https://doi.org/10.1016/j.ijbiomac.2020.11.162

Peres, S., Magalhães, M. C. F., Abreu, M. M., Leitão, S., Santos, A., & Cerejeira, M. J. (2016). Interaction of contaminated sediment from a salt marsh with estuarine water: evaluation by leaching and ecotoxicity assays and salts from leachate evaporation. *Journal of Soils and Sediments*, *16*(5), 1612–1624. https://doi.org/10.1007/s11368-016-1355-z

Perez-Martinez, V., Bello-Rocha, Lady, Rodríguez-Rodriguez, C., Sierra, C. A., & Castellanos, D. A. (2024). Obtention and characterization of PLA/PHBV thin sheets by solvent casting and extrusion with application in food packaging. *Bulletin of Materials Science*, *47*(1). https://doi.org/10.1007/s12034-023-03133-9

Pérez-Rivero, C., López-Gómez, J. P., & Roy, I. (2019). A sustainable approach for the downstream processing of bacterial polyhydroxyalkanoates: State-of-the-art and latest developments. *Biochemical Engineering Journal*, *150*. https://doi.org/10.1016/j.bej.2019.107283

Philip, S., Keshavarz, T., & Roy, I. (2007). Polyhydroxyalkanoates: biodegradable polymers with a range of applications. *Journal of Chemical Technology & Biotechnology*, *82*, 233–247. https://doi.org/10.1002/jctb

Pilapitiya, P. G. C. N. T., & Ratnayake, A. S. (2024). The world of plastic waste: A review. *Cleaner Materials*, *11*. https://doi.org/10.1016/j.clema.2024.100220

Pinhal, S., Ropers, D., Geiselmann, J., De Jong, H., & Metcalf, W. W. (2019). Acetate Metabolism and the Inhibition of Bacterial Growth by Acetate. *Journal of Bacteriology*, *201*(13), 147–166. https://doi.org/10.1128/JB.00147-19

Pinter, E., Welle, F., Mayrhofer, E., Pechhacker, A., Motloch, L., Lahme, V., Grant, A., & Tacker, M. (2021). Circularity study on pet bottle-to-bottle recycling. *Sustainability*, *13*, 1–15. https://doi.org/10.3390/su13137370

Pinto-Ibieta, F., Serrano, A., Cea, M., Ciudad, G., & Fermoso, F. G. (2021). Beyond PHA: Stimulating intracellular accumulation of added-value compounds in mixed microbial cultures. *Bioresource Technology*, *337*. https://doi.org/10.1016/j.biortech.2021.125381

Poiana, M. A., Alexa, E., Munteanu, M. F., Gligor, R., Moigradean, D., & Mateescu, C. (2015). Use of ATR-FTIR spectroscopy to detect the changes in extra virgin olive oil by adulteration with soybean oil and high temperature heat treatment. *Open Chemistry*, *13*(1), 689–698. https://doi.org/10.1515/chem-2015-0110

Policastro, G., Panico, A., & Fabbricino, M. (2021). Improving biological production of poly(3-hydroxybutyrate-co-3-hydroxyvalerate) (PHBV) co-polymer: a critical review. *Reviews in Environmental Science and Biotechnology, 20* (2), 479–513. https://doi.org/10.1007/s11157-021-09575-z

Ponjavic, M., Malagurski, I., Lazic, J., Jeremic, S., Pavlovic, V., Prlainovic, N., Maksimovic, V., Cosovic, V., Atanase, L. I., Freitas, F., Matos, M., & Nikodinovic-Runic, J. (2023). Advancing PHBV Biomedical Potential with the Incorporation of Bacterial Biopigment Prodigiosin. *International Journal of Molecular Sciences*, *24*(3). https://doi.org/10.3390/ijms24031906

Qi, X., Yan, W., Cao, Z., Ding, M., & Yuan, Y. (2022). Current advances in the biodegradation and bioconversion of polyethylene terephthalate. *Microorganisms*, *10*(1). https://doi.org/10.3390/microorganisms10010039

Qin, P., Wu, L., Li, B., Li, N., Pan, X., & Dai, J. (2021). *Superior Gas Barrier Properties of Biodegradable PBST vs. PBAT Copolyesters: A Comparative Study*. https://doi.org/10.3390/polym

Queirós, D., Fonseca, A., Lemos, P. C., & Serafim, L. S. (2015). Long-term operation of a two-stage polyhydroxyalkanoates production process from hardwood sulphite spent liquor. *Journal of Chemical Technology and Biotechnology*, *91*(9), 2480–2487. https://doi.org/10.1002/jctb.4841

Rai, R., Keshavarz, T., Roether, J. A., Boccaccini, A. R., & Roy, I. (2011). Medium chain length polyhydroxyalkanoates, promising new biomedical materials for the future. *Materials Science and Engineering R: Reports*, *72*(3), 29–47. https://doi.org/10.1016/j.mser.2010.11.002

Raj, B., Rahul, J., Singh, P. K., Rao, V. V. L. K., Kumar, J., Dwivedi, N., Kumar, P., Singh, D., & Strzałkowski, K. (2023). Advancements in PET Packaging: Driving Sustainable Solutions for Today's Consumer Demands. *Sustainability*, *15*. https://doi.org/10.3390/su151612269

Rangel, C., Carvalho, G., Oehmen, A., Frison, N., Lourenço, N. D., & Reis, M. A. M. (2023). Polyhydroxyalkanoates production from ethanol- and lactate-rich fermentate of confectionary industry effluents. *International Journal of Biological Macromolecules*, *229*, 713–723. https://doi.org/10.1016/j.ijbiomac.2022.12.268

Rao, A., Haque, S., El-Enshasy, H. A., Singh, V., & Mishra, B. N. (2019). RSM–GA based optimization of bacterial PHA production and In Silico modulation of citrate synthase for enhancing PHA production. *Biomolecules*, *9*(12). https://doi.org/10.3390/biom9120872

Rawte, T., Padte, M., & Mavinkurve, S. (2002). Incidence of marine and mangrove bacteria accumulating polyhydroxyalkanoates on the mid-west coast of India. *World Journal of Microbiology & Biotechnology*, *18*, 655–659. https://doi.org/10.1023/A:1016872631403

Raza, Z. A., Abid, S., & Banat, I. M. (2018). Polyhydroxyalkanoates: Characteristics, production, recent developments and applications. *International Biodeterioration & Biodegradation*, *126*, 45–56. https://doi.org/10.1016/j.ibiod.2017.10.001

Razaif-Mazinah, M. R. M., Anis, S. N. S., Harun, H. I., Rashid, K. A., & Annuar, M. S. M. (2016). Unusual poly(3-hydroxyalkanoate) (PHA) biosynthesis behavior of pseudomonas putida bet001 and *delftia tsuruhatensis* bet002 isolated from palm oil mill effluent. *Biotechnology and Applied Biochemistry*, *64*(2), 259–269. https://doi.org/10.1002/bab.1482

Rebocho, A. T., Pereira, J. R., Freitas, F., Neves, L. A., Alves, V. D., Sevrin, C., Grandfils, C., & Reis, M. A. M. (2019). Production of medium-chain length polyhydroxyalkanoates by Pseudomonas citronellolis grown in apple pulp waste. *Applied Food Biotechnology*, *6*(1), 71–82. http://dx.doi.org/10.22037/afb.v6i1.2179

Rebocho, A. T., Pereira, J. R., Neves, L. A., Alves, V. D., Sevrin, C., Grandfils, C., Freitas, F., & Reis, M. A. M. (2020). Preparation and characterization of films based on a natural p(3hb)/mcl-pha blend obtained through the co-culture of *Cupriavidus necator* and *Pseudomonas citronellolis* in apple pulp waste. *Bioengineering*, *7*(2). https://doi.org/10.3390/bioengineering7020034

Reddy, C. S. K., Ghai, R., & Kalia, V. C. (2003). *Polyhydroxyalkanoates : an overview*. *87*, 137–146.

Reddy, M. V., & Mohan, S. V. (2012). Effect of substrate load and nutrients concentration on the polyhydroxyalkanoates (PHA) production using mixed consortia through wastewater treatment. *Bioresource Technology*, *114*, 573–582. https://doi.org/10.1016/j.biortech.2012.02.127

Reddy, V. U. N., Ramanaiah, S. V., Reddy, M. V., & Chang, Y. C. (2022). Review of the Developments of Bacterial Medium-Chain-Length Polyhydroxyalkanoates (mcl-PHAs). *Bioengineering*, *9*(5), 1–24. https://doi.org/10.3390/bioengineering9050225

Reis, M., Albuquerque, M., Villano, M., & Majone, M. (2011). Mixed Culture Processes for Polyhydroxyalkanoate Production from Agro-Industrial Surplus/Wastes as Feedstocks. *Comprehensive Biotechnology, 2nd Edi.*, *6*, 669–683. https://doi.org/10.1016/B978-0-08-088504-9.00464-5

Ren, T., Patel, M. K., & Blok, K. (2008). Steam cracking and methane to olefins: Energy use, CO2 emissions and production costs. *Energy*, *33*(5), 817–833. https://doi.org/10.1016/j.energy.2008.01.002

Rodrigues, M., Cravo, A., Freire, P., Rosa, A., & Santos, D. (2020). Temporal assessment of the water quality along an urban estuary (Tagus estuary, Portugal). *Marine Chemistry*, *223*. https://doi.org/10.1016/j.marchem.2020.103824

Rodrigues, T., Torres, C. V., Freitas, P., Neves, L. A., Carvalheira, M., Reis, M. A. M., & Freitas, F. (2024). Conversion of tomato waste into a poly(3-hydroxybutyrate-co-3-hydroxyvalerate-co-3-hydroxyhexanoate) by a mixed microbial community. *Journal of Environmental Chemical Engineering*, *12*(6). https://doi.org/10.1016/j.jece.2024.114755

Ronkay, F. (2023). Becoming the symbol of recycling instead of consumption – 50 years of PET bottles. *Express Polymer Letters*, *17*(12), 1180–1181. https://doi.org/10.3144/expresspolymlett.2023.89

Ru, J., Huo, Y., & Yang, Y. (2020). Microbial Degradation and Valorization of Plastic Wastes. *Frontiers in Microbiology*, *11*. https://doi.org/10.3389/fmicb.2020.00442

Sabapathy, P. C., Devaraj, S., Meixner, K., Anburajan, P., Kathirvel, P., Ravikumar, Y., Zabed, H. M., & Qi, X. (2020). Recent developments in Polyhydroxyalkanoates (PHAs) production – A review. *Bioresource Technology, 306*. https://doi.org/10.1016/j.biortech.2020.123132

Sachan, R. S. K., Devgon, I., Al-Tawaha, A. R. M. S., & Karnwal, A. (2024). Optimizing Polyhydroxyalkanoate production using a novel Bacillus paranthracis isolate: A response surface methodology approach. *Heliyon*, *10*. https://doi.org/10.1016/j.heliyon.2024.e35398

Sadler, J. C., & Wallace, S. (2021). Microbial synthesis of vanillin from waste poly(ethylene terephthalate). *Green Chemistry*, *23*(13), 4665–4672. https://doi.org/10.1039/d1gc00931a

Saini, R. K., Prasad, P., Shang, X., & Keum, Y. S. (2021). Advances in lipid extraction methods—a review. *International Journal of Molecular Sciences*, *22*(24). https://doi.org/10.3390/ijms222413643

Saisriyoot, M., Sahaya, T., Thanapimmetha, A., Chisti, Y., & Srinophakun, P. (2016). Production of potential fuel oils by *Rhodococcus opacus* grown on petroleum processing wastewaters. *Journal of Renewable and Sustainable Energy*, *8*(6). https://doi.org/10.1063/1.4971875

Salam, M. D., Varma, A., Prashar, R., & Choudhary, D. (2021). Review on Efficacy of Microbial Degradation of Polyethylene Terephthalate and Bio-upcycling as a Part of Plastic Waste Management. *Applied Ecology and Environmental Sciences*, *9*(7), 695–703. https://doi.org/10.12691/aees-9-7-8

Salehizadeh, H., & Van Loosdrecht, M. C. M. (2004). Production of polyhydroxyalkanoates by mixed culture: Recent trends and biotechnological importance. *Biotechnology Advances*, *22*(3), 261–279. https://doi.org/10.1016/j.biotechadv.2003.09.003

Salvador, M., Abdulmutalib, U., Gonzalez, J., Kim, J., Smith, A. A., Faulon, J. L., Wei, R., Zimmermann, W., & Jimenez, J. I. (2019). Microbial genes for a circular and sustainable bio-PET economy. *Genes, 10*(5). https://doi.org/10.3390/genes10050373

Samak, N. A., Jia, Y., Sharshar, M. M., Mu, T., Yang, M., Peh, S., & Xing, J. (2020). Recent advances in biocatalysts engineering for polyethylene terephthalate plastic waste green recycling. *Environment International*, *145*. https://doi.org/10.1016/j.envint.2020.106144

Samrot, A. V, Samanvitha, S. K., Shobana, N., Renitta, E. R., Senthilkumar, P., Kumar, S. S., Abirami, S., Dhiva, S., Bavanilatha, M., Prakash, P., Saigeetha, S., Shree, K. S., & Thirumurugan, R. (2021). The Synthesis, Characterization and Applications of Polyhydroxyalkanoates (PHAs) and PHA-based Nanoparticles. *Polymers*, *13*. https://doi.org/ 10.3390/polym13193302

Sanahuja, A. B., Teruel, N. G., Carratalá, M. L. M., & Selva, M. C. G. (2011). Characterization of almond cultivars by the use of thermal analysis techniques. Application to cultivar authenticity. *JAOCS, Journal of the American Oil Chemists' Society*, *88*(11), 1687–1693. https://doi.org/10.1007/s11746-011-1847-3

Sang, T., Wallis, C. J., Hill, G., & Britovsek, G. J. P. (2020). Polyethylene terephthalate degradation under natural and accelerated weathering conditions. *European Polymer Journal*, *136*. https://doi.org/10.1016/j.eurpolymj.2020.109873

Sangroniz, A., Zhu, J. B., Tang, X., Etxeberria, A., Chen, E. Y. X., & Sardon, H. (2019). Packaging materials with desired mechanical and barrier properties and full chemical recyclability. *Nature Communications*, *10*(1), 1–7. https://doi.org/10.1038/s41467-019-11525-x

Santos, E. S., Abreu, M. M., Peres, S., Magalhães, M. C. F., Leitão, S., Pereira, A. S., & Cerejeira, M. J. (2017). Potential of Tamarix africana and other halophyte species for phytostabilisation of contaminated salt marsh soils. *Journal of Soils and Sediments*, *17*(5), 1459–1473. https://doi.org/10.1007/s11368-015-1333-x

Šaraba, V., Milovanovic, J., Nikodinovic-Runic, J., Budin, C., de Boer, T., & Ciric, M. (2023). Brackish Groundwaters Contain Plastic- and Cellulose-Degrading Bacteria. *Microbial Ecology*, *86*(4), 2747–2755. https://doi.org/10.1007/s00248-023-02278-8

Saratale, R. G., Cho, S. K., Kadam, A. A., Ghodake, G. S., Kumar, M., Bharagava, R. N., Varjani, S., Nair, S., Kim, D. S., Shin, H. S., & Saratale, G. D. (2022). Developing Microbial Co-Culture System for Enhanced Polyhydroxyalkanoates (PHA) Production Using Acid Pretreated Lignocellulosic Biomass. *Polymers*, *14*(4), 726. https://doi.org/ 10.3390/polym14040726

Sasoh, M., Masai, E., Ishibashi, S., Hara, H., Kamimura, N., Miyauchi, K., & Fukuda, M. (2006). Characterization of the terephthalate degradation genes of *Comamonas* sp. strain E6. *Applied and Environmental Microbiology*, *72*(3), 1825–1832. https://doi.org/10.1128/AEM.72.3.1825-1832.2006

Satta, A., Zampieri, G., Loprete, G., Campanaro, S., Treu, L., & Bergantino, E. (2024). Metabolic and enzymatic engineering strategies for polyethylene terephthalate degradation and valorization. In *Reviews in Environmental Science and Biotechnology, 23* (2), 351–383. https://doi.org/10.1007/s11157-024-09688-1

Satti, S. M., Hashmi, M., Subhan, M., Shereen, M. A., Fayad, A., Abbasi, A., Shah, A. A., & Ali, H. M. (2024). Bio-upcycling of plastic waste: a sustainable innovative approach for circular economy. *Water, Air, and Soil Pollution*, *235*(382), 1–14. https://doi.org/10.1007/s11270-024-07122-4

Scarborough, M. J., Lawson, C. E., DeCola, A. C., & Gois, I. M. (2022). Microbiomes for sustainable biomanufacturing. *Current Opinion in Microbiology*, *65*, 8–14. https://doi.org/10.1016/j.mib.2021.09.015

Schaerer, L. G., Wood, E., Aloba, S., Byrne, E., Bashir, M. A., Baruah, K., Schumann, E., Umlor, L., Wu, R., Lee, H., Orme, C. J., Wilson, A. D., Lacey, J. A., Ong, R. G., & Techtmann, S. M. (2023). Versatile microbial communities rapidly assimilate ammonium hydroxide-treated plastic waste. *Journal of Industrial Microbiology and Biotechnology*, *50*(1). https://doi.org/10.1093/jimb/kuad008

Schaerer, L. G., Wu, R., Putman, L. I., Pearce, J. M., Lu, T., Shonnard, D. R., Ong, R. G., & Techtmann, S. M. (2023). Killing two birds with one stone: chemical and biological upcycling of polyethylene

terephthalate plastics into food. *Trends in Biotechnology*, *41*(2), 184–196. https://doi.org/10.1016/j.tibtech.2022.06.012

Scheirs, J., & Long, T. E. (2005). *Modern polyesters: chemistry and technology of polyesters and copolyesters* (First). John Wiley & Sons.

Serafim, L. S., Lemos, P. C., Albuquerque, M. G. E., & Reis, M. A. M. (2008). Strategies for PHA production by mixed cultures and renewable waste materials. *Applied Microbiology and Biotechnology*, *81*(4), 615–628. https://doi.org/10.1007/s00253-008-1757-y

Shah, S., & Kumar, A. (2020). Polyhydroxyalkanoates: Advances in the synthesis of sustainable bioplastics. *European Journal of Environmental Sciences*, *10*(2), 76–88. https://doi.org/10.14712/23361964.2020.9

Shen, M., Song, B., Zeng, G., Zhang, Y., Huang, W., Wen, X., & Tang, W. (2020). Are biodegradable plastics a promising solution to solve the global plastic pollution? *Environmental Pollution*, *263*. https://doi.org/10.1016/j.envpol.2020.114469

Shields-Menard, S. A., Amirsadeghi, M., Sukhbaatar, B., Revellame, E., Hernandez, R., Donaldson, J. R., & French, W. T. (2015). Lipid accumulation by Rhodococcus rhodochrous grown on glucose. *Journal of Industrial Microbiology and Biotechnology*, *42*(5), 693–699. https://doi.org/10.1007/s10295-014-1564-7

Shigematsu, T., Yumihara, K., Ueda, Y., Numaguchi, M., Morimura, S., & Kida, K. (2003). Delftia tsuruhatensis sp. nov., a terephthalate-assimilating bacterium isolated from activated sludge. *International Journal of Systematic and Evolutionary Microbiology*, *53*(5), 1479–1483. https://doi.org/10.1099/ijs.0.02285-0

Sierra-García, I. N., Alvarez, J. C., De Vasconcellos, S. P., De Souza, A. P., Dos Santos Neto, E. V., & De Oliveira, V. M. (2014). New hydrocarbon degradation pathways in the microbial metagenome from brazilian petroleum reservoirs. *PLOS ONE*, *9*(2). https://doi.org/10.1371/journal.pone.0090087

Silva, F., Matos, M., Pereira, B., Ralo, C., Pequito, D., Marques, N., Carvalho, G., & Reis, M. A. M. (2022). An integrated process for mixed culture production of 3-hydroxyhexanoate-rich polyhydroxyalkanoates from fruit waste. *Chemical Engineering Journal*, *427*. https://doi.org/10.1016/j.cej.2021.131908

Silva, J. B., Pereira, J. R., Marreiros, B. C., Reis, M. A. M., & Freitas, F. (2021). Microbial production of medium-chain length polyhydroxyalkanoates. *Process Biochemistry*, *102*, 393–407. https://doi.org/10.1016/j.procbio.2021.01.020

Silva, R. A., Grossi, V., Olivera, N. L., & Alvarez, H. M. (2010). Characterization of indigenous Rhodococcus sp. 602, a strain able to accumulate triacylglycerides from naphthyl compounds under nitrogen-starved conditions. *Research in Microbiology*, *161*(3), 198–207. https://doi.org/10.1016/j.resmic.2010.01.007

Silva, T. A., Freitas, M. C., Andrade, C., Taborda, R., Freire, P., Schmidt, S., & Antunes, C. (2013). Geomorphological response of the salt-marshes in the Tagus estuary to sea level rise. *Journal of Coastal Research*, *65*, 582–587. https://doi.org/10.2112/si65-099.1

Singh, A. K., & Mallick, N. (2009). SCL-LCL-PHA copolymer production by a local isolate, Pseudomonas aeruginosa MTCC 7925. *Biotechnology Journal*, *4*(5), 703–711. https://doi.org/10.1002/biot.200800307

Singh, N., Hui, D., Singh, R., Ahuja, I. P. S., Feo, L., & Fraternali, F. (2017). Recycling of plastic solid waste: A state of art review and future applications. *Composites Part B: Engineering*, *115*(15), 409–422. https://doi.org/10.1016/j.compositesb.2016.09.013

Singh, N., Ogunseitan, O. A., Wong, M. H., & Tang, Y. (2022). Sustainable materials alternative to petrochemical plastics pollution: A review analysis. *Sustainable Horizons*, *2*. https://doi.org/10.1016/j.horiz.2022.100016

Sinha, V., Patel, M. R., & Patel, J. V. (2010). Pet waste management by chemical recycling: A review. *Journal of Polymers and the Environment*, *18*(1), 8–25. https://doi.org/10.1007/s10924-008-0106-7

Smith, R. L., Bissel, J., & McGrath, C. (2014). Biodegradation of Poly(3-Hydroxybutyrate) Produced from *Cupriavidus necator* with Different Concentrations of Oleic Acid as Nutritional Supplement. US008722383B2.

Soni, V. K., Singh, G., Vijayan, B. K., Chopra, A., Kapur, G. S., & Ramakumar, S. S. V. (2021). Thermochemical Recycling of Waste Plastics by Pyrolysis: A Review. *Energy and Fuels*, *35*(16), 12763–12808. https://doi.org/10.1021/acs.energyfuels.1c01292

Soong, Y. H. V., Sobkowicz, M. J., & Xie, D. (2022). Recent Advances in Biological Recycling of Polyethylene Terephthalate (PET) Plastic Wastes. *Bioengineering*, *9*(3), 98. https://doi.org/10.3390/bioengineering9030098

Sruamsiri, D., Thayanukul, P., & Suwannasilp, B. B. (2020). In situ identification of polyhydroxyalkanoate (PHA)-accumulating microorganisms in mixed microbial cultures under feast/famine conditions. *Scientific Reports*, *10*(1), 1–10. https://doi.org/10.1038/s41598-020-60727-7

Štrukil, V. (2021). Highly Efficient Solid-State Hydrolysis of Waste Polyethylene Terephthalate by Mechanochemical Milling and Vapor-Assisted Aging. *ChemSusChem*, *14*(1), 330–338. https://doi.org/10.1002/cssc.202002124

Suhaimi, N. A. S., Muhamad, F., Abd Razak, N. A., & Zeimaran, E. (2022). Recycling of polyethylene terephthalate wastes: A review of technologies, routes, and applications. *Polymer Engineering and Science*, *62*(8), 2355–2375. https://doi.org/10.1002/pen.26017

Sun, R., Zheng, H., Yin, S., Zhang, X., You, X., Wu, H., Suo, F., Han, K., Cheng, Y., Zhang, C., & Li, Y. (2022). Comparative study of pyrochar and hydrochar on peanut seedling growth in a coastal salt-affected soil of Yellow River Delta, China. *Science of the Total Environment*, *833*. https://doi.org/10.1016/j.scitotenv.2022.155183

Suri, K., Singh, B., Kaur, A., & Singh, N. (2019). Impact of roasting and extraction methods on chemical properties, oxidative stability and Maillard reaction products of peanut oils. *Journal of Food Science and Technology*, *56*(5), 2436–2445. https://doi.org/10.1007/s13197-019-03719-4

Suwanawat, N., Parakulsuksatid, P., Nitayapat, N., & Sanpamongkolchai, W. (2019). Biodegradation of terephthalic acid by *Rhodococcus biphenylivorans* isolated from soil. *International Journal of*

Environmental Science and Development, *10*(1), 30–33. https://doi.org/10.18178/ijesd.2019.10.1.1141

Suzuki, M., Tachibana, Y., & Kasuya, K. ichi. (2021). Biodegradability of poly(3-hydroxyalkanoate) and poly(ε-caprolactone) via biological carbon cycles in marine environments. *Polymer Journal*, *53*(1), 47–66. https://doi.org/10.1038/s41428-020-00396-5

Tajparast, M., & Frigon, D. (2015). Genome-scale metabolic model of *Rhodococcus jostii* RHA1 (iMT1174) to study the accumulation of storage compounds during nitrogen-limited condition. *BMC Systems Biology*, *9*(1). https://doi.org/10.1186/s12918-015-0190-y

Tamang, P., Banerjee, R., Köster, S., & Nogueira, R. (2019). Comparative study of polyhydroxyalkanoates production from acidified and anaerobically treated brewery wastewater using enriched mixed microbial culture. *Journal of Environmental Sciences*, *78*, 137–146. https://doi.org/10.1016/j.jes.2018.09.001

Tamang, P., & Nogueira, R. (2021). Valorisation of waste cooking oil using mixed culture into short- and medium-chain length polyhydroxyalkanoates: Effect of concentration, temperature and ammonium. *Journal of Biotechnology*, *342*, 92–101. https://doi.org/10.1016/j.jbiotec.2021.10.006

Tan, G. Y. A., Chen, C. L., Li, L., Ge, L., Wang, L., Razaad, I. M. N., Li, Y., Zhao, L., Mo, Y., & Wang, J. Y. (2014). Start a research on biopolymer polyhydroxyalkanoate (PHA): A review. *Polymers*, *6*(3), 706–754. https://doi.org/10.3390/polym6030706

Tan, H. T., Chek, M. F., Neoh, S. Z., Ang, S. L., Yoshida, S., Hakoshima, T., & Sudesh, K. (2022). Characterization of the polyhydroxyalkanoate (PHA) synthase from Ideonella sakaiensis, a bacterium that is capable of degrading and assimilating poly(ethylene terephthalate). *Polymer Degradation and Stability*, *206*. https://doi.org/10.1016/j.polymdegradstab.2022.110160

Taniguchi, I., Yoshida, S., Hiraga, K., Miyamoto, K., Kimura, Y., & Oda, K. (2019). Biodegradation of PET: Current Status and Application Aspects. *ACS Catalysis*, *9*(5), 4089–4105. https://doi.org/10.1021/acscatal.8b05171

Thachnatharen, N., Shahabuddin, S., & Sridewi, N. (2021). The Waste Management of Polyethylene Terephthalate (PET) Plastic Waste: A Review. *IOP Conference Series: Materials Science and Engineering*, *1127*(1). https://doi.org/10.1088/1757-899x/1127/1/012002

Thomsen, T. B., Almdal, K., & Meyer, A. S. (2023). Significance of poly(ethylene terephthalate) (PET) substrate crystallinity on enzymatic degradation. *New Biotechnology*, *78*, 162–172. https://doi.org/10.1016/j.nbt.2023.11.001

Thu, N. T. T., Hoang, L. H., Cuong, P. K., Viet-Linh, N., Nga, T. T. H., Kim, D. D., Leong, Y. K., & Nhi-Cong, L. T. (2023). Evaluation of polyhydroxyalkanoate (PHA) synthesis by Pichia sp. TSLS24 yeast isolated in Vietnam. *Scientific Reports*, *13*(1), 1–14. https://doi.org/10.1038/s41598-023-28220-z

Tilsted, J. P., Bauer, F., Deere Birkbeck, C., Skovgaard, J., & Rootzén, J. (2023). Ending fossil-based growth: Confronting the political economy of petrochemical plastics. *One Earth*, *6*(6), 607–619. https://doi.org/10.1016/j.oneear.2023.05.018

Tiso, T., Narancic, T., Wei, R., Pollet, E., Beagan, N., Schröder, K., Honak, A., Jiang, M., Kenny, S. T., Wierckx, N., Perrin, R., Avérous, L., Zimmermann, W., O'Connor, K., & Blank, L. M. (2021). Towards bio-upcycling of polyethylene terephthalate. *Metabolic Engineering*, *66*, 167–178. https://doi.org/10.1016/j.ymben.2021.03.011

Torres, C. A. V., Antunes, S., Ricardo, A. R., Grandfils, C., Alves, V. D., Freitas, F., & Reis, M. A. M. (2012). Study of the interactive effect of temperature and pH on exopolysaccharide production by Enterobacter A47 using multivariate statistical analysis. *Bioresource Technology*, *119*, 148–156. https://doi.org/10.1016/j.biortech.2012.05.106

Townsend, K. R., Lu, H. C., Sharley, D. J., & Pettigrove, V. (2019). Associations between microplastic pollution and land use in urban wetland sediments. *Environmental Science and Pollution Research*, *26*(22), 22551–22561. https://doi.org/10.1007/s11356-019-04885-w

Trakunjae, C., Boondaeng, A., Apiwatanapiwat, W., Kosugi, A., Arai, T., Sudesh, K., & Vaithanomsat, P. (2021). Enhanced polyhydroxybutyrate (PHB) production by newly isolated rare actinomycetes *Rhodococcus* sp. strain BSRT1-1 using response surface methodology. *Scientific Reports*, *11*(1). https://doi.org/10.1038/s41598-021-81386-2

Trifunović, D., Schuchmann, K., & Müller, V. (2016). Ethylene glycol metabolism in the acetogen Acetobacterium woodii. *Journal of Bacteriology*, *198*(7), 1058–1065. https://doi.org/10.1128/JB.00942-15

Tripathi, L., Wu, L.-P., Chen, J., & Chen, G.-Q. (2012). Synthesis of Diblock copolymer poly-3-hydroxybutyrate -block-poly-3-hydroxyhexanoate [PHB-b-PHHx] by a β-oxidation weakened Pseudomonas putida KT2442. *Microbial Cell Factories*, *11*(1). https://doi.org/10.1186/1475-2859-11-44

Umemura, R. T., & Felisberti, M. I. (2021). Plasticization of poly(3-hydroxybutyrate) with triethyl citrate: Thermal and mechanical properties, morphology, and kinetics of crystallization. *Journal of Applied Polymer Science*, *138*(10), 1–14. https://doi.org/10.1002/app.49990

Urtuvia, V., Ponce, B., Andler, R., & Díaz-Barrera, A. (2023). Relation of 3HV fraction and thermomechanical properties of poly(3–hydroxybutyrate–co–3–hydroxyvalerate) produced by Azotobacter vinelandii OP. *International Journal of Biological Macromolecules*, *253*. https://doi.org/10.1016/j.ijbiomac.2023.127681

Vahur, S., Teearu, A., Peets, P., Joosu, L., & Leito, I. (2025, January 12). *Database of ATR-FT-IR spectra of various materials. ATR-FT-IR spectrum of fresh soybean oil (4000–225 cm^{-1})*. University of Tartu. https://spectra.chem.ut.ee/paint/binders/soybean-oil/

Valentino, F., Beccari, M., Fraraccio, S., Zanaroli, G., & Majone, M. (2014). Feed frequency in a Sequencing Batch Reactor strongly affects the production of polyhydroxyalkanoates (PHAs) from volatile fatty acids. *New Biotechnology*, *31*(4), 264–275. http://dx.doi.org/10.1016/j.nbt.2013.10.006

Valentino, F., Morgan-Sagastume, F., Campanari, S., Villano, M., Werker, A., & Majone, M. (2017). Carbon recovery from wastewater through bioconversion into biodegradable polymers. *New Biotechnology*, *37*, 9–23. https://doi.org/10.1016/j.nbt.2016.05.007

Van der Vegt A. K. (2002). *From Polymers to Plastics* (First edit). VSSD. http://www.vssd.nl/hlf/m028.htm

Verlinden, R. A. J., Hill, D. J., Kenward, M. A., Williams, C. D., & Radecka, I. (2007). Bacterial synthesis of biodegradable polyhydroxyalkanoates. *Journal of Applied Microbiology*, *102*(6), 1437–1449. https://doi.org/10.1111/j.1365-2672.2007.03335.x

Vermeer, C. M., Nielsen, M., Eckhardt, V., Hortensius, M., Tamis, J., Picken, S. J., Meesters, G. M. H., & Kleerebezem, R. (2022). Systematic solvent screening and selection for polyhydroxyalkanoates (PHBV) recovery from biomass. *Journal of Environmental Chemical Engineering*, *10*(6). https://doi.org/10.1016/j.jece.2022.108573

Villano, M., Beccari, M., Dionisi, D., Lampis, S., Miccheli, A., Vallini, G., & Majone, M. (2010). Effect of pH on the production of bacterial polyhydroxyalkanoates by mixed cultures enriched under periodic feeding. *Process Biochemistry*, *45*(5), 714–723. https://doi.org/10.1016/j.procbio.2010.01.008

Villano, M., Valentino, F., Barbetta, A., Martino, L., Scandola, M., & Majone, M. (2014). Polyhydroxyalkanoates production with mixed microbial cultures: From culture selection to polymer recovery in a high-rate continuous process. *New Biotechnology*, *31*(4), 289–296. https://doi.org/10.1016/j.nbt.2013.08.001

Voss, I., & Steinbüchel, A. (2001). High cell density cultivation of Rhodococcus opacus for lipid production at a pilot-plant scale. *Applied Microbiology and Biotechnology*, *55*(5), 547–555. https://doi.org/10.1007/s002530000576

Vural, C., Vural, C., & Ozdemir, G. (2020). Monitoring of the degradation of aromatic hydrocarbons by bioaugmented activated sludge. *Journal of Chemical Technology and Biotechnology*, *95*(1), 52–62. https://doi.org/10.1002/jctb.6200

Wahlen, B. D., Willis, R. M., & Seefeldt, L. C. (2011). Biodiesel production by simultaneous extraction and conversion of total lipids from microalgae, cyanobacteria, and wild mixed-cultures. *Bioresource Technology*, *102*(3), 2724–2730. https://doi.org/10.1016/j.biortech.2010.11.026

Walker, S., & Rothman, R. (2020). Life cycle assessment of bio-based and fossil-based plastic : A review. *Journal of Cleaner Production*, *261*, 1–15. https://doi.org/10.1016/j.jclepro.2020.121158

Walker, T. R., & Fequet, L. (2023). Current trends of unsustainable plastic production and micro(nano)plastic pollution. *TrAC - Trends in Analytical Chemistry*, *160*, 116984. https://doi.org/10.1016/j.trac.2023.116984

Wang, H., Ye, J. W., Chen, X., Yuan, Y., Shi, J., Liu, X., Yang, F., Ma, Y., Chen, J., Wu, F., Lan, Y., Wu, Q., Tong, Y., & Chen, G. Q. (2023). Production of PHA copolymers consisting of 3-hydroxybutyrate and 3-hydroxyhexanoate (PHBHHx) by recombinant *Halomonas bluephagenesis*. *Chemical Engineering Journal*, *466*. https://doi.org/10.1016/j.cej.2023.143261

Wang, J. J., Dodla, S. K., Delaune, R. D., Hudnall, W. H., & Cook, R. L. (2011). Soil carbon characteristics in two Mississippi river deltaic Marshland profiles. *Wetlands*, *31*(1), 157–166. https://doi.org/10.1007/s13157-010-0130-y

Wang, L., & Cui, Y. W. (2024). Simultaneous treatment of epichlorohydrin wastewater and polyhydroxyalkanoate recovery by halophilic aerobic granular sludge highly enriched by Halomonas sp. *Bioresource Technology*, *391*. https://doi.org/10.1016/j.biortech.2023.129951

Wang, Y., Kretschmer, K., Zhang, J., Mondal, A. K., Guo, X., & Wang, G. (2016). Organic sodium terephthalate@graphene hybrid anode materials for sodium-ion batteries. *RSC Advances*, *6*(62), 57098–57102. https://doi.org/10.1039/c6ra11809g

Wang, Y., Yamada, S., Asakawa, N., Yamane, T., Yoshie, N., & Inoue, Y. (2001). Comonomer compositional distribution and thermal and morphological characteristics of bacterial poly(3-hydroxybutyrate-co-3-hydroxyvalerate)s with high 3-hydroxyvalerate content. *Biomacromolecules*, *2*(4), 1315–1323. https://doi.org/10.1021/bm010128o

Wang, Y., Zhang, Y., Song, H., Wang, Y., Deng, T., & Hou, X. (2019). Zinc-catalyzed ester bond cleavage: Chemical degradation of polyethylene terephthalate. *Journal of Cleaner Production*, *208*, 1469–1475. https://doi.org/10.1016/j.jclepro.2018.10.117

Webb, H. K., Arnott, J., Crawford, R. J., & Ivanova, E. P. (2013). Plastic degradation and its environmental implications with special reference to poly(ethylene terephthalate). *Polymers*, *5*(1), 1–18. https://doi.org/10.3390/polym5010001

Wedulo, A., Atuhaire, D. K., Ochwo, S., Muwanika, V., Rwendeire, A. J. J., & Nakavuma, J. L. (2014). Characterisation and evaluation of the efficiency of petroleum degrading bacteria isolated from soils around the oil exploration areas in western Uganda. *African Journal of BIotechnology*, *13*(48), 4458–4470. https://doi.org/10.5897/A2014AJB2014.13888

Wei, T., & Fang, Q. (2022). Regulating the monomer of polyhydroxyalkanoate from mixed microbial culture: with particular emphasis on substrate composition: A review. *Environmental Engineering Research*, *27*(5), 0–1. https://doi.org/10.4491/eer.2021.333

Weinstein, J. E., Dekle, J. L., Leads, R. R., & Hunter, R. A. (2020). Degradation of bio-based and biodegradable plastics in a salt marsh habitat: Another potential source of microplastics in coastal waters. *Marine Pollution Bulletin*, *160*. https://doi.org/10.1016/j.marpolbul.2020.111518

Wendy, Y. B. D., Fauziah, M. Z. N., Baidurah, Y. S., Tong, W. Y., & Lee, C. K. (2022). Production and characterization of polyhydroxybutyrate (PHB) BY Burkholderia cepacia BPT1213 using waste glycerol as carbon source. *Biocatalysis and Agricultural Biotechnology*, *41*. https://doi.org/https://doi.org/10.1016/j.bcab.2022.102310

Werker, A. G., Johansson, P. S. T., & Magnusson, P. O. G. (2015). *Process for the extraction of polyhydroxyalkanoates from biomass*. US 20150368393A1.

Werker, A., Lorini, L., Villano, M., Valentino, F., & Majone, M. (2022). Modelling Mixed Microbial Culture Polyhydroxyalkanoate Accumulation Bioprocess towards Novel Methods for Polymer Production Using Dilute Volatile Fatty Acid Rich Feedstocks. *Bioengineering*, *9*(3). https://doi.org/10.3390/bioengineering9030125

Werner, A. Z., Clare, R., Mand, T. D., Pardo, I., Ramirez, K. J., Haugen, S. J., Bratti, F., Dexter, G. N., Elmore, J. R., Huenemann, J. D., Peabody, G. L., Johnson, C. W., Rorrer, N. A., Salvachúa, D., Guss, A. M., & Beckham, G. T. (2021). Tandem chemical deconstruction and biological upcycling

of poly(ethylene terephthalate) to β-ketoadipic acid by Pseudomonas putida KT2440. *Metabolic Engineering*, *67*, 250–261. https://doi.org/10.1016/j.ymben.2021.07.005

Wojnowska-Baryła, I., Bernat, K., & Zaborowska, M. (2022). Plastic Waste Degradation in Landfill Conditions: The Problem with Microplastics, and Their Direct and Indirect Environmental Effects. *International Journal of Environmental Research and Public Health*, *19*(20). https://doi.org/https://doi.org/10.3390/ ijerph192013223

Wongfaed, N., O-Thong, S., Sittijunda, S., & Reungsang, A. (2023). Taxonomic and enzymatic basis of the cellulolytic microbial consortium KKU-MC1 and its application in enhancing biomethane production. *Scientific Reports*, *13*(1), 1–27. https://doi.org/10.1038/s41598-023-29895-0

Wongsirichot, P., Barroso-Ingham, B., Hamilton, A., Parroquin Gonzalez, M., Romero Jimenez, R., Hoeven, R., & Winterburn, J. (2024). Food wastes for bioproduct production and potential strategies for high feedstock variability. *Waste Management*, *184*, 1–9. https://doi.org/10.1016/j.wasman.2024.05.027

Wu, F., Misra, M., & Mohanty, A. K. (2021). Challenges and new opportunities on barrier performance of biodegradable polymers for sustainable packaging. *Progress in Polymer Science*, *117*. https://doi.org/10.1016/j.progpolymsci.2021.101395

Wu, M., & Wang, H. (2024). Re-considering and designing microbiomes for future waste biorefinery. *Microbial Biotechnology*, *17*(1), 1–5. https://doi.org/10.1111/1751-7915.14395

Wu, S., Tao, S., Ye, X., Wang, A., Liu, Z., Ran, C., Liang, H., Li, H., Yang, Y., Zhang, W., & Liu, J. T. (2023). Characteristics of Sedimentary Organic Matter in Tidal Estuaries: A Case Study from the Minjiang River Estuary. *Water*, *15*(9). https://doi.org/10.3390/w15091682

Yang, Q., Wu, Z., & Tao, C. (2014). Study on biodegradability of terephthalic acid in polyester fabric alkali-peeling process wastewater. *Water Science and Technology*, *69*(2), 328–334. https://doi.org/10.2166/wst.2013.714

Yang, X. (2013). Rapid Determination of Eight Related Aromatic Acids in the p-Phthalic Acid Mother Liquid Using an Agilent 1260 Infi nity LC System and an Agilent Poroshell 120 SB-C18 Column (Application Note). In *Agilent Technologies, Co. Ltd*. Agilent Technologies, Co. Ltd.

Yogesh, C., Pathak, B., & Fulekar, M. H. (2012). PHA - Production Application and its Bioremediation in Environment. *International Research Journal of Environment Sciences*, *1*(2), 46–52.

Yoshida, S., Hiraga, K., Takehana, T., Taniguchi, I., Yamaji, H., Maeda, Y., Toyohara, K., Miyamoto, K., Kimura, Y., & Oda, K. (2016). A bacterium that degrades and assimilates poly(ethylene terephthalate). *Science*, *351*(6278), 1196–1199. https://doi.org/10.1126/science.aaf8305

Zarrinmehr, M. J., Daneshvar, E., Nigam, S., Gopinath, K. P., Biswas, J. K., Kwon, E. E., Wang, H., Farhadian, O., & Bhatnagar, A. (2022). The effect of solvents polarity and extraction conditions on the microalgal lipids yield, fatty acids profile, and biodiesel properties. *Bioresource Technology*, *344*. https://doi.org/10.1016/j.biortech.2021.126303

Zhang, Y. J., Li, Q., Zhang, Y. X., Wang, D., & Xing, J. M. (2012). Optimization of Succinic acid fermentation with Actinobacillus succinogenes by response surface methodology (RSM). *Journal*

of Zhejiang University: Science B (Biomedicine & Biotechnology), *13*(2), 103–110. https://doi.org/10.1631/jzus.B1100134

Zhang, Y., Wusiman, A., Liu, X., Wan, C., Lee, D. J., & Tay, J. H. (2018). Polyhydroxyalkanoates (PHA) production from phenol in an acclimated consortium: Batch study and impacts of operational conditions. *Journal of Biotechnology*, *267*, 36–44. https://doi.org/10.1016/j.jbiotec.2018.01.001

Zhang, Y.-M., Sun, Y.-Q., Wang, Z.-J., & Zhang, J. (2013). The environmental fate of phthalate esters: A literature review. *Chemosphere*, *109*(7/8), 1–4. https://doi.org/10.1590/sajs.2013/20120019

Zhang, Z., Wang, Y., Wang, X., Zhang, Y., Zhu, T., Peng, L., Xu, Y., Chen, X., Wang, D., Ni, B. J., & Liu, Y. (2024). Towards scaling-up implementation of polyhydroxyalkanoate (PHA) production from activated sludge: Progress and challenges. *Journal of Cleaner Production*, *447*. https://doi.org/https://doi.org/10.1016/j.jclepro.2024.141542

Zhao, J., Cui, Y. W., Zhang, H. Y., & Gao, Z. L. (2021). Carbon Source Applied in Enrichment Stage of Mixed Microbial Cultures Limits the Substrate Adaptability for PHA Fermentation Using the Renewable Carbon. *Applied Biochemistry and Biotechnology*, *193*(10), 3253–3270. https://doi.org/10.1007/s12010-021-03587-9

Zhao, K., Deng, Y., Chen, J. C., & Chen, G.-Q. (2003). Polyhydroxyalkanoate (PHA) scaffolds with good mechanical properties and biocompatibility. *Biomaterials*, *24*, 1041–1045. https://doi.org/S0142-9612(02)00426-X

Zhao, Q., Bai, J., Lu, Q., & Zhang, G. (2017). Effects of salinity on dynamics of soil carbon in degraded coastal wetlands: Implications on wetland restoration. *Physics and Chemistry of the Earth*, *97*, 12–18. https://doi.org/10.1016/j.pce.2016.08.008

Zhao, Q., Zhao, H., Gao, Y., Zheng, L., Wang, J., & Bai, J. (2020). Alterations of bacterial and archaeal communities by freshwater input in coastal wetlands of the Yellow River Delta, China. *Applied Soil Ecology*, *153*. https://doi.org/10.1016/j.apsoil.2020.103581

Zheng, Y., Su, F., Li, H., Song, F., Wei, C., & Cui, P. (2024). Structure and Function of Soil Bacterial Communities in the Different Wetland Types of the Liaohe Estuary Wetland. *Microorganisms*, *12*(10). https://doi.org/10.3390/microorganisms12102075

Zhong, Y., Godwin, P., Jin, Y., & Xiao, H. (2020). Biodegradable polymers and green-based antimicrobial packaging materials: A mini-review. *Advanced Industrial and Engineering Polymer Research*, *3*(1), 27–35. https://doi.org/10.1016/j.aiepr.2019.11.002

Zhou, J. J., Shen, J. T., Jiang, L. L., Sun, Y. Q., Mu, Y., & Xiu, Z. L. (2017). Selection and characterization of an anaerobic microbial consortium with high adaptation to crude glycerol for 1,3-propanediol production. *Applied Microbiology and Biotechnology*, *101*(15), 5985–5996. https://doi.org/10.1007/s00253-017-8311-8

Zhou, T., Wang, S., Zhang, W., Yin, F., Cao, Q., Lian, T., & Dong, H. (2023a). Comparison of different aerobic sludge on enriching polyhydroxyalkanoate mixed microbial culture using lactic acid fermentation broth of agricultural wastes. *Chemical Engineering Journal*, *475*. https://doi.org/10.1016/j.cej.2023.146000

Zhou, T., Wang, S., Zhang, W., Yin, F., Cao, Q., Lian, T., & Dong, H. (2023b). Polyhydroxyalkanoates production from lactic acid fermentation broth of agricultural waste without extra purification: The effect of concentrations. *Environmental Technology and Innovation*, *32*. https://doi.org/10.1016/j.eti.2023.103311

Zhou, W., Bergsma, S., Colpa, D. I., Euverink, G. J. W., & Krooneman, J. (2023). Polyhydroxyalkanoates (PHAs) synthesis and degradation by microbes and applications towards a circular economy. *Journal of Environmental Management*, *341*. https://doi.org/10.1016/j.jenvman.2023.118033

Zhou, X., Sun, Z., Yan, H., Feng, X., Zhao, H., Liu, Y., Chen, X., & Yang, C. (2021). Produce petrochemicals directly from crude oil catalytic cracking, a techno-economic analysis and life cycle society-environment assessment. *Journal of Cleaner Production*, *308*. https://doi.org/https://doi.org/10.1016/j.jclepro.2021.127283

Zuñiga, C., Zaramela, L., & Zengler, K. (2017). Elucidation of complexity and prediction of interactions in microbial communities. *Microbial Biotechnology*, *10*(6), 1500–1522. https://doi.org/10.1111/1751-7915.12855

APPENDIXES

Appendix A

Table A 1. One-way ANOVA results for kinetic and stoichiometric parameters of the three assays performed by *Rhodococcus* sp. Ave7 using REX-TPA.

Source	ANOVA Analysis						Bonferroni´s Multiple Comparison Test		
	SS	df	F value	*p*-value	Significance	R^2	A vs B	A vs C	B vs C
CDW (g/L)	2.3	8	240	<0.00001	Yes	0.99	Significant (p<0.05)	Significant (p<0.05)	Significant (p<0.05)
μ_{max} (h^{-1})	0.0062	8	0.1	0.9063	No	0.032	Not significant (p>0.05)	Not significant (p>0.05)	Not significant (p>0.05)
$Y_{X/TPA}$ (g_X/g_{TPA})	0.095	8	46	0.0002	Yes	0.94	Highly significant (p<0.001)	Not significant (p>0.05)	Significant (p<0.05)
TAG (g/L)	0.091	8	21	0.002	Yes	0.87	Significant (p<0.05)	Highly significant (p<0.0001)	Not significant (p>0.05)
TAG wt.%	14	8	32	0.0006	Yes	0.92	Highly significant (p<0.001)	Significant (p<0.05)	Not significant (p>0.05)
r_{TAG} (g/(L.day))	0.011	8	33	0.0006	Yes	0.92	Not significant (p>0.05)	Significant (p<0.01)	Highly significant (p<0.0001)
$Y_{TAG/TPA}$ (g_{TAG}/g_{TPA})	0.0038	8	1100	<0.00001	Yes	1	Significant (p<0.05)	Significant (p<0.05)	Significant (p<0.05)
PHA (g/L)	0.46	8	870	<0.00001	Yes	1	Not significant (p>0.05)	Significant (p<0.05)	Significant (p<0.05)
PHA wt.%	260	8	840	<0.00001	Yes	1	Significant (p<0.05)	Highly significant (p<0.001)	Highly significant (p<0.001)
r_{PHA} (g/(L.day))	0.57	8	85000	<0.00001	Yes	1	Significant (p<0.05)	Highly significant (p<0.001)	Highly significant (p<0.001)
$Y_{PHA/TPA}$ (g_{TAG}/g_{TPA})	0.0029	8	440	<0.00001	Yes	0.99	Not significant (p>0.05)	Highly significant (p<0.001)	Highly significant (p<0.001)

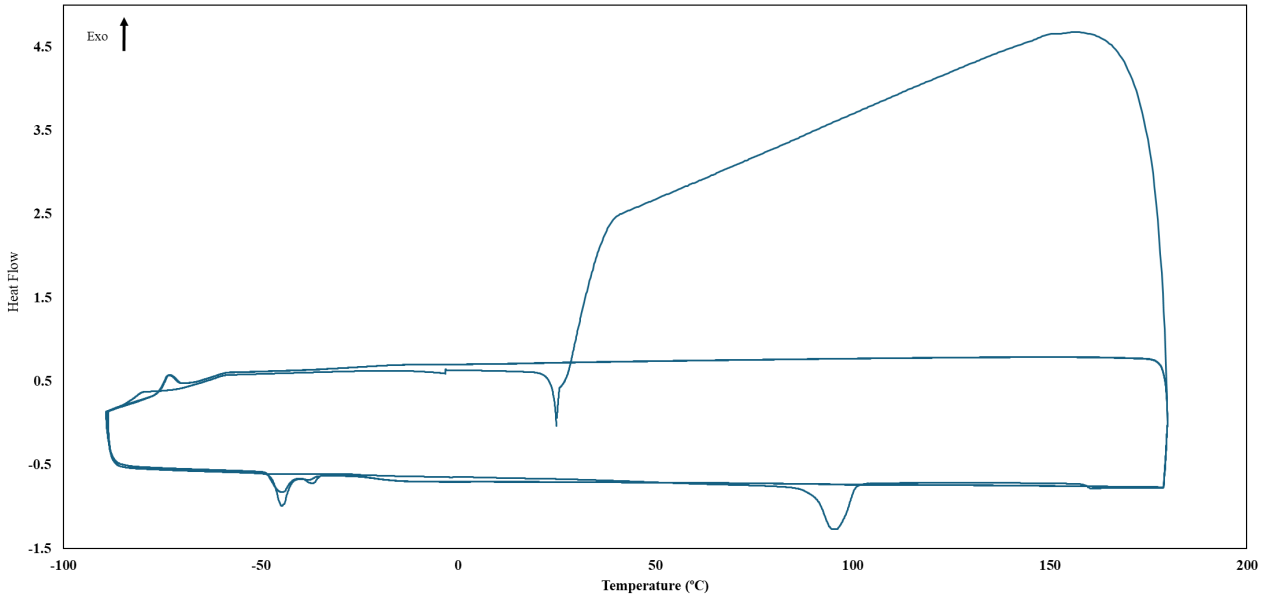

Figure A. 1 - Differential scanning calorimetry (DSC) thermogram of PHBV produced by *Rhodococcus* sp.Ave7.

Appendix B

Table B. 1. One-way ANOVA results for the three PHA production assays, A, B and C, performed at 69, 89 and 113 days, respectively of marshland microbiome selection using REX-TPA as feedstock.

One-way ANOVA					
P-value	0.9897				
P-value summary	ns				
Are means signif. different? (P < 0.05)	No				
Number of groups	3				
F	0.010				
R squared	0.0017				
Bartlett's test for equal variances					
Bartlett's statistic (corrected)	0.095				
P value	0.9538				
P value summary	ns				
Do the variances differ signif. (*P*<0.05)	No				
ANOVA Table	SS	df	MS		
Treatment (between columns)	17	2	8.4		
Residual (within columns)	9600	12	800		
Total	9700	14			
Bonferroni's Multiple Comparison Test	Mean Diff.	t	Significant? *P* < 0.05?	Summary	95% CI of diff
Assay A vs Assay B	0.76	0.042	No	ns	-49 to 51
Assay A vs Assay C	-1.8	0.098	No	ns	-52 to 48
Assay B vs Assay C	-2.5	0.14	No	ns	-52 to 47

Table B. 2. One-way ANOVA results for the molecular weight, PDI and thermal properties of the PHB produced from marshland microbiome selection using REX-TPA as feedstock.

One-way ANOVA					
P-value	0.8641				
P-value summary	ns				
Are means signif. different? ($P < 0.05$)	No				
Number of groups	3				
F	0.15				
R squared	0.014				
Bartlett's test for equal variances					
Bartlett's statistic (corrected)	0.97				
P value	0.6154				
P value summary	Ns				
Do the variances differ signif. ($P < 0.05$)	No				
ANOVA Table	SS	df	MS		
Treatment (between columns)	4200	2	2100		
Residual (within columns)	300000	21	14000		
Total	310000	23			
Bonferroni's Multiple Comparison Test	Mean Diff.	t	Significant? P <0.05?	Summary	95% CI of diff
PHB_A vs PHB_B	-20	0.34	No	ns	-180 to 140
PHB_A vs PHB_C	-32	0.54	No	ns	-190 to 120
PHB_B vs PHB_C	-12	0.20	No	ns	-170 to 140

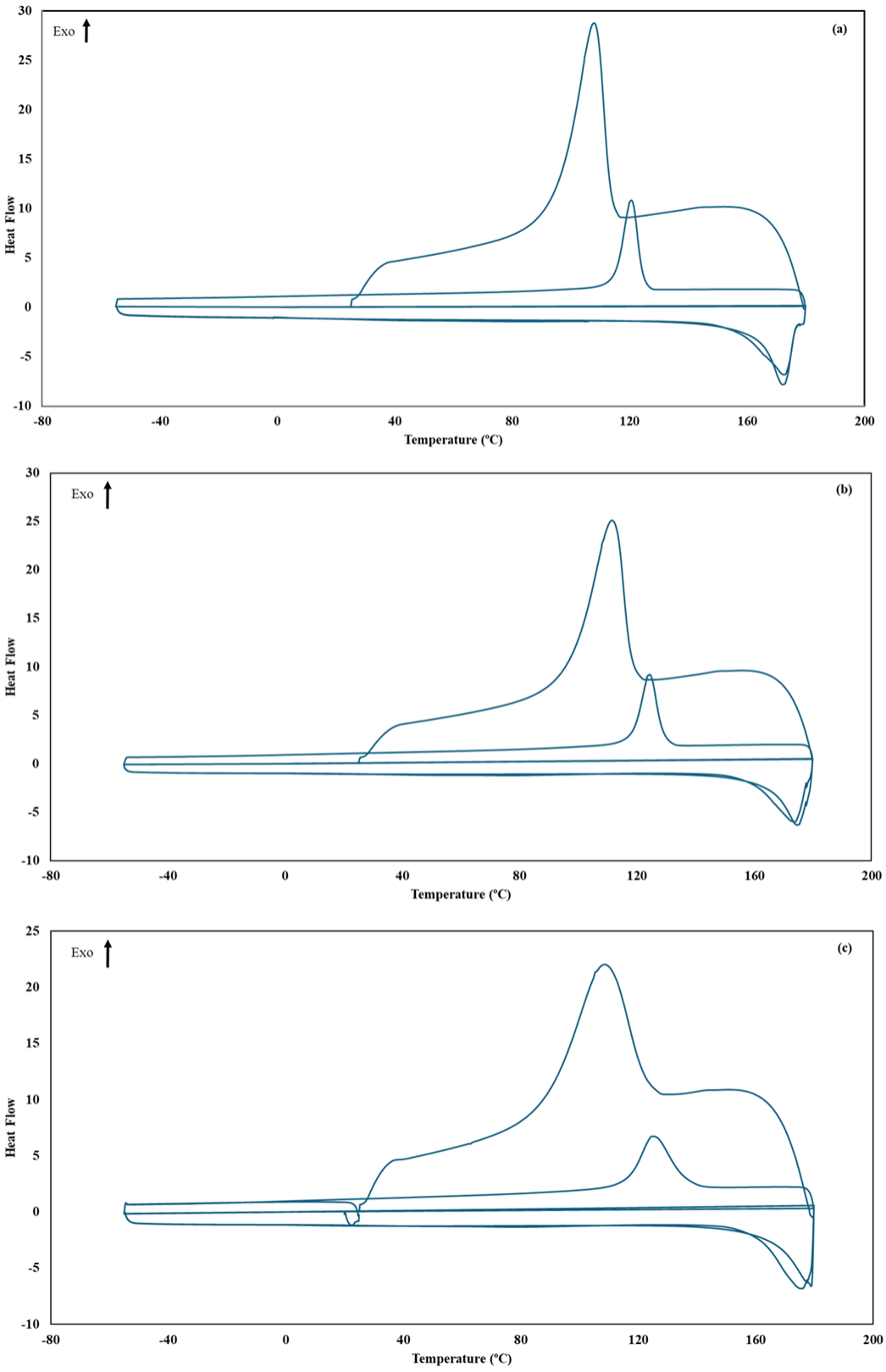

Figure B. 1 - Differential scanning calorimetry (DSC) thermogram of PHB produced at 69 (a), 89 (b) and 113 (c) days by marshland microbiome using REX-TPA as feedstock.

2025

ANA TERESA MATALOTO REBOCHO

BIOLOGICAL UPCYCLING OF MIXED PET WASTE
INTO HIGH VALUE PRODUCTS